

Frans Laakso

Studies on High Speed
Uplink Packet Access
Performance Enhancements



JYVÄSKYLÄ STUDIES IN COMPUTING 206

Frans Laakso

Studies on High Speed
Uplink Packet Access
Performance Enhancements

Esitetään Jyväskylän yliopiston informaatioteknologian tiedekunnan suostumuksella
julkisesti tarkastettavaksi yliopiston Agora-rakennuksen Gamma-salissa
joulukuun 19. päivänä 2014 kello 12.

Academic dissertation to be publicly discussed, by permission of
the Faculty of Information Technology of the University of Jyväskylä,
in building Agora, Gamma hall, on December 19, 2014 at 12 o'clock noon.



UNIVERSITY OF JYVÄSKYLÄ

JYVÄSKYLÄ 2014

Studies on High Speed
Uplink Packet Access
Performance Enhancements

JYVÄSKYLÄ STUDIES IN COMPUTING 206

Frans Laakso

Studies on High Speed
Uplink Packet Access
Performance Enhancements



UNIVERSITY OF JYVÄSKYLÄ

JYVÄSKYLÄ 2014

Editors

Timo Männikkö

Department of Mathematical Information Technology, University of Jyväskylä

Pekka Olsbo, Ville Korhonen

Publishing Unit, University Library of Jyväskylä

URN:ISBN:978-951-39-5984-5

ISBN 978-951-39-5984-5 (PDF)

ISBN 978-951-39-5983-8 (nid.)

ISSN 1456-5390

Copyright © 2014, by University of Jyväskylä

Jyväskylä University Printing House, Jyväskylä 2014

ABSTRACT

Laakso, Frans

Studies on High Speed Uplink Packet Access Performance Enhancements

Jyväskylä: University of Jyväskylä, 2014, 96 p.(+included articles)

(Jyväskylä Studies in Computing

ISSN 1456-5390; 206)

ISBN 978-951-39-5983-8 (nid.)

ISBN 978-951-39-5984-5 (PDF)

Finnish summary

Diss.

The purpose of this thesis is to address a variety of performance related aspects in terms of Third Generation (3G) mobile networks. From a practical perspective, wireless network sets a very demanding environment for different services due to, e.g., limited User Equipment (UE) battery power, transmission delays, packet loss and varying network performance. This thesis addresses the aforementioned challenges by evaluating different transmit diversity options, battery saving opportunities, Interference Coordination (IC), Range Extension (RE) and Dual-Carrier (DC) in Uplink (UL). The studies are conducted with the help of time driven quasi-static system level simulator where, e.g., fading, propagation and Radio Resource Management (RRM) functionality is explicitly taken into account.

Keywords: WCDMA, HSUPA, Interference Coordination, Transmit Diversity, Beamforming, Antenna Switching, CPC, DTx, Battery Savings, Rake, LMMSE, VoIP, System Level Performance, Simulations

Author Frans Laakso
Department of Mathematical Information Technology
University of Jyväskylä
Finland

Supervisors Professor Tapani Ristaniemi
Department of Mathematical Information Technology
University of Jyväskylä
Finland

Dr. Janne Kurjenniemi
Magister Solutions, Ltd.
Finland

Reviewers Professor Peter Chong
School of Electrical & Electronic Engineering
Nanyang Technological University
Singapore

Professor Zekeriya Uykan
Faculty of Engineering
Dogus University
Turkey

Opponent Professor Jyri Hämäläinen
Aalto University
Finland

ACKNOWLEDGEMENTS

The studies related to this thesis are done in co-operation with the University of Jyväskylä, Magister Solutions Ltd., Nokia Research Center, Nokia Siemens Networks and Renesas Mobile Europe. First of all, I wish to express my gratitude to the Department of Mathematical Information Technology for providing the initial opportunity to work on this research area. This dissertation has taken its time and it would not have been possible without the help of many people. I would especially like to thank my supervisors Professor Tapani Ristaniemi and Dr. Janne Kurjenniemi for their support and encouragement at every stage of my thesis.

I would like to thank all the co-authors who have participated in the research work of the included articles. It has been a privilege to work with you and this thesis simply would not have been completed without you.

Also I would like to express my gratitude to all the colleagues from Magister Solutions for the exceptional working atmosphere. Our daily get-togethers have been important moments for talking about life in general, and for sharing and developing ideas concerning our research and studies.

Additionally, I would like to express my gratitude to the Jenny and Antti Wihuri Foundation, Nokia Foundation, Ulla Tuominen Foundation and the Department of Mathematical Information Technology for the financial support provided for the research. Special thanks to the Ernst and Ossi Hirvelä Foundation for their financial support and for providing apartments for students.

I am grateful to the examiners of my thesis, Professors Peter Chong and Zekeriya Uykan, for their constructive comments and Professor Jyri Hämäläinen for being my opponent.

I am also grateful to all of my friends who always helped me to clear my mind and to take a look at my problems in a new perspective. A good distraction is sometimes most welcome, even if it is not appreciated at that very moment.

Last but most importantly, my warmest thanks go to my father Leo and mother Airi for their love and patience, and for the live energy they have been sharing with me during my whole live, and to my sister Tutta and brothers Jyrki and Jari for their support and wise advice.

Jyväskylä, November 22, 2014
Frans Laakso

ABBREVIATIONS

| | |
|----------|--|
| 1G | First Generation |
| 2G | Second Generation |
| 3G | Third Generation |
| 3GPP | Third Generation Partnership Project |
| 4G | Fourth Generation |
| 5G | Fifth Generation |
| ACK | Acknowledgment |
| AS | Active Set |
| AVI | Actual Value Interface |
| BER | Bit Error Rate |
| BFTD | Beamforming Transmit Diversity |
| BS | Base Station |
| BSC | Base Station Controller |
| CDM | Code Division Multiplexing |
| CDMA | Code Division Multiple Access |
| CL | Closed Loop |
| CLBF | Closed Loop Beamforming |
| CLPC | Closed Loop Power Control |
| CLTD | Closed Loop Transmit Diversity |
| CN | Core Network |
| CPC | Continuous Packet Connectivity |
| CRC | Cyclic Redundancy Check |
| CS | Combining Set |
| CT | Core and Terminals |
| DC | Dual-Carrier |
| DC-HSDPA | Dual-Carrier HSDPA |
| DC-HSUPA | Dual-Carrier HSUPA |
| DCH | Dedicated Channel |
| DL | Downlink |
| DPCCH | Dedicated Physical Control Channel |
| DPDCH | Dedicated Physical Data Channel |
| DRX | Discontinuous Reception |
| DS-CDMA | Direct-Sequence Code Division Multiple Access |
| DTX | Discontinuous Transmission |
| E-AGCH | E-DCH Absolute Grant Channel |
| E-DCH | Enhanced Dedicated Channel |
| E-DPCCH | Enhanced Dedicated Physical Control Channel |
| E-DPDCH | Enhanced Dedicated Physical Data Channel |
| E-HICH | E-DCH Hybrid ARQ Indicator Channel |
| E-RGCH | E-DCH Relative Grant Channel |

| | |
|----------|---|
| E-TFCI | Enhanced Transport Format Combination Indicator |
| E-UTRAN | Evolved UMTS Terrestrial Radio Access Network |
| Eb/No | Energy per Bit to Noise Ratio |
| Ec/No | Energy per Chip to Noise Ratio |
| EDGE | Enhanced Data rates for GSM Evolution |
| ETSI | European Telecommunications Standards Institute |
| FDD | Frequency Division Duplex |
| FDMA | Frequency Division Multiple Access |
| FER | Frame Error Rate |
| GERAN | GSM/EDGE Radio Access Network |
| GPRS | General Packet Radio Service |
| GSM | Global System for Mobile Communications |
| HARQ | Hybrid Automatic Repeat-reQuest |
| HetNet | Heterogeneous Networks |
| HS-DPCCH | High Speed Downlink Physical Control Channel |
| HS-SCCH | High Speed Shared Control Channel |
| HSDPA | High Speed Downlink Packet Access |
| HSPA | High Speed Packet Access |
| HSUPA | High Speed Uplink Packet Access |
| IC | Interference Coordination |
| ILPC | Inner Loop Power Control |
| ITU | International Telecommunication Union |
| LA | Link Adaptation |
| LMMSE | Linear Minimum Mean Squared Error |
| LTE | Long Term Evolution |
| MAC | Medium Access Control |
| MAI | Multiple Access Interference |
| Max C/I | Maximum Carrier to Interference Ratio |
| MC | Multi-Carrier |
| ME | Mobile Equipment |
| MIMO | Multiple Input Multiple Output |
| MRC | Maximum Ratio Combining |
| NACK | Negative Acknowledgment |
| NMT | Nordic Mobile Telephone |
| Node-B | Base Station |
| NST | Non-Scheduled Transmissions |
| OL | Open Loop |
| OLBF | Open Loop Beamforming |
| OLPC | Open Loop Power Control |
| OLPC | Outer Loop Power Control |
| OLTD | Open Loop Transmit Diversity |

| | |
|---------|--|
| OVSF | Orthogonal Variable Spreading Factor |
| PA | Power Amplifier |
| PC | Power Control |
| PedA | Pedestrian A |
| PF | Proportional Fair |
| PG | Processing Gain |
| QoS | Quality of Service |
| QPSK | Quadrature Phase Shift Keying |
| RAN | Radio Access Network |
| RAN1 | Radio Access Network Radio Layer 1 |
| RE | Range Extension |
| RF | Radio Frequency |
| RLC | Radio Link Control |
| RNC | Radio Network Controller |
| RoT | Rise over Thermal |
| RR | Round Robin |
| RRM | Radio Resource Management |
| RTT | Round-Trip Time |
| Rx | Receive |
| S-DPCCH | Secondary Dedicated Physical Control Channel |
| S-HARQ | Super-HARQ |
| SA | System Architecture |
| SATD | Switched Antenna Transmit Diversity |
| SI | Study Item |
| SINR | Signal to Interference and Noise Ratio |
| SIR | Signal to Interference Ratio |
| SMS | Short Message Service |
| SON | Self-Organizing Network |
| TDD | Time Division Duplex |
| TDM | Time Division Multiplexing |
| TDMA | Time Division Multiple Access |
| TPC | Transmission Power Control |
| TR | Technical Requirement |
| TS | Technical Specification |
| TSG | Technical Specification Group |
| TTI | Transmission Time Interval |
| Tx | Transmit |
| UE | User Equipment |
| UL | Uplink |
| UL DTX | Uplink Discontinuous Transmission |
| ULTD | Uplink Transmit Diversity |
| UMTS | Universal Mobile Telecommunications System |
| UPH | Uplink Power Headroom |

| | |
|-------|--|
| USIM | UMTS Subscriber Identity Module |
| UTRAN | UMTS Terrestrial Radio Access Network |
| VehA | Vehicular A |
| VoIP | Voice over IP |
| WA | Wrap-Around |
| WCDMA | Wideband Code Division Multiple Access |
| WG | Working Group |
| WI | Work Item |

LIST OF FIGURES

| | | |
|-----------|---|----|
| FIGURE 1 | 3GPP release timeline | 25 |
| FIGURE 2 | UMTS architecture | 29 |
| FIGURE 3 | FDMA, TDMA and CDMA principles..... | 30 |
| FIGURE 4 | Spreading/despreading operation [HT07]..... | 31 |
| FIGURE 5 | Multipath propagation | 32 |
| FIGURE 6 | Slow and fast fading of propagated signal in respect to receiver-transmitter distance | 34 |
| FIGURE 7 | Maximum ratio combining with the Rake receiver | 39 |
| FIGURE 8 | Multiple access interference | 40 |
| FIGURE 9 | Block diagram of LMMSE receiver | 41 |
| FIGURE 10 | Power control in WCDMA..... | 42 |
| FIGURE 11 | The new channels introduced as part of HSUPA | 47 |
| FIGURE 12 | Synchronous HARQ in HSUPA | 47 |
| FIGURE 13 | HSUPA discontinuous transmission | 51 |
| FIGURE 14 | Time domain Interference Coordination -scenario..... | 53 |
| FIGURE 15 | Illustration of dual-carrier operation..... | 55 |
| FIGURE 16 | Example of VoIP traffic with different TTIs | 56 |
| FIGURE 17 | The selected Range Extension -scheme..... | 57 |
| FIGURE 18 | HARQ mapping when switching from normal 2 ms TTI to 2 ms TTI RE | 58 |
| FIGURE 19 | HARQ mapping when switching from 2 ms TTI RE to normal 2 ms TTI operation..... | 59 |
| FIGURE 20 | The principle of SATD | 61 |
| FIGURE 21 | High level block diagram of SATD [3GP11a] | 61 |
| FIGURE 22 | Genie aided switching (TX1) | 62 |
| FIGURE 23 | TPC aided switching 1 (TX2)..... | 63 |
| FIGURE 24 | TPC aided switching 2 (TX3)..... | 64 |
| FIGURE 25 | DPCCH aided switching (TX4)..... | 64 |
| FIGURE 26 | Periodical switch (TX5)..... | 64 |
| FIGURE 27 | SATD power selection algorithms..... | 65 |
| FIGURE 28 | High level block diagram of OLBF [3GP11a]..... | 66 |
| FIGURE 29 | Principle of CLBF without pilot pre-coding | 70 |
| FIGURE 30 | Principle of CLBF with pre-coded pilots..... | 71 |
| FIGURE 31 | Illustration of the simulation flow..... | 77 |
| FIGURE 32 | Simulation scenario with wrap-around | 79 |

LIST OF TABLES

TABLE 1 The phase adjustments corresponding to the feedback com-
mands for the time slots 74

TABLE 2 System level simulator classification and the main attributes 76

CONTENTS

| | |
|---------------------------|--|
| ABSTRACT | |
| ACKNOWLEDGEMENTS | |
| ABBREVIATIONS | |
| LIST OF FIGURES | |
| LIST OF TABLES | |
| CONTENTS | |
| LIST OF INCLUDED ARTICLES | |

| | | |
|---------|--|----|
| 1 | INTRODUCTION | 17 |
| 1.1 | Research Problem | 18 |
| 1.2 | Related Studies..... | 20 |
| 1.2.1 | Interference Coordination..... | 20 |
| 1.2.2 | Dual-Carrier..... | 21 |
| 1.2.3 | Range Extension | 22 |
| 1.2.4 | Transmit Diversity | 23 |
| 1.3 | The Third Generation Partnership Project | 24 |
| 1.4 | Main Contribution..... | 25 |
| 1.5 | Outline of the Dissertation..... | 27 |
| 2 | UNIVERSAL MOBILE TELECOMMUNICATIONS SYSTEM | 28 |
| 2.1 | UMTS Radio Access Network Architecture | 28 |
| 2.2 | Brief Introduction to WCDMA..... | 30 |
| 2.2.1 | Basics of Spreading and Despreading | 31 |
| 2.3 | Multipath Radio Channels..... | 32 |
| 2.3.1 | Attenuation..... | 33 |
| 2.3.1.1 | Distance Attenuation | 33 |
| 2.3.1.2 | Slow and Fast Fading | 33 |
| 2.4 | Multi-Antenna Techniques | 34 |
| 2.4.1 | Receive Diversity | 35 |
| 2.4.2 | Transmit Diversity | 35 |
| 2.5 | Macro Diversity..... | 36 |
| 2.6 | Receivers | 37 |
| 2.6.1 | Mathematical Signal Model | 37 |
| 2.6.2 | Rake Receiver..... | 38 |
| 2.6.3 | Intra- and Inter-cell Interference..... | 39 |
| 2.6.4 | Linear Minimum Mean Squared Error Chip-level Equalizer | 40 |
| 2.6.4.1 | LMMSE Receiver Coefficient Calculation | 41 |
| 2.7 | Power Control..... | 42 |
| 2.8 | Handovers in WCDMA..... | 43 |
| 3 | HIGH SPEED UPLINK PACKET ACCESS..... | 45 |
| 3.1 | HSUPA Channels | 46 |
| 3.2 | Fast Layer 1 Retransmissions | 46 |

| | | |
|---------|---|----|
| 3.3 | Scheduling..... | 48 |
| 3.3.1 | Scheduling Algorithms | 48 |
| 3.3.2 | User Multiplexing..... | 49 |
| 3.4 | Continuous Packet Connectivity | 50 |
| 3.4.1 | Uplink Discontinuous Transmission | 50 |
| 4 | HSUPA PERFORMANCE ENHANCEMENTS | 52 |
| 4.1 | Interference Coordination..... | 52 |
| 4.2 | Dual-Carrier | 54 |
| 4.2.1 | Scheduling with DC-HSUPA | 55 |
| 4.3 | Range Extension..... | 56 |
| 4.3.1 | Mode Switching Criteria for Range Extension | 57 |
| 4.3.2 | HARQ Operation with Range Extension | 58 |
| 4.4 | Transmit Diversity | 59 |
| 4.4.1 | Switched Antenna Transmit Diversity | 60 |
| 4.4.1.1 | SATD Algorithms | 60 |
| 4.4.2 | Open Loop Beamforming Transmit Diversity | 65 |
| 4.4.2.1 | OLBF SINR Calculation | 67 |
| 4.4.2.2 | OLBF Algorithms | 68 |
| 4.4.3 | Closed Loop Beamforming Transmit Diversity | 69 |
| 4.4.3.1 | CLBF SINR Calculation | 71 |
| 4.4.3.2 | CLBF Algorithms..... | 72 |
| 4.4.3.3 | CLBF Feedback Methods | 73 |
| 5 | RESEARCH TOOLS | 75 |
| 5.1 | Simulator Types | 75 |
| 5.2 | Simulation Flow | 76 |
| 6 | SIMULATION RESULTS..... | 78 |
| 6.1 | Simulation Scenarios and Assumptions | 78 |
| 6.2 | Interference Coordination Results | 79 |
| 6.3 | Dual-Carrier Results | 80 |
| 6.4 | Range Extension Results | 81 |
| 6.5 | Transmit Diversity Results..... | 82 |
| 6.5.1 | Results on Switched Antenna Transmit Diversity..... | 82 |
| 6.5.2 | Results on Open Loop Beamforming | 84 |
| 6.5.3 | Results on Closed Loop Beamforming | 84 |
| 7 | CONCLUSION | 87 |
| | YHTEENVETO (FINNISH SUMMARY) | 89 |
| | REFERENCES..... | 91 |
| | INCLUDED ARTICLES | |

LIST OF INCLUDED ARTICLES

- PI Frans Laakso, Kari Aho, Thomas Chapman, Tapani Ristaniemi. Applicability of Interference Coordination in Highly Loaded HSUPA Network. *IEEE 71st Vehicular Technology Conference: VTC2010-Spring*, 2010.
- PII Ilmari Repo, Kari Aho, Sami Hakola, Thomas Chapman, Frans Laakso. Enhancing HSUPA System Level Performance with Dual Carrier Capability. *5th IEEE International Symposium on Wireless Pervasive Computing (ISWPC)*, 2010.
- PIII Frans Laakso, Kari Aho, Ilmari Repo, Thomas Chapman. Extended HSUPA Coverage and Enhanced Battery Saving Opportunities with Multiple TTI Lengths. *21st IEEE International Symposium on Personal, Indoor and Mobile Radio Communications (PIMRC 2010)*, 2010.
- PIV Frans Laakso, Kari Aho, Ilmari Repo, Thomas Chapman. Streamlining HSUPA TTI Lengths without Compromising HSUPA Capacity. *IEEE 73rd Vehicular Technology Conference: VTC2011-Spring*, 2011.
- PV Kari Aho, Ilmari Repo, Petri Eskelinen, Frans Laakso. Introducing Switched Antenna Transmit Diversity for High Speed Uplink Packet Access. *18th International Conference on Telecommunications*, 2011.
- PVI Petri Eskelinen, Ilmari Repo, Kari Aho, Frans Laakso. On HSUPA Open Loop Switched Antenna Transmit Diversity Performance in Varying Load Conditions. *IEEE 73rd Vehicular Technology Conference: VTC2011-Spring*, 2011.
- PVII Ilmari Repo, Kari Aho, Petri Eskelinen, Frans Laakso. Switched Antenna Transmit Diversity Imperfections and Their Implications to HSUPA Performance. *18th International Conference on Telecommunications*, 2011.
- PVIII Frans Laakso, Kari Aho, Ilmari Repo, Petri Eskelinen, Marko Lampinen. Beamforming Transmit Diversity Using Power Control Commands for High Speed Uplink Packet Access. *IEEE 74th Vehicular Technology Conference: VTC2011-Fall*, 2011.
- PIX Tuomas Hiltunen, Frans Laakso, Petri Eskelinen, Kari Aho, Ilmari Repo, Arto Lehti. Introducing Dual Pilot Closed Loop Transmit Diversity for High Speed Uplink Packet Access. *IEEE 74th Vehicular Technology Conference: VTC2011-Fall*, 2011.
- PX Petri Eskelinen, Frans Laakso, Kari Aho, Tuomas Hiltunen, Ilmari Repo, Arto Lehti. Impact of Practical Codebook Limitations on HSUPA Closed Loop Transmit Diversity. *IEEE 74th Vehicular Technology Conference: VTC2011-Fall*, 2011.

- PXI Petri Eskelinen, Frans Laakso, Marko Lampinen. Impact of Amplitude Component on HSUPA Closed Loop Transmit Diversity Performance. *IEEE 75th Vehicular Technology Conference: VTC2012-Spring*, 2012.
- PXII Frans Laakso, Petri Eskelinen, Marko Lampinen. Performance of Absolute and Recursive Feedback Methods with HSUPA Closed Loop Transmit Diversity. *23rd IEEE International Symposium on Personal, Indoor and Mobile Radio Communications (PIMRC 2012)*, 2012.
- PXIII Frans Laakso, Petri Eskelinen, Marko Lampinen. Uplink Weight Signaling for HSUPA Closed Loop Transmit Diversity. *23rd IEEE International Symposium on Personal, Indoor and Mobile Radio Communications (PIMRC 2012)*, 2012.

1 INTRODUCTION

The way people can use electronic devices for communication has dramatically changed within the time span of just a few decades. Since the 1980's First Generation (1G) networks, also known as Nordic Mobile Telephone (NMT) networks [HB03], commercial wireless cellular technologies have evolved through the 1990's Second Generation (2G) Global System for Mobile Communications (GSM) networks [EVBH09] to the wide spread use of current 3G networks utilizing Wideband Code Division Multiple Access (WCDMA) [HT07]. WCDMA Release 99 specification work was completed at the end of 1999 and was followed by the first commercial deployment during 2002 [HT11]. At the same time the services evolved from the 1G's analogue voice calls through digital voice calls, Short Message Service (SMS) [EVBH09] and limited packet data capabilities of 2G into the more packet data focused 3G.

While the WCDMA's initial 384 kbps data rate [HT07] was a vast improvement over the packet data capabilities of 2G, the deployment of a large variety of new services, such as mobile internet access and multimedia streaming, create constant demand for higher data rates and better performance. Wireless cellular networks have experienced rapid evolution in terms of data rates, but wireline networks are still able to provide the highest data rates. As such, applications designed for wireline networks drive the evolution of the wireless data rates as customers are used to wireline performance and expect the wireless networks to perform on comparable levels.

Challenges such as this are being met through High Speed Packet Access (HSPA) evolutions [HT06] to 3G networks. The standards for Downlink (DL) and UL HSPA evolutions, known as High Speed Downlink Packet Access (HSDPA) and High Speed Uplink Packet Access (HSUPA), were completed in March 2002 and December 2004, followed by commercial deployments in 2005 and 2007 [HT11]. The first phase of the HSPA evolution, also known as HSPA+, was completed in June 2007 and the deployments started during 2009 [HT11]. With the latest evolutions, HSPA can reach theoretical downlink peak data rates on a scale of hundreds of megabits per second [HTT14].

The new possibilities offered by these devices and growing variety of ser-

vices have increased the number of mobile subscribers tremendously. The first billion landmark was passed in 2002, the second billion in 2005, the third billion 2007, the fourth billion by the end of 2008 and the fifth billion in the middle of 2010 [HT11]. Voice communication has become mobile in a massive way and mobile phones are the preferred method of voice communication, with mobile networks covering over 90% of the world's population [HT11]. More than 550 operators have deployed the HSPA network in more than 200 countries by 2014, and all WCDMA networks have been upgraded to support HSPA and many networks also support HSPA+ with 21 Mbps and 42 Mbps [HTT14]. With the continuing evolution for new technologies, the deployment of Fourth Generation (4G) Long Term Evolution (LTE) networks and plans for the Fifth Generation (5G), the way in which people communicate and interact is bound to continue changing.

The studies on various performance enhancements, such as Interference Coordination (IC), Dual-Carrier (DC), Range Extension (RE) and transmit diversity, presented in this thesis, have been conducted in support of the HSUPA standardization work aiming to further improve the HSUPA performance. In the following sections, the research problem, related studies and motivation for this thesis are further elaborated.

1.1 Research Problem

A number of further optimization steps are required in HSPA to support even more users and higher capacity. When considering satisfactory user experience in the cellular network, various factors ranging from optimizing the Radio Resource Management (RRM) functions to UE battery consumption need to be addressed, while at the same time preventing performance loss from the networks point of view. These optimization areas include, for example, the use of additional carriers, minimization of signaling load, optimization of UE power consumption, control of uplink interference and the use of uplink transmit diversity. Regarding RRM functions, this thesis covers the following aspects.

As the traffic data volume increases also the signaling volumes are also increasing in the network. As such, the increased signaling traffic and uplink interference can become the limiting factor in network capacity. This relates especially to modern smartphone applications, which typically create relatively small packet sizes that are transmitted frequently, causing continuous channel allocations and releases. This high signaling also causes more uplink interference because of the control channel overhead. Therefore, uplink interference control solutions are needed in the smartphone dominated networks. The HSUPA time domain interference coordination, studied in this thesis, aims to provide enhancements especially for the power restricted cell edge UEs.

The most straightforward solution for increasing capacity is to add more carriers to the existing sites. This solution is cost efficient as existing sites, antennas, and infrastructure solutions can be reused. As operators may have multi-

ple spectrum bands available, HSUPA dual-carrier operation has the potential to provide benefits when compared to single carrier operations. In theory, the UEs could double their peak data rate with adequate power resources.

The very first 3G devices suffered from high power consumption, high cost and poor quality. Since then, battery power consumption during a voice call has dropped from more than 400 mA to below 100 mA on the latest devices [HTT14]. The major improvement in power consumption shows the importance of radio frequency and baseband technology evolution. Continuous Packet Connectivity (CPC) in the uplink, more specifically Uplink Discontinuous Transmission (UL DTX), is studied for improved UE power saving opportunities. CPC introduces the possibility to eliminate continuous transmission and reception in HSPA networks. Regarding UL DTX, this means that the control channel used, e.g., for power control, is not transmitted continuously, thus minimizing the power consumption and reducing the interference levels in the system. As such, UL DTX introduces periods when the UE can turn off the transmit circuitry for power saving purposes. However, incorrectly configured UL DTX can potentially lead to severe performance loss due to the absence of power control. Additionally, the specifications define that in HSUPA systems, UEs can be configured to use either a 2 or 10 ms Transmission Time Interval (TTI). These two have different properties defining the purpose for which they should be used. The 2 ms TTI provides shorter transmission periods, but it requires higher instantaneous transmission power. Alternatively, the 10 ms TTI requires lower transmission power, but the transmission period is longer. Issues with UL DTX, different TTI lengths and uplink Range Extension (RE) for improving the coverage of UEs using 2 ms TTI are investigated in this thesis. Due to the intolerance to excessive packet loss and delays, Voice over IP (VoIP) is used as a use case for the studies on mixed TTI and RE.

Earlier the size, cost and power resources in the UE have been a limiting factor for using transmit diversity, i.e., deploying additional Transmit (Tx) antennas to the UE. In addition to the diversity gain, the received combined signal power is theoretically doubled with two Tx antennas when compared to single antenna transmission [3GP11a]. Due to technological advancements and continuously increasing performance requirements, uplink transmit diversity has become a more attractive solution. In the meetings of an organization standardization known as the Third Generation Partnership Project (3GPP) possible schemes, assumptions and performance of Open Loop Beamforming (OLBF) and Switched Antenna Transmit Diversity (SATD) were evaluated and discussed. Initially the work focused on Open Loop (OL) schemes, which do not require any newly standardized dynamic feedback signaling between the network and UE, but later on expanded to include Closed Loop Beamforming (CLBF) with feedback mechanisms. These uplink transmit diversity schemes are studied in this thesis for improvements in the UE performance in general.

Taking previously mentioned aspects into account this thesis aims to answer the following questions:

- Does interference coordination provide added value in the HSPA uplink

and if so, in which situations?

- In which situations are UEs able to utilize dual-carrier HSUPA with the limited available power they have and how does dual-carrier performance compare against two single carrier systems?
- Is CPC able to provide battery saving opportunities without compromising the capacity and quality of service and if so, in which situations and how does the use of two TTI lengths affect the cell capacity and achievable UE battery saving opportunities with CPC?
- Is range extension capable of providing the coverage of 10 ms TTI without compromising the capacity and quality of service?
- Is SATD, with algorithms applicable to real networks, able to provide gain over a system without transmit diversity and how does a varying cell load and non-ideal conditions, such as antenna imbalance and antenna correlation, affect the SATD performance?
- How does OLBF and CLBF, with ideal algorithms, perform against a system without transmit diversity and are the said techniques able to provide gain over a system without transmit diversity with an algorithm applicable to real networks?
- How does different cell loading, antenna imbalance, antenna correlation, feedback delays, antenna pre-coding weight update intervals, codebook sizes and feedback mechanisms affect the CLBF performance?

To answer the above mentioned questions, a wide variety of quasi-static system level simulations are performed. The use of this kind of a simulation tool is strongly advocated by the complexity of a purely analytical approach to RRM, and on the other hand the expense and time requirements of real world physical network trials. The used research tools are presented in detail in Chapter 5.

1.2 Related Studies

The purpose of this section is to point out some of the most important studies related to the topics in this thesis. The aim is to provide further understanding on the researched topics and, in combination with Section 1.1, further elaborate how this thesis deepens the previous studies.

1.2.1 Interference Coordination

There are several approaches for interference cancellation and coordination in wireless networks. Prior to this study, interference cancellation has been considered for HSUPA, see, e.g., [SZZ14] and [BGL⁺08], but studies on interference coordination have mainly focused on HSDPA and LTE cellular networks. Regarding HSDPA, for example in [LCSA06] a simple interference mitigation scheme to enhance cell edge user data rate through network coordination is proposed. It

is demonstrated in the paper, by the use of simulations, that the scheme significantly improves cell edge user throughput without lowering the total system capacity and spectral efficiency. Recent HSDPA studies consider more advanced schemes, such as Heterogeneous Networks (HetNet) interference coordination schemes, see, e.g., [ZCWY13].

Interference coordination with different mechanisms is widely studied in LTE, see, e.g., [Nec08], [BPG⁺09], [XJH07] and [Sim07]. Since the LTE frequency band is divided into resource blocks and the same blocks are used in each cell, in one of the approaches some of the blocks are restricted to be scheduled to only UEs near the cell center. Scheduling is restricted according to patterns of blocks and these patterns are arranged according to a certain frequency reuse pattern between the cells. Considering the neighboring cells, this arrangement allows for cell edge UEs to be scheduled into different blocks, thus reducing the inter-cell interference and throughput. As with HSDPA, more recently also the LTE interference coordination studies are also considering more advanced approaches, such as utilizing Self-Organizing Network (SON) solution with focus on interference coordination objectives, see, e.g., [BC13].

In this thesis, the existing HSUPA studies are broadened through investigating the possibilities to apply the basic principles of LTE type interference coordination approach with resource restrictions to HSUPA, where a similar effect is achieved by the means of time-domain coordination. For this kind of coordination to function, the Base Stations (Node-Bs) need to be synchronized for implementing coordinated scheduling of different user groups also in the neighboring cells. As the uplink receive timings need to be synchronized between each Node-B, an advanced timing mechanism needs to be introduced. This could be achieved, for example, by alignment of the downlink timings.

1.2.2 Dual-Carrier

In Releases 5 and 6, HSDPA and HSUPA are defined to utilize a single 5 MHz bandwidth. In Release 8, dual-carrier functionality with 5+5 MHz bandwidth is specified for HSDPA. The results for a performance study regarding the dual-carrier operation for HSDPA are presented in [dAKH⁺09]. Based on the results, with dual-carrier a peak data rate twice the amount of a single carrier can be achieved for a single user. In addition, different gain sources, such as multi-user diversity and frequency selectivity, are identified. In [JBG⁺09] the dual-carrier HSDPA studies are extended further to cover Multi-Carrier (MC) operation. Based on the results, the achievable data rates of a multi-carrier system increases proportionally to the number of carriers, providing that the system is not fully saturated.

This thesis deepens the existing studies by evaluating the performance of dual-carrier also in HSUPA. At the time, the conducted studies were used to support the 3GPP standardization work on improving the HSUPA data rates to meet end user expectations of future mobile broadband services. The work in 3GPP led to standardizing dual-carrier for HSUPA in Release 9, see, e.g., [HT11], [HTT14].

1.2.3 Range Extension

As the computational power and performance of mobile devices continue to increase, controlling energy consumption and extending battery life becomes more and more critical. As such, possible power savings are almost as important as the radio network performance when small hand-held devices are in question. However, the capacity and coverage of the network should not be compromised in the name of power savings. The network coverage is typically limited by the uplink and the HSUPA capacity depends on the number of parameters, including such settings as TTI length, number of retransmissions and relative channel power allocation.

Power savings at the UE side in the uplink can be achieved, e.g., as a by-product when applying Release 7 UL DTX. The idea of UL DTX is to stop transmitting the control channels when the UE is in the idle mode, thus decreasing the amount of interference and consuming less power. However, too aggressive use of UL DTX has the potential to compromise the power control and lead to reduced performance. Regarding 3G systems, the impact of UL DTX has been studied extensively, see, e.g., [BJ06], [FCMR07], [FCRaR07] and [CCRa⁺08] and been shown to provide noticeable gains in terms of capacity and meeting the delay requirements. Additionally, optimizing the link efficiency for UL DTX is investigated in, e.g., [DWKT07]. VoIP performance in general with Release 7 enhancements, including aspects relevant to this thesis, such as UL DTX, is investigated in [HKM⁺06].

Regarding UL DTX performance from a link performance point of view, studied in [BJ06], it is concluded that with UL DTX the power control stability can be maintained and additional advantage in terms of performance can be achieved. Articles [FCMR07], [FCRaR07] and [CCRa⁺08] deepen the analysis in terms of system simulations. In [FCMR07] it is shown that substantial gains can be seen in terms of VoIP performance and the highest absolute performance can be achieved when 2 ms TTI and gating is used. In [FCRaR07] static and dynamically activated Medium Access Control (MAC) layer bundling of two VoIP packets in a single frame is proposed and compared against the single packet per frame transmission. Studies are conducted with 10 ms TTI and the results indicate noticeable gains of bundling when UL DTX is used. It is also concluded in [DWKT07] that the use of UL DTX can be beneficial for both 2 and 10 ms TTI. In [HKM⁺06] it is concluded that the VoIP over HSUPA spectral efficiency with Release 7 enhancements is expected to be twice the efficiency of the Release 99 solution.

This thesis deepens the knowledge on HSUPA performance with different TTI lengths when VoIP is considered as a use case. This thesis will increase the knowledge, e.g., on the impact of UL DTX power saving opportunities not only with different TTI lengths, but also when a mix of both TTI lengths is in use in the network. This thesis also presents a Range Extension (RE) scheme for avoiding potential coverage problems when only the 2 ms TTI length is in use. Additionally, existing studies concentrate mainly on the system wide performance,

whereas this thesis addresses the performance also from the user device perspective by the means of Tx antenna activity measurements. Thus, this thesis provides further knowledge on the conditions where users are able to better maintain a good quality of service and the network will have a better radio resource utilization.

1.2.4 Transmit Diversity

The demand for increasing spectral efficiency in mobile communications systems motivates the search for more powerful techniques. With the aid of various diversity techniques, transmissions with better signal quality can be used for improving the systems performance in terms of the achievable performance, capacity and the Quality of Service (QoS) measures. Multi-antenna techniques can be seen as a joint name for a set of techniques with a common theme that they rely on the use of multiple antennas at the receiver and/or the transmitter. Multiple antennas can be used to provide additional diversity against fading on the radio channel, 'shape' the overall antenna beam in a certain way or to create what can be seen as multiple parallel communication 'channels' over the radio interface [DPSB08]. Regarding this thesis, multiple transmitter antennas are used with both the beamforming and the Switched Antenna Transmit Diversity (SATD) studies.

SATD in HSUPA is not studied extensively, but, e.g., in [ZCLY11] SATD is part of an evaluation of various HSUPA transmit diversity schemes. The study concludes, that the investigated Closed Loop (CL) SATD is able to provide gain over the baseline without transmit diversity. Additionally, based on the study, the performance of CL is better than that of Open Loop (OL) due to more accurate feedback information.

Open Loop Beamforming (OLBF) schemes for HSUPA are studied, e.g., in [SWFK12] and [WAH⁺10]. A practical OLBF algorithm using the feedback commands of the existing fast power control loop is investigated in [SWFK12]. The results show, that the transmit power at the UE can be reduced noticeably when compared to the reference case of only one Tx antenna, thus improving the UE's battery life. Article [WAH⁺10] includes results on field tests showing gain for the studied scheme.

Closed Loop Beamforming (CLBF) in HSUPA is investigated in, e.g., [ZCLY11], [MTS⁺11], [ZJ12] and [JHBS12]. Based on the results in [ZCLY11], the performance of CLBF is better than the baseline case without transmit diversity and that of CL SATD. According to [MTS⁺11], the application of CLBF can improve the average system throughput noticeably, owing to a lower UE transmit power and reduced inter-cell interference. The results in [ZJ12] show, that CLBF can provide clear gain in saving UE transmission power consumption over the baseline without Multiple Input Multiple Output (MIMO) transmission while little gain in improving throughput. Additionally, in [JHBS12] various CLBF schemes are investigated, [MTS⁺11] considers also HSUPA MIMO scheme performance and beamforming benefits for HSUPA is investigated in [GWY07].

This thesis complements the existing studies by investigating SATD, OLBf and CLBF system level performance with a wide variety of algorithms in numerous different parameter options, e.g., codebook sizes and signaling delays, with different feedback options and in non-ideal conditions, such as with antenna correlation and imbalance. All of the studies are made in accordance with 3GPP parameterization and with the same simulation tool, which enables an easier comparison of different studied schemes. As such, the scope of the HSUPA transmit diversity studies presented in this thesis is exceptionally comprehensive. The work in 3GPP led to standardizing uplink CLBF in Release 11, see, e.g., [HTT14].

1.3 The Third Generation Partnership Project

The research presented in this thesis is used in support of standardization work in an organization known as the Third Generation Partnership Project (3GPP). As such, a brief introduction to 3GPP is in order.

WCDMA had been chosen as 3G technology in early 1998 by various standardization forums, like European Telecommunications Standards Institute (ETSI). During 1998 parallel work proceeded in the forums, but it was resource consuming for companies with a global presence and there was a possibility to have different specifications depending on the discussions within each forum. As such, the 3GPP forum [3GP14b] was created at the end of 1998 by the USA, Europe, South Korea and Japan with the intention to introduce a new single global standard for mobile communication based on the WCDMA technology. Later on other countries, such as China, joined the 3GPP. Different companies, like Nokia, are members through their respective standardization organization. [HT07]

The initial target was to produce Technical Specifications (TSs) and Technical Requirements (TRs) for a 3G mobile system, but later on the maintenance and development of the GSM including evolved radio access technologies, e.g., General Packet Radio Service (GPRS) and Enhanced Data rates for GSM Evolution (EDGE) were also included. At the moment the 4G technologies, such as LTE, are also being standardized in 3GPP [HT11]. Figure 1 shows a timeline which indicates the Releases so far, including future Releases expected to take place before 2017.

3GPP work is divided into Technical Specification Group (TSG):

- TSG Radio Access Network (RAN), with the main focus on the radio interface, internal interfaces between Node-B and Radio Network Controller (RNC), and interface from RNC to Core Network (CN).
- TSG Core and Terminals (CT), with the main focuses including the core network, signaling between terminals and core network.
- TSG System Architecture (SA), with the main focus on the services and overall system architecture.

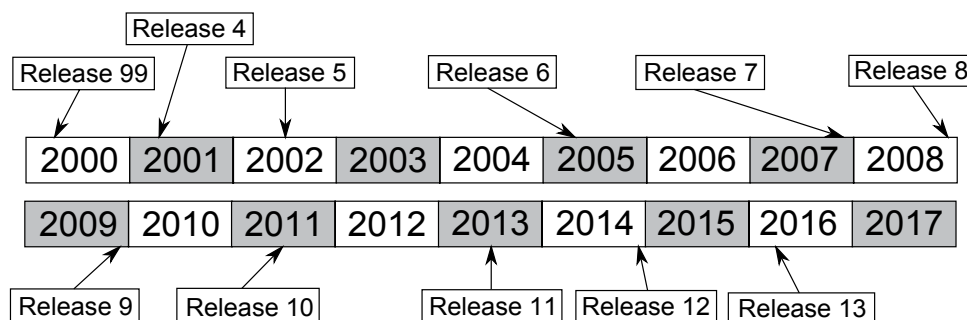


FIGURE 1 3GPP release timeline

- TSG GSM/EDGE Radio Access Network (GERAN), with the main focus on the same as those of TSG RAN for the GSM/GPRS/EDGE based radio interface.

Each TSG is divided into several Working Groups (WGs). For example, TSG RAN has the following WGs:

- TSG RAN WG1 - Physical channel structures and mapping, physical layer multiplexing, channel coding and error detection, spreading, modulation and other physical layer procedures, measurements and their provision to the upper layers
- TSG RAN WG2 - Radio interface architecture and protocols between UE and RAN, services offered by the physical layer to upper layers, cell selection and re-selection procedures, UE capabilities for UE - RAN interface, definition of RRM strategies to be supported by RAN
- TSG RAN WG3 - Overall UMTS Terrestrial Radio Access Network (UTRAN) and Evolved UMTS Terrestrial Radio Access Network (E-UTRAN) architecture, synchronization in UTRAN and E-UTRAN, interface protocols for RNC - RNC (Iur), Node-B - RNC (Iub) and RNC - CN (Iu) communication
- TSG RAN WG4 - Requirements for radio link, RRM performance and accuracy of measurements, radio system scenario analysis and simulation
- TSG RAN WG5 - Development of UE conformance test specifications

The research presented in this thesis is mostly related to the RAN WG1 aspects.

1.4 Main Contribution

During the work on the subject of the dissertation, the author has produced and co-authored several publications. Article [PI] evaluates the performance of highly loaded HSUPA network with and without network wide static Interference Coordination (IC). IC alternates the priorities for user transmission periods

throughout the network to achieve reduced interference levels and higher performance. In the published article, a large variety of combinations including, e.g., different schedulers, cell center/edge user definitions (user splits) and interference targets are investigated. The performance is analyzed using a quasi-static system level simulator. The author of this thesis is the first author of the article and has the main responsibility for the IC code implementation, simulations and result analysis.

Article [PII] analyzes how Dual-Carrier (DC) capability can enhance HSUPA performance in comparison to using only single carrier. DC operation gives the UE the possibility to transmit simultaneously using two 5 MHz bands, theoretically doubling the peak data rates and user throughput. The analysis is conducted with a quasi-static system level simulation tool. In addition to implementation support, the author is a contributor for the analysis and article writing. The study in 3GPP led to standardizing HSUPA dual-carrier for Release 9, see, e.g., [HT11].

Article [PIII] evaluates the benefit of exploiting a mixture of 2 or 10 ms Transmission Time Intervals (TTIs) within a cell instead of only one. The study is quantified by means of studying the achievable coverage of Voice over IP (VoIP) and possible battery saving benefits. Article [PIV] expands on the mixed TTI study by proposing a 2 ms Range Extension (RE) scheme for HSUPA networks to avoid potential coverage problems and usage of multiple TTI lengths. With range extension, UEs in poor radio conditions are configured to send bundles of 2 ms TTI transmissions without Hybrid Automatic Repeat-reQuest (HARQ) feedback to improve their coverage. The results are acquired by using a quasi-static system level simulation tool. The author of this thesis is the first author in both of the articles and has the main responsibility for the code implementation, simulations and result analysis regarding both the mixed TTI and the RE scheme.

Articles [PVI], [PVI] and [PVII] are devoted to the Switched Antenna Transmit Diversity (SATD) scheme using switching between two Tx antennas without additional feedback information. In the published articles, the diversity scheme performance is investigated against the baseline performance without transmit diversity in various conditions. These include, e.g., varying load conditions, antenna imbalance, correlation and the existence of multiple different SATD algorithms in the network simultaneously. The performance is analyzed using a quasi-static system level simulator. Regarding the SATD studies, the author of this thesis is a contributor for the result analysis and article writing.

Articles [PVIII], [PIX], [PX], [PXI], [PXII] and [PXIII] are devoted to Beamforming Transmit Diversity (BFTD). With beamforming, multiple Tx antennas are utilized and the UE's transmitter applies a weight vector to the Tx antennas in order to amplify the received signal. The investigated beamforming techniques are benchmarked in various conditions against the baseline system performance without transmit diversity. The author of this thesis is the first author of the articles [PVIII], [PXII] and [PXIII], and has the main responsibility for the beamforming code implementation, simulations and result analysis. The studies in 3GPP led to standardizing HSUPA transmit diversity for Release 11, see, e.g., [HTT14].

1.5 Outline of the Dissertation

The rest of the dissertation is organized as follows.

Chapter 2 presents the basics on Universal Mobile Telecommunications System (UMTS), a 3G mobile cellular system for networks based on the GSM standard, and WCDMA, which is a commonly adopted radio interface in UMTS. The purpose of the chapter is to introduce the most important UMTS and WCDMA aspects related to this thesis in order to give the reader adequate knowledge to read and review the included studies.

Chapter 3 describes the most essential features and properties of HSPA up-link evolution, called HSUPA, in relation to this thesis. The key features, such as the HSUPA channels, multiplexing and Hybrid Automatic Repeat-reQuest (HARQ), are presented.

Chapter 4 is devoted to the research conducted in this thesis. The chapter introduces multiple separate techniques for, e.g., controlling interference, improving the system or user throughput, reducing delays or extending cell range.

Chapter 5 presents the research tool used to perform studies regarding this thesis. The used tool is a comprehensive system level radio network simulator designed, e.g., for studying RRM algorithms to obtain capacity and coverage estimates, to support standardization work and network planning by optimizing the radio network parameters.

Chapter 6 contains the results obtained with the system level simulator introduced in Chapter 5. The scenarios and assumptions used in the studies are presented first, followed by the simulation result analysis. Finally, **Chapter 7** concludes the thesis.

2 UNIVERSAL MOBILE TELECOMMUNICATIONS SYSTEM

Universal Mobile Telecommunications System (UMTS) is a 3G mobile cellular system for networks based on the GSM standard. UMTS is developed and maintained by the 3GPP and WCDMA is the most commonly adopted radio interface in UMTS [HT07]. Both UMTS and WCDMA are widely described in [HT07] and in 3GPP specifications [3GP14b]. The purpose of this chapter is to introduce the most important UMTS and WCDMA aspects related to this thesis in order to give the reader adequate knowledge to read and review the included studies.

2.1 UMTS Radio Access Network Architecture

The data-handling capabilities of second-generation systems are limited, and as such one of the major aims of UMTS was to have better capabilities to transfer data traffic. UMTS itself is a complete system architecture that was designed for flexible delivery of any type of services. New radio access technologies were required and a new logical radio access network was needed. However, the UMTS architecture contains many comparable elements to 2G GSM/GPRS networks, which, e.g., reduces the cost of upgrading and enables relatively easy interoperability between networks; the handsets are backwards compatible and there is signaling to support, e.g., inter-system handovers between UMTS and GSM, or UMTS and LTE [HT07] [HT11].

UMTS network can be divided into three logical domains:

- User Equipment (UE) consists of Mobile Equipment (ME) and UMTS Subscriber Identity Module (USIM) smartcard. UE is not necessary a mobile phone but can also be any data terminal with no voice capability
- UMTS Terrestrial Radio Access Network (UTRAN) which handles all radio-related functionality

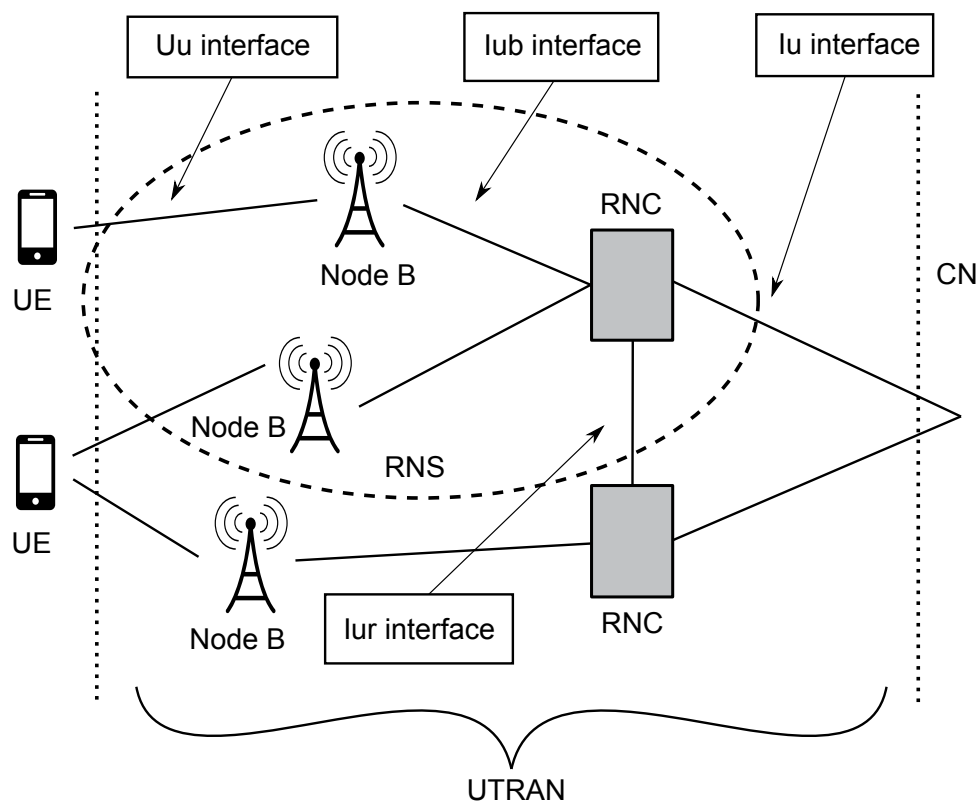


FIGURE 2 UMTS architecture

- Core Network (CN) which is responsible for transport functions, including switching and routing calls and data as well as tracking the users

The UTRAN architecture, illustrated in Figure 2, consists of elements such as RNC and Node-B [HT07]. Compared to the 2G systems, RNC corresponds roughly to the GSM Base Station Controller (BSC). Node-B, owned by RNC, corresponds roughly to the Base Station (BS) in GSM systems. RNC controls the operation of multiple Node-Bs, managing resources such as allocating capacity for data transmissions and providing signaling for, e.g., call set-up and handovers. Node-B can operate a group of antennas and performs the air interface processes, such as channel coding, rate adaptation, spreading, synchronization, power control, and is responsible for RRM.

UTRAN can contain multiple RNCs which are responsible for controlling the radio resources and Node-Bs within their domain. RNCs are connected to each other via Iur interface. Node-B is responsible for handling the data flow between Uu, i.e., between UE and Node-B and Iub, i.e., between Node-B and RNC interfaces. Finally, UTRAN is connected to CN via Iu interface. CN is responsible for routing the connections between external networks and UMTS.

In this thesis the network element terminology, such as Node-B and Base

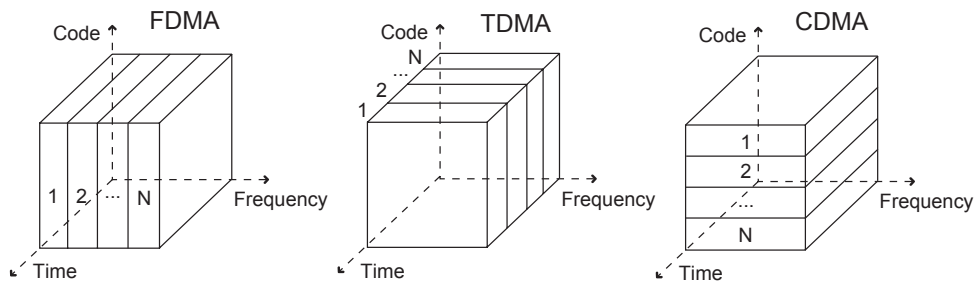


FIGURE 3 FDMA, TDMA and CDMA principles

Station (BS), will be used solely to describe UMTS network elements unless separately otherwise specified.

2.2 Brief Introduction to WCDMA

Wideband Code Division Multiple Access (WCDMA) is a wideband Direct-Sequence Code Division Multiple Access (DS-SS-CDMA) system, i.e. user information bits are spread over a wide bandwidth by multiplying the user data with quasi-random bits, known as chips, derived from Code Division Multiple Access (CDMA) spreading codes [HT07]. In contrast to Time Division Multiple Access (TDMA), where different timeslots are allocated for different users, or to Frequency Division Multiple Access (FDMA), where different users have different frequencies, in CDMA the users share the same frequency and time plane and different users are identified from each other by using codes, as illustrated in Figure 3.

The WCDMA chip rate of 3.84 Mcps results in a carrier bandwidth of approximately 5 MHz. In addition to supporting higher user data rates, the wide carrier bandwidth of WCDMA also has certain performance benefits, such as increased multipath diversity, introduced in Section 2.3. WCDMA supports highly variable user data rates and the deployment of multiple carriers to increase capacity. [HT07]

Additionally, WCDMA supports two basic modes of operation: Frequency Division Duplex (FDD) and Time Division Duplex (TDD). In FDD mode, separate 5 MHz carrier frequencies are used for the uplink and downlink respectively, whereas in TDD only one 5 MHz is shared in time between the uplink and downlink. [HT07]

The codes are applied in WCDMA as follows [HT07]: In uplink the channelization codes are used to separate the physical data and control channels, and the scrambling codes are used to separate the UEs. In downlink the channelization codes are used to separate connections to different users within one cell, and scrambling codes are used to separate the Node-B sectors. The following subsection presents the basic principles of the spreading operation.

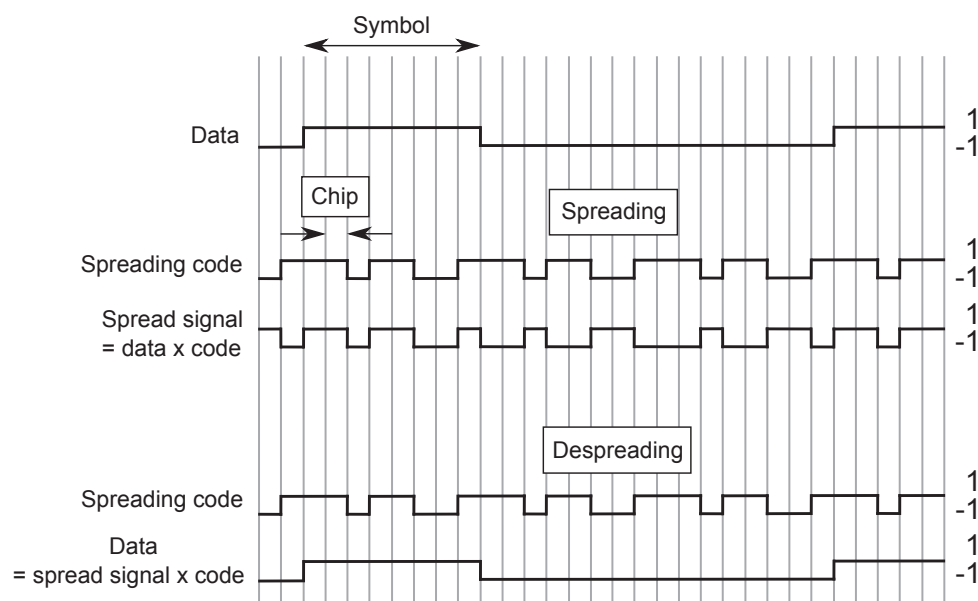


FIGURE 4 Spreading/despreading operation [HT07]

2.2.1 Basics of Spreading and Despreading

The information signal is spread in WCDMA over the whole frequency band both in the uplink and downlink. With spreading the transmissions are more robust against interference and jamming, and additionally more secure. As described in [HT07], the spreading operation is done by multiplying each user data bit with a sequence of code bits, i.e., the spreading code. The resulting encoded sequences of bits are called chips and the length of the spreading codes determine the bit rate; a shorter code results in a higher bit rate, but the chip requires a better Signal to Interference and Noise Ratio (SINR) to be correctly received.

In the spreading and despreading operation, illustrated in Figure 4, at the transmitter side the user data is multiplied chip by chip with the spreading code. The data is then transmitted and at the receiver side the signal is despread by multiplying the unscrambled data with the same spreading code.

This despread signal is then integrated, i.e., summed together over the length of spreading code. If the values of the integrated signal vary close to the used spreading factor and its negated value, the receiver identifies that the signal is meant for it. Alternatively, if the integrated values vary around zero, the transmission is from an interfering source.

It is worth noting that in CDMA based systems the power of the own signal increases on average by the used spreading factor relative to the interference present. This effect is known as Processing Gain (PG) and is a fundamental aspect of all CDMA systems. Processing gain gives CDMA based systems robustness to cope with the self-interference resulting from reusing the carrier frequencies in

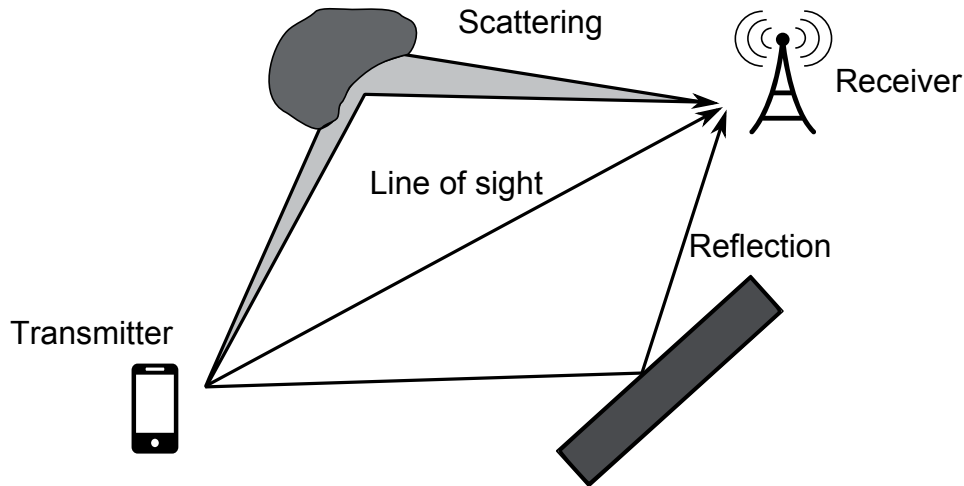


FIGURE 5 Multipath propagation

geographically close proximity. However, the processing gain comes at the price of an increased transmission bandwidth. [HT07]

2.3 Multipath Radio Channels

The transmitted radio signal propagation is characterized by multiple reflections, diffractions and attenuation of the signal energy, as illustrated in Figure 5. As the name suggests, multipath is the propagation phenomenon which results in copies of the original radio signals, referred as multipath components, reaching the receiver by multiple paths. In spread spectrum systems a receiver can separate different multipath components if the delay between the components is at least one chip in duration. These components have variations in, e.g., amplitude and phase, but with an assumption that the multipath components do not fully correlate, a receiver capable of taking advantage of the multipath components can enhance the quality of a received signal and mitigate, e.g., the effects of fast fading. This gain from multipath components is referred to as multipath diversity gain. This diversity can be captured with a Rake receiver or with some other linear detector or channel equalizer.

More details about multipath radio channels can be found in [HT07], [BPS98] and [HTW03]. A mathematical modeling of a multipath radio channel can be seen in [Nih08]. Receivers, e.g., above mentioned Rake receiver, are introduced

in Section 2.6. The following subsections contain a brief introduction into the first forms of signal attenuation, i.e., distance attenuation, slow and fast fading.

2.3.1 Attenuation

Attenuation limits the range of radio signals and is affected by the materials a signal must travel through. Attenuation can be categorized into three major components: distance attenuation, shadowing, i.e., slow fading and fast fading. These components are briefly described in the following subsections.

2.3.1.1 Distance Attenuation

Distance attenuation, i.e., path loss is the reduction in a signals energy as it propagates over the air from the transmitter to the receiver. Exact calculation of path loss is typically possible only for simpler cases, such as free space loss, i.e., propagation in a vacuum. For practical applications the radio wave propagation models are typically based on statistically measured and averaged losses along typical classes of radio links.

The Okumura-Hata model is widely used for coverage calculation in macro-cell network planning. The model is based on the empirical measurements made by Y. Okumura in Tokyo at frequencies up to 1920 MHz [OOKF68]. A mathematical model, adapted by M. Hata, was created based on these measurements [Hat80]. Initially the Okumura-Hata model was applicable only for lower bandwidths, but it was later extended with COST 231 model [Dam99], which made it applicable for bandwidths in range of $1500 \leq f(\text{MHz}) \leq 2000$. This combined model is called COST-Hata model and it is widely applied to UMTS frequencies exceeding 2000 MHz, even though originally the models frequencies were restricted to below that. More information about various propagation models can be found in [LWN05] and [Sey05].

2.3.1.2 Slow and Fast Fading

The terms slow and fast fading refer to the rate at which the magnitude and phase change imposed by the channel on the signal changes. The coherence time is a measure of the minimum time required for the magnitude change or phase change of the channel to become uncorrelated from its previous value.

Slow fading arises when the coherence time of the channel is large relative to the delay constraint of the channel. In this regime, the amplitude and phase change imposed by the channel can be considered roughly constant over the period of use. Slow fading can be caused by events such as shadowing, where obstacles such as a hill or large building can obscure the main signal path between the UE and Node-B. The amount of slow fading, and signal attenuation in general, depends greatly on the environment. A flat rural area with only a few trees has noticeably less obstacles in the signal's path compared to an urban area with tall buildings. Slow fading varies as the UE moves and with short distances

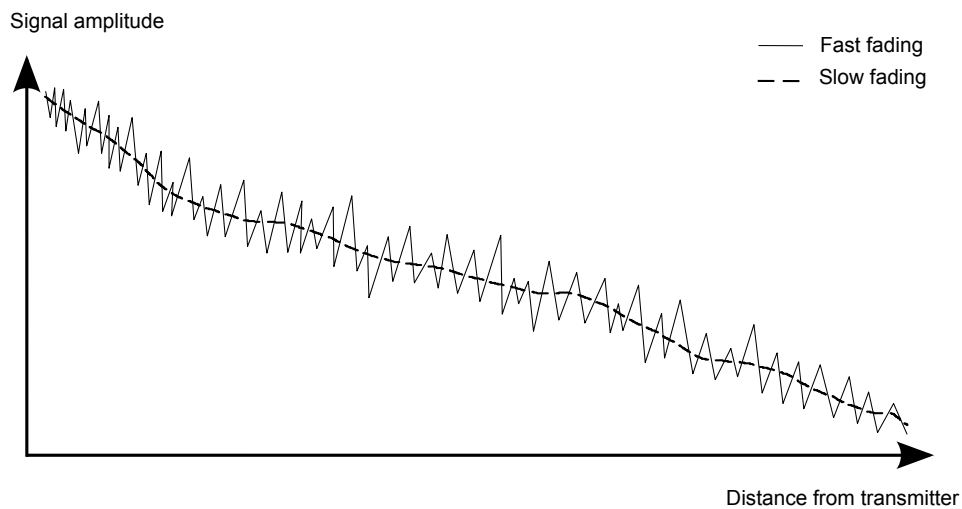


FIGURE 6 Slow and fast fading of propagated signal in respect to receiver-transmitter distance

the slow fading values correlate. In simulators the received power change caused by shadowing is often modeled using log-normal distribution with a correlation distance [3GP98] [Sey05].

As mentioned before, when the signal is, for example, reflected from a surface of a building it can create a multipath component of the transmitted signal. When these multipath components arrive at different times to the receiver, the components can cause either a constructive addition to the arriving plane waves if their amplitudes and phases match, or a destructive addition if their phases do not match. The resulting constructive addition is a signal with larger energy than any of its components. Alternatively, the resulting destructive addition is often a signal with very small or zero energy, and the channel is said to be in fade. The speed of amplitude variation of received signal is influenced by the speed of the receiver and transmitter, and therefore the variations can be very intensive. This kind of fading is referred to as fast fading [Sey05]. Fast fading occurs when the coherence time of the channel is small relative to the delay constraint of the channel. As a distinction to slow fading, this can be generally understood as a situation where the channel does not remain constant during one symbol duration. In this regime, the amplitude and phase change imposed by the channel varies considerably over the period of use. Both slow and fast fading of a propagated signal in respect to receiver-transmitter distance is illustrated in Figure 6. [Sey05]

2.4 Multi-Antenna Techniques

Multi-antenna techniques can be seen as a joint name for a set of techniques with a common theme that rely on the use of multiple antennas at the receiver and/or

the transmitter, in combination with more or less advanced signal processing. Multiple antennas can be used to provide additional diversity against fading on the radio channel, 'shape' the overall antenna beam in a certain way, e.g., to maximize the overall antenna gain in the direction of the target receiver/transmitter or to create what can be seen as multiple parallel communication 'channels' over the radio interface. [DPSB08]

Regarding the studies in this thesis, multiple receiver antennas are used with all of the researched enhancements. Multiple transmitter antennas are used with both the beamforming and the switched antenna transmit diversity studies. Additionally, as the name suggests, in the beamforming studies the antenna beam is also shaped in order to maximize the signal strength. Only the usage of multiple parallel communication channels, often referred to as spatial multiplexing or MIMO antenna processing, is not in the scope of this thesis.

2.4.1 Receive Diversity

A receiver with multiple Receive (Rx) antennas for collecting the multipath components uses receive diversity [HTW03]. This is perhaps the most straightforward and historically the most commonly used multi-antenna configuration. The less the separate multipath components resemble each other, the more usable they are when forming the combined signal. Hence, increasing the number of receiving antennas increases the number of separate signal paths and larger number of usable components can be received. However, adequate antenna spacing is required for the new signal paths to be independent. If this is achieved, the additional received multipath components can improve the quality of the received signal. [HTW03]

The receivers and related signal processing is introduced in Section 2.6. The impact of receive diversity is studied extensively, e.g., in [Nih08]. More information about receive diversity can be found in [HTW03] and [DPSB08].

2.4.2 Transmit Diversity

In contrast to the receive diversity receiver with multiple antennas, in transmit diversity the transmitter has multiple Transmit (Tx) antennas for transmitting the signal. As with the receive diversity, adequate antenna spacing is required in order to achieve independent fading for the antennas. Without any knowledge about the channel conditions of the different Tx antennas, multiple Tx antennas provide only diversity. However, if the information about, e.g., the relative channel phases is available at the transmitter side, the overall antenna beam can be shaped in the direction of a target receiver. This is known as beamforming. [HTW03]

As defined in [HTW03], transmit diversity methods fall into two classes: Open Loop (OL) and Closed Loop (CL). Open Loop Transmit Diversity (OLTD) techniques apply various receiver-independent algorithms at the transmitter side to combat the fading channel and do not require additional feedback from the

receiver. Closed Loop Transmit Diversity (CLTD) techniques are designed to improve system performance over the open loop ones, but require feedback from the receiver to function. More information about transmit diversity can be found in [HTW03] and [DPSB08].

Regarding 3G systems, a downlink OL and two CL transmit diversity modes with two Tx antennas were included as early as in 3GPP Release 4 [DPSB08]. The space-time block code, introduced in [3GP02], was adopted as an open loop transmit diversity method for two Tx antennas.

Regarding the CL, two different feedback modes with slightly different trade-offs in effective constellation resolution and signaling robustness were adopted. In Mode 1 the length of the feedback word is one bit, and the Node-B interpolates between two consecutive feedback words making the transmit weight to follow a time-varying Quadrature Phase Shift Keying (QPSK) constellation. In Mode 2 the feedback word consists of four bits where three bits are assigned to phase and one bit to gain. Thus, Mode 1 maintains equal power transmission from both antennas while with Mode 2 the antennas transmit with different power. Mode 2 was later removed from Release 5 onwards because it was never implemented in the networks [HTT14].

2.5 Macro Diversity

Instead of utilizing only one source transmitter, the receiver can also collect the multipath components from different cells or sectors, and combine the signals in a predefined manner. This is referred to as macro diversity combining. The sectors used for combining are chosen according to the UE's measurements and form a Combining Set (CS). Two different methods for macro diversity combining were introduced in 3GPP Release 6 [3GP07a].

In the first method, a receiver with selective combining receives and simultaneously decodes the same packets from different sectors which are in its CS. After the reception and decoding, the received packets are processed at the Radio Link Control (RLC) layer where a Cyclic Redundancy Check (CRC) is performed. Based on the CRC, the first correctly received packet is selected. The packet is lost if all copies of the packet fail the CRC.

In the second method, a receiver using soft combining receives and stores all the packets from different CS sectors. These packets are then aligned in time and combined soft values are formed for them. After combining, the receiver decodes the combined packet and checks whether the packet was received correctly or not.

2.6 Receivers

Different types of receivers have been developed during the 3G evolution. These receivers aim, e.g., to decrease the impact of multipath propagation or mitigate the interference from other cells. Not all of these receivers are used in this study as some of them are too old and are mainly to be taken into account in the simulation as legacy user equipment. For the purposes of this thesis, Rake and Linear Minimum Mean Squared Error (LMMSE) diversity receivers are considered.

2.6.1 Mathematical Signal Model

For the receivers it is necessary to describe the signal model in more detail. This is especially important for the beamforming transmit diversity research presented in this thesis.

A radio channel can be fully characterized by its time-variant impulse response, $\mathbf{h}(t)$. In a mobile radio channel, the impulse response consists of several time-delayed components. This kind of channel is referred to as a multipath channel, introduced in Section 2.3. As defined in [Nih08], if it is assumed there exists N_{Rx} Rx-antennas, the received chip sequence equals to:

$$\mathbf{y}(t) = \mathbf{H}^T \mathbf{x}(t) + \mathbf{n}(t), \quad (1)$$

where \mathbf{H} is the channel matrix between the transmitter and receiver, $\mathbf{n}(t)$ is the noise vector consisting of both the neighboring sector interference and the thermal noise over the bandwidth. The transmitted chip stream $\mathbf{x}(t)$ is

$$\mathbf{x}(t) = [x(t + F + L - D) \dots x(t) \dots x(t - D)]^T, \quad (2)$$

In (2) L is the delay spread of the channel normalized to the chip interval, D is the delay parameter satisfying $(0 \leq D \leq F)$ and F is the length of the linear filter \mathbf{w} which the receiver uses in filtering \mathbf{y} in order to obtain the estimate $\tilde{\mathbf{x}}$ for the transmitted chip sequence \mathbf{x} :

$$\tilde{\mathbf{x}}(t) = \mathbf{w}^T \mathbf{y}(t). \quad (3)$$

Multiplication of the channel coefficient matrix \mathbf{H}^T in (1) models the convolution with the impulse response of the channel. \mathbf{H} is the $(F + L) \times (F \cdot N_{Rx})$ matrix given by the following equation:

$$\mathbf{H} = \begin{bmatrix} \mathbf{h} & 0 & 0 & \dots & 0 \\ 0 & \mathbf{h} & 0 & \dots & 0 \\ 0 & 0 & \mathbf{h} & \dots & 0 \\ \vdots & \vdots & \vdots & \ddots & \vdots \\ 0 & 0 & 0 & \dots & \mathbf{h} \end{bmatrix}^T, \quad (4)$$

where \mathbf{h} is the $N_{Rx} \cdot (L + 1)$ channel impulse response matrix defined by

$$\mathbf{h} = \begin{bmatrix} \mathbf{h}_1[0] & \mathbf{h}_1[1] & \dots & \mathbf{h}_1[L] \\ \mathbf{h}_2[0] & \mathbf{h}_2[1] & \dots & \mathbf{h}_2[L] \\ \vdots & \vdots & \ddots & \vdots \\ \mathbf{h}_{N_{Rx}}[0] & \mathbf{h}_{N_{Rx}}[1] & \dots & \mathbf{h}_{N_{Rx}}[L] \end{bmatrix}, \quad (5)$$

where $\mathbf{h}_i(l)$ is the channel impulse of i^{th} Rx-antenna at the delay l .

2.6.2 Rake Receiver

The Rake receiver is a radio receiver designed to counter the effects of multipath fading by using several 'sub-receivers' called fingers. Each of the fingers receives individual multipath components and each of the components arriving at the receiver more than a chip length apart can be distinguished from each other by the Rake receiver. Each component is then decoded independently and combined in order to make the most use of the different transmission characteristics of each transmission path, and thus improve the reliability of the information. [HT07]

The combining method used in the Rake receiver is Maximum Ratio Combining (MRC). The principle of MRC is to combine all the multipath components in a co-phased and weighted manner in order to have the highest achievable Signal to Interference and Noise Ratio (SINR) at the receiver at all times. As illustrated in Figure 7, the individual multipath components are received with the fingers of the Rake receiver and then modified with a channel estimate. Each channel estimate is acquired individually for each finger from known pilot channel measurements. Finally, the multipath components are combined by summing them together. As such, the phases of the Rake reception algorithm can be described briefly as follows [HT07]:

- Received multipath components, often referred as taps, are identified from the signal
- Correlation receivers, i.e., Rake fingers are allocated for each multipath component
- Pilot symbol is used to form a channel estimation, which is used to track the phase shift induced by the channel for each of the fingers
- The phase shifts are reversed
- The fingers are combined coherently

MRC is an appropriate antenna-combining strategy when the received signal is mainly impaired by noise [DPSB08]. However, in many cases of mobile communication the received signal is mainly impaired by interference from other transmitters within the system, rather than by noise. In situations with only a single dominating interferer, performance can be improved if the antenna weights are selected so that the interferer is suppressed. More information about the Rake receiver and MRC can be seen in [DPSB08], [HT07], [LWN05] and [PS07]. As defined in [Nih08], Rake receiver can be modeled by linear filtering as follows:

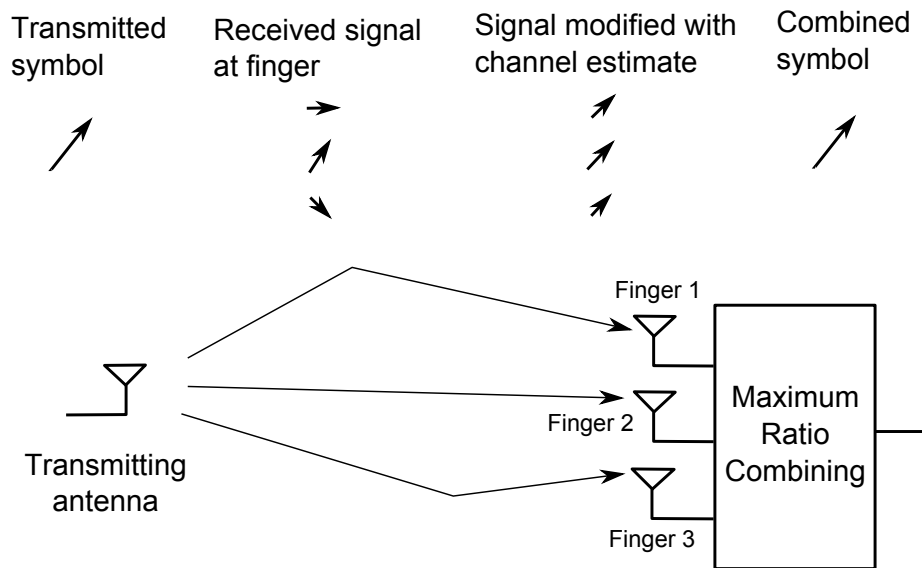


FIGURE 7 Maximum ratio combining with the Rake receiver

$$\mathbf{w}_{RAKE} = \mathbf{H}^H \delta_D \quad (6)$$

where H is the channel impulse response matrix and

$$\delta_D = [0 \ \dots \ 0 \ 1 \ 0 \ \dots \ 0]^T \quad (7)$$

represents the delay of the equalizer.

2.6.3 Intra- and Inter-cell Interference

WCDMA uses Orthogonal Variable Spreading Factor (OVSF) codes to spread user data in both uplink and downlink [3GP12a]. Orthogonal signals are fully separated and can be received without any interference from each other. However, a delay shift between the OVSF codes can increase the cross-correlation considerably. This means that two transmissions transmitted at different times, but received at the same time have non-orthogonal spreading codes, and interfere with each other. This type of interference emanating from the multipath propagation of the serving cell signal is called intra-cell interference, or so-called Multiple Access Interference (MAI), presented in Figure 8.

The Rake receiver can exploit the multipath diversity by finding and combining the multipath components of the same transmission arriving at the receiver in the span of multiple chip-times, but the delayed and overlapping components cause interference to each other. The spreading code problem with compromised orthogonality occurs only in frequency-selective channels, where several multipath components are received more than a chip-time apart. In flat-fading channel only one multipath component arrives at the receiver, i.e., the

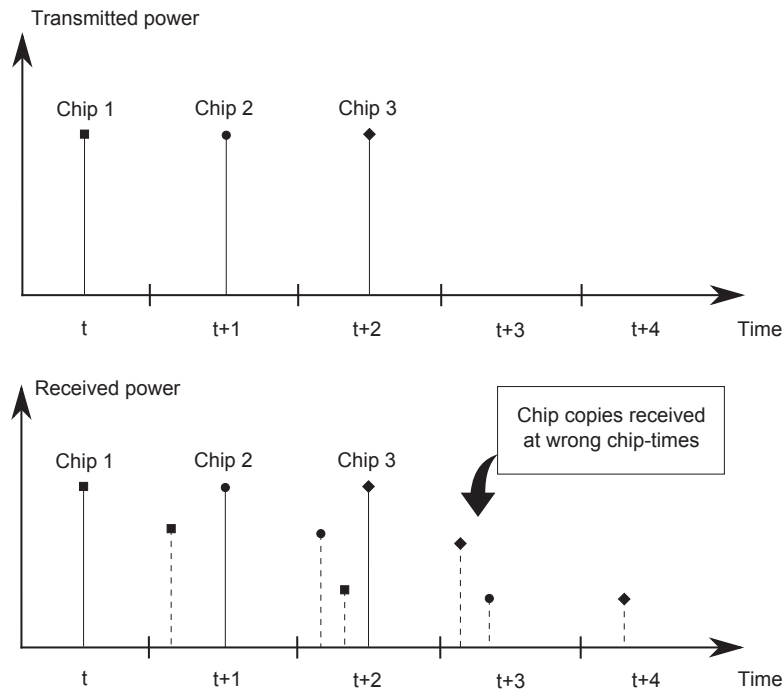


FIGURE 8 Multiple access interference

sent signal is received only once, thus the signals remain orthogonal.

In the border regions between two or more cells, inter-cell interference is in a more dominant role. The scrambling codes used to separate different base stations are not orthogonal, thus inter-cell interference is present regardless of the delay profile of the radio channel. Due to the different nature of inter-cell interference, the same methods of mitigation with intra-cell interference are not possible. However, by estimating the interfering neighboring sector signal characteristics their effect can also be mitigated. More information about intra- and inter-cell interference can be found, e.g., in [PS07] and [HT07].

2.6.4 Linear Minimum Mean Squared Error Chip-level Equalizer

Compared to the MRC -based receiver filtering, a better alternative is to select a filter setting that provides a trade-off between signal corruption due to radio-channel frequency selectivity, and noise/interference. This can be done, e.g., by selecting the filter to minimize the mean-square error between the equalizer output and the transmitted signal. The Linear Minimum Mean Squared Error (LMMSE) equalizer with receiver diversity can be used in frequency-selective channels to make the channel flat again and restore the orthogonality lost due to time-shift between the signals [Nih08].

LMMSE -chip-level equalization is relatively simple and performs well in frequency-selective channels. However, the equalizer complexity depends on the

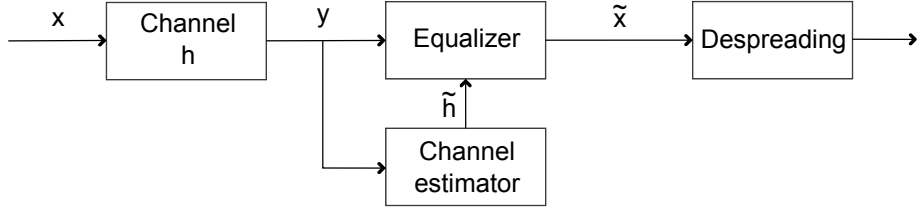


FIGURE 9 Block diagram of LMMSE receiver

delay spread of the channel: in channels with a larger delay spread, a longer and more complex equalizer is needed, thus making the delay spread a limiting factor for the use of chip-level equalizer in practice [DPSB08]. More information about LMMSE can be found in [DPSB08] and [PS07].

2.6.4.1 LMMSE Receiver Coefficient Calculation

The main concept of LMMSE diversity receiver is to restore the orthogonality by equalizing the received signal from the serving cell at the chip level before despreading, as shown in Figure 9. The equalization is done by using an adaptive calculation of the receiver coefficient. [DAO01]

To calculate the receiver coefficient vector \mathbf{w} of length $N_{Rx} \cdot F$ the following quadratic cost function should be minimized:

$$F(\mathbf{w}) = E \left\{ \left| \mathbf{w}^T \mathbf{r}(t) - \mathbf{s}(t - \tau) \right|^2 \right\}, \quad (8)$$

which is the distance between the received chip sequence $\mathbf{r}(t)$ equalized and the $(t - \tau)$ -th transmitted chip $\mathbf{s}(t - \tau)$ for a given value of delay $\tau \in \{-F + D + 1, -F + D + 2, \dots, D + L\}$. The value of \mathbf{w} , which minimizes the cost function $F(\mathbf{w})$, is found by deriving (8) in respect to \mathbf{w}^T [Bra83]:

$$\frac{\partial F}{\partial \mathbf{w}^T} = 0. \quad (9)$$

After rearranging the equation (9) can be rewritten as:

$$(\mathbf{H}^T \mathbf{H}^* + \mathbf{C}_w) \mathbf{w}^* - (\mathbf{H}^T \delta_\tau) = 0, \quad (10)$$

where \mathbf{C}_w is the white noise autocorrelation matrix, and δ_τ is a zero vector with the unit on the position τ . Therefore, the LMMSE receiver coefficient is equal to:

$$\mathbf{w}_{LMMSE} = (\mathbf{H}^H \mathbf{H} + \mathbf{C}_w)^{-1} \mathbf{H}^H \delta_\tau. \quad (11)$$

According to the [KZL00] and [KZ00] the equation for LMMSE receiver coefficient calculation can be expressed as:

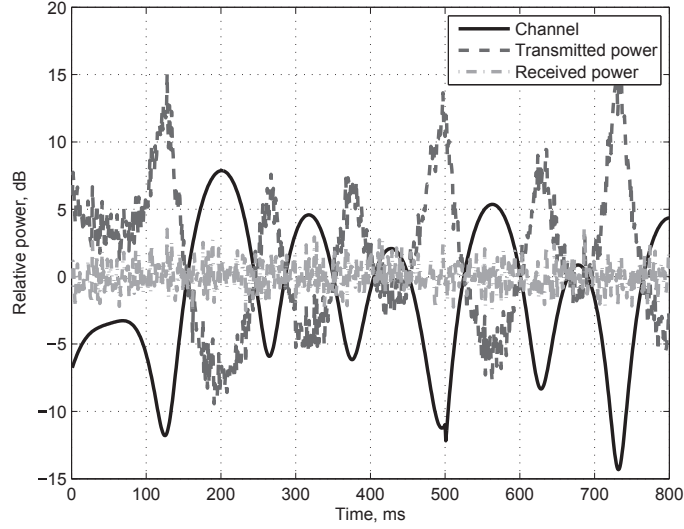


FIGURE 10 Power control in WCDMA

$$\mathbf{w}_{LMMSE} = \mathbf{C}_w^{-1} \mathbf{H}^H (\mathbf{H} \mathbf{C}_w^{-1} \mathbf{H}^H + \mathbf{I})^{-1} \delta_\tau. \quad (12)$$

Equations (11) and (12) present the same calculation in alternative forms. As such, both of these equations can be used for LMMSE receiver coefficient calculation. The delay can be optimized for LMMSE as presented in [KZL00].

2.7 Power Control

Dynamic Power Control (PC) is one of the most important aspects of WCDMA. As the name suggests, power control dynamically adjusts the radio-link transmit power to compensate for variations and differences in the instantaneous channel conditions, illustrated in Figure 10. The aim of these adjustments is to maintain a near constant Signal to Interference Ratio (SIR) at the receiver to successfully transmit data without a too high error probability. In principle, transmit-power control increases the power at the transmitter when the radio link experiences poor radio conditions and vice versa. Thus, the transmit power is in essence inversely proportional to the channel quality. As such, PC mitigates the effects of fading and ensures that each user receives and transmits with just enough energy to prevent blocking of distant users (near-far -effect), and that the users won't exceed reasonable interference levels. [HT07]

The near-far -effect is possible in situations where the UEs are in different radio channel conditions due to, e.g., interference, distance attenuation (path loss)

or shadowing. UEs in bad channel conditions need higher transmission power for a similar signal interference ratio as the UEs in good channel conditions. As such, when the UE in bad channel conditions increase their transmission power to compensate, other UEs experience higher interference, and might be forced to increase their transmission power as well, creating a cycle with UEs increasing their transmission power. The UEs with the lowest resources will experience high interference and possibly be even blocked by UEs with higher amounts of resources at their disposal due to better channel conditions. [HT07]

The power control can be divided into Open Loop Power Control (OLPC), also referred as slow power control, and to Closed Loop Power Control (CLPC), referred as fast power control. OLPC is too inaccurate due to the essentially uncorrelated fast fading between uplink and downlink, caused by the large frequency separation of the uplink and downlink bands of the WCDMA FDD - mode. As such, open loop power control is used to compensate, e.g., distance attenuation at the beginning of the call when the power levels are not yet controllable with pilot symbols. When the connection has been established, CLPC becomes active. [HT07]

As described in [HT07], the CLPC can be further divided into two parts: the Inner Loop Power Control (ILPC) and the Outer Loop Power Control (OLPC). In the uplink ILPC, the Node-B performs frequent estimates of the received signal levels and compares it to target signal levels: If the measured signal level is higher than the target signal level, Node-B will command the UE to lower the transmission power; if it is too low it will command the UE to increase its transmission power. OLPC, on the other hand, is designed to adjust the target value for ILPC. OLPC can be used to control, e.g., the quality of service but generally the update resolution is lower than with ILPC. As such, as long as the UE has the necessary transmission power available, CLPC will prevent the power imbalance among all the uplink signals received at Node-B. Similar CLPC technique is also used in the WCDMA downlink to provide a marginal amount of additional power to UEs at the cell edge, as they suffer from increased inter-cell interference. More information about power control can be found in [HT07] and [DPSB08].

2.8 Handovers in WCDMA

In general, a handover is an action related to an ongoing call where one radio channel is switched to another in order to guarantee the defined quality of service and continuity of an established call. WCDMA supports three handover categories: intra-frequency handovers, inter-frequency handover and inter-system handovers. Intra-frequency handover means a handover procedure within the same frequency and system, inter-frequency between different frequencies but within the same system and inter-system is a handover to another system, e.g., from WCDMA to GSM. [HT07]

Different handover categories support only certain types of handovers and

the types can be divided into soft, softer and hard handover [HT07]. A soft handover is done between different Node-Bs and softer handover happens between different sectors of a single Node-B. In both of these the actual handover functionality is similar and the transition should be seamless, thus the service should continue uninterrupted. In contrast, with hard handover the handover source is released first and then the destination is connected, thus a short interruption in the service is expected. The set of cells the UE is communicating with is known as the Active Set (AS). The RNC determines, based on measurements from the UE, the Node-Bs forming the AS. Handover categories, types and procedures are covered in detail in [HT07] and [DPSB08], but in regards to this thesis, the intra-frequency soft and softer handovers are the most important ones.

3 HIGH SPEED UPLINK PACKET ACCESS

High Speed Packet Access (HSPA) introduces improved packet data capabilities for both uplink and downlink WCDMA. The downlink evolution is called High Speed Downlink Packet Access (HSDPA) and it was introduced in Release 5. The uplink evolution called High Speed Uplink Packet Access (HSUPA) was introduced in Release 6. HSPA was targeted for higher capacities and coverage for non-real time traffic with high transmission rate requirements. These requirements were met by the means of innovative techniques such as fast Layer 1 retransmissions referred as Hybrid Automatic Repeat-reQuest (HARQ), Link Adaptation (LA), Node-B controlled scheduling and shortened Transmission Time Interval (TTI).

Release 5 allowed a maximum downlink data rate of 14 Mbps, although the first networks supported only 1.8 and 3.6 Mbps. Since then, the data rates have been increasing in 3GPP releases and the peak rate in Release 11 is up to 336 Mbps in downlink and 35 Mbps in uplink. Similar improvements were achieved with latency, which affects end user performance since many interactive applications benefit from the low latency. The typical latency in WCDMA Release 99 networks was 150-200 ms while HSDPA Release 5 enabled latencies below 80 ms, and the combination of HSDPA and HSUPA in Release 6 gave even sub-30 ms latency. Latency here refers to Round-Trip Time (RTT), which is the two-way latency through the mobile and the core network. [HTT14]

As HSDPA is not in the focus of this thesis, the following sections deal mainly with the most essential features and properties of HSUPA related to this thesis. The key features of HSUPA such as the HSUPA channels, multiplexing and HARQ are presented, respectively, in Sections 3.1, 3.3.2 and 3.2. Section 3.3 presents some well-known types of schedulers. Excellent sources of additional information about HSPA are, e.g., [3GP14e], [3GP13b], [HT07], [HT06], [DPSB08] and for the very latest HSPA development [HTT14]. A more detailed explanation of the physical layer aspects can be found in the 3GPP specification [3GP14d].

3.1 HSUPA Channels

HSUPA is not a standalone feature as it requires existing WCDMA channels, such as Release 99 Dedicated Channel (DCH). Regarding the Release 99 Dedicated Channel (DCH), the Dedicated Physical Control Channel (DPCCH) is unchanged and the need for the Dedicated Physical Data Channel (DPDCH) depends on the possible uplink services mapped to the DCH. Dedicated Physical Control Channel (DPCCH) is used, e.g., for fast power control.

A new uplink transport channel, Enhanced Dedicated Channel (E-DCH), was introduced in Release 6. As with DCH, E-DCH is also mapped to separate physical control and data channels. The E-DCH can be configured simultaneously with one or several DCHs. Thus, high-speed packet-data transmission on the E-DCH can occur at the same time as services using the DCH from the same UE. E-DCH initially supported two network configurable TTI lengths: an optional 2 ms TTI and a mandatory 10 ms TTI. In principle, different UEs can be configured with different TTIs. Downlink control signaling is necessary for the operation of the E-DCH. [DPSB08]

User data is carried on the Enhanced Dedicated Physical Data Channel (E-DPDCH) while the new control information uses the Enhanced Dedicated Physical Control Channel (E-DPCCH). Depending on the instantaneous data rate, the number of E-DPDCHs and their spreading factors are both varied. In addition to the transport channel, new channels for scheduling control were also introduced with HSUPA: E-DCH Absolute Grant Channel (E-AGCH), E-DCH Relative Grant Channel (E-RGCH) and E-DCH Hybrid ARQ Indicator Channel (E-HICH) [DPSB08].

E-AGCH is used to inform the absolute scheduling value, i.e., an absolute power level that the UE should adopt. E-AGCH can in principle allow transition between minimum and maximum data rates as well as any smaller data rate changes in between the two extremes [HT07]. The absolute grant channel is sent only from the serving cell. E-RGCH is a relative scheduling channel which transmits step up/down commands. A non-serving cell can transmit only hold/down commands in order to reduce and keep the interference levels reasonable. A new channel for retransmission control, E-HICH, carries the information whether a particular base station has received the uplink packet correctly or not. The new channels introduced as part of HSUPA are illustrated in Figure 11. [DPSB08]

3.2 Fast Layer 1 Retransmissions

Compared to the earlier WCDMA architecture, HSPA introduced new functionality to Node-B, fast retransmissions being among these changes. In Release 99, retransmissions can be employed only from RNC, but after the introduction of HSPA retransmissions can be initiated also from Node-B. The main benefit is

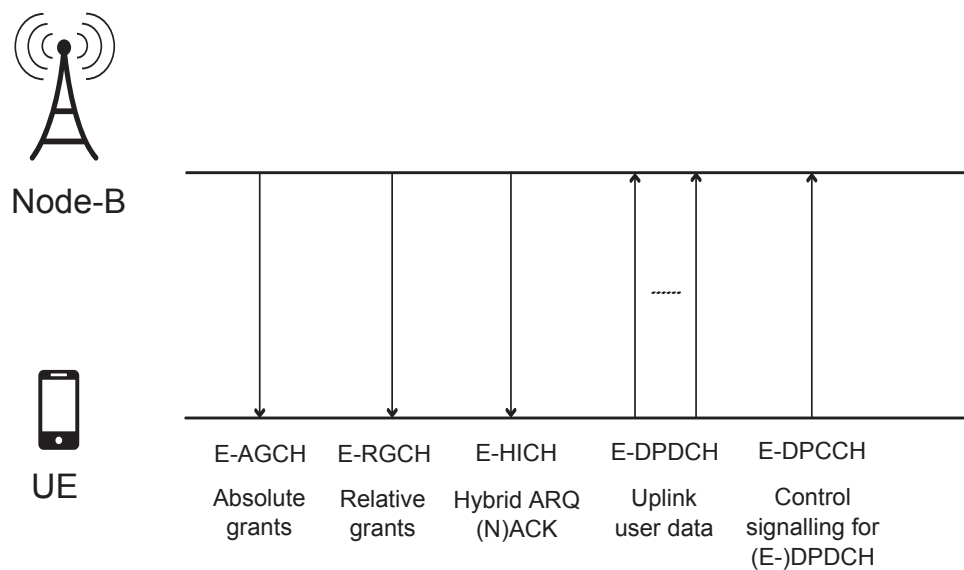


FIGURE 11 The new channels introduced as part of HSUPA

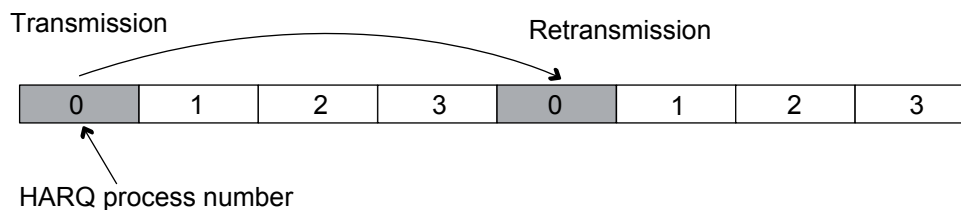


FIGURE 12 Synchronous HARQ in HSUPA

the fast indication about the need of retransmission, leading to noticeably lower round trip times compared to the Release 99 retransmission procedure.

With fast layer 1 retransmissions, or Hybrid Automatic Repeat-reQuest (HARQ), the receiving decoder does not immediately forget the received symbols if the transmission fails, but combines the symbols over multiple retransmissions. In this way HARQ provides robustness against occasional transmission errors. The retransmissions can operate in two modes: with identical retransmissions, commonly referred to as soft or chase combining, or with non-identical retransmissions, known also as incremental redundancy combining [HT06]. The HARQ operation is synchronous, i.e., retransmissions are not explicitly scheduled and always occur at a predefined time after the initial transmission, and consists of multiple parallel stop-and-wait processes for separate transmissions, illustrated in Figure 12. [DPSB08]

For each transport block received in the uplink, a single bit is transmitted from the Node-B to the UE to indicate successful decoding or to request a retransmission of the erroneously received transport block. When the UE is in soft

handover the HARQ protocol is terminated in multiple cells, i.e., the transmitted data may be successfully received in multiple Node-Bs and all involved Node-Bs attempt to decode the data. If the UE receives an indication of successful reception from at least one of the Node-Bs, the UE considers the data to be successfully received. [DPSB08]

3.3 Scheduling

The scheduler is one of the most important elements of HSUPA and it controls when and at what data rate the UE is allowed to transmit. Since Release 5, the scheduler is located in Node-B instead of RNC. As described in Section 2.6 and Section 2.7, by increasing the transmission power, the UE can transmit at a higher data rate. However, due to the non-orthogonal uplink, the transmission from one UE causes interference on other terminals. If the interference level is too high, transmissions may not be received properly. On the other hand, a too low interference level may indicate that the UEs are artificially throttled and full system capacity is not exploited. Therefore, Node-B has a scheduler to allow users to transmit with as high a data rate as possible without exceeding the maximum tolerable interference level in the cell. [DPSB08]

Even if the UE transmits at an acceptable intra-cell interference level, neighboring cells may experience non-acceptable inter-cell interference levels. Therefore, the UEs in soft handover also monitor the scheduling information from the non-serving cells, as those can request all their non-served users to lower their data rate by transmitting an overload indicator. [DPSB08]

Two different scheduling schemes are defined for HSUPA: scheduled transmissions and Non-Scheduled Transmissions (NSTs) [HT06]. The scheduled transmissions are controlled by Node-B, while the NSTs are controlled by RNC which defines a minimum data rate for the UE to use without any previous request. The NSTs aim to better meet the tight delay requirements of certain applications, such as VoIP, by reducing signaling overhead and processing delays.

The scheduling framework is based on scheduling grants sent by the Node-B scheduler to control the UE transmission activity and scheduling requests sent by the UEs to request resources. Based on measurements of the interference level, the scheduler controls the scheduling grant in each terminal to maintain the interference level in the cell at a desired target while still taking the UE's requests into account. The HARQ retransmissions are transmitted with the same rate as the initial transmission. [DPSB08]

3.3.1 Scheduling Algorithms

Although scheduling algorithms are very important, they are not standardized by the 3GPP, which makes the algorithms an interesting research topic for the academia and industry. In the following, three basic types of scheduling algo-

rithms are introduced: Round Robin (RR), Maximum Carrier to Interference Ratio (Max C/I) and Proportional Fair (PF).

Round Robin (RR) [HT06] is one of the simplest scheduling algorithms and often used as a benchmarking reference for more advanced scheduling algorithms. With RR the users are served in sequential order, i.e., all users are handled without priority. RR is very easy to implement and provides high fairness as the users get served equally, but radio resources might be wasted and the network throughput suffers as the channel conditions are not taken fully into account.

Compared to RR, Maximum Carrier to Interference Ratio (Max C/I) [HT06] schedules users purely according their channel conditions. The user with the best channel conditions at any given time will be scheduled. This maximizes the network throughput, but user fairness can suffer significantly and the users in the worst channel conditions might never get scheduled.

Between these two types, Proportional Fair (PF) [HT06] tries to maintain a balance between maximizing the network throughput by serving users in good channel conditions and at the same time allowing all users at least a minimum level of service. In practice, with PF each user is given a scheduling priority inversely proportional to anticipated resource consumption, but factoring in the occasions the user has been scheduled previously.

As defined in [HT07], the the PF priority metric p for user n can be calculated as:

$$p_n = \frac{d_n}{r_n}, \quad (13)$$

where d_n is the instantaneously supported data rate for user n , obtained with the link adaptation algorithm, and r_n is the average served throughput for user n . The average served user throughput r_n is calculated as [HT06]:

$$r_n = \begin{cases} (1 - a) \times r_{n_old} + a \times d_n, & \text{if the user is served} \\ (1 - a) \times r_{n_old}, & \text{if the user is not served} \end{cases} \quad (14)$$

where r_{n_old} is the old value of r_n and a is the forgetting factor. By adjusting the value of forgetting factor, the PF scheduler can either improve throughput or fairness.

3.3.2 User Multiplexing

As described in Section 3.3, scheduling aims for efficient use of system resources and tries to balance the interference levels and data rates. With certain services, such as VoIP, the required data rates are relatively low compared to, e.g., multimedia streaming services. As such, fully exploiting the available resources in any given TTI may require scheduling multiple users at the same time. A variety of multiplexing schemes have been developed for these purposes [HT06]. For the research presented in this thesis, three user multiplexing schemes are presented: Code Division Multiplexing (CDM), Time Division Multiplexing (TDM) and CDM/TDM.

With pure CDM all the users are first provided a minimum bit rate, but based on the priority metric, requested allocations and the scheduler's Rise over Thermal (RoT) level, the users can have additional higher allocations. TDM allows only one user to be scheduled in each TTI, resulting in increased queuing times but also reducing the interference levels. As with CDM, in TDM the re-transmissions are prioritized over new transmissions due to synchronous HARQ operation. In a combination of the following, CDM/TDM, the minimum bit rate for all users is not guaranteed, but multiple users can be scheduled in each TTI, depending on the RoT level that the scheduler is aiming for.

3.4 Continuous Packet Connectivity

Continuous Packet Connectivity (CPC) is a 3GPP standardization item (e.g. [3GP07b], [3GP10a], [3GP10c]) aiming to improve system capability to meet challenges such as having high numbers of users in the system, users staying connected for long periods of time, UE battery consumption and bursty or sporadic traffic types. CPC, introduced in Release 7, targets these challenges through three main features:

- UL Discontinuous Transmission (UL DTX)
- DL Discontinuous Transmission (DL DRX)
- Restricted High Speed Shared Control Channel (HS-SCCH)

In brief, Discontinuous Transmission (DTX) and Discontinuous Reception (DRX) eliminate the need for continuous transmission and reception when data is not exchanged. Prior to Release 7, DPCCCH was required to be transmitted continuously regardless of whether there is need for data to be transmitted or not, creating unnecessary interference to the cell and draining the UE battery. Similarly, HS-SCCH was required to be monitored continuously in downlink. From the perspective of this thesis the most essential is naturally UL DTX, which is described in more detail in the following. More information about CPC can be seen in [HTT14], [DPSB08] and [HT07].

3.4.1 Uplink Discontinuous Transmission

An ideal approach for transmissions would be to have the UE stay silent when there is no data to be transmitted and activate the control channels just for the data transmission periods. However, that could compromise, e.g., the fast power control which would be updated only during the data transmission times. As a solution, with Uplink Discontinuous Transmission (UL DTX) the transmission of DPCCCH is controlled both by data transmissions and also various timers, illustrated in Figure 13. This enables the power control to function with sufficient accuracy while still offering reduction in interference levels and battery consumption. The operation can be described shortly as follows:

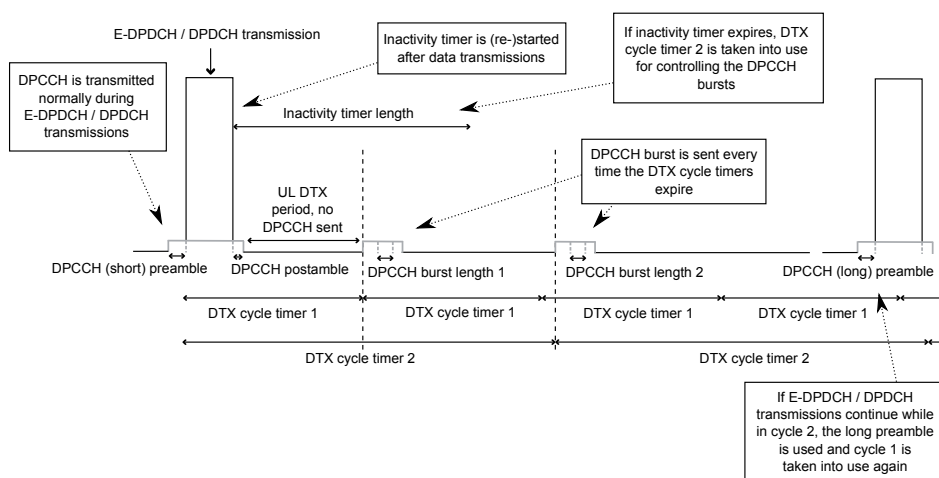


FIGURE 13 HSUPA discontinuous transmission

- *Data transmission* - DPCCH is transmitted continuously throughout the data transmissions.
- *DTX cycle 1 and 2* - Cycles control the periodic DPCCH bursts that are sent regardless of whether there is any actual data transmission or not. UE uses cycle 1 when there has been data transmission during the past inactivity timer length.
- *DPCCH burst 1 and 2* - Defines the length of DPCCH bursts initialized by cycle 1 or cycle 2 timers, respectively.
- *DPCCH preamble* - Before the actual data transmission or DPCCH burst is initiated either a short or a long burst is transmitted to allow the fast power control to correct the UE's transmit power levels. The long DPCCH burst is sent if UE is in DTX cycle 2 and data transmission is initialized, otherwise the short burst is sent.
- *DPCCH postamble* - After the data transmission or DPCCH burst has ended, DPCCH is still transmitted as long as the postamble length defines.
- *Inactivity timer* - Transitions from DTX cycle 1 to 2 are controlled by inactivity timer. Once the timer expires, UE moves from cycle 1 to cycle 2. The timer is restarted after each data transmission.

4 HSUPA PERFORMANCE ENHANCEMENTS

The research presented in this thesis consists of multiple separate techniques for, e.g., controlling the interference, improving system or user throughput, reducing delays, extending the cell range and utilizing uplink transmit diversity. These techniques are introduced in the following sections. More in depth information can be seen in the included articles [PI] - [PXIII].

4.1 Interference Coordination

Limited UE power resources and interference are among the main factors limiting the uplink system performance. In uplink, the interference consists of three main components: intra-cell interference, inter-cell interference and thermal noise. As described in Section 2.6.3, intra-cell interference is caused by non-orthogonal signals of the UEs in the same cell. If intra-cell interference is successfully mitigated, the next largest interference source is inter-cell interference.

Inter-cell interference mitigation has been studied extensively as part of the development of the LTE -standard, see, e.g., [Nec08], [BPG⁺09], [XJH07] and [Sim07] for an overview, and there are several approaches to IC in LTE. Since the frequency band is divided into resource blocks and the same blocks are used in each cell, in one approach some of the blocks are restricted to be scheduled to only UEs near to the cells center. The pattern of blocks, in which the scheduling is restricted, is arranged between the cells according to a certain frequency reuse pattern. Considering the neighboring cells, this arrangement allows for cell edge UEs to be scheduled in different blocks, thus reducing the inter-cell interference, and improving user and cell throughput.

Inspired by the approaches for LTE, the time domain Interference Coordination (IC), presented in this thesis ([PI]), aims to limit the inter-cell interference by restricting the users power of E-DPDCH in a predefined manner. The scheduled TTIs are divided into cell center and cell edge periods. The users are categorized into two groups, cell edge and cell center users, and these groups are scheduled

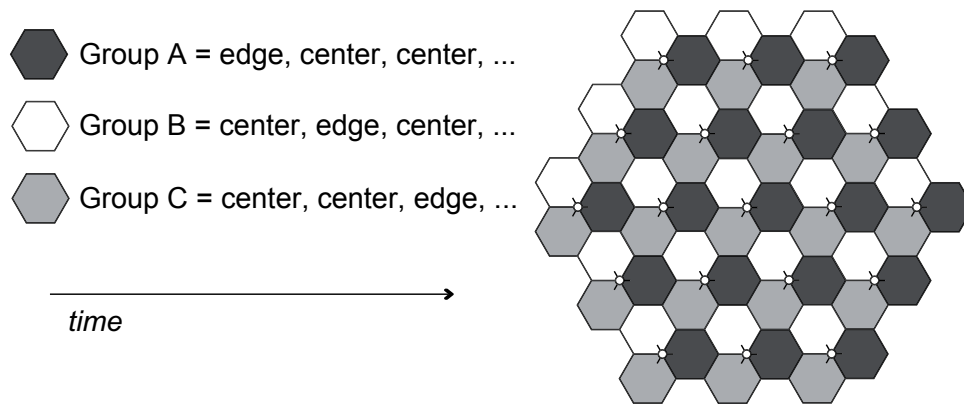


FIGURE 14 Time domain Interference Coordination -scenario

differently depending on which period is active. As such, during the cell center period, the cells allow the normal scheduling and multiplexing operation only for center UEs. Alternatively, when the cells are in the edge period, only the cell edge or, depending on the configuration, all UEs may be scheduled with unrestricted E-DPDCH.

In the studied scheme the cell edge periods are restricted to one third of all TTIs and cell center periods consist of the remaining two thirds of the TTIs. The IC operation with the described configuration is illustrated in Figure 14. This operation could be achieved by activating and deactivating HARQ processes or, alternatively, with RNC restricting the maximum data rate for UEs in certain HARQ processes and time periods. It should be noted, that activating and deactivating HARQ processes is possible in the Release 6 specification, thus applicable to legacy UEs, whereas specifying a different minimum data rate in some HARQ processes would require changes in specification. Taking all into account, time domain IC sets the following basic restrictions and requirements for the system:

- Node-Bs have to be synchronized as the center/edge periods have to be synchronized between separate Node-Bs
- The criteria for selecting the cell edge/center users need to be defined
- The scheduling procedure needs to be modified accordingly to the IC operation

In this thesis, a user is classified as a cell edge user if the Energy per Chip to Noise Ratio (E_c/N_o) difference between the users serving cell and any other cell is smaller than a certain value defined by a parameter. As such, the exact proportion of edge and center users will vary from cell to cell. The edge/center user percentages quoted in this thesis refer to the average number across all of the cells. In regard to scheduling, the following modifications are in effect:

- With CDM and CDM/TDM scheduling during the cell edge period, the cell edge users are scheduled first according to the priority metric. But after

that there is the possibility to also schedule cell center users if that mode is configured. Otherwise cell center users will be scheduled only with the minimum transmission rate.

- With CDM and CDM/TDM scheduling during the cell center period only the cell center users are scheduled according to priority metric. Cell edge users will be allocated only with a configured minimum transmission rate.
- With TDM scheduling only one user is scheduled at each transmission time interval. As such, only the set of scheduling candidates need to be modified to make sure the users classified for the period are available.

4.2 Dual-Carrier

Prior to Release 9, HSUPA was defined to utilize a single carrier with 5 MHz bandwidth. Following the development of the baseband processing capabilities, the work in 3GPP turned towards enabling a single device to use larger bandwidth than the original WCDMA bandwidth. Defining a larger bandwidth with the new chip rate would have been a non-backwards compatible solution, so it was chosen to consider using multiple 5 MHz carriers for a single device. As operators may have multiple 5 MHz spectrum bands available and as Dual-Carrier (DC) for HSDPA was already specified in Release 8 [HT11], the logical continuum was to study the possibility of Dual-Carrier HSUPA (DC-HSUPA), illustrated in Figure 15. Study in 3GPP led to standardizing Dual-Carrier HSUPA (DC-HSUPA) for Release 9, see, e.g., [HTT14], [HT11], [3GP11b], [3GP12b], [3GP10b], [3GP12c], [3GP13c] and [3GP13d], and the results of this research have been utilized to support the DC-HSUPA standardization work. Following the standardization of DC-HSUPA, Multi-Carrier (MC) HSDPA was specified in Release 10 [HTT14], [HT11], 8-carrier HSDPA with MIMO and uplink MIMO in Release 11 [HTT14], [3GP14a], [3GP13a]. However, as the author has not published research on multi-carrier or MIMO, in this thesis only DC-HSUPA is considered ([PII]).

Enabling dual-carrier operation for HSUPA can provide many benefits for both the network and the UEs compared to single carrier operation. With adequate power resources UEs could in theory double their peak data rate. A number of the most significant dual-carrier benefits are listed below:

- The UE(s) may transmit with the highest Enhanced Transport Format Combination Indicator (E-TFCI) but still have reserve power. As such, with dual-carrier the UE(s) may use the reserve power on the other carrier to increase their total transmission rate.
- The UE(s) may transmit with a higher code rate or modulation as the transmission could be divided over two carriers to get higher link efficiency.
- Due to the rise over thermal limit, the scheduler may not be able to allocate as many resources as the UE(s) would be able to use. This limitation can be alleviated with the use of dual-carrier as the UE(s) may use the reserve power on the other carrier to increase their total transmission rate.

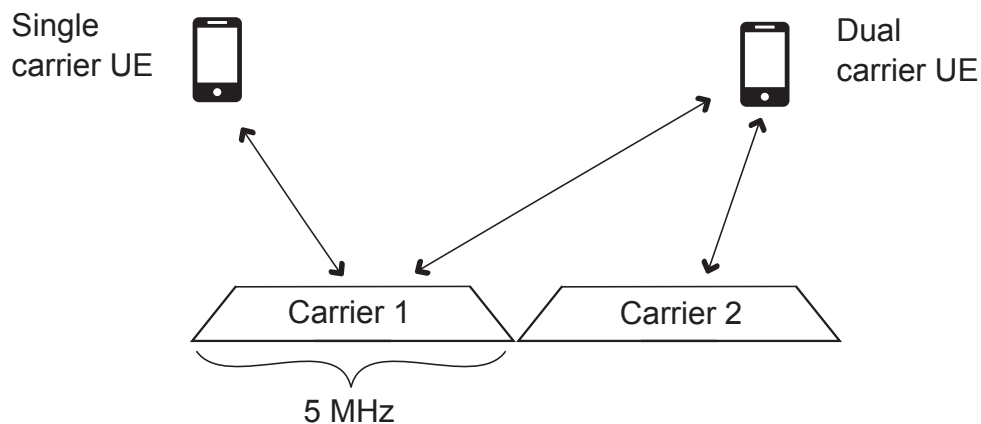


FIGURE 15 Illustration of dual-carrier operation

- Dual-carriers enable load balancing between carriers and give more room for maximizing the use of resources. The network and UE(s) experience less interference as less users transmit at the same time on E-DPDCH.

The main restrictions and requirements for DC-HSUPA operation, as defined in 3GPP Release 9 specification, are listed briefly as follows:

- DC-HSUPA requires Dual-Carrier HSDPA (DC-HSDPA) for operating.
- The carriers belong to the same Node-B and are adjacent.
- UE has a single Power Amplifier (PA) and the total transmit power is shared between carriers.
- The control channels are transmitted on both carriers.

Additionally, a large enough available spectrum and UEs supporting the feature are required to implement dual-carrier in practice.

4.2.1 Scheduling with DC-HSUPA

Scheduling with dual-carrier follows the principles defined in Section 3.3. However, due to the presence of two carriers, slight scheduling modifications are needed in order to maximize resource utilization.

Rather than sending pure transmission rate requests to Node-B, the UE reports periodically the unallocated power level which is referred as power headroom. Node-B can use the power headroom reports as a means to differentiate UEs with good channel conditions and those with poor channel conditions. This way Node-B can avoid scheduling the UE with power that it is not able to provide and prioritize users with higher headroom.

Proportional Fair (PF) scheduling based on power headroom criteria is chosen as the basis for the scheduling, which is done according to UE's primary carrier. The primary carrier is static during the simulation and all UEs have the same primary carrier. This means that the primary carrier is always scheduled

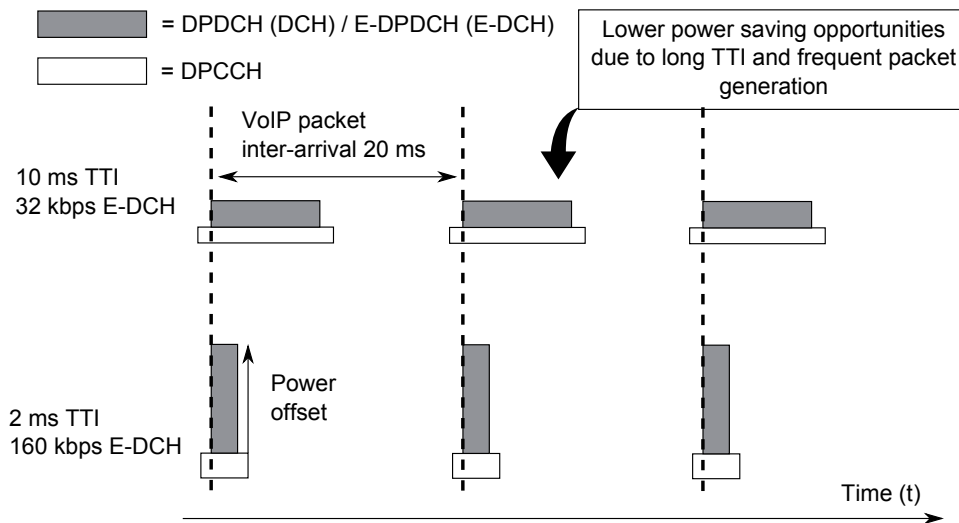


FIGURE 16 Example of VoIP traffic with different TTIs

first and UE's total power headroom is the metric for PF scheduler. The UEs also make their rate requests in that same carrier order.

4.3 Range Extension

3GPP has specified that terminals can be configured to use either 2 or 10 ms TTI in HSUPA systems. The 2 ms TTI length can provide higher battery saving opportunities due to shorter transmit times but on the other hand a 10 ms TTI can extend the coverage for power limited UEs that cannot utilize 2 ms TTI, illustrated in Figure 16. The purpose of the Range Extension (RE) -scheme presented in this thesis ([PIII] and [PIV]) is to avoid potential coverage problems when using only the 2 ms TTI length.

With RE, UEs in poor radio conditions are configured to send bundles of 2 ms TTI transmissions without HARQ feedback if the UE is found to be coverage limited, thus eliminating the need to configure two different TTIs. This makes it possible for the scheduler to manage only one TTI instead of two, and as such reduce the number of required radio link reconfiguration procedures. Additionally, various services have tight delay requirements and as such the shorter 2 ms TTI in conjunction with RE enables the coverage limited UEs to meet the requirements better. Furthermore, Release 7 enhancements such as UL DTX, presented in Section 3.4.1, are less beneficial in conjunction with the longer 10 ms TTI, as presented in Figure 16. Thus, UEs can gain additional benefit from the 2 ms TTI RE -technique, which avoids the necessity to utilize the 10 ms TTI in larger cells.

In this thesis, RE is modeled with a scheme with three Super-HARQ (S-HARQ) processes, i.e., bundles of consecutive 2 ms TTI transmissions of same

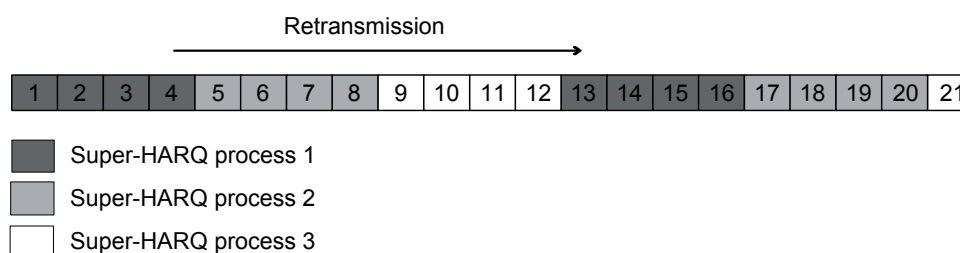


FIGURE 17 The selected Range Extension -scheme

packet. The scheme was selected due to similarity to TTI bundling in LTE, presented in, e.g., [SM09] and [HW09]. In the selected scheme, each RE bundle consists of four consecutive 2 ms transmissions and there are three S-HARQ processes as Figure 17 illustrates. In other words, the RTT for S-HARQ processes is 12 TTIs and three packets can be accommodated at a time. Each S-HARQ is assumed to have a maximum of three transmissions per S-HARQ.

Unlike with the normal 2 ms transmission, where the HARQ feedback (Acknowledgment (ACK) or Negative Acknowledgment (NACK)) is sent after every individual transmission, in RE mode the feedback is sent at the end of the RE -bundle. The Node-B combines all of the received transmissions in the bundle before decoding in order to accumulate higher SINR at its receiver. Regarding the power control, as the number of repeated TTIs is higher than the number of non repeated TTIs, the E-DPDCH power offset for repeated TTIs is lower than non repeated TTIs in order to keep the power control stable. Additionally, as a requirement, Node-Bs must know which UE uses RE and when.

4.3.1 Mode Switching Criteria for Range Extension

In the presented RE -scheme, the UEs can dynamically utilize RE and the decision to use either normal 2 ms TTI transmissions or RE mode is made at the beginning of the HARQ cycle; every 8 TTIs when in 2 ms mode and every 12 TTIs when in RE -mode. In this study this is referred to as the switch point, illustrated in Figure 18 and Figure 19. For the UE to switch from operational mode to another, certain conditions must be met.

To make the switch from normal to RE -mode there must be data to be transmitted either in the HARQ channel or in the buffer. Additionally, the Uplink Power Headroom (UPH), i.e., the available UE transmit power after DPCCH, must be below the threshold value:

- If the UPH is higher than the set threshold value, the UE should make a regular 2 ms TTI transmission, as the UE is expected to have sufficient power to meet the required SIR level
- If the UPH is less than the set threshold value, the UE should switch to RE -mode

The UE is forced to make the switch from RE -mode to normal mode if there is no

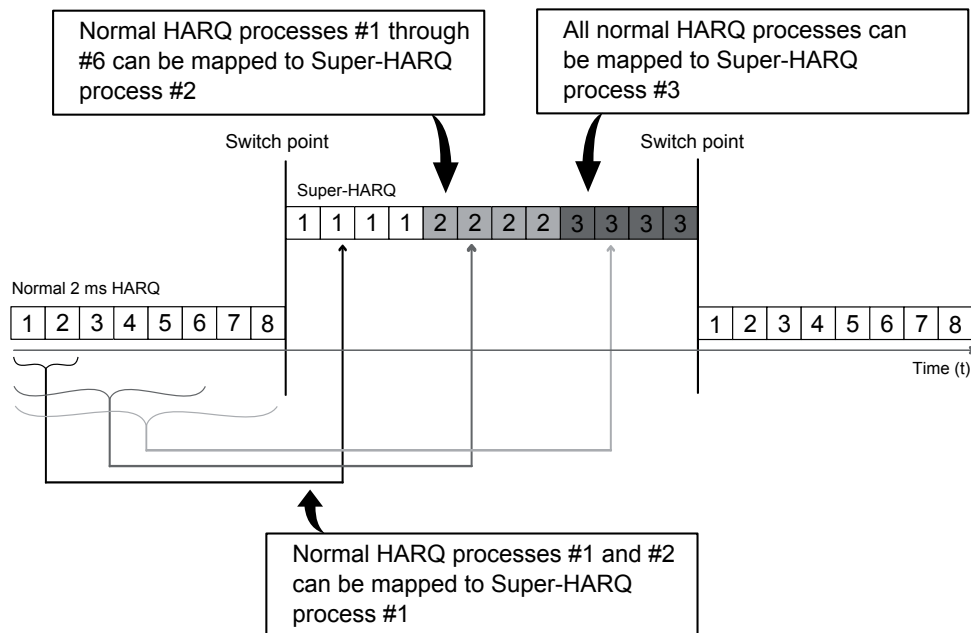


FIGURE 18 HARQ mapping when switching from normal 2 ms TTI to 2 ms TTI RE

data to be transmitted. Otherwise, the switch can be made if the UPH is above the threshold value. The threshold value for switching is optimized based on the targeted QoS criteria and defines the ratio between normal 2 ms TTI users and RE users. If the UE is not at the switch point, it will continue its transmissions in the current mode even if the criteria for switching would indicate otherwise.

4.3.2 HARQ Operation with Range Extension

In the studied scheme, the RTT defines which HARQ channel can be mapped to which S-HARQ. When moving from normal to RE -mode, illustrated in Figure 18, the HARQ channels are mapped as follows:

- HARQ channels 1 and 2 can be mapped to S-HARQ process 1 even though full 16 ms RTT has not passed
- HARQ channels 1 through 6 can be mapped to S-HARQ process 2
- All HARQ channels can be mapped to S-HARQ process 3

If there are more than three HARQ processes in use when the UE moves to RE -mode, prioritization of HARQ channels depends on the delay. Excess packets and pending HARQ will have to wait until one or more S-HARQ processes become available.

When moving from RE mode to normal mode, illustrated in Figure 19, due to RTT requirements the S-HARQ channels are mapped to HARQ channels as follows:

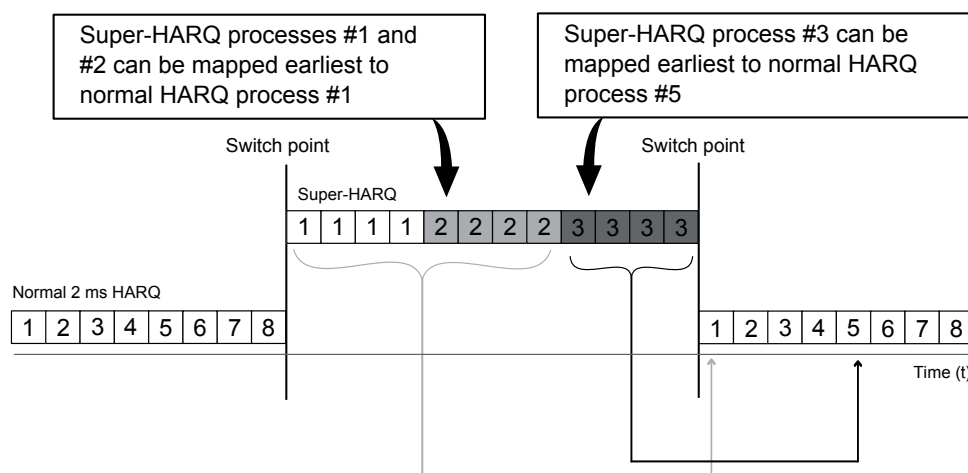


FIGURE 19 HARQ mapping when switching from 2 ms TTI RE to normal 2 ms TTI operation

- S-HARQ processes 1 and 2 can be mapped to HARQ channel 1 and onwards
- All S-HARQ processes can be mapped to HARQ channel 5 and onwards

4.4 Transmit Diversity

Release 99 contained support for Node-B transmit diversity, but Release 5 HSDPA and 6 HSUPA were basically designed around a single antenna, single frequency band, and single-carrier operation. Following the standardization of downlink MIMO in Release 7, uplink MIMO and uplink Closed Loop Transmit Diversity (CLTD) were specified in Release 11 [HTT14], [3GP14a], [3GP13a]. CLTD is a separate feature from the standard perspective, thus, it can be used by UEs which do not support MIMO. However, as the author has not published research on MIMO, it is not considered in this thesis.

In October 2009 a Study Item (SI) regarding Uplink Transmit Diversity (ULTD) for HSPA was opened in 3GPP to cover Open Loop Transmit Diversity (OLTD) options for uplink. The study is focused on schemes that do not require any newly standardized dynamic feedback signaling between network and UE. Previously transmit diversity has been considered mainly for downlink (e.g. [HT07] and [HT11]) for instance due to cost and size requirements of the small handheld terminals. However, due to the increasing demand for higher performance also in the uplink, diversity techniques were considered as potential performance enhancement for HSUPA as well.

During various Radio Access Network Radio Layer 1 (RAN1) work group [3GP14c] meetings possible schemes, assumptions and performance of Open Loop Beamforming (OLBF) and Switched Antenna Transmit Diversity (SATD) were

evaluated and discussed. The work under the study item aimed at, e.g., evaluating the potential benefits of the indicated UL transmit diversity techniques, investigating the impacts on UE implementation and how to ensure that the UE operating an uplink transmit diversity will not cause any detrimental effects on the overall systems performance. These findings are summarized in the 3GPP Technical Report 25.863 [3GP11a].

In December 2010 a Work Item (WI) on uplink transmit diversity was opened. In this WI the performance associated with uplink CLTD was evaluated. In contrast to OL, with CL Node-B controls the pre-coding vector, i.e., the antenna weights, which the UEs apply. The summary of findings related to uplink CLTD can be seen in 3GPP contribution R1-113408 [3GP11c].

The studied uplink transmit diversity schemes may be categorized into two types of algorithms:

- transmission from one Tx antenna (e.g. SATD)
- simultaneous transmission from two Tx antennas (e.g. transmit beamforming)

Based on feedback mechanisms, the algorithms can be further categorized into Open Loop (OL) and Closed Loop (CL) algorithms. In the following sections, the uplink transmit diversity schemes and algorithms studied in this thesis are presented.

4.4.1 Switched Antenna Transmit Diversity

With Switched Antenna Transmit Diversity (SATD) ([PV], [PVI] and [PVII]) the UE transmits the DPCCCH, Enhanced Dedicated Physical Control Channel (E-DPCCH), E-DPDCH and High Speed Downlink Physical Control Channel (HS-DPCCH) as in the current specifications. As a difference, with SATD the UE possesses two Tx antennas and is able to switch its Radio Frequency (RF) chain between the antennas, illustrated in Figure 21 and Figure 20. As described in [3GP11a], SATD can ideally provide a 3 dB gain over the operation with single Tx antenna.

In the studied technique, the UE decides independently at each evaluation interval which Tx antenna to use, meaning the scheme is an open loop scheme and the network is not aware of UEs using SATD. In soft handover it may be the case that the best UE antenna may differ for different cells. For this thesis, it is assumed that the UE bases its antenna selection on the serving Node-B. Note that, as the switch is invisible to the network, any filtering of channel estimates between slots at Node-B will smear the channel impulse responses from the two antennas after switching.

4.4.1.1 SATD Algorithms

Five different SATD algorithms for deciding the best antenna are presented in this section: Genie Aided Switching (TX1), Transmission Power Control (TPC)

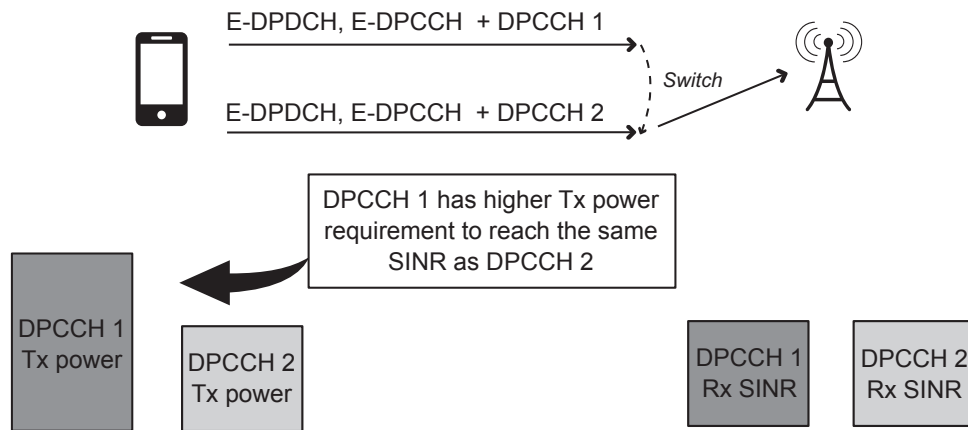


FIGURE 20 The principle of SATD

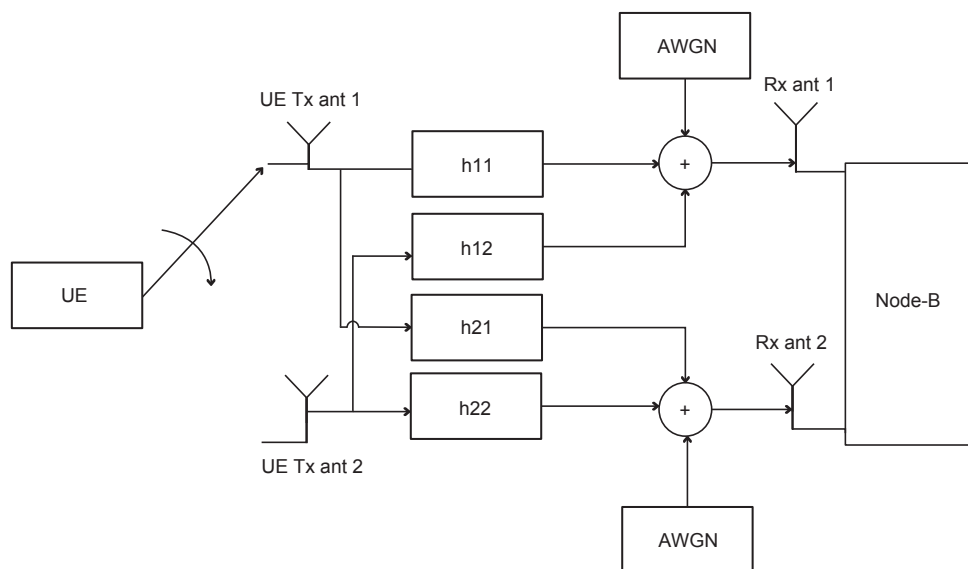


FIGURE 21 High level block diagram of SATD [3GP11a]

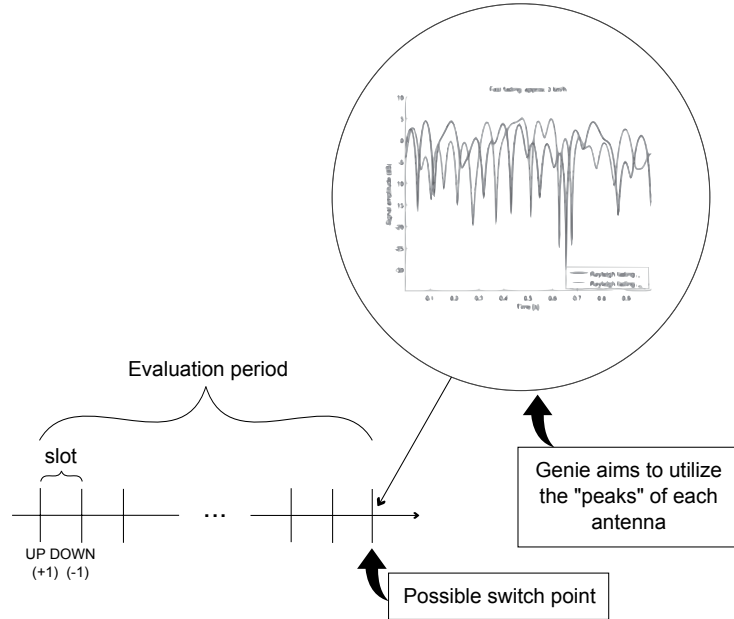


FIGURE 22 Genie aided switching (TX1)

Aided Switching 1 (TX2), TPC Aided Switching 2 (TX3), DPCCH Aided Switching (TX4), Periodical Switch (TX5). Out of these, the Genie algorithm is not realistic as it has perfect knowledge for deciding which antenna to use. As such, the Genie represents an upper bound for the UE transmit diversity algorithms performance and functions as a benchmark. The rest of the algorithms are practical algorithms, i.e., the algorithms use existing performance indicators to decide the used antenna.

Genie Aided Switching (TX1)

With Genie aided switching, illustrated in Figure 22, the UE makes switching decisions every evaluation period, e.g., radio frame (10 ms), based on an ideal knowledge of the channel impulse responses from the two antennas. The selected Tx antenna ($j = 1, 2$) is the one that maximizes:

$$\frac{1}{15} \sum_{k=1}^{15} \sum_{l=1}^L \left(|h_{1,j}(l,k)|^2 + |h_{2,j}(l,k)|^2 \right) \quad (15)$$

where k is a slot index, l is a multipath index and $h_{i,j}(l,k)$ represents the channel impulse response from between Tx antenna j and Receive (Rx) antenna i . In practice this algorithm can be implemented simply by selecting the antenna with best fading conditions as the outcome will be the same as with the equation above.

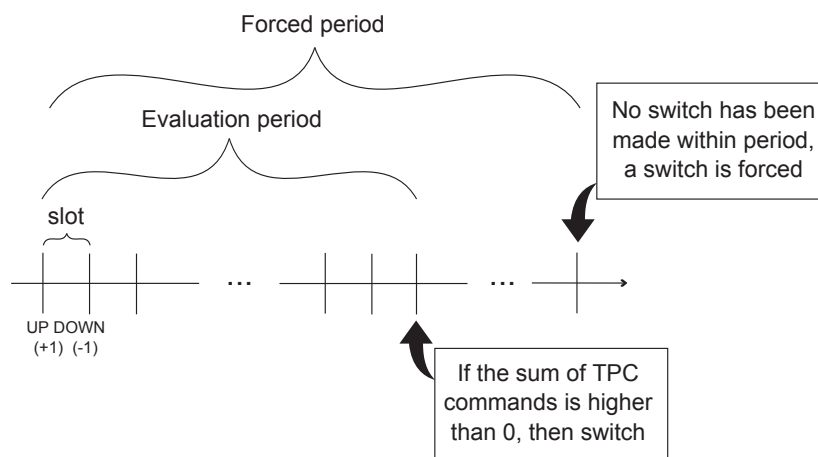


FIGURE 23 TPC aided switching 1 (TX2)

TPC Aided Switching 1 (TX2)

With TPC command aided switching, the UE will every time interval, e.g., radio frame (10 ms), check the sum of TPC commands where power **UP** command represents +1 and power **DOWN** -1. With **TX2**, illustrated in Figure 23, if the sum of the commands is higher than 0 then the switch is made as that would indicate that the current antenna needs on average more power than in the previous evaluation period and other antenna could potentially be in a better situation. In addition, a forced switch is made every forced switch time interval if the sum of TPC commands does not trigger the switch earlier.

TPC Aided Switching 2 (TX3)

With TPC aided **TX3**, illustrated in Figure 24, the UE switches Tx antennas periodically every time interval, e.g., radio frame (10 ms), and then monitors the following PC command for the new antenna. If the command after the switch is **DOWN**, the current antenna is kept in use, otherwise the previous antenna is switched back into use.

DPCCH Aided Switching (TX4)

TX4, illustrated in Figure 25, is based on the UE periodically checking every time interval the last known DPCCH level of each antenna and switching to the antenna indicated the best. A forced switch is made every forced switch time interval if the performance indicator level does not trigger the switch earlier.

Periodical Switch (TX5)

TX5 is based on a periodical switch between antennas, illustrated in Figure 26. This means that antennas are changed every time interval, e.g., radio frame (10 ms), regardless of the channel conditions of different antennas.

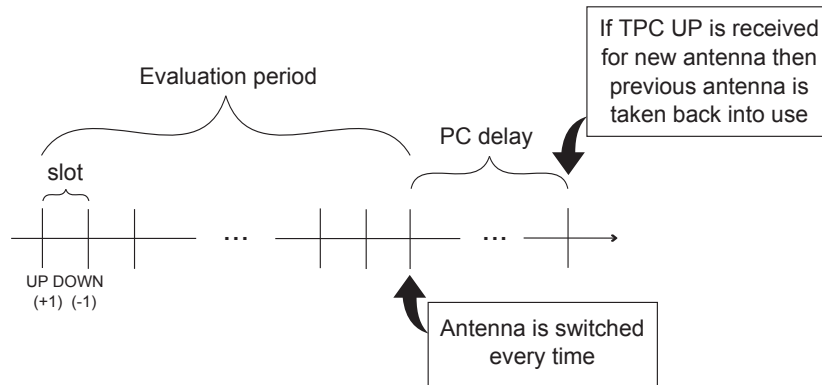


FIGURE 24 TPC aided switching 2 (TX3)

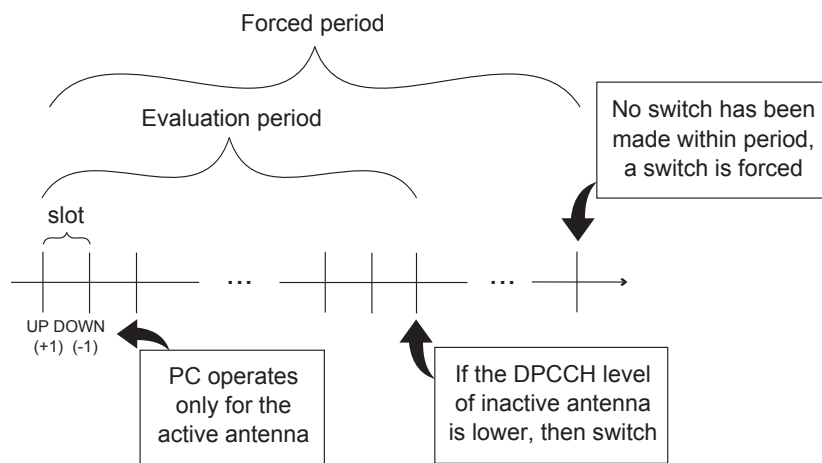


FIGURE 25 DPCCH aided switching (TX4)

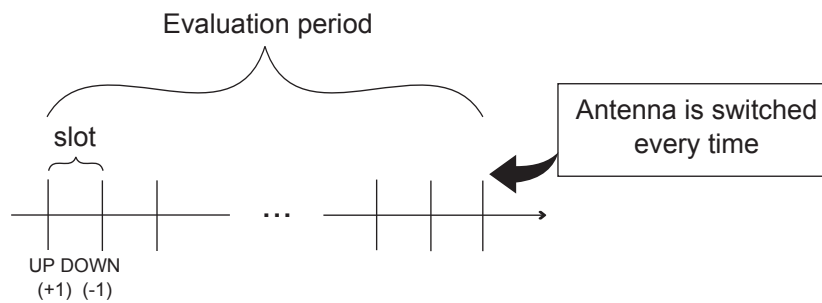


FIGURE 26 Periodical switch (TX5)

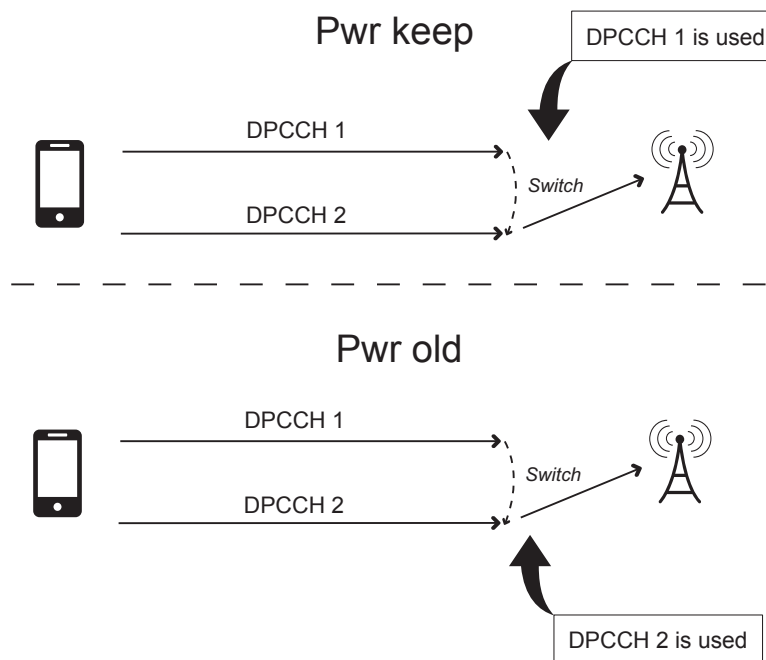


FIGURE 27 SATD power selection algorithms

Power Selection Algorithms

In addition to switching algorithms, the DPCCH transmit power level for the new antenna also needs to be decided after each switch. Two different power algorithms, illustrated in Figure 27, are modeled and studied in this thesis. These algorithms are described shortly as follows:

- With **Pwr keep** the power level of the antenna where the transmission in switching from is used
- With **Pwr old** the last known power level of the antenna where the transmission in switching to is used

4.4.2 Open Loop Beamforming Transmit Diversity

In addition to SATD, the study item regarding uplink transmit diversity for HSPA [3GP11a] covers the study of beamforming transmit diversity schemes without channel state feedback. These studied schemes are called Open Loop Transmit Diversity (OLTD) schemes and they should not be mixed with the space-time block codes. Previously transmit diversity has only been considered for downlink and both OL space-time block codes and CL beamforming based on channel state feedback have been specified for the downlink [HTT14].

Different Open Loop Beamforming (OLBF) transmit diversity concepts are presented in, e.g., [WAH⁺10] and [3GP11a]. As explained in [WAH⁺10], the di-

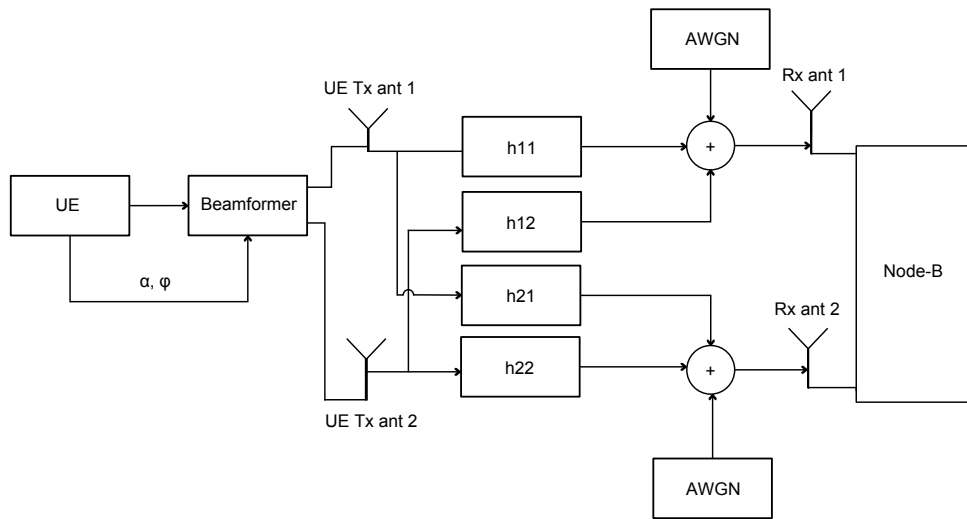


FIGURE 28 High level block diagram of OLBF [3GP11a]

iversity transmitter employing beamforming can provide two types of gain; coherent gain from beamforming and incoherent gain from mitigation of channel fades, i.e., the classical diversity gain. If the radio channels of different Tx antennas are highly correlated, which typically is the case in small hand-held devices, they can be used to form a beam and the coherent gain becomes dominant. Beamforming can be seen as a form of spatial filtering which separates the signals of different UEs due to which the interference seen by Node-B is lower than without beamforming especially in heavily loaded cells. More information about beamforming can be seen in, e.g., [HBN08], [DPSB08] and [HT07].

The OLBF scheme studied in this thesis ([PVIII]), illustrated in Figure 28, contains a single power control loop based on the post receiver combined SINR across all Tx and Rx antennas at Node-B and each antenna branch is transmitted with half of the total transmit power. Only one DPCCH is sent and the coded, modulated, spread and filtered signal transmitted from each antenna is the same; however a phase offset, determined by weight vectors, is applied between the antennas. As such the phase adjustments are also applied to the HS-DPCCH, E-DPCCH and E-DPDCH. Regarding the soft handover, the selected weights are applied to all of the links in UEs AS.

The phase offset is set autonomously by the UE and should maximize the SINR at the receiver. The network is not aware of the phase offset applied by the UE, but will receive a pilot signal based on a combination of the two transmitter antenna signals and base its channel estimation on this. Changing of the phase offset by the UE will result in a change in the channel estimate; however filtering of the channel estimates will smear these changes. The phase offset may be changed by the UE for every slot.

4.4.2.1 OLBF SINR Calculation

The SINR calculation for the downlink receive diversity system, presented in [Nih08], has been modified for uplink with a 2x2 antenna configuration which incorporates both beamforming transmit diversity and diversity reception, shown in (16). The channel coefficient matrix of the numerator has been replaced with a new combined channel coefficient matrix H_c . The denominator (17), i.e., the interference part of the SINR equation consists of the self-interference from E-DCH and the pilot, and also the noise and other UE interference. The assumption is made that the other UE interference is white.

$$SINR = S_f \frac{P_{E-DCH}}{N_c P} \frac{P |w^T H_c^T \delta|^2}{I} \quad (16)$$

where

$$I = P_{tot} w^T H_c^T \widehat{\delta} \widehat{\delta}^T H_c^* w^* + w^T C_w w^* \quad (17)$$

In the formula above, P_{E-DCH}/P is the fraction of the total transmit power used by all E-DPDCHs and N_c is the number of *spreading factor* = 4 (SF4) equivalent codes used for E-DPDCH. The effective processing gain S_f is equal to 4, as the SF2 codes are transmitted with twice the power of the SF4 codes. P_{tot} is the total UE transmit power used by E-DPDCH, E-DPCCH and the DPCCH.

Based on in Section 2.6.1, H_c is a $(F + L) \times (F \times N_{Rx})$ combined channel coefficient matrix, which represents the effective channels from the beamforming transmitter to the Rx antennas 1 and 2. Multiplication by the channel coefficient matrix models the convolution between the transmitted signal and the channel. The channel coefficient matrix is defined as

$$\mathbf{H}_c = \begin{bmatrix} \mathbf{h}_c & 0 & 0 & \dots & 0 \\ 0 & \mathbf{h}_c & 0 & \dots & 0 \\ 0 & 0 & \mathbf{h}_c & \dots & 0 \\ \vdots & \vdots & \vdots & \ddots & \vdots \\ 0 & 0 & 0 & \dots & \mathbf{h}_c \end{bmatrix}^T, \quad (18)$$

wherein matrix h_c includes the path loss, shadowing, antenna gain and fast fading components and is formed by weighting the impulse responses between the Tx and Rx antennas ($h_{11}, h_{12}, h_{21}, h_{22}$) with the Tx antenna weights (w_1, w_2):

$$\mathbf{h}_c = \begin{bmatrix} w_1 \mathbf{h}_{11}[0] + w_2 \mathbf{h}_{21}[0] & \dots & w_1 \mathbf{h}_{11}[L] + w_2 \mathbf{h}_{21}[L] \\ w_1 \mathbf{h}_{12}[0] + w_2 \mathbf{h}_{22}[0] & \dots & w_1 \mathbf{h}_{12}[L] + w_2 \mathbf{h}_{22}[L] \end{bmatrix} \quad (19)$$

As defined in Section 2.6.2 and Section 2.6.4.1, the delay of equalizer is presented in (20) by δ and is defined with $\widehat{\delta}$ as follows:

$$\delta = [0 \ \dots \ 0 \ 1 \ 0 \ \dots \ 0]^T \quad (20)$$

$$\hat{\delta} = \text{diag}([1 \ \dots \ 1 \ 0 \ 1 \ \dots \ 1]) \quad (21)$$

C_w is the combined covariance matrix for the noise and other UE interference. The calculation of the receiver filter w is presented in (22) for Rake and in (23) for LMMSE.

$$\mathbf{w}_{\text{RAKE}} = \mathbf{H}_c^H \quad (22)$$

$$\mathbf{w}_{\text{LMMSE}} = \sqrt{P_{\text{tot}}} H_c \left(P_{\text{tot}} H_c H_c^T + C_w \right)^{-1} \delta \quad (23)$$

4.4.2.2 OLBF Algorithms

In this thesis, two different OLBF algorithms for deciding the used beamforming weight vectors are presented: the so called Genie algorithm and a realistic 'practical algorithm'. As with SATD, the Genie is not a realistic option for real networks but represents an upper performance boundary. Likewise, the practical algorithm uses existing performance indicators to formulate the used weights, and as such is applicable to real networks.

Genie Aided Beamforming

In the Genie scenario [3GP11a], the UE has perfect knowledge of the channel impulse responses from the two antennas. The phase offset between antennas is implemented by applying a beamforming weight to each antenna. The beamforming weights $\underline{w} = [w_1 \ w_2]^H$ are adjusted every slot (0.67msec); in each slot, they are calculated to maximize:

$$\sum_{l=1}^L \underline{w}^H H_l(k)^H H_l(k) \underline{w} \quad (24)$$

where $H_l(k)$ is a 2x2 matrix of channels between Tx and Rx antennas for the l^{th} multipath in the k^{th} slot. The calculation is done to all of the links in the UE's AS and the weight resulting in the highest power is selected. To simplify the evaluation of the above formulation, a limited set of 8 weight vectors is defined. Each weight vector is defined as

$$[w_1 \ w_2] = [1 \ e^{-j\theta}] \quad (25)$$

where $\theta = \{0, 0.25\pi, 0.5\pi, 0.75\pi, \pi, 1.25\pi, 1.5\pi, 1.75\pi\}$. The weight selection is calculated and applied on a slot by slot basis and no delays are assumed with the application of weights.

TPC Aided Practical Algorithm

In the practical OLB scenario [3GP11a], the UE does not have access to channel impulse response vectors and must estimate every slot the weight vector to apply based on the TPC commands and the following algorithm:

Let TPC command *DOWN* be represented by -1 and TPC command *UP* by $+1$.

1. Initial relative phase between two transmitters is $\Delta\varphi = -\delta/2$ for the first slot (#1 slot). ϵ is kept zero until two TPC commands become available to the UE.
2. Apply relative phase for the next slot $\Delta\varphi = \Delta\varphi + \delta$
3. Determine new relative phase: (TPC1 and TPC2 correspond to slot $(1,2),(3,4), \dots, (i*2 - 1, i*2)$, where $i = 1$ to n)
 - if $TPC1 > TPC2$, $\Delta\varphi = \Delta\varphi + \epsilon$
 - if $TPC2 > TPC1$, $\Delta\varphi = \Delta\varphi - \epsilon$
 - otherwise, no change
4. Apply relative phase for the next slot $\Delta\varphi = \Delta\varphi - \delta$ and go to step 2.

For the algorithm above, $\Delta\varphi$ represents the weight phase offset which is defined by applying relative phase shifts with parameter defined values δ and ϵ . As such the total available amount of different weights depends on the relative shift values. Smaller relative shift values result in a larger amount of possible weight phase offsets and vice versa. For purposes of this study the relative shift values δ and ϵ were defined by 3GPP simulation assumptions.

The above algorithm can be implemented with asymmetric or symmetric phase shifts. With asymmetric phase implementation, the phase of the transmit signal from the first antenna is kept constant and the relative phase is applied only to the transmit signal from the second antenna. With symmetric phase implementation, half of the relative phase is applied to the transmit signal from the first antenna and the other half of the relative phase is applied with an opposite sign to the transmit signal from the second antenna.

As with the Genie, the practical algorithm weight selection is also done on a slot by slot basis and no additional delays are assumed with the actual use of the weights. However, as power control commands are used to formulate the weights, the delay with TPC commands affects the practical algorithm performance.

4.4.3 Closed Loop Beamforming Transmit Diversity

In the studied Closed Loop Beamforming (CLBF) scheme, two DPCCs are transmitted independently from different antennas. As DPCC is the channel carrying the pilot symbols, two DPCCs are needed in order to obtain knowledge of the whole channel matrix. As with the OLB scheme presented in Section 4.4.2,

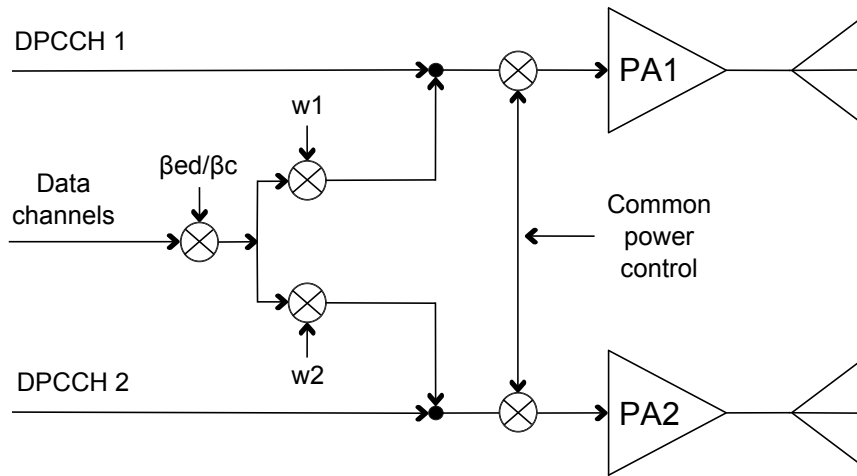


FIGURE 29 Principle of CLBF without pilot pre-coding

CLBF is carried out by pre-coding the signal with weight vectors prior to transmission.

In the initial evolution of the CL scheme, described in [PIX] and illustrated in Figure 29, both DPCCHs are transmitted without pre-coding, whereas beamforming weights $[w_1 \ w_2]$ are applied to, e.g., the HS-DPCCH, E-DPCCH and E-DPDCH. In the latest evolution of the scheme, described in [PX], [PXI], [PXII] and [PXIII] and illustrated in Figure 30, beamforming weights $[w_1 \ w_2]$ are applied to, e.g., DPCCH, DPDCH, HS-DPCCH, E-DPCCH and E-DPDCHs, whereas beamforming weights $[w_3 \ w_4]$ are applied to the Secondary Dedicated Physical Control Channel (S-DPCCH).

All of the evolutions of the scheme include a single power control loop based on the post receiver combined SINR across all Tx and Rx antennas at Node-B. However, while the first evolution has an equal power distribution and each antenna branch is transmitting with half of the total transmit power, in the second evolution the total transmit power for the two antenna branches may be divided if the signaled pre-coding weights contain amplitude components, which define the power offset, i.e., the power split between antennas. As such, the antennas may have an equal power split or either of the antennas may have a larger portion of the power.

The pilot channels are transmitted using different OVSF codes, but, since the branches combine over the air, the traffic to pilot ratio β_{ed}/β_c is set as E-DPDCH power over the total power on DPCCH and S-DPCCH. In the following subsections, Section 4.4.3.1 and Section 4.4.3.2, only the latest evolution with four weights pre-coding with two pilots is considered.

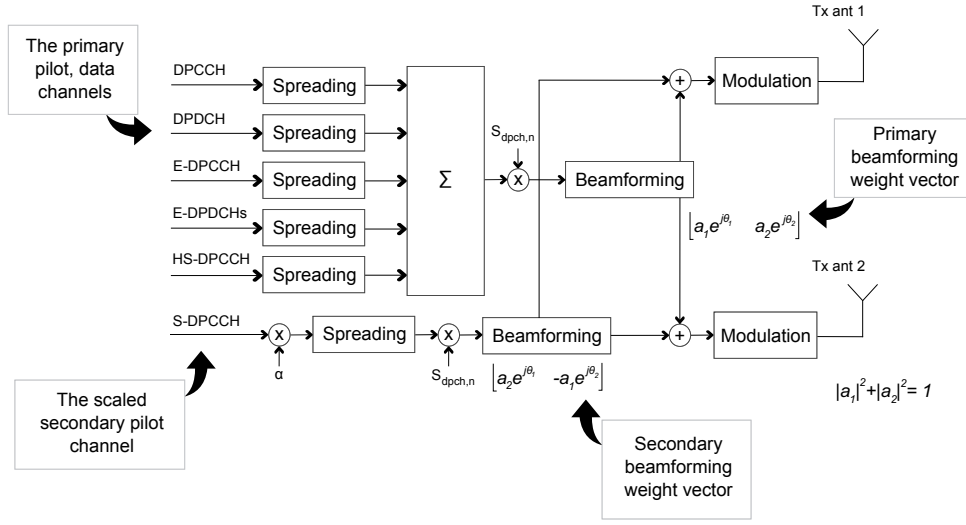


FIGURE 30 Principle of CLBF with pre-coded pilots

4.4.3.1 CLBF SINR Calculation

The SINR calculation for downlink receive diversity system, presented in [Nih08], has been modified for uplink CLBF (26). The channel coefficient matrix of the numerator has been replaced with a new combined channel coefficient matrix H_c . The denominator (27), i.e., the interference part of the SINR equation consists of the self-interference from E-DCH and the pilots, and also of the noise and other UE interference. The assumption is made that the other UE interference is white.

$$SINR = S_f \frac{P_{E-DCH}}{N_c P} \frac{P |w^T H_c^T \delta|^2}{I} \quad (26)$$

where

$$I = P_{tot} w^T H_c^T \delta \delta^T H_c^* w^* + P_{S-DPCCH} w^T H_2^T \delta H_2^* w^* + w^T C_w w^* \quad (27)$$

In the formula above, P_{E-DCH}/P is the fraction of the total transmit power used by all E-DPDCHs and N_c is the number of *spreading factor* = 4 (SF4) equivalent codes used for E-DPDCH. The effective processing gain S_f is equal to 4, as the SF2 codes are transmitted with twice the power of the SF4 codes. P_{tot} is the total UE transmit power used by E-DPDCH, E-DPCCH and the DPCCH. Respectively, $P_{S-DPCCH}$ is the transmit power of S-DPCCH.

Based on in Section 2.6.1, H_c and H_2 are $(F + L) \times (F \times N_{Rx})$ combined channel coefficient matrices, which represent the effective channels from the beamforming transmitter to the Rx antennas 1 and 2. Here F is the length of the receive filter w , L equals the length of the channel normalized to chip interval and N_{Rx} is

the number of Rx antennas. Multiplication by the channel coefficient matrix models the convolution between the transmitted signal and the channel. The channel coefficient matrix H_c is defined as

$$\mathbf{H}_c = \begin{bmatrix} \mathbf{h}_c & 0 & 0 & \dots & 0 \\ 0 & \mathbf{h}_c & 0 & \dots & 0 \\ 0 & 0 & \mathbf{h}_c & \dots & 0 \\ \vdots & \vdots & \vdots & \ddots & \vdots \\ 0 & 0 & 0 & \dots & \mathbf{h}_c \end{bmatrix}^T, \quad (28)$$

wherein matrix h_c includes the path loss, shadowing, antenna gain and fast fading components and is formed by weighting the impulse responses between the Tx and Rx antennas ($h_{11}, h_{12}, h_{21}, h_{22}$) with the Tx antenna weights w_1, w_2 :

$$\mathbf{h}_c = \begin{bmatrix} w_1 \mathbf{h}_{11}[0] + w_2 \mathbf{h}_{21}[0] & \dots & w_1 \mathbf{h}_{11}[L] + w_2 \mathbf{h}_{21}[L] \\ w_1 \mathbf{h}_{12}[0] + w_2 \mathbf{h}_{22}[0] & \dots & w_1 \mathbf{h}_{12}[L] + w_2 \mathbf{h}_{22}[L] \end{bmatrix} \quad (29)$$

H_2 follows the definition of H_c , but with the Tx antenna weights w_3, w_4 for the S-DPCCH. As defined in Section 2.6.2 and Section 2.6.4.1, the delay of equalizer is presented in (30) by δ and is defined with $\hat{\delta}$ as follows:

$$\delta = [0 \quad \dots \quad 0 \quad 1 \quad 0 \quad \dots \quad 0]^T \quad (30)$$

$$\hat{\delta} = \text{diag}([1 \quad \dots \quad 1 \quad 0 \quad 1 \quad \dots \quad 1]) \quad (31)$$

C_w is the combined covariance matrix for the noise and other UE interference. The calculation of the receiver filter w is presented in (32) for Rake and in (33) for LMMSE.

$$\mathbf{w}_{RAKE} = \mathbf{H}_c^H \quad (32)$$

$$\mathbf{w}_{LMMSE} = \sqrt{P_{tot}} H_c \left(P_{tot} H_c H_c^T + C_w \right)^{-1} \delta \quad (33)$$

4.4.3.2 CLBF Algorithms

In contrast to OLBf, with CL Node-B selects the beamforming weights for the UE. As such, Node-B is also aware of the transmission phase changes and can maintain an optimal channel estimation. If the UE is in soft handover, the weights selected by the serving Node-B are used and also signaled in the uplink to inform non-serving Node-Bs about the used weights. The antenna weights are selected from a limited set of possibilities also known as the codebook.

The weight selection is updated on a slot by slot basis. To select the weights, Node-B evaluates the SINR with each of the weight possibilities based on the received pilots and the weights maximizing the SINR in the current slot are selected. In general, the weight selection operation resembles the open loop Genie

algorithm, described in Section 4.4.2.2, as with both the weights maximizing the SINR are also selected based on channel impulse response. However, with CL additional delays are assumed for applying the weights in the transmitter to model the feedback delay and it is possible to have signaling errors with the weights.

The phase offset between antennas is implemented by applying a beamforming weight to each antenna. The beamforming weights $\underline{w} = [w_1 \ w_2]^H$ are adjusted every slot; in each slot, they are calculated to maximize:

$$\sum_{l=1}^L \underline{w}^H H_l(k)^H H_l(k) \underline{w} \quad (34)$$

where $H_l(k)$ is a 2×2 matrix of channels between Tx and Rx antennas for the l^{th} multipath in the k^{th} slot. The calculation in (34) is done only for the link between the UE and the serving Node-B, but the weight resulting in the highest power is selected and applied for all links. The primary pilot (DPCCH), E-DPCCH, E-DPDCH and HS-DPCCH channels are pre-coded with the primary beamforming weight vector

$$[w_1 \ w_2] = [a_1 e^{j\theta_1} \ a_2 e^{j\theta_2}] \quad (35)$$

where, as an example, the phase $\theta_i = \{0, \frac{\pi}{4}, \frac{3\pi}{4}, \frac{5\pi}{4}, \frac{7\pi}{4}\}$ with a codebook size of four. Amplitude a_i belongs to a finite set depending on the case. The beamforming phase offset is denoted by $\theta_2 - \theta_1$ and the relation of a_1 to a_2 reflects the selected codebook power offset, i.e., the power split between the Tx antennas. Different codebook options are investigated in [PX] and [PXI]. The S-DPCCH is pre-coded with the orthogonal secondary beamforming weight vector

$$[w_3 \ w_4] = [a_2 e^{j\theta_1} \ -a_1 e^{j\theta_2}] \quad (36)$$

4.4.3.3 CLBF Feedback Methods

Two distinctive feedback methods are investigated in this thesis; the absolute and the recursive feedback methods. In the absolute feedback method, the information for the whole beamforming weight vector is transmitted in every feedback period, whereas in the recursive feedback method, one bit per feedback update period is transmitted. For the recursive feedback method, the feedback bits of multiple concurrent time slots are combined to form the pre-coding weight vector. This approach has the potential to offer increased tolerance against individual signaling errors as only part of the weight vector would have incorrect information in the case of a signaling error. In addition, the recursive method requires less signaling bits per time slot, which would offer increased motivation to use such a scheme. However, compared to the absolute scheme, a single signaling error affects the weight selection for a longer time period as the full weight vector is constructed from the information over multiple time slots.

The use of a pre-coded pilot means that a channel estimate for the demodulation is directly available from the channel estimate. However, the non-beamformed

TABLE 1 The phase adjustments corresponding to the feedback commands for the time slots

| Bit | Even slot | Uneven slot |
|-----|-----------|-------------|
| 0 | 0 | $\pi/2$ |
| 1 | π | $-\pi/2$ |

channel needs to be calculated in order to derive the channel for feedback calculation. The receiver uses the already signaled beamforming weight to solve the non-beamformed channel. The applied beamforming weight in the transmitter is not necessarily the same as the assumed one in the receiver if feedback error occurs and the receiver is not aware of the feedback error. This causes error propagation for the recursive feedback method. The absolute feedback method also suffers from the error propagation but the memory effect is shorter.

The absolute feedback method is simple, as all the necessary information bits are sent in one signaling message, and does not require a specialized algorithm. However, the recursive feedback method does require an algorithm, which is described in the following subsection.

Recursive Feedback Method

The recursive feedback method for this study was adapted from downlink Closed Loop Mode 1 -transmit diversity [3GP14d]. In each slot, UE calculates the optimum phase adjustment, ϕ , for antenna 2, which is then quantized into ϕ_Q having two possible values as follows:

$$\phi_Q = \begin{cases} \pi, & \text{if } \pi/2 < \phi - \phi_r(i) \leq 3\pi/2 \\ 0, & \text{otherwise} \end{cases} \quad (37)$$

where

$$\phi_r(i) = \begin{cases} 0, & i = 2k, \forall k \in Z \\ \pi/2, & i = 2k + 1, \forall k \in Z \end{cases} \quad (38)$$

If $\phi_Q = 0$, a command '0' is send to the UE. Correspondingly, if $\phi_Q = \pi$, command '1' is send to the UE. Due to rotation of the constellation the received commands are interpreted according to Table 1, which shows the mapping between phase adjustment, ϕ_i , and received feedback command for each uplink slot.

The weight w is then calculated by averaging the received phases over two consecutive slots. Algorithmically, w is calculated as follows:

$$w = \frac{\sum_{i=n-1}^n \cos(\phi_i)}{2} + j \frac{\sum_{i=n-1}^n \sin(\phi_i)}{2} \quad (39)$$

where $\phi_i \in \{0, \pi, \pi/2, -\pi/2\}$.

5 RESEARCH TOOLS

The research tool used in this thesis is a comprehensive system level radio network simulator designed, e.g., for studying Radio Resource Management (RRM) -algorithms to obtain capacity and coverage estimates, to support standardization work and network planning by optimizing the radio network parameters. As the complexity of the radio network behavior makes it extremely hard to calculate comprehensive and accurate analytical results and, on the other hand, physical network trials would be time consuming and expensive, a configurable system level simulator with parameters for, e.g., network traffic, user terminals, network configuration, RRM algorithms and physical layer is a valuable tool for studying the radio networks performance and enhancements.

The used simulation tool enables detailed simulation of users in multiple cells with realistic call generation, propagation and fading, adopted from [3GP98], and updated according to 3GPP requirements for each research topic. In addition to the articles included in this thesis, the used simulator has been utilized in support of 3GPP standardization work, in other international articles and conferences, see, e.g., [FCMR07] and [FCRaR07], as well as in a doctoral thesis [Aho10]. The confidence analysis of the used quasi-static simulator is presented in [Aho10].

5.1 Simulator Types

The simulator implementation is often a compromise between building an accurate model of a network and keeping the computing efforts manageable. In order to reduce the complexity and computational requirements of the simulator, a division into link and system level simulators has been made. In a link level simulator, the connection between one UE and the base station is modeled on a very detailed level, e.g., chip or symbol level. The resulting link level data can be used as it is for varying studies or it can be used as an input in a system level simulator. An example of this is a so called Actual Value Interface (AVI), presented in [HSM⁺97], through which the produced link level data for received Frame Er-

TABLE 2 System level simulator classification and the main attributes

| | Static | Quasi-static | Dynamic |
|---------------------------------|----------------------------|---|---------------------------------|
| <i>Algorithms</i> | Simplified | Extensively modeled | Fully modeled |
| <i>Computational Complexity</i> | Low | Mediocre | High |
| <i>Mobility</i> | Static | Static | Yes |
| <i>Slow Fading</i> | Fixed | Fixed | Varying |
| <i>Fast Fading</i> | Fixed | Varying | Varying |
| <i>Time Domain</i> | No | Yes | Yes |
| <i>Use Cases</i> | Coverage predictions, etc. | RRM study excluding explicit mobility, etc. | Mobility study, RRM study, etc. |

ror Rate (FER) or Bit Error Rate (BER) vs. Energy per Bit to Noise Ratio (Eb/No) performance is used in the system level simulator to model the individual link performance, thus reducing the computational complexity for system level simulations. With the exception of the use of an AVI, link level simulators are out of the scope of this thesis.

System level simulators can be further classified into three main types: static, quasi-static, and dynamic. The main attributes for the different system simulator types are listed in Table 2. As the table shows, static simulators provide fast but simplified solution for quick evaluations, see, e.g., [NBL05]. For both static and quasi-static approaches, the statistical confidence is achieved by running multiple drops, i.e., independent simulation iterations. In each step, e.g., the UE locations and slow fading are randomized, but the statistics are gathered and averaged over all drops. In the dynamic simulations the statistical confidence is achieved through long simulations and mobility, i.e., the UEs are actually moving within the scenario. The simulator used to test the performance of different concepts in this thesis is a proprietary quasi-static simulator.

5.2 Simulation Flow

With the used simulator the simulation flow includes three fundamental phases: simulation setup, simulation run and finalizing the simulation. As multiple simulation drops are used in the quasi-static approach, there is also a reset phase between the drops, see Figure 31. During the simulation setup all of the objects, including the simulation scenario, RNCs, Node-Bs and UEs, are generated according to the user defined parameters. In the simulation run phase the actual simulation procedure is executed. This phase starts with a warm up period, during which the initial load for the network should reach the targeted realistic level. After the warm up period ends, the statistics collection begins. The simulation runs in a slot resolution, i.e., all relevant actions are performed and statistics are collected for each 0.667 ms slot. The relevant actions in every simulation slot con-

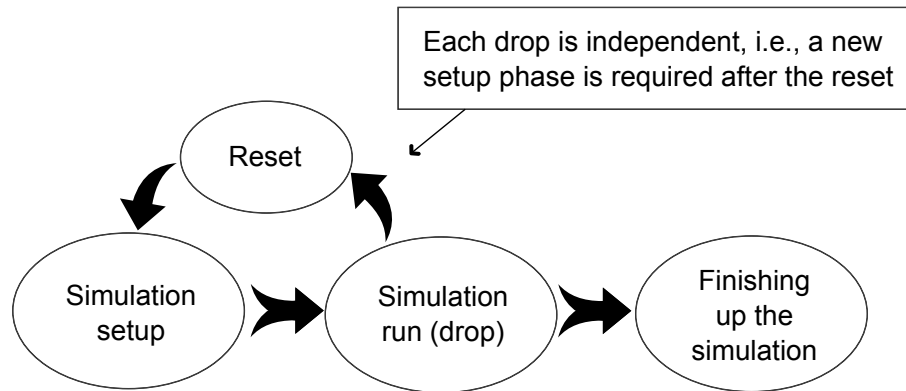


FIGURE 31 Illustration of the simulation flow

sist of, e.g., interference calculation for all active connections and adjusting the power control. All the elements involved in the simulated system (UEs, NodeBs, RNCs) execute their own actions before the simulation moves on to the next time slot. The simulation run will stay active until the last simulation time slot for the drop is reached. After the simulation run, the simulation flow resets and returns to the setup phase, providing that there are more drops to be run. In the reset phase all active variables, with the exception of statistics, are reset, e.g., UEs and existing connections are destroyed. After the parameter defined number of drops have been simulated, at the end of the last drop the statistics over all drops will be saved and the simulation is finalized by destroying all the created elements.

6 SIMULATION RESULTS

Uplink is characterized by power limited terminals and high interference levels and, as such, is often considered to limit the overall coverage of services. As the users are producing and uploading more and more media content themselves instead of just consuming it, the bandwidth requirements for the uplink continues to increase noticeably. Moreover, with certain service types, such as speech, the high number of simultaneous connections can strain the available radio network resources. In the following subsections these challenges are addressed via multiple HSUPA enhancements.



This chapter presents the results obtained with the system level simulator introduced in Chapter 5. The scenarios and assumptions used in the studies are presented first, followed by the simulation result analysis. Regarding the results, interference coordination and dual-carrier in HSUPA are addressed first in studies presented in articles [PI] and [PII], respectively. These topics are followed by articles [PIII] and [PIV] regarding studies on coverage extension and battery saving possibilities in HSUPA. Articles [PV] through [PXIII] focus on different schemes for uplink transmit diversity, namely Switched Antenna Transmit Diversity (SATD) and Beamforming Transmit Diversity (BFTD).

6.1 Simulation Scenarios and Assumptions

The studies presented in this thesis are conducted in hexagonal macro cellular scenarios utilizing Wrap-Around (WA). The purpose of wrap-around is to model the interference correctly also for the outer cells. This is achieved by limiting the UE placement around the actual simulation area, but replicating the cell transmissions around the whole simulation area to offer a more realistic interference situation throughout the scenario. As such, a UE is able to make a handover to the outer cells.

Two different tiered WA layouts are used in this thesis: in the first WA scenario, two tiers are used to form 21 cells with 7 Node-Bs. In the second, and

- Two wrap-around scenarios

- Three tiers 
 - Hexagonal network of 19 sites
3 sectors per site
- Two tiers 
 - Hexagonal network of 7 sites
3 sectors per site

- Non-wrap-around scenarios

- 1 site with 1-3 sectors (used mainly for debugging purposes)

- Statistics gathered from all sectors

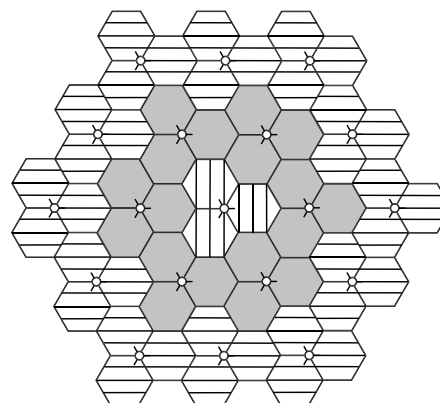


FIGURE 32 Simulation scenario with wrap-around

more often used scenario, three tiers are used to form 57 cells with 19 Node-Bs. Figure 32 illustrates the network structure of the used wrap-around scenarios.

The main parameters for the simulations are presented in conjunction with the included articles [PI] - [PXIII]. The used channel models are based on a tapped-delay line model in coherence with the International Telecommunication Union (ITU) recommendations [IR97]. The model is characterized by the number of taps, the time delay relative to the first tap, the average power relative to the strongest tap, and the Doppler spectrum of each tap. The used power profiles are modified from the ITU power delay profiles so that the delay and power between paths are normalized to at least one chip-time [3GP98].

6.2 Interference Coordination Results

Section 4.1 presents the motivation and principles of interference coordination in HSUPA networks. In brief, Interference Coordination (IC) alternates the priorities for user transmission periods throughout the network to achieve reduced interference levels and higher performance. Article [PI] evaluates the IC performance against a network without IC in a high load situation. A large variety of combinations including, e.g., different schedulers, user splits and RoT targets are investigated.

The results presented in article [PI] indicate that IC can bring gain in certain scenarios. As can be expected, in general the highest gains are attained with heavily loaded network. However, based on the results, the gain with the investigated setup is limited to users already in good channel conditions and, on top of that, the gain comes at the expense of fairness and even leading to users already in poorer channel conditions to experience performance loss. Moreover, it

is shown that the major part of the gain comes from splitting users into different groups and scheduling these groups without any network wide interference coordination. As such, results comparable to the investigated scheme could also be achieved without network wide coordination and by just adjusting the scheduling parameters. As the investigated scheme is based on time domain coordination, there are less available transmission periods for each user group when compared to the scheme without IC. As such, in low load situations the imbalance in fairness is most noticeable as the transmissions are more limited by transmission periods than RoT. A similar effect can be seen when comparing low RoT targets to higher RoT targets.

In conclusion, the IC scheme presented in [PI], has the potential to offer limited performance improvements, albeit at a cost. As such, there are limited amounts of potential use cases. One option is to use UL DTX, which is not used in this study but is investigated in, e.g., article [PIII], in combination with IC. UL DTX could potentially have reduced the interference levels more, resulting in higher performance together with IC, especially with a suitable service such as VoIP. Additionally, the required UE bandwidth is relatively low with VoIP, which could make it easier to modify the scheduling to favor the edge users more, thus improving IC fairness and potentially eliminate the losses. However, modifications to scheduling depend heavily on the suitable center / edge user distribution, i.e., scheduling should guarantee quality of service for both user groups.

6.3 Dual-Carrier Results

As described earlier in Section 4.2, Dual-Carrier (DC) capability for HSUPA was introduced to 3GPP Release 9 through the standardization work supported in part by the results presented in article [PII]. The article presents simulation results regarding how dual-carrier capability can enhance HSUPA performance in comparison to using only a single carrier.

Based on the results presented in [PII], with single carrier the UEs have reserve transmit power available especially in smaller cells. As the results show, with dual-carrier operation in smaller cells with low load this reserve power can roughly double the burst throughput. In larger cells the UEs are more power limited and the gains are focused on users in good channel conditions, as expected, as these users have the most reserve power available. With DPCCCH gating, i.e., UL DTX, the UEs in worse channel conditions obtain additional gain from dual-carrier operation especially with higher loads. This indicates that the control channel overhead is getting higher in dual-carrier systems compared to two single carrier systems. In conclusion, based on the results, dual-carrier operation is a viable way to improve peak UE throughput for users in good channel conditions and especially with low cell loads.

6.4 Range Extension Results

As described earlier in Section 3.1, HSUPA defines two Transmission Time Interval (TTI) lengths: an optional 2 ms TTI and a mandatory 10 ms TTI. These two have different properties defining the purpose for which they should be used. The 2 ms TTI provides shorter transmission periods and longer periods of silence, but it requires higher instantaneous transmission power. Alternatively, the 10 ms TTI requires lower transmission power, but the transmission period is longer, thus reducing the number of possible retransmissions and possible battery saving opportunities with Uplink Discontinuous Transmission (UL DTX). Article [PIII] investigates the issues with these two TTI lengths from the perspective of capacity and achievable battery saving opportunities with VoIP over HSUPA.

One of the main results in article [PIII] is that UL DTX is able to provide noticeable gains when compared to operation without UL DTX. This gain is most noticeable in highly loaded cells, where a large number of UEs generate high interference, thus adversely affecting the cells capacity. The results also show that a mixture of TTIs is able to provide gain over utilizing a single TTI length. With the mixed TTI approach the larger coverage of the longer 10 ms TTI and better battery saving opportunities of the shorter 2 ms TTI can be combined, thus providing battery savings while avoiding coverage problems. These battery savings are achieved due to UEs with better channel conditions being able to utilize the shorter 2 ms TTI, while the more limited UEs utilize the 10 ms TTI for better coverage. The most significant improvements of the mixed TTI approach can be seen in larger cells, where the 10 ms TTI is more often needed as the 2 ms TTI consumes more power resources from already power limited cell edge UEs. It is shown in [PIII], that in the simulated scenarios a mixed TTI configuration with roughly a third of the users configured to 10 ms TTI and the rest for 2 ms TTI provides a comparable capacity level with the pure 10 ms TTI setup, while at the same time providing noticeably improved battery saving opportunities.

The mixed TTI study, presented in article [PIII], is further extended in article [PIV] by proposing a 2 ms TTI Range Extension (RE) -scheme. With RE, the 2 ms TTI transmissions are repeated if the UE is found to be coverage limited, thus eliminating the need to configure two different TTIs for the cell. This enables the scheduler to manage only one TTI instead of two, and as such reduce the number of required radio link reconfiguration procedures. Other benefits include a better capability for coverage limited UEs to meet tighter delay requirements with various services and more possibilities for coverage limited UEs to utilize UL DTX.

The results show that in the smaller cells RE performs on the same level as pure 2 ms TTI setup. This is due to the fact that the smaller cells are interference limited rather than power limited, and as such there is no need for UEs to use RE. It is important to note, that while RE improves the probability to get transmissions through in power outage situation, it does not reduce the interference. In larger cells, where the mixed TTI approach investigated in article [PIII] is seen to

be most beneficial, range extension clearly outperforms the pure 2 ms TTI, both with and without UL DTX. Additionally, in larger cells the cost of RE in terms of possible battery saving opportunities is very minimal when compared to the 2 ms TTI. Taking both the noticeable coverage improvement and the minimal increase in Tx antenna activity into account, the benefits offered by RE clearly outweigh the negative effects.

6.5 Transmit Diversity Results

Transmit diversity is considered as one way to improve system capacity and performance. In general, transmit diversity exploits the principle of providing the receiver with multiple faded replicas of the same information-bearing signal. The results for transmit diversity are presented in this section. The results of different schemes are divided into following subsections: the results for Switched Antenna Transmit Diversity (SATD), introduced in Section 4.4.1, are presented first in Section 6.5.1. The results for Open Loop Beamforming (OLBF), introduced in Section 4.4.2, are presented next in Section 6.5.2. Finally, the results for Closed Loop Beamforming (CLBF), introduced in Section 4.4.3, are presented in Section 6.5.3.

6.5.1 Results on Switched Antenna Transmit Diversity

Switched Antenna Transmit Diversity (SATD) is a transmit diversity scheme where only one Tx antenna is active at any given time even though the UE is equipped with multiple Tx antennas. The investigated SATD algorithms are open loop algorithms, i.e., the algorithms function without additional feedback information for selecting the Tx antenna. This section presents the results for SATD investigated in articles [PV], [PVI] and [PVII]. The results cover the performance of five different algorithms in system level in various conditions against baseline performance without transmit diversity. These conditions include various non-ideal conditions which occur in real implementations, e.g., varying load conditions, antenna imbalance, correlation and the existence of multiple different SATD algorithms in the network simultaneously.

Regarding the different algorithms introduced in Section 4.4.1.1, the results in article [PV] show that the Genie (TX1) algorithm, can provide gains with all cell loading points and channels. However, with the much faster changing Vehicular A (VehA) channel the gains are significantly lower. With the more practical algorithms the performance varies: with some algorithms gains can be achieved, but improper switching decisions with other algorithms can lead to loss in performance even in slower changing Pedestrian A (PedA) channel. The faster changing VehA channel is an even more difficult environment for the practical algorithms operating without feedback about the channel state. TX5, based only on periodic changing of Tx antennas, results in poorest performance and can result even in losses. Practical algorithms TX2 and TX4, utilizing available averaged

channel information, are able to provide gain but do not reach the upper limit. **TX3** indicates gain with low load, but once the load increases the performance gain turns into a loss.

In addition, the power selection algorithms studied in article [PV] do not show very significant difference. In general, **Pwr keep**, i.e. keeping the same DPCCH power in use for both antennas regardless of the switch, is showing slightly higher performance. However, the antennas in [PV] are considered to be rather similar with the exception of channel conditions and a relatively small short term antenna imbalance.

The gain from SATD is caused mainly by additional diversity and due to UEs being able to utilize the antenna which is in better channel condition, leading to a reduction in the average required DPCCH and total transmission power. Due to reduced transmission power the interference levels are also reduced and the Node-B is able to schedule higher allocations to the UEs.

Regarding the varying load conditions, studied in article [PVI], the gain from SATD is more noticeable either in cells with higher loads, or in larger cells where the UEs are more likely to be power limited. This is due to the fact that with lower loads in small cells, the transmit power is not generally an issue and power savings when SATD is assumed do not increase throughput, but when offered load increases gain from antenna switching becomes more apparent as the performance enhancements from SATD are mainly due to lowered interference conditions and transmit power requirements. By increasing the offered load, interference becomes more and more dominant, causing DPCCH power to be increased accordingly. Due to being able to utilize the antenna which has the higher channel gain, SATD uses less DPCCH and total power. Thus, SATD causes less interference which in turn enables Node-B to schedule higher allocations. The result of higher allocations is again increased interference within the system, but with greater traffic-to-pilot ratio. Moreover, the reduction in DPCCH transmit power helps especially the performance of power limited cell edge users as these UEs can utilize the decreased DPCCH power by increasing the transmit power of the data channel, thus having higher probability for a successful transmission. In general, SATD improves the systems ability to serve higher offered loads.

Regarding the non-ideal conditions, e.g., antenna imbalance and correlation investigated in article [PVII], it was shown that especially long term antenna imbalance can reduce the achievable gain by SATD since it reduces the time when the second antenna is better. The results indicate that assuming -4 dB long term imbalance decreases cell throughput when compared to ideal cases without imbalance with both the ideal **TX1** and the practical **TX2** algorithms. Even when only short term imbalance is assumed a small consistent drop in throughput is observed.

It was also shown in [PVII] that antenna correlation, present inherently in real implementations, has an impact on SATD performance especially in PedA channel. The investigated SATD algorithms have gain over baseline with a low 0 and 0.3 correlation and the cell throughput with practical algorithms can result in slight loss when the correlation increases to 0.7. The practical algorithms do

not suffer from increased correlation as much as the ideal **TX1** algorithm. In the faster changing VehA channel the practical algorithms are not able to keep up with the rapid changes in channel conditions and as such the gains over baseline are smaller even with zero correlation.

In a real network, it is possible that UEs will have different antenna selection schemes that may affect the systems level performance. Using this kind of mixture of different SATD algorithms simultaneously might lead to system performance being lowered close to, or below baseline level, as shown in article [PVII].

6.5.2 Results on Open Loop Beamforming

Beamforming is a form of transmit diversity where the overall antenna beam from multiple Tx antennas is shaped in the direction of a target receiver based on the information on channel phases. Open Loop Beamforming (OLBF) applies various receiver-independent algorithms at the transmitter side to combat the fading channel without additional feedback from the receiver. A practical scheme relying on existing power control commands to calculate the beamforming weight vector is investigated in article [PVIII]. This scheme is benchmarked against an ideal algorithm, capable of always selecting the optimal weight vector, in various conditions such as different cell sizes, varying cell loads, different channel models and receivers.

The results in [PVIII] show that the investigated practical scheme is able to provide gains in the slower changing PedA channel, but with more complex and faster changing VehA channel the power control command dependent practical algorithm is not able to provide gains over the baseline. This is due to the fact that the power control dependent algorithm is not able to follow up on the faster changing VehA channel fast enough. This trend does not change with different receivers, but in general with LMMSE the absolute performance is higher, while the relative gains remain similar regardless of the receiver. Similarly, the relative gains from OLBF are slightly larger with lower cell loads or larger cells.

As seen in [PVIII], the gains with beamforming are fundamentally due to the signal energy being received more efficiently and, on the other hand, the power of the interfering signals being lower due to the spatial filtering. As the UEs are required to use less power than in the baseline case and the power control is able to reduce the transmit powers, less power is needed to get the transmissions through and higher bit rates can be scheduled without generating more interference to the cell or exceeding the maximum UE transmit power.

6.5.3 Results on Closed Loop Beamforming

In contrast to OLBF, with Closed Loop Beamforming (CLBF) the the overall antenna beam from multiple Tx antennas is shaped in the direction of a target receiver based on the information on channel phases provided from the receiver side. The performance of CLBF is studied in articles [PIX] - [PXIII]. The performance of a CLBF scheme without pilot pre-coding is investigated in article

[PIX] in various conditions such as different cell sizes, varying cell loads, different channel models and receivers. Followed by this study, the performance of a CLBF scheme with pre-coded pilots is investigated in articles [PX] - [PXIII]. This latter study also considers the performance in various conditions such as different cell sizes, varying cell loads, different channel models and receivers, but also investigates the impact of different codebook sizes, delays and update intervals related to antenna weights, the impact of a weight vector amplitude component, the performance of two different feedback methods and applicability of signaling the used pre-coding weights back to the Node-B in order to ensure correct decoding at the Node-B receiver.

According to the simulation results presented in article [PIX] the CLBF is beneficial in all of the studied cases, although the gains are higher in the slower changing PedA channel than in faster varying VehA, which is due to a more frequency selective channel and higher UE velocity of VehA. However, in contrast to OLB, CLBF is able to provide clear gains also with VehA. The relative gains from CLBF are larger with higher cell loads or larger cells, and the simulations show that in the VehA channel, which has a richer multipath profile, LMMSE brings a clear gain over the Rake receiver. However, the relative performance improvement related to the CLTD is almost equal for both receivers. The gain mechanism of CLBF is similar to other transmit diversity algorithms, such as open loop beamforming; a better receiver SINR can be achieved by using two Tx antennas with adjusted phases without increasing the total transmission power, which enables scheduling of UEs with higher bit rates.

Based on the study presented in article [PX], the largest studied codebook size of eight provides the best performance, as expected. However, the size of the codebook can be reduced from eight to four with only a few percent penalties in performance. Reducing the size of the codebook further to two weights results in more significant performance loss. Additionally, it is shown that the pre-coding weight update interval and delay are critical especially for channels with high vehicular speeds and short coherence time of channel. In terms of a weight update interval the best performance is achieved with the shortest possible interval. With long intervals the performance in a faster fading VehA channel can be compromised. As increasing the codebook size and shortening the weight signaling interval increases the signaling overhead, it is important to find a suitable balance with performance. Finally, increasing the signaling feedback delays results in similar effects as increasing the update intervals, thus additional feedback delays should be avoided.

As shown in article [PXI], including amplitude components into the codebook increases the performance of cell edge users and the higher the antenna imbalance the higher the benefit for these users. With amplitude components CLBF can adapt to the power limitation caused by the long distance to the serving Node-B and also mitigate the impact of power loss caused by antenna imbalance. As such, the amplitude component can provide increased coverage and fairness in the system. However, the cell center UEs in better channel conditions do not gain from the additional amplitude components. Similarly, as the cell center UEs

form a major part of it, the systems performance will decrease in all situations if any of the studied amplitude components are included in the CLBF codebook. It is also important to note, that including the amplitude component will increase the number of available beamforming weights, thus also increasing the feedback requirements by generating more signaling overhead in the downlink direction.

According to the studies on feedback methods, presented in article [PXII], both of the investigated feedback methods are capable of providing gain over the baseline in simulated conditions. When comparing the performance between the recursive and the absolute feedback methods, the benefit of having the absolute feedback comes from increased tolerance for weight signaling bit errors, translating into higher achievable throughput rates. Moreover, it is shown that the higher the BER, the higher is the benefit from absolute feedback over recursive as the longer memory effect with the recursive feedback signaling error propagation results in a large enough impact to overcome the increased individual signaling error tolerance from distributing the weight signaling bits over multiple time slots. However, the recursive feedback method requires less signaling bits per slot, thus reducing the signaling overhead. As such, the expected BER is in a major role when selecting a suitable feedback method.

The study on uplink weight signaling for decoding error correction, presented in article [PXIII], shows, that the benefits from improved error correction can increase the performance over the case without uplink signaling especially with higher BER and the difference in performance can already be seen with the error rates below 10%. However, as uplink weight signaling requires additional signaling bits, the method may not be justified if weight feedback BER is expected to be low. It is also seen in [PXIII] that the improvement is more noticeable with the recursive feedback method, which corroborates with the more drastic error specific propagation with the said method, as seen in [PXII]. However, these results are obtained without uplink signaling errors and as such present the upper bound on achievable performance. Additionally, even though the investigated uplink signaling method is relatively straightforward, new bi-directional weight signaling is needed and as such introduces new challenges.

7 CONCLUSION

The purpose of this thesis is to address variety of performance related aspects in terms of Third Generation (3G) mobile networks. From a practical perspective, wireless network sets a very demanding environment for different services due to, e.g., limited User Equipment (UE) battery power, transmission delays, packet loss and varying network performance. This thesis addresses the aforementioned challenges by evaluating different uplink transmit diversity schemes, battery saving opportunities, interference coordination and dual-carrier uplink. The studies are conducted with the help of a time driven quasi-static system level simulator where, e.g., fading, propagation and RRM functionality is explicitly taken into account.

Interference Coordination (IC) is addressed in this thesis as potential uplink performance enhancement. The results of the studied scenarios show that even though IC can bring gain in certain scenarios, the majority of the gain comes at the expense of fairness leading to users that already have higher throughput benefiting most from the situation. Moreover, it is shown that gain can be achieved without any network wide interference coordination, thus the studied IC scheme is not such an attractive option. However, by combining IC with other techniques, such as the Uplink Discontinuous Transmission (UL DTX), the studied IC scheme could be reconsidered in future studies, especially for highly loaded small cells.

Followed by the standardization of downlink dual-carrier in Release 8, this thesis evaluates the motivation and applicability of dual-carrier in uplink. The results show that the UEs have reserve power available for dual-carrier operation especially in small cells. Based on the dual-carrier simulations, with low loads the burst throughput can be close to twice the throughput of a single carrier. With UL DTX, the gains from uplink dual-carrier are more substantial also with higher loads. The studies in the Third Generation Partnership Project (3GPP) led to the standardization of uplink dual-carrier in Release 9.

Apart from addressing the performance from a radio network point of view, this thesis evaluates the possible battery saving opportunities for UEs through continuous packet connectivity features and switching off additional antennas. The results show that the uplink discontinuous transmissions are highly benefi-

cial providing battery saving opportunities and at the same time increasing the uplink capacity due to decreased interference. The achieved battery saving gains are higher with 2 ms TTI than with 10 ms TTI, but the coverage can be compromised in some situations by utilizing only the 2 ms TTI. As such, utilizing a mixture of both available TTIs in the uplink can extend the coverage whilst providing optimized battery saving opportunities. The mixed TTI study is further extended by proposing a 2 ms TTI Range Extension (RE) -scheme, where the transmissions are repeated if the UE is found to be coverage limited, thus eliminating the need to configure two different TTIs for the cell. The results show that RE is most beneficial in larger cells, where it brings noticeable coverage improvement with minimal increase in Tx antenna activity into account. In the smaller cells range extension performs on the same level as pure 2 ms TTI setup.

Besides evaluating the aforementioned performance enhancements, this thesis evaluates in detail the numerous uplink transmit diversity schemes. These include, e.g., Transmit (Tx) antenna switching scheme with multiple algorithms for deciding the Tx antenna, and both Open Loop Beamforming (OLBF) and Closed Loop Beamforming (CLBF) transmit diversity schemes with simultaneous transmission from two Tx antennas. Based on the results, Switched Antenna Transmit Diversity (SATD) is capable of bringing gain to the system, but the performance and the amount of gain depends heavily on the chosen algorithm and channel conditions, and improper switching decisions can lead to loss of performance. The gain from SATD is caused mainly by additional diversity and due to UEs being able to utilize the antenna which is in better channel condition, leading to a reduction in the average required DPCH and total transmission power.

Regarding beamforming, the studied Open Loop (OL) -scheme is able to provide gains in a slower changing channel, but with the more complex and faster changing channel the power control command dependent practical algorithm is not able to provide gains over the baseline. This is due to the fact that the power control dependent algorithm is not able to follow up on the faster changing channel fast enough. In contrast to the OL -scheme, the CLBF is beneficial in a wide variety of studied cases, including the faster varying channels problematic for the studied OLBF -scheme. The beamforming gain mechanism is similar to other transmit diversity approaches; a better receiver SINR can be achieved by using two Tx antennas with adjusted phases without increasing the total transmission power, which enables scheduling of UEs with higher bit rates. The studies in 3GPP led to the standardization of uplink CLTD in Release 11.

YHTEENVETO (FINNISH SUMMARY)

Ensimmäiset kolmannen sukupolven (3G) langattomat WCDMA (Wideband Code Division Multiple Access) tekniikkaa käyttävät 3G-verkot otettiin käyttöön jo vuonna 2002. Tämän jälkeen niin 3G-verkkojen suorituskyky kuin määrätkin ovat kasvaneet merkittävästi ja niiden tarjoamat tiedonsiirtonopeudet ovat saavuttaneet mittavan suosion käyttäjien keskuudessa. Monipuolisten palveluiden tarjoaminen vaatii kuitenkin alati suurempia tiedonsiirtonopeuksia, jotta edelleen kasvavaan käyttäjämäärään sekä tiedonsiirron volyyymiin pystytään vastaamaan. Tästä johtuen 3GPP:n (Third Generation Partnership Project) toimesta tutkitaan edelleen keinoja WCDMA -tekniikan suorituskyvyn parantamiseksi.

WCDMA -tekniikan kehityksen ensimmäinen evoluutio tunnetaan nimellä HSPA (High Speed Packet Access), joka voidaan jakaa tukiasemalta matkaviestimelle tapahtuvaan alalinkin liikenteeseen suunnattuun HSDPA (High Speed Download Packet Access) -laajennukseen ja matkaviestimeltä tukiasemalle tapahtuvaan ylälinkin liikenteeseen suunnattuun HSUPA (High Speed Uplink Packet Access) -laajennukseen.

Kolmannen sukupolven verkkoja käyttävien asiakkaiden volyyymi on niin suuri, että vaikka kilpailevia ja kehittyneempiä tekniikoita on jo olemassa, 3G on ylivoimaisesti hallitseva langaton laajakaistatekniikka maailmalla. Operaattorit ovat investoineet suuria rahamääriä olemassa oleviin verkkoihin, joiden uusiminen kokonaan ei olisi aina kustannustehokasta. Näistä syistä jo olemassa olevien verkkojen elinkaarta jatketaan ja suorituskykyä kasvatetaan edelleen. Uudempien verkkotekniikoiden, kuten LTE:n (Long Term Evolution), yleistymisestä huolimatta kolmannen sukupolven verkkoihin liittyvä tutkimus on edelleen hyvin aktiivista ja ajankohtaista, myös koska usein tietty tutkimuksen aiheena oleva tekninen parannus ei rajoitu pelkästään yhteen verkkotekniikkaan, vaan hyväksi havaittuja ratkaisuja käytetään useammassa verkkotekniikassa.

Tässä väitöskirjatyössä tutkitaan HSUPA-matkaviestinverkkojen suorituskykyä, mahdollisia parannuksia sekä ongelmakohtia. Langaton matkaviestinverkko asettaa palveluille haasteelliset toimintaolosuhteet mm. erilaisten viiveiden, virheiden sekä radioresurssien hallinnan myötä. Tämä väitöskirjatyö pyrkii vastaamaan näihin haasteisiin tutkimalla eri lähetysdiversiteettivaihtoehtoja, tehonsäästömahdollisuuksia, häiriön koordinoitua sekä taajuuskaistojen lisäämistä ylälinkkiin. Tutkimusmenetelmänä käytetään ohjelmistopohjaista radioverkkosimulaattoria, jolla pyritään mallintamaan reaali maailman matkaviestinjärjestelmää hyvin tarkasti. Simulaattorissa käytetyt mallit mm. signaalin etenemiselle, häilymälle sekä radioresurssien hallinta-algoritmeille ovat yleisesti hyväksytyjä ja tunnettuja.

Yksi teoreettinen mahdollisuus parantaa solun laidalla olevien käyttäjien suorituskykyä on suorittaa häiriön koordinoitua ylälinkissä. Usein juuri näillä käyttäjillä käytettävissä oleva lähetysteho on rajoitettu ja ylimääräinen häiriö vain huonontaa tilannetta. Väitöskirjatyössä tutkitaan, kuinka aikajakoinen koko verkon laajuinen lähetyksien koordinoitua voisi parantaa tilannetta. Lähetyk-

set pyritään koordinoimaan siten, että solun laidalla olevien käyttäjien kanssa samanaikaisesti saisivat lähettää vain niitä ympäröivissä soluissa keskellä solua olevat käyttäjät.

Väitöskirjatyössä tutkitaan myös mahdollisuutta lisätä hyvässä tilanteessa olevien käyttäjien maksimitiedonsiirtonopeuksia lisäämällä käytössä olevia taajuuskaistoja, samalla vähentäen lähetyksistä syntyvää häiriötä. HSPA:n alalinkissä tämä on jo tehty aiemmin, mutta ylälinkissä on huomioitava päätelaitteiden huomattavasti rajoittuneempi teho, tehonsäätö sekä ohjauskanavien tuoma häiriö.

Radioverkon toiminnan ja palvelunlaadun takaamisen lisäksi merkittävä osa-alue hyvän käyttäjäkokemuksen osalta on myös päätelaitteen akunkulutus. Väitöskirjatyössä tutkitaan, millaiset tehonsäätömahdollisuudet ohjauskanavien lähetyksien rajoittamisella voidaan saavuttaa. Lähetyksiä rajoitettaessa on erityisen tärkeää huomioida, että tehonsäätöt eivät saa vaarantaa palvelun laatua saati verkon toimintaa. Tehonsäätömahdollisuuksia tutkitaan myös käyttämällä eripituisia lähetysvälejä eri suhteissa. Lyhyemmällä väleillä yksittäisen lähetyksen pituus on lyhyempi, mutta vaadittava energia suurempi. Vastaavasti pidemmillä väleillä yksittäisen lähetyksen pituus on pidempi, mutta energia pienempi. Pidempien lähetysvälien etuna on suurempi peittoalue, mutta haittapuolena rajoitetumpi tiedonsiirtonopeus ja pidemmät lähetyksiantennien aktiiviset jaksot. Lyhyempien lähetysvälien rajoitetun peittoalueen ongelman ratkaisemiseksi tässä väitöskirjassa tutkitaan tekniikkaa, jossa yksittäisen lähetyksen sijaan lähetetään nopea sarja lähetyksiä.

Väitöskirjan laajin kokonaisuus keskittyy ylälinkin lähetyksidiversiteetin tutkimiseen, jossa aihepiiriin lukeutuvat keilanmuodostus- ja antenninvaihtotekniikat. Ylälinkin lähetyksidiversiteetissä päätelaitteessa on käytössä useita lähetyksiantenneja. Antenninvaihtotekniikoissa vain yksi lähetyksiantenni on kerrallaan käytössä ja käytettävä antenni pyritään valitsemaan suosien lähetyksiantennia, joka on edullisemmassa kanavatilantessa. Keilanmuodostuksessa on samanaikaisesti käytössä useita lähetyksiantenneja, joilla lähetyksestä muodostetaan suunnattu keila hyödyntäen kanavatilannetta ja säätämällä antennien välistä vaihetta sen mukaisesti. Keilanmuodostukseen liittyvässä tutkimuksessa hyödynnetään sekä avoimen, että suljetun silmukan menetelmää. Avoimen silmukan menetelmässä päätelaite tekee itsenäisesti lähetyksiantenneihin liittyvät päätökset, kun taas suljetun silmukan menetelmässä tukiasema osallistuu aktiivisesti päätöksentekoon.

REFERENCES

- [3GP98] 3GPP TR 101 112 (UMTS 30.03). Selection procedures for the choice of radio transmission technologies of the UMTS, April 1998.
- [3GP02] 3GPP TS 25.211 v3.12.0. Physical channels and mapping of transport channels onto physical channels (FDD), September 2002.
- [3GP07a] 3GPP TS 25.308 v6.4.0. High speed downlink packet access (HSDPA), overall description, stage 2 (Release 6), March 2007.
- [3GP07b] 3GPP TS 25.903 v7.0.0. Continuous connectivity for packet data users (Release 7), March 2007.
- [3GP10a] 3GPP TS 25.214 v7.17.0. Physical layer procedures (FDD) (Release 7), December 2010.
- [3GP10b] 3GPP TS 25.215 v9.2.0. Physical layer measurements (FDD) (Release 9), March 2010.
- [3GP10c] 3GPP TS 25.321 v7.19.0. Medium Access Control (MAC) protocol specification (Release 7), December 2010.
- [3GP11a] 3GPP TR 25.863 v11.0.0. Uplink transmit diversity for high speed packet access (HSPA) (Release 11), December 2011.
- [3GP11b] 3GPP TS 25.319 v9.7.0. Enhanced uplink, overall description, stage 2 (Release 9), December 2011.
- [3GP11c] 3GPP TSG-RAN WG1 #66bis, R1-113408, Nokia Siemens Networks, Nokia. Summary of the of the uplink closed loop transmit diversity performance results, October 2011.
- [3GP12a] 3GPP TR 25.213 v11.2.0. Spreading and modulation (FDD), June 2012.
- [3GP12b] 3GPP TS 25.214 v9.8.0. Physical layer procedures (FDD) (Release 9), March 2012.
- [3GP12c] 3GPP TS 25.321 v9.10.0. Medium Access Control (MAC) protocol specification (Release 9), December 2012.
- [3GP13a] 3GPP TS 25.306 v11.8.0. UE Radio Access capabilities (Release 11), December 2013.
- [3GP13b] 3GPP TS 25.319 v11.8.0. Enhanced uplink, overall description, stage 2 (Release 11), December 2013.
- [3GP13c] 3GPP TS 25.331 v9.17.0. Radio Resource Control (RRC) protocol specification (Release 9), December 2013.

- [3GP13d] 3GPP TS 25.433 v9.10.0. UTRAN Iub interface Node B Application Part (NBAP) signalling (Release 9), December 2013.
- [3GP14a] 3GPP. Overview of 3GPP Release 11 v0.1.9, June 2014.
- [3GP14b] 3GPP. Third generation partnership project homepage, <http://www.3gpp.org>. Cited, June 2014.
- [3GP14c] 3GPP. Third generation partnership project homepage, RAN WG1 (Radio layer 1), <http://3gpp.org/RAN1-Radio-layer-1>. Cited, July 2014.
- [3GP14d] 3GPP TS 25.214 v11.8.0. Physical layer procedures (FDD) (Release 11), March 2014.
- [3GP14e] 3GPP TS 25.308 v11.8.0. High speed downlink packet access (HSDPA), overall description, stage 2 (Release 11), March 2014.
- [Aho10] Kari Aho. *Enhancing System Level Performance of Third Generation Cellular Networks Through VoIP and MBMS Services*. PhD thesis, Faculty of Information Technology, University of Jyväskylä, 2010.
- [BC13] M. Behjati and J. Cosmas. Self-organizing network interference coordination for future LTE-advanced networks. In *Broadband Multimedia Systems and Broadcasting (BMSB), 2013 IEEE International Symposium on*, pages 1 – 5. IEEE, 2013.
- [BGL⁺08] Wei Bai, Yuehong Gao, Jing Liu, Xin Zhang, and Dacheng Yang. A novel resource allocation method for HSUPA with successive interference cancellation. In *Vehicular Technology Conference, 2008. VTC 2008-Fall. IEEE 68th*, pages 1 – 5. IEEE, 2008.
- [BJ06] M. Bertinelli and J. Jaatinen. VoIP over HSUPA: link level performance study. In *Wireless Communication Systems, 2006. ISWCS '06. 3rd International Symposium on*, pages 485 – 489. IEEE, 2006.
- [BPG⁺09] G. Boudreau, J. Panicker, Ning Guo, Rui Chang, Neng Wang, and S. Vrzic. Interference coordination and cancellation for 4G networks. In *Communications Magazine, IEEE (Volume:47 , Issue: 4)*, volume 47, pages 74 – 81. IEEE, 2009.
- [BPS98] E. Biglieri, J. Proakis, and S. Shamai. Fading channels: Information-theoretic and communications aspects. In *Information Theory, IEEE Transactions on*, volume 44, pages 2619 – 2692. IEEE, 1998.
- [Bra83] D.H. Brandwood. A complex gradient operator and its application in adaptive array theory. *Communications, Radar and Signal Processing, IEE Proceedings F*, 130(1):11 – 16, February 1983.

- [CCRa⁺08] Tao Chen, G. Charbit, K. Ranta-aho, O. Fresan, and T. Ristaniemi. VoIP end-to-end performance in HSPA with packet age aided HSDPA scheduling. In *Personal, Indoor and Mobile Radio Communications, 2008. PIMRC 2008. IEEE 19th International Symposium on*, pages 1 – 5. IEEE, 2008.
- [dAKH⁺09] D.M. de Andrade, A. Klein, H. Holma, I. Viering, and G. Liebl. Performance evaluation on dual-cell HSDPA operation. In *Vehicular Technology Conference Fall (VTC 2009-Fall), 2009 IEEE 70th*, pages 1 – 5. IEEE, 2009.
- [Dam99] E. Damosso. *Digital mobile radio towards future generation systems: COST action 231*. Directorate General Telecommunications, Information Society, Information Market, and Exploitation Research, 1999.
- [DAO01] P. Darwood, P. Alexander, and I. Oppermann. LMMSE chip equalisation for 3GPP WCDMA downlink receivers with channel coding. In *Communications, 2001. ICC 2001. IEEE International Conference on*, volume 5, pages 1421 – 1425. IEEE, 2001.
- [DPSB08] E. Dahlman, S. Parkvall, J. Skold, and P. Beming. *3G Evolution: HSPA and LTE for Mobile Broadband*. Elsevier Ltd, second edition, 2008.
- [DWKT07] C. Delgado, J. Wigard, T.E. Kolding, and J. Tito. Optimizing link efficiency for gated DPCCH transmission on HSUPA. In *Personal, Indoor and Mobile Radio Communications, 2007. PIMRC 2007. IEEE 18th International Symposium on*, pages 1 – 5. IEEE, 2007.
- [EVBH09] J. Eberspächer, H-J Vögel, C. Bettstetter, and C. Hartmann. *GSM - Architecture, Protocols and Services*. John Wiley & Sons, third edition, 2009.
- [FCMR07] O. Fresan, Tao Chen, E. Malkamaki, and T. Ristaniemi. DPCCH gating gain for Voice over IP on HSUPA. In *Wireless Communications and Networking Conference, 2007.WCNC 2007. IEEE*, pages 4274 – 4278. IEEE, 2007.
- [FCRaR07] O. Fresan, Tao Chen, K. Ranta-aho, and T. Ristaniemi. Dynamic packet bundling for VoIP transmission over Rel'7 HSUPA with 10ms TTI length. In *Wireless Communication Systems, 2007. ISWCS 2007. 4th International Symposium on*, pages 508 – 512. IEEE, 2007.
- [GWY07] Weijiang Guo, Chenwei Wang, and Dacheng Yang. Research on the potential benefit of beamforming in HSUPA. In *Wireless Communications, Networking and Mobile Computing, 2007. WiCom 2007. International Conference on*, pages 783 – 786. IEEE, 2007.

- [Hat80] M. Hata. Empirical formula for propagation loss in land mobile radio services. In *Vehicular Technology, IEEE Transactions on*, volume 29, pages 317 – 325, 1980.
- [HB03] L. Harte and D. Bowler. *Introduction to Mobile Telephone Systems - 1G, 2G, 2.5G, and 3G Wireless Technologies and Services*. Althos Publishing, second edition, 2003.
- [HBN08] L. Hanzo, J. Blogh, and Song Ni. *3G, HSPA and FDD versus TDD Networking: Smart Antennas and Adaptive Modulation*. John Wiley & Sons, second edition, 2008.
- [HKM⁺06] H. Holma, M. Kuusela, E. Malkamaki, K. Ranta-aho, and Chen Tao. VoIP over HSPA with 3GPP Release 7. In *Personal, Indoor and Mobile Radio Communications, 2006 IEEE 17th International Symposium on*, pages 1 – 5. IEEE, 2006.
- [HSM⁺97] S. Hämmäläinen, P. Slanina, Hartman M., Leppeteläinen A., Holma H., and O. Salonaho. A novel interface between link and system simulations. In *Proc. of ACTS Mobile Communications Summit*, 1997.
- [HT06] Harri Holma and Antti Toskala. *HSDPA/HSUPA for UMTS: High Speed Radio Access for Mobile Communications*. John Wiley & Sons, 2006.
- [HT07] Harri Holma and Antti Toskala. *WCDMA for UMTS - HSPA evolution and LTE*. John Wiley & Sons, fourth edition, 2007.
- [HT11] Harri Holma and Antti Toskala. *LTE for UMTS: Evolution to LTE-Advanced*. John Wiley & Sons, second edition, 2011.
- [HTT14] Harri Holma, Antti Toskala, and Pablo Tapia. *HSPA+ Evolution to Release 12: Performance and Optimization*. John Wiley & Sons, first edition, 2014.
- [HTW03] A. Hottinen, O. Tirkkonen, and R. Wichman. *Multi-Antenna Transceiver Techniques for 3G and Beyond*. John Wiley & Sons, 2003.
- [HW09] Jing Han and Haiming Wang. Principle and performance of TTI bundling for VoIP in LTE FDD mode. In *Wireless Communications and Networking Conference, 2009. WCNC 2009. IEEE*, pages 1 – 6. IEEE, 2009.
- [IR97] ITU-R. Guidelines for evaluation of radio transmission technologies for IMT-2000, recommendation, ITU-R M.1225, 1997.
- [JBG⁺09] K. Johansson, J. Bergman, D. Gerstenberger, M. Blomgren, and A. Wallen. Multi-carrier HSPA evolution. In *Vehicular Technology Conference, 2009. VTC Spring 2009. IEEE 69th*, pages 1 – 5. IEEE, 2009.

- [JHBS12] Yibo Jiang, Jilei Hou, A. Bharadwaj, and S. Sambhwani. Design aspects of closed loop beamforming transmit diversity in HSUPA. In *Communications (ICC), 2012 IEEE International Conference on*, pages 6061 – 6065. IEEE, 2012.
- [KZ00] T.P. Krauss and M.D. Zoltowski. Oversampling diversity versus dual antenna diversity for chip-level equalization on CDMA downlink. In *Sensor Array and Multichannel Signal Processing Workshop. 2000. Proceedings of the 2000 IEEE*, pages 47 – 51. IEEE, 2000.
- [KZL00] T.P. Krauss, M.D. Zoltowski, and G. Leus. Simple MMSE equalizers for CDMA downlink to restore chip sequence: Comparison to zero-forcing and RAKE. In *Acoustics, Speech, and Signal Processing, 2000. ICASSP '00. Proceedings. 2000 IEEE International Conference on*, volume 5, pages 2865 – 2868. IEEE, 2000.
- [LCSA06] Shupeng Li, Fang-Chen Cheng, Lei Song, and N. Ansari. WLC04-6: Network coordination and interference mitigation for HSDPA and EV-DO forward link. In *Global Telecommunications Conference, 2006. GLOBECOM '06. IEEE*, pages 1 – 5. IEEE, 2006.
- [LWN05] J. Laiho, A. Wacker, and T. Novosad. *Radio Network Planning and Optimisation for UMTS*. John Wiley & Sons, second edition, 2005.
- [MTS⁺11] R. Maslennikov, A. Trushanin, M. Shkerin, M. Shashanov, and P. Czerepinski. Analysis of multiple antenna transmission for HSUPA. In *ITS Telecommunications (ITST), 2011 11th International Conference on*, pages 762 – 767. IEEE, 2011.
- [NBL05] J. Niemelä, J. Borkowski, and J. Lempiäinen. Performance of static WCDMA simulator. In *Proc. IEEE International Symposium on Wireless Personal Multimedia and Communications*, volume 2, pages 1266 – 1270, September 2005.
- [Nec08] M.C. Necker. Interference coordination in cellular OFDMA networks. In *Network, IEEE (Volume:22 , Issue: 6)*, volume 22, pages 12 – 19. IEEE, 2008.
- [Nih08] Timo Nihtilä. *Performance of Advanced Transmission and Reception Algorithms for High Speed Downlink Packet Access*. PhD thesis, Faculty of Information Technology, University of Jyväskylä, 2008.
- [OOKF68] Y. Okumura, E. Ohmori, T. Kawano, and K. Fukuda. Field strength and its variability in the VHF and UHF land mobile service. In *Review of the Electronic Communication Laboratories*, volume 16, pages 825 – 873, 1968.
- [PS07] John G. Proakis and Masoud Salehi. *Digital Communications*. McGraw-Hill, fifth edition, 2007.

- [Sey05] John S. Seybold. *Introduction to RF Propagation*. John Wiley & Sons, 2005.
- [Sim07] A. Simonsson. Frequency reuse and intercell interference coordination in E-UTRA. In *Vehicular Technology Conference, 2007. VTC2007-Spring. IEEE 65th*, pages 3091 – 3095. IEEE, 2007.
- [SM09] R. Susitaival and M. Meyer. LTE coverage improvement by TTI bundling. In *Vehicular Technology Conference, 2009. VTC Spring 2009. IEEE 69th*, pages 1 – 5. IEEE, 2009.
- [SWFK12] S. Schroeter, R. Weigel, G. Fischer, and A. Koelpin. A practical beamsteering algorithm with low phase fluctuation for WCDMA/HSUPA uplink using transmit power control bits as feedback. In *Microwave Radar and Wireless Communications (MIKON), 2012 19th International Conference on*, volume 2, pages 641 – 646. IEEE, 2012.
- [SZZ14] Sharad Sambhwani, Wei Zhang, and Wei Zeng. Uplink interference cancellation in HSPA: Principles and practice, <http://www.qualcomm.com/media/documents/>, Qualcomm, Inc. white paper, 2009. Cited, July 2014.
- [WAH⁺10] S. Wang, E. Abreu, H. Harel, K. Kludt, and P. Chen. Mobile transmit beam-forming diversity on UMTS/HSUPA networks. In *Sarnoff Symposium, 2010 IEEE*, pages 1 – 6. IEEE, 2010.
- [XJH07] Y. Xiang, Luo, J., and C. Hartmann. Inter-cell interference mitigation through flexible resource reuse in OFDMA based communication networks. In *Proc. 13th European Wireless Conference EW2007*, pages 1 – 4, 2007.
- [ZCLY11] Chi Zhang, Yongyu Chang, Shuhui Liu, and Dacheng Yang. The analysis and evaluation of uplink transmit diversity schemes in multi-user HSUPA system. In *Vehicular Technology Conference (VTC Spring), 2011 IEEE 73rd*, pages 1 – 5. IEEE, 2011.
- [ZCWY13] Chi Zhang, Yongyu Chang, Ke Wang, and Dacheng Yang. Cross-tier interference coordination for heterogeneous network in MF-HSDPA system. In *Vehicular Technology Conference (VTC Spring), 2013 IEEE 77th*, pages 1 – 5. IEEE, 2013.
- [ZJ12] Zhang Zhang and Liu Jinhua. Uplink MIMO for HSPA. In *Communications (ICC), 2012 IEEE International Conference on*, pages 6056 – 6060. IEEE, 2012.

ORIGINAL PAPERS

PI

**APPLICABILITY OF INTERFERENCE COORDINATION IN
HIGHLY LOADED HSUPA NETWORK**

by

Frans Laakso, Kari Aho, Thomas Chapman, Tapani Ristaniemi 2010

IEEE 71st Vehicular Technology Conference: VTC2010-Spring

Reproduced with kind permission of IEEE.

Applicability of Interference Coordination in Highly Loaded HSUPA Network

Frans Laakso*, Kari Aho[†], Thomas Chapman[‡] and Tapani Ristaniemi*,

* University of Jyväskylä, P.O. Box 35, FIN-40014, Jyväskylä, Finland
E-mail: {frans.laakso,tapani.ristaniemi}@jyu.fi

[†] Magister Solutions Ltd., Rautpohjankatu 8, FIN-40700, Jyväskylä, Finland.
E-mail: {kari.aho}@magister.fi

[‡] Roke Manor Research Ltd, Hampshire, SO51 0ZN, United Kingdom
E-mail: {thomas.chapman}@roke.co.uk

Abstract—This paper evaluates the performance of highly loaded *High Speed Uplink Packet Access (HSUPA)* network with and without network wide static *Interference Coordination (IC)*. IC alternates the priorities for user transmission periods throughout the network to achieve reduced interference levels and higher performance. A large variety of combinations including, e.g., different schedulers, cell center/edge user definitions (user splits) and interference targets are investigated in this paper. Performance is analyzed using a quasi-static system level simulator which is also used to support *Third Generation Partnership Project (3GPP)* standardization work. The simulator contains detailed and commonly accepted models, for instance, for channel profiles, fading and propagation. The study indicated that IC can bring gain in certain scenarios. However, the gain comes at the expense of fairness leading to users that already have high throughput benefiting from the situation. Moreover, it was shown that the major part of the gain comes from splitting users to different groups and scheduling these groups without any network wide interference coordination.

I. INTRODUCTION

High Speed Uplink Packet Access (HSUPA), a packet evolution of *Wideband Code Division Multiple Access (WCDMA)*, was standardised in the *Third Generation Partnership Project (3GPP)* Release 6 with the name of *Enhanced Dedicated Channel (EDCH)*. HSUPA is the uplink counterpart of the *High Speed Downlink Packet Access (HSDPA)* that was already introduced in Release 5. Both channels were conceived in order to achieve higher capacity and coverage for high transmission rates by the means of, e.g., *Hybrid Automatic Repeat Request (HARQ)*, fast scheduling and shortened *Transmission Time Interval (TTI)* [1].

In general the total system coverage is limited by the uplink due to mainly two factors: very limited power resources of the *User Equipment (UE)* and interference levels. Interference in the uplink consists of three components: intra-cell (i.e., own cell) interference, inter-cell interference (i.e., other cell) and thermal noise. Intra-cell interference arises because the signals between UEs are not orthogonal when arriving at the base station. This is why multi-user interference cancellation is beneficial to be used [2]. If the intra-cell interference is successfully mitigated, then the next largest source of interference is inter-cell interference. Mitigation of inter-cell interference has been studied extensively as part of the development of

the *Long Term Evolution (LTE)* standard. For an overview, see, e.g., [3] [4] [5] [6]. There are several approaches to interference coordination in LTE. In one approach, since the frequency band is divided into resource blocks and the same blocks are used in each cell, some of the blocks are restricted to be scheduled to only UEs near to the cell center. The pattern of blocks in which the scheduling is restricted is arranged between the cells according to a certain frequency re-use pattern. Considering neighbouring cells, this arrangement allows for cell edge UEs to be scheduled into different blocks, thus reducing the inter-cell interference and improving user (and cell) throughput and availability of higher data rates.

The purpose of this paper is to investigate the applicability of the LTE-type interference coordination principles to HSUPA, by the means of time domain coordination. For the coordination to operate, the base stations need to be synchronized so that coordinated scheduling of cell center users and cell edge users in the neighbouring cells can be implemented properly. Furthermore, an advanced timing mechanism needs to be introduced in order to synchronize uplink receive timings at each Node B. This could be achieved, for example, by alignment of the downlink timings.

II. SIMULATION ASSUMPTIONS AND MODELING ISSUES

The purpose of this section is to present the modeling issues and simulation assumptions related to this paper. The study is conducted with quasi-static system level simulator which is also used to support 3GPP standardization work and has been utilized and presented in various performance evaluations of HSUPA, see, e.g., [7] and [8]. The simulator models the complexity of HSUPA network in detail including commonly accepted models for, e.g., channel profiles, fading and propagation. In order to keep computing efforts at more sensible level, mobility is defined implicitly in the simulator, instead of explicit dynamic approach.

A. Interference coordination

Interference coordination for HSUPA is implemented as time domain coordination. Hence, it requires that the base stations are synchronized so that in certain cells only the cell edge users transmit while in the neighboring cells only

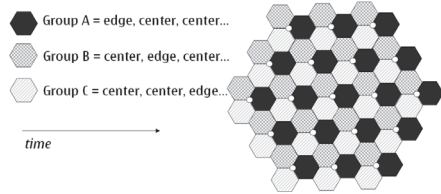


Fig. 1. Simulation scenario with interference coordination

the center users are allowed to transmit and thus inter-cell interference experienced during cell edge user scheduling periods should be lower. This is illustrated in Fig. 1. The figure also reveals that the coordination has a spatial aspect as well. For the purpose of the simulations, 9 HARQ processes are assumed as it allows a straightforward division of the HARQ processes into 3 groups, and application of a re-use pattern of 3.

The *Enhanced Dedicated Physical Data Channel (E-DPDCH)* power of cell edge users is restricted in some of the time periods (referred as 'center' period in Fig. 1), whereas any UE or only cell edge UEs may be scheduled with a high E-DPDCH power in other time periods (referred as 'edge' period in Fig. 1). The proportion of edge and center users and the power restriction applied to edge users depends on the simulation configuration. Such a scheduling could be achieved by activating/deactivating HARQ processes, or alternatively by the means of *Radio Network Controller (RNC)* restricting the maximum data rate applicable to UEs in certain HARQ processes in certain time periods. It should be noted that activating/deactivating HARQ processes is possible in the Release 6 specifications and thus applicable to legacy UEs, whereas specifying a different minimum data rate in some HARQ processes would require a specification change and thus would require new terminals.

In this study it is assumed that cell edge users' E-DPDCH is restricted 2/3 of the TTIs and any UE (i.e., including cell center users) can be scheduled in the remaining 1/3 of the TTIs. However, during the latter, edge users are prioritized.

A user is classified as cell edge user if the E_c/N_0 difference between the user's serving cell and any other cell is smaller than a certain value defined by a parameter. Thus, the exact proportion of edge and center users will vary between cells. The percentage for 'edge/center' splits quoted in this paper refer to the average number across all of the cells.

B. Scheduling and resource allocation

Transmissions and the power needed for each transmission are characterized by the transmission rate, the radio conditions, the intra-cell and inter-cell interference and the thermal noise. A UE is required to make possible retransmissions with the same rate as the first transmission and thus the rate should be chosen such that the required power is sufficiently less than the maximum power to allow the possibility for retransmissions

with higher power requirements. Thus, rather than sending pure transmission rate requests to the Node B, in this study UEs report periodically the unallocated power level which is referred as power headroom. In this way the Node B can avoid scheduling the UEs with power that they are not able to provide and prioritize users with higher headroom. Moreover, the prioritization of users in the Node B scheduler is based on *Proportional Fair (PF)* scheduling.

Multiplexing of users that are allowed to transmit in the same TTI can be done in one of three ways in HSUPA: *Code Division Multiplexing (CDM)*, *Time Division Multiplexing (TDM)* or with combination of those two which is referred as CDM/TDM scheduling. With pure CDM all users are provided with minimum bit rate but according to the priority metric (and requests) users can have higher allocations. TDM allows only one user to be scheduled in each TTI resulting in increased queuing times but also reduced interference levels. Combination of those two, CDM/TDM, does not guarantee minimum bit rate for all users but multiple users can be scheduled in each TTI depending on the *Rise over Thermal (RoT)* level that the scheduler is aiming at. Compared to CDM, the total sum power per cell with CDM/TDM can be lower, but then the impact on power consumption would also be smaller.

Scheduling/multiplexing requires some changes to the basic operation when interference coordination is applied. Recall that there are two periods of operation: cell center period and cell edge period. With CDM the following actions are taken:

- During both periods all the users are prioritized according to the PF metric but the priority of users who are not in turn is modified so that they will have lower priority than the users whose turn it is.
- During cell center periods only cell center users are scheduled according to priority metric and they are the only ones that are allowed to have higher transmission rates than the minimum transmission rate defined as a parameter. Therefore, the cell edge users will get only that minimum transmission rate.
- During cell edge periods the cell edge users are scheduled first according to priority metric. But after that there is a possibility to schedule also cell center users if that mode is enabled.

C. Traffic model

Full buffer traffic model was selected for simulations in order to reach necessary system load and higher interference levels. With full buffer traffic model each UE always has an unlimited amount of data available in the buffer.

D. Simulation scenario and parameters

Simulations are carried out in wrap-around macro cell scenario, which consists of 19 base station sites with 3 sectors (or cells) each resulting in a layout of 57 hexagonal cells. The wrap-around scenario means that the UE placement is limited around the 57 cells, but the cell transmissions are replicated outside the simulation area to offer more realistic interference for every UE in the network.

TABLE I
SIMULATION PARAMETERS.

| Parameter | Value |
|---------------------------|--|
| Cell layout | Hexagonal grid, 3 sector/site, 19 sites/57 sectors, wrap around |
| Inter-site distance | 500 m |
| NodeB receiver | LMMSE |
| Antenna FTB | 20 dB |
| Node B antenna gain | 14 dBi |
| Node B noise figure | 5 dB |
| Node B Rx antennas | 2 |
| UE antenna gain | 0 dB |
| UE Tx power | 24 dBm |
| Shadow fading | 8 dB |
| Shadowing correlation | 1 between sectors, 0.5 between sites |
| Channel profile | Pedestrian A 3kmph |
| Number of users / sector | 10 & 20 users |
| Maximum user bit rate | 768 kbps |
| Scheduling algorithm | Proportional Fair |
| Traffic model | Full Buffer |
| User multiplexing | [CDM, CDM/TDM] |
| Re-use pattern for IC | 3 |
| Cell Edge user proportion | [19, 49, 78] % |
| Number of HARQ processes | 9 |
| RoT operating point | 3-7dB |

For each interference coordination simulation, the users are classified as 'cell edge' or 'cell center'. The proportion of cell edge users is varied in different simulation runs. Values (19, 49, 78 %) were chosen to represent typical 'low', 'medium' and 'high' edge user proportions.

The maximum user bit rate was selected based on previous simulation campaigns, which identified the best suited maximum user transmission rates for the used channel profile, namely 768 kbps for Pedestrian A 3kmph. The main parameters for the simulations described in this paper are listed shortly in Table I.

III. RESULTS ANALYSIS

This section presents the simulation results and analysis on the basis of the results. Key performance indicators are sector throughput vs. RoT and user throughput distributions.

A. Throughput analysis

Regarding average sector throughput, the results analyzed in this section can be found in Table II for low sector load, namely 10 UEs/sector, and in Table III for high sector load, namely 20 UEs/sector. The user throughput results are available in Fig. 2, Fig. 3 and Fig. 4.

With the CDM scheduler and lower load IC brings gain only in limited cases in terms of average sector throughput when compared to the baseline cases (i.e., with no IC), see Table II. The amount of loss/gain is dependent on the user split, i.e., how many users are considered as cell edge users and on the used RoT target.

With low splits and lower RoT targets there are enough 'good' center users (i.e., users capable of high data rates within RoT limit) to make up for the reduced transmission possibilities due to splitting users into groups and fill the

TABLE II
IC GAINS [%] WITH LOW SECTOR LOAD, PEDESTRIAN A 3KMPH.

| IC simulation case | RoT target | | | | |
|-----------------------|------------|--------|--------|--------|--------|
| | 3 dB | 4 dB | 5 dB | 6 dB | 7 dB |
| Center UEs allowed | | | | | |
| Low split, CDM | 5.01 | 3.31 | 1.74 | -0.17 | -2.05 |
| Medium split, CDM | 12.54 | 5.27 | -2.06 | -8.05 | -11.83 |
| High split, CDM | -7.33 | -19.88 | -29.00 | -34.68 | -38.34 |
| Low split, CDM/TDM | 5.76 | 0.41 | -7.26 | -8.37 | -8.44 |
| Medium split, CDM/TDM | 27.63 | 20.00 | 13.72 | 9.55 | 5.59 |
| High split, CDM/TDM | 19.57 | 4.77 | -3.79 | -8.79 | -12.54 |
| Center UEs denied | | | | | |
| Low split, CDM | -9.06 | -14.76 | -20.58 | -25.59 | -29.10 |
| Medium split, CDM | -3.76 | -17.09 | -26.24 | -32.08 | -35.75 |
| High split, CDM | -18.32 | -32.53 | -41.09 | -46.27 | -49.57 |
| Low split, CDM/TDM | 1.73 | -2.34 | -5.65 | -8.10 | -9.87 |
| Medium split, CDM/TDM | 27.05 | 16.14 | 7.75 | 1.25 | -4.03 |
| High split, CDM/TDM | 20.43 | 4.37 | -6.05 | -12.87 | -18.13 |

TABLE III
IC GAINS [%] WITH HIGH SECTOR LOAD, PEDESTRIAN A 3KMPH.

| IC simulation case | RoT target | | | | |
|-----------------------|------------|-------|-------|-------|--------|
| | 3 dB | 4 dB | 5 dB | 6 dB | 7 dB |
| Center UEs allowed | | | | | |
| Low split, CDM | 10.46 | 6.12 | -2.21 | -7.95 | -12.74 |
| Medium split, CDM | 28.59 | 24.36 | 21.25 | 18.58 | 16.19 |
| High split, CDM | 42.32 | 30.37 | 22.45 | 17.48 | 13.58 |
| Low split, CDM/TDM | 25.00 | 16.24 | 6.72 | 1.93 | -0.84 |
| Medium split, CDM/TDM | 52.59 | 36.89 | 25.88 | 19.06 | 16.09 |
| High split, CDM/TDM | 100.86 | 74.48 | 64.54 | 59.67 | 55.82 |
| Center UEs denied | | | | | |
| Low split, CDM | 12.25 | 5.20 | 1.01 | -1.34 | -3.24 |
| Medium split, CDM | 34.15 | 25.40 | 19.50 | 15.35 | 12.39 |
| High split, CDM | 45.92 | 31.41 | 20.98 | 13.86 | 7.74 |
| Low split, CDM/TDM | 38.79 | 16.94 | 5.55 | 1.24 | -0.60 |
| Medium split, CDM/TDM | 66.38 | 42.00 | 28.07 | 20.99 | 17.77 |
| High split, CDM/TDM | 108.62 | 78.19 | 67.06 | 61.33 | 57.26 |

available RoT capacity, see Fig. 2 for lower RoT target average user throughput performance. However, with higher RoT targets the 'good' users suffer from limited data rate in addition to the lost transmission periods and as such the results show minor loss, see Fig. 3 for higher RoT target average user throughputs.

In terms of cell throughput, with high splits and low system load there are not enough 'good' center users to compensate the loss of transmission periods as the maximum bit rate is already limited. The effect shows already with low RoT targets and when the target increases, the effect is further emphasized. In other words, RoT is not fully utilized in all periods which leads to lowered system throughput. Additionally, preventing center user scheduling with lower load during edge periods reduces the system load and as such amplifies the effects of reduced transmission periods and data rate limit. This happens due to reduced number of possible scheduling TTIs for center users, which results in lower amounts of good throughputs.

With higher load IC can bring gain especially with relatively high edge user splits, see Table III. This indicates that IC requires also relatively high sector load, so that enough load

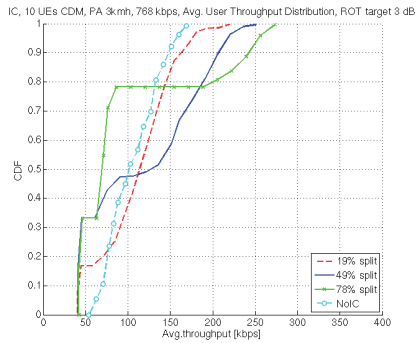


Fig. 2. CDF of user throughput, CDM with low load, RoT target 3 dB, center user scheduling is allowed during the edge user periods.

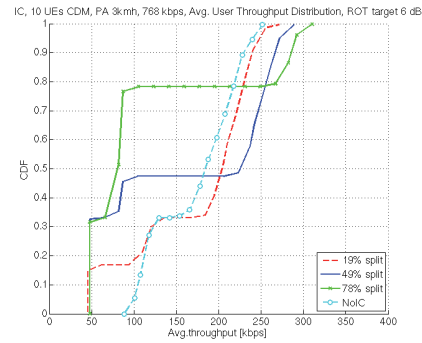


Fig. 3. CDF of user throughput, CDM with low load, RoT target 6 dB, center user scheduling is allowed during the edge user periods.

TABLE IV
CDM BASELINE GAINS [%] COMPARED TO CDM/TDM, PEDESTRIAN A
3KMPH.

| CDM baseline | 3 dB | 4 dB | 5 dB | 6 dB | 7 dB |
|--------------|--------|--------|-------|-------|-------|
| 10 UEs | 49.21 | 34.82 | 25.50 | 19.52 | 14.96 |
| 20 UEs | 163.79 | 100.93 | 82.69 | 75.41 | 70.59 |

for cell center TTIs exists. As with lower sector load case, the IC gains are mostly result of the necessary amount of 'good' center users getting noticeably better performance.

In general the higher load results support the lower load conclusions as the higher system load balances out the loss of transmission periods and data rate limit. However, in higher load case the system is fully loaded and as such the absolute performance starts to decline. IC improves this situation by balancing the load as does preventing center user scheduling during edge periods.

Regarding user throughput, the low edge user splits lead to a higher number of poor throughput users without benefiting significantly to the good users due to the load being already relatively high. On the other hand, with higher cell edge user splits it is possible for the fewer good users to achieve higher user throughputs, see Fig. 4.

With higher load the system is already too saturated for center user scheduling during the edge periods to have a noticeable effect on performance. However, the center users can take advantage of the cell edge users being denied to send during 2/3 of the time.

B. CDM and CDM/TDM scheduler performance

In general, the CDM/TDM scheduler demonstrated poorer performance and more sensitivity to sector load than than CDM scheduler with both the baseline and the center/edge split simulations, as can be seen from Tables II, III and IV. Lower CDM/TDM throughput performance, when compared to CDM, is the result of different data rate distributions within

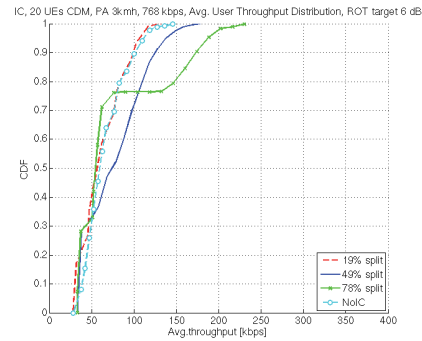


Fig. 4. CDF of user throughput, CDM with high load, RoT target 6 dB, center user scheduling is allowed during the edge user periods.

the system. With CDM every user is guaranteed to have minimum bit rate instead of zero bit rate with CDM/TDM. The trend is that with CDM system there are usually noticeably larger amount of these lower data rate transmissions and a slightly lower number of highest data rate transmissions, when compared to the CDM/TDM system. This larger number of lower data rate transmissions results in higher total sector throughput than the fewer amount of higher data rates.

The sensitivity can be seen from lower sector load IC simulations, where the results show similar behaviour to pure CDM with higher load, see Tables II and III. With lower load and a CDM/TDM scheduler edge/center splitting results in losses in general. As with the CDM scheduler, the effects of losing transmission periods and data rate limit affects CDM/TDM performance.

With higher load and a CDM/TDM scheduler, IC can bring gain especially with higher edge user splits and lower RoT

TABLE V
IMPACT OF COORDINATION, HIGH LOAD WITH CDM SCHEDULER, RoT
TARGET 3 DB, PEDESTRIAN A 3KMPH.

| Simulation case | Gain with IC [%] | Gain with only splitting users into groups [%] |
|-----------------|------------------|--|
| Low split | 10,46 | 11,44 |
| Medium split | 28,59 | 29,08 |
| High split | 42,32 | 40,85 |

targets, see Table III. However, the absolute capacity numbers are already noticeably degenerated and CDM/TDM offers lower absolute throughputs than pure CDM. Even after the IC gains, CDM/TDM throughputs are at best of the same order as CDM without IC.

The general trends with CDM/TDM scheduler user throughputs with and without center user scheduling during edge periods are rather similar to pure CDM case. When the system is heavily loaded the good users will not get high enough throughputs and thus the average sector throughput is also lower.

C. CDM scheduler without interference coordination

All of the simulation cases above are interference coordinated cases, i.e., there should be only edge users transmitting in one cell and center users in all of the surrounding cells. The purpose of this section is to analyze the situation when this kind of coordination is not done.

In terms of sector throughput all of the simulated cases with and without coordination provide similar numbers. In general these results indicate that there is no need for IC as the same benefit can be acquired just by introducing an algorithm which divides users into cell edge and cell center users, for comparison see Table V. In other words, this means that the reported gains can be achieved solely with a modified PF scheduler, which adjusts the forgetting factor according to the edge user split and increases cell throughput at the expense of fairness.

IV. CONCLUSION

The purpose of this study was to evaluate the impact of interference coordination to the HSUPA performance with full buffer traffic. Different types of schedulers, user splits, scenarios were investigated to examine potential performance enhancement possibilities.

General findings are that with high load, IC brings more gain when compared to corresponding baseline case but the absolute throughput numbers are lower than with low load. This happens when system has high enough load for 'good' users, which raise the throughput levels on the expense of the 'poorer' users, and balance out the loss of transmission periods and data rate limit, both of which resulted in performance degeneration with lower system load. Additionally, the effect of losing transmission periods and data rate limit is emphasized with higher RoT targets as transmissions are more limited by transmission periods and the data rate limit than RoT.

In general, the inter-cell interference levels are very similar between cell edge and cell center periods (i.e., coordination of the edge/center periods between cells does not seem to influence interference), but in order to further improve performance, different *Continuous Packet Connectivity (CPC)* features could be investigated in conjunction with IC.

Another issue to be considered is IC effects to multi-user diversity. It is possible that IC has an impact to multi-user diversity in some situations due to dividing users to groups with separate transmission periods, and as such has a negative effect on performance.

Regarding different user multiplexing options, in general level the pure CDM system performs better than CDM/TDM system if the performance is evaluated according to sector/user throughput. With CDM/TDM the results show lower throughput performance, when compared to CDM, and this happens due to different data rate distribution within the system. However, with CDM/TDM the gain from edge/center user splitting exists already with lower sector load.

In addition, a situation in which cell center users are not allowed to be scheduled during edge periods was investigated. Based on these results, in lower load situation the pure CDM scheduler is not attractive as there are even losses instead of any visible gains. However, with high load the system does not suffer when center users are not allowed to be scheduled during edge periods as higher system load balances out the loss of transmission periods and data rate limit.

Finally, the impact of random group assignment was studied, i.e., the situation without actual interference coordination. The study on that matter shows in our simulation cases that in terms of throughput the system does not gain that much from using interference coordination between cells but most of the gain comes from cell edge/center user split.

V. ACKNOWLEDGMENTS

This study is a collaborative work between Nokia and Nokia Siemens Networks. The authors would like to thank all of their co-workers and colleagues for their comments and support.

REFERENCES

- [1] H. Holma and A. Toskala, *HSDPA/HSUPA for UMTS*, 1st ed. John Wiley & Sons Ltd, 2006.
- [2] S. Verdu, *Multuser Detection*, 1st ed. Cambridge University Press, 1998.
- [3] M. C. Necker, "Interference coordination in cellular ofdma networks," *IEEE Networks*, vol. 22, pp. 12–19, November-December 2008.
- [4] G. Boudreau and et.al., "Interference coordination and cancellation for 4g networks," *IEEE Communications Magazine*, vol. 47, pp. 74–81, April 2009.
- [5] Y. Xiang, J. Luo, and C. Hartmann, "Inter-cell interference mitigation through flexible resource reuse in ofdma based communication networks," in *European Wireless 2007 (EW 2007)*, April 2007.
- [6] A. Simonsson, "Frequency reuse and intercell interference co-ordination in e-utra," in *Vehicle Technology Conference, 2007. VTC2007-Spring. IEEE 65th*, April 2007.
- [7] O. Fresan, C. Tao, E. Malkamaki, and T. Ristaniemi, "DPCC gating gain for Voice over IP on HSUPA," in *Proc. IEEE Wireless Communications and Networking Conference (WCNC'07)*, China, March 2007.
- [8] M. Zhang, T. Chen, and J. Hu, "Throughput-based and power-based load control in hsupa," in *Wireless Communications, Networking and Mobile Computing, 2005. Proceedings. 2005 International Conference on*, vol. 2, September 2005, pp. 969–973.

PII

**ENHANCING HSUPA SYSTEM LEVEL PERFORMANCE WITH
DUAL CARRIER CAPABILITY**

by

Ilmari Repo, Kari Aho, Sami Hakola, Thomas Chapman, Frans Laakso 2010

5th IEEE International Symposium on Wireless Pervasive Computing (ISWPC)

Reproduced with kind permission of IEEE.

Enhancing HSUPA System Level Performance with Dual Carrier Capability

Ilmari Repo^{*}, Kari Aho[†], Sami Hakola[‡], Thomas Chapman[§], Frans Laakso^{*},

^{*} University of Jyväskylä, P.O. Box 35, FIN-40014, Jyväskylä, Finland
E-mail: {ilmari.repo,frans.laakso}@jyu.fi

[†] Magister Solutions Ltd., Rautopohjankatu 8, FIN-40700, Jyväskylä, Finland.
E-mail: {kari.aho}@magister.fi

[‡] Nokia, Elektriikkatie 3, PL 50, FIN-90571, Oulu, Finland.

E-mail: {sami.hakola}@nokia.com

[§] Roke Manor Research Ltd, Hampshire, SO51 0ZN, United Kingdom
E-mail: {thomas.chapman}@roke.co.uk

Abstract—The purpose of this paper is to analyze how dual carrier capability can enhance High Speed Uplink Packet Access performance in comparison to using only single carrier. Dual carrier operation gives the User Equipment the possibility to transmit simultaneously using two 5 MHz bands, theoretically doubling the peak data rates and user throughput. The analysis is conducted with a system level simulation tool. This paper first indicates with single carrier simulations that, especially in small cells, terminals have spare power available for dual carrier operation. These observations are verified with dual carrier simulations by showing that the burst throughput can be practically doubled. In the larger cells only the users in good position can fully benefit from using dual carrier.

I. INTRODUCTION

The first commercial *Third Generation (3G)* wireless networks utilizing *Wideband Code Division Multiple Access (WCDMA)* as a radio interface were deployed in 2002. [1] WCDMA offered for the first time high data rates and relatively low latencies for packet switched connections over cellular networks. Due to increasing requirements of e.g. multimedia applications packet data capabilities of WCDMA were later enhanced even further, first in the downlink in *Third Generation Partnership Project (3GPP) Release 5 (Rel'5)* and a couple of years later in *Release 6 (Rel'6)* which introduced enhancements for the uplink counterpart. Namely these evolutions are called *High Speed Downlink Packet Access (HSDPA)* and *High Speed Uplink Packet Access (HSUPA)*. The most important improvements included *Hybrid Automatic Repeat Requests (HARQ)*, shortened *Transmission Time Interval (TTI)*, fast scheduling in *Node B* and adaptive modulation and coding schemes [2].

The development of 3G technology and networks is still going on and new improvements are being discussed. Currently 3GPP is standardizing the possibility to use HSUPA beyond current 5 MHz bandwidth by introducing multi carrier operation [3]. Release 8 specified *Dual Carrier (DC)* for HSDPA and thus natural continuum for the work is DC also in the uplink. Dual Carrier operation would give the *User Equipment (UE)* the possibility to transmit simultaneously with two carriers if it has adequate power resources. DC

operation would theoretically double the peak data rates and throughput as well as increase resource utilization for situations where there would be an imbalance between loads on separate carriers. If a UE is using Dual Carrier it is able to use either or both of the carriers on a fast basis without radio bearer reconfiguration. Another gain from using multiple carriers comes from the fact that there may be frequency diversity that can be exploited. In this paper we study performance and feasibility of dual carrier HSUPA in system level using both single and dual carrier simulations.

The rest of this paper is organized as follows. In the next section modeling issues and assumptions regarding dual carrier are presented. The most important simulation parameters and simulation scenarios are also introduced. In the following section simulation results are analyzed starting for both single carrier pre-analysis and dual carrier simulations. Finally the most important findings and future work are summarized in the conclusions.

II. SIMULATION ASSUMPTIONS AND MODELING ISSUES

The purpose of this section is to cover briefly the modeling issues and simulation assumptions related to the studies presented in this paper. As a research tool we use quasi-static system level simulator which enables detailed simulation of users in multiple cells with realistic propagation and fading models. The tool has been previously used and presented in various performance and performance enhancement evaluations of HSUPA, see e.g. [4], [5] and [6]. The following subsections aim to provide a brief overview of the most critical dual carrier related modeling aspects in this paper.

From the UE perspective, Dual Carrier operation implies that the UE has the ability to send data on adjacent 5 MHz bands at the same time. However the *Power Amplifier* requirements are the same as for single carrier which means that maximum total power of both carriers is 24 dB or 250 mW. The Node B needs two receivers in order to support Dual Carrier, but unlike UEs, its limiting factor is not power but noise rise. The received total power needs to be within certain limits in order to be able to decode transmissions from all

UEs. A value of 6 dB is generally used as a maximum *Rise over Thermal (RoT)* target. When using dual carrier, the RoT targets are separate for each carrier so the UE transmission power is the limiting factor in multi carrier uplink as it does not double.

A. Power Control

Dual Carrier uses separate fast power control for each carrier which means that the *Dedicated Physical Control Channel (DPCCH)* must be transmitted on both carriers in order to keep *Signal-to-Interference Ratio (SIR)* target and to maintain synchronization.

B. Fading

Slow fading is assumed to be same for both carriers and as the UEs are geographically static the slow fading is also constant during simulation. Fast fading is modeled independently for each carrier and is completely uncorrelated. A velocity of 3 km/h is assumed for fast fading.

C. Scheduling

The power needed for each transmission is characterized by the transmission rate, the radio conditions, the intra-cell and inter-cell interference and the thermal noise. In HSUPA a UE is required to make HARQ retransmissions with the same rate as the first transmission. This implies that the data rate should be chosen so that the required power is sufficiently less than the maximum power to allow the possibility for retransmissions with higher power requirements in case channel conditions have worsened. Thus, rather than sending pure transmission rate requests to the Node B, in this study the UE reports periodically the unallocated power level which is referred as power headroom. This way the Node B can avoid scheduling the UE with power that it is not able to provide and prioritize users with higher headroom.

The Node B can use the power headroom reports as a means to differentiate UEs with good channel conditions and those with poor channel conditions. Proportional fair scheduling based on power headroom criteria is chosen also as the basis for our studies. In this study the scheduling for Dual Carrier UEs is done according to their primary carrier (C1), which is static during simulation and is the same for all UEs. This means that the first carrier gets always scheduled first and UEs total power headroom is the metric for proportional fair scheduler. UEs also make their rate requests in that same carrier order.

Multiplexing of users that are allowed to transmit in the same TTI can be done in HSUPA using *Code Division Multiplexing (CDM)*, *Time Division Multiplexing (TDM)* or with a combination of those two. CDM multiplexing was used in this study which means that all UEs are provided at least with a minimum bit rate when they have data to send, but according to the priority metric and *rate requests* users can have higher allocations. A minimum data rate of 24 kbps was selected.

D. Traffic and channel models

This paper considers a bursty traffic as traffic model which is based on 3GPP assumptions [6] and uses a truncated lognormal distribution with parameters $\sigma = 0.35$ and $\mu = 11.675$ and a constraint on the maximum file size. Burst *Interarrival Time (IAT)* is modeled as exponential distribution with parameter $\lambda = 0.05$ which gives a mean IAT of 20 seconds. This means that there can be multiple bursts per UE during the simulation time which is set to 60 seconds. Bursts are transferred without higher layer acknowledgements or retransmissions so when UE happens to be power limited, it is possible that not all generated data not transferred completely after HARQ transmissions. The traffic source is common for both carriers. All UEs are active from the beginning of the simulation and thus cause interference even when they are not sending data. The reason why bursty traffic is considered is that it resembles typical behaviour in cellular networks in that only some users are active at a time. The 3GPP *Typical Urban (TU6)* channel model was used in simulations.

E. DPCCH Gating

DPCCH gating is part of *Continuous Packet Connectivity (CPC)* and it enables a UE to shut down its transmitter when it does not have data to send. CPC may also be used along with dual carrier. The benefit of gating for UEs is that it can save battery life, while the downside is that the fast power control sync is lost and it needs a short time to resume. From Node B point of view gating enables more efficient resource usage as idle users transmit DPCCH less often, reducing overhead in the RoT. Simplified modeling for gating is assumed in this study to keep the scope reasonable. DPCCH is transmitted only when user has *Enhanced Dedicated Physical Data Channel (E-DPDCH)* transmission i.e. a burst is being transmitted. Thus, e.g. *High Speed Dedicated Physical Control Channel (HS-DPCCH)* gating preambles/postambles are not explicitly modeled.

F. Simulation scenario and parameters

Simulations are carried out in a macro cell scenario as presented in Fig. 1. The scenario consists of 7 base station sites with 3 sectors each resulting in a layout of 21 hexagonal cells. UE placement is limited to around the center cells, but wrap-around means that cell transmissions are replicated outside the simulation area to offer more realistic interference conditions. Soft handover is also modeled and UEs can be connected to up to 3 Node Bs. The *Inter-site distance (ISD)* is varied in order to simulate different cell sizes. Penetration loss also differs between cell sizes as described in [7].

Simulation parameters are mainly based on [7] and the most important ones are listed in Table I. In the DC simulations both carriers are active from the beginning and DC is enabled for every UE in cell regardless of their geographical position.

III. RESULTS ANALYSIS

In this section we present and analyze the simulation results based upon UE transmit power distribution and active user,

TABLE I
SIMULATION PARAMETERS.

| Parameter | Value |
|------------------------------|---|
| Simulation time | 60 s |
| Time resolution | 1 slot i.e. 0.6667 s |
| Channel profile | Typical Urban (TU6) |
| TTI length | 2 ms |
| HARQ Processes | 8 |
| Max. HARQ Transmissions. | 4 |
| RoT Target | 6.0 dB |
| Bandwidth | 5, 10 MHz |
| Number of sectors | 21 (Wrap-Around) |
| Inter Site Distance (ISD) | 0.5, 1.732 km |
| Penetration Loss | 10, 20 dB (depending on ISD) |
| Node B Scheduler | proportional fair (PF), Primary Carrier First |
| Power Headroom Reporting | instant |
| Fast fading speed | 3 km/h |
| Slow fading deviation | 8 dB |
| Path Loss Model | $128.1 + 37.6 \times \log_{10}(R)$, R in kilometers |
| UE Maximum Transmit Power | 250 mW = 24 dBm |
| Correlation between carriers | Uncorrelated |
| Burst Size Distribution | log-normal, $\sigma = 0.35$, $\mu = 11.675$, mean 0.125 Mbytes |
| Burst Max. Size | 0.3125 Mbytes |
| Burst IAT Distribution | exponential with $\lambda = 0.05$, mean 20 seconds |

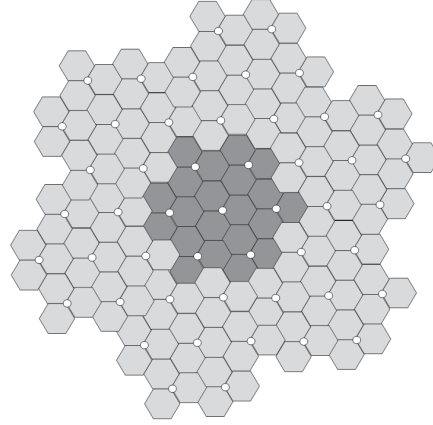


Fig. 1. Simulation scenario. UEs are placed within the darker area in the middle and rest is wrap-around.

burst and cell throughputs. Rise over Thermal in the Node B is also analyzed. The metrics are analyzed via both *Cumulative Distribution Functions (CDF)* to give view of the distribution of throughputs throughout the cell and bar plots to indicate the mean throughput levels with different parameter settings. Active user throughput is calculated by dividing UEs correctly sent data by the time it took to transfer it. This differs from burst throughput in that whereas burst throughput may have more than one sample from a UE, user throughput has one sample per UE that is averaged over the users bursts. In simulation result figures the 'N' notation indicates the number of users per 5 MHz bandwidth per sector. This kind of comparison is used to be able to better observe the actual spectral efficiency relative to the used bandwidth.

A. Pre-analysis for Dual Carrier

Before implementing and running dual carrier simulations, a series of single carrier simulations was carried out in order to examine which UEs and in which type of cells there would be benefit from dual carrier, and whether dual carrier could be feasible. Figure 2 shows the transmit power of single carrier UEs in 500 m and 1732 m cells. In the 500 m cell UEs are not power limited but rather, RoT limited. This means that the Node B has to restrict capacity in order to keep the noise rise over thermal within certain limits. This is illustrated in Figure 3, which shows both the *Average RoT* and *Average Active RoT*. Active RoT is only collected from a Node B when there is at least one UE transmitting a burst in that cell whereas Average RoT is collected every slot. In contrast to 500 m cell in 1732 m cell most UEs are power limited and are not expected to greatly benefit from dual carrier operation. The reason that the tails of transmit power distributions get lower

when the number of UEs is increased comes from the fact that with more simultaneously active users, the RoT target is shared with other active UEs. This means they are not able to use the maximal transmit power to fill RoT by themselves and leads to lower transmit power. Figure 2 shows that the average sector throughputs are similar regardless of the cell size as may be expected due to traffic model.

According to this pre-analysis with single carrier simulations it seems probable that UEs in smaller cells would be able to benefit from multiple carriers but in larger cells there is not as much expected gain.

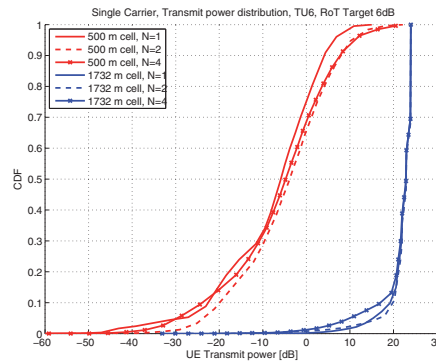


Fig. 2. Single carrier UE transmit power CDF in 500 m and 1732 m cells.

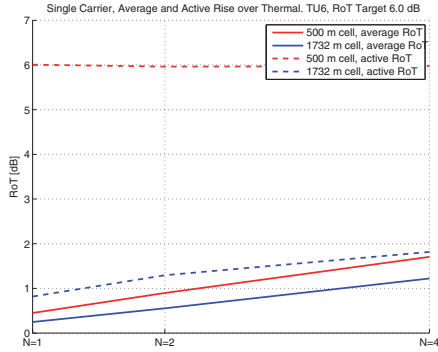


Fig. 3. Single carrier UE RoT Distribution in both 500 m and 1732 m cells.

B. Dual Carrier performance

Figure 4 shows the burst throughputs for a 500 m cell. The curves reveal that, especially for $N = 1$ and $N = 2$, users can benefit from dual carrier, as their throughput is practically doubled (see explanation for 'N' notation in Section III). When the cell gets more loaded the benefits of dual carrier reduce. The reasons for this kind of behaviour lies in the fact that the DPCCCH overhead gets larger when number of users increases and the observed RoT in the base station gets partially filled by interference caused by UEs that are in between bursts and only transmitting DPCCCH. Figure 5 shows the corresponding burst throughput in the larger cell. The tails of the CDFs are same for both single and dual carrier indicating that dual carrier does not increase burst throughput for the worst users who are located near cell edges. Instead, only the users near cell center can benefit and even from those only a fraction can actually double their throughput.

Mean achieved user throughputs for both cell sizes are presented in Figure 8. It is quite clear that in the smaller cell most UEs can increase their bit rates and the performance approaches that of two times single carrier. However in the large cell mean user data rates are not significantly increased from single carrier as many users do not have sufficient transmit power to utilize the second carrier.

It should be noted that the mean cell throughput does not improve when compared with corresponding single carrier case. This is a property of the traffic model as the amount of generated and transferred traffic during simulations are the same. The gains for dual carrier come in form of increased burst and user throughputs. Figure 6 shows the throughput of different carriers as well as the total sum of them. In 500 m cell the throughputs of carriers are similar, which is due to the fact that the scheduler schedules UEs on both carriers as UEs' power headrooms are sufficiently large to support transmission on the second carrier. However in the larger 1732 m cell, as UEs are power limited, their power headroom for the second carrier are typically low, which results in different

throughput among carriers. The total cell throughput still stays around the same, as the traffic model is similar. This kind of approach causes the first carrier to be more loaded than the second in case the UEs run out of transmit power when they are scheduled to the second carrier. For greater power and interference efficiency, the scheduling algorithm could take into account UEs instantaneously better carriers and schedule them first.

Active RoTs are plotted in Figure 7.

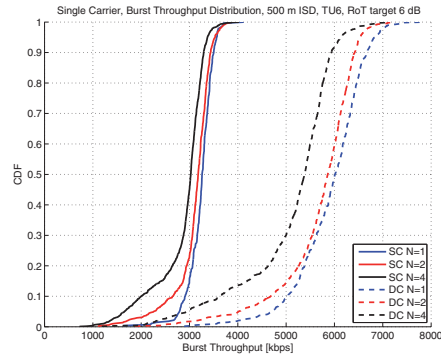


Fig. 4. Dual Carrier burst throughput CDF in 500 m cell.

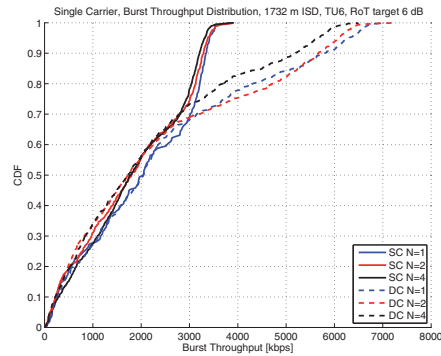


Fig. 5. Dual Carrier burst throughput CDF in 1732 m cell.

C. Analysis of DPCCCH gating

Simulations were run with DPCCCH gating to examine how much gating affects the results. Burst throughputs for gating are presented in Figure 9 for the 500 m cell, and they can be compared to Figure 4 which shows the same scenario without gating. It can be observed that for $N = 4$ the throughput is increased. This indicates that when the number of UEs is increased, the benefit of gating becomes more obvious as the DPCCCH overhead coming from other UEs can be mitigated.

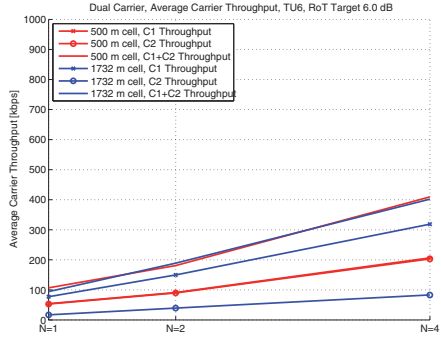


Fig. 6. Dual Carrier carrier throughputs for both 500 m and 1732 m cells.

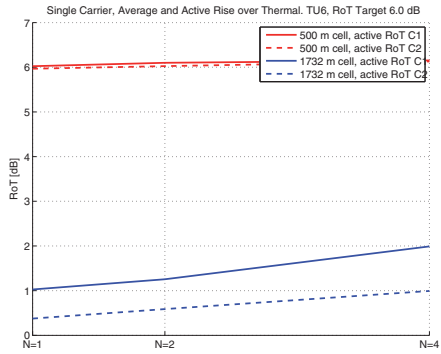


Fig. 7. Dual Carrier Average Active RoT per carrier in both 500 m and 1732 m cells.

IV. CONCLUSION

The purpose of this study was to investigate the feasibility and both system level and user experienced gains of Dual Carrier HSUPA. The study indicates that with bursty traffic in small cells and with relatively low load it is possible to achieve peak bit rates that exceed the capacity of two single carrier systems. This indicates that dual carrier is beneficial for UEs in good radio positions. In larger cells the benefits of dual carrier are not as visible, largely due to UEs being power limited as this paper shows via single carrier pre-analysis. This study can in the future be extended, for instance, by researching the impact of higher cell load and different types of scheduling algorithms.

V. ACKNOWLEDGEMENTS

This study is a collaborative work between Nokia and Nokia Siemens Networks. The authors would like to thank all of their co-workers and colleagues for their comments and support.

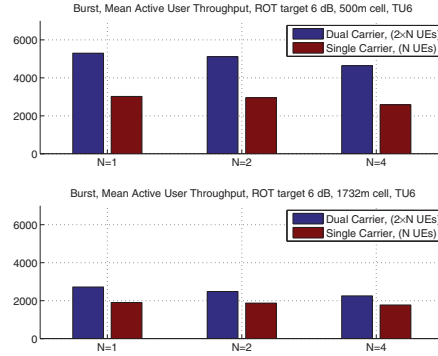


Fig. 8. Mean user throughput in 500 m and 1732 m cells, TU6, ROT Target 6 dB.

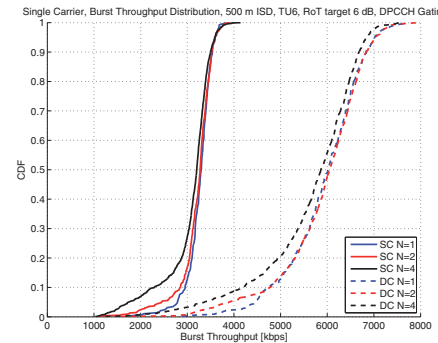


Fig. 9. Dual Carrier burst throughput CDF with DPCCH gating in 500 m cell.

REFERENCES

- [1] H. Holma and A. Toskala, Eds., *WCDMA for UMTS*, 4th ed. John Wiley & Sons Ltd, 2007.
- [2] H. Holma and A. Toskala, *HSDPA/HSUPA for UMTS*, 1st ed. John Wiley & Sons Ltd, 2006.
- [3] "Multi-carrier evolution," 3GPP Work Item Description, December 2008.
- [4] O. Fresan, T. Chen, E. Malkamaki, and T. Ristaniemi, "Dpcch gating gain for voice over ip on hsupa," March 2007, pp. 4274-4278.
- [5] T. Chen, G. Charbit, K. Ranta-aho, O. Fresan, and T. Ristaniemi, "Voip end-to-end performance in hspa with packet age aided hspa scheduling," Sept. 2008, pp. 1-5.
- [6] T. Chen, M. Kuusela, and E. Malkamaki, "Uplink capacity of voip on hsupa," vol. 1, May 2006, pp. 451-455.
- [7] "System Simulation Assumptions for Dual Carrier HSUPA Performance Evaluation," 3GPP TSG RAN WG1 contribution R1-090508, January 2009.

PIII

**EXTENDED HSUPA COVERAGE AND ENHANCED BATTERY
SAVING OPPORTUNITIES WITH MULTIPLE TTI LENGTHS**

by

Frans Laakso, Kari Aho, Ilmari Repo, Thomas Chapman 2010

21st IEEE International Symposium on Personal, Indoor and Mobile Radio
Communications (PIMRC 2010)

Reproduced with kind permission of IEEE.

Extended HSUPA Coverage and Enhanced Battery Saving Opportunities with Multiple TTI Lengths

Frans Laakso
University of Jyväskylä
P.O. Box 35
FIN-40014 Jyväskylä, Finland
firstname.lastname@jyu.fi

Ilmari Repo
University of Jyväskylä
P.O. Box 35
FIN-40014 Jyväskylä, Finland
firstname.lastname@jyu.fi

Kari Aho
Magister Solutions
Rautpohjankatu 8
FIN-40600 Jyväskylä, Finland
firstname.lastname@magister.fi

Thomas Chapman
Roke Manor Research Ltd.
S051 0ZN
Hampshire, United Kingdom
firstname.lastname@roke.co.uk

Abstract—3GPP has specified that terminals can be configured to use either 2 or 10 ms transmission time interval in high speed uplink packet access systems. The purpose of this paper is to evaluate the benefit of exploiting a mixture of both of the transmissions time intervals within a cell instead of only one. The study is quantified by means of studying the achievable coverage of voice over IP and possible battery saving benefits. The analysis is conducted with a system level simulator modeling network and terminal behavior in detail. The paper indicates that utilizing a mixture of both transmission time intervals can extend coverage whilst providing enhanced battery saving opportunities.

Keywords: VoIP, capacity, scheduling

I. INTRODUCTION

Traditionally voice has been transferred via circuit switched networks, but recently IP-based applications have started to gain more and more popularity. Their popularity has been one of the driving forces enabling the deployment of wireless cellular networks. The *Third Generation Partnership Project's* (3GPP's) Releases 5 and 6 took a major step by introducing *High Speed Downlink Packet Access (HSDPA)* and *High Speed Uplink Packet Access (HSUPA)* evolutions [1], respectively. For the first time voice could be transmitted over a packet switched network with higher spectral efficiency than a traditional circuit switched network. Following from the HSDPA and HSUPA evolutions, 3GPP has introduced number of enhancements that further improve and make IP based voice services possible. For instance, architectural framework and IP multimedia subsystem to provide a secure and reliable means for wireless and wire line communication, and *Continuous Packet Connectivity (CPC)* features improving, e.g., the battery life and reducing the interference levels.

II. MOTIVATION AND RELATED STUDIES

Previous studies regarding HSUPA performance have focused on situation where only one *Transmit Time Interval*

(TTI) length is configured for all terminals in a cell. The impact of various new techniques, such as *Discontinuous DPCCCH transmissions (UL DTX)*, i.e., *Dedicated Physical Control Channel (DPCCCH)* gating [2] [3] [4] [5] [6] and optimized schedulers [5] [7] [8] have been studied extensively with VoIP and been shown to provide noticeable gains in terms of capacity and meeting the delay requirements. Additionally, the effects of mobility have been investigated with system level simulations [9] and live network studies [10] [11].

As HSUPA specifies that terminals can be configured with either 10 ms (mandatory) or 2 ms (optional) TTI this paper extends the previous studies by allowing UEs to be configured to use either one of those TTIs in the same simulation environment. The benefit of allowing both TTIs is that the 2 ms TTI length can provide higher battery saving opportunities due to shorter transmit times but on another hand 10 ms TTI can extend the coverage for power limited UEs that cannot utilize 2 ms TTI, see Figure 1. . In this study, the terminals are split into TTI groups in such a way that 2 ms TTI is specified to be used closer to Node B and 10 ms TTI is assigned to users near the cell edge.

Moreover, this paper extends previous studies by evaluating the performance from two-fold perspective: maximum achievable capacity per cell and battery saving opportunities. Capacity is defined through user quality of service and battery saving opportunities defined by the times when turning of the transmit circuitry is possible, i.e., no data or mandatory control transmissions are present.

III. DISCONTINUOUS DPCCCH TRANSMISSIONS

Before 3GPP Release 7, DPCCCH was defined to be transmitted continuously regardless whether there is actual user data to be transmitted or not, thus highly loading the cell and draining the UE battery with continuous transmissions. An ideal solution for mitigating the impact of those would be to keep the UE silent during the periods when it is not

transmitting any data and activate the control channels just for the transmissions periods but that could compromise the fast power control.

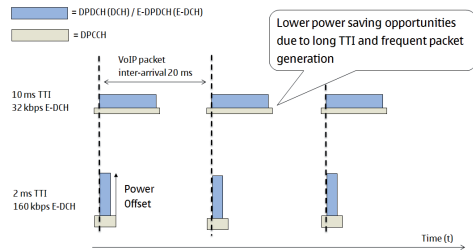


Figure 1. Example of VoIP traffic with different TTIs

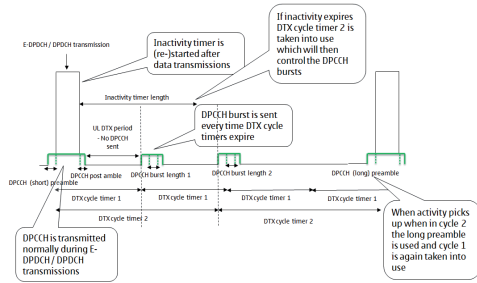


Figure 2. Uplink discontinuous transmission

Release 7 addresses this problem with discontinuous DPCCH transmissions [12] [13]. With UL DTX the transmission of DPCCH is controlled by data transmissions and various different timers which are illustrated in Figure 2. and described shortly as follows:

- **Data transmission:** DPCCH is transmitted continuously throughout the data transmissions.
- **DPCCH preamble:** before the actual data transmission or DPCCH burst is initiated either short or long burst is transmitted to allow the fast power control to correct the UE's transmit power levels. The long DPCCH burst is sent if UE is in DTX cycle 2 and data transmission is initialized, otherwise short is sent.
- **DPCCH postamble:** after the data transmission or DPCCH burst has ended, DPCCH is still transmitted as long as the postamble length defines.
- **Inactivity timer:** transitions from DTX cycle 1 to 2 are controlled by inactivity timer. Once the timer expires, UE moves from cycle 1 to cycle 2. The timer is (re-)started after each data transmission.
- **DTX cycle 1 and 2:** control the periodic DPCCH bursts that are sent regardless is there actual data transmission or not. UE uses cycle 1 when there has been data transmission during the past inactivity timer length.

- **DPCCH burst 1 and 2:** define the length of DPCCH bursts initialized by cycle 1 or cycle 2 timers, respectively.

IV. VOIP OVER HSUPA

In this section, key HSUPA features and assumptions related to VoIP in terms of this study are depicted. These include delay requirements, *Hybrid Automatic Repeat Request (HARQ)* transmissions, scheduling and TTI length classifier.

A. Delay Requirements

One of the most critical factors effecting VoIP quality is the delay. Total transmission delay is the sum of the compression, decompression, processing, buffering/queuing, transmission and the network delays. According to ITU e-model [14], the maximum acceptable mouth-to-ear delay for voice is in the order of 250 ms. In the respect of HSPA networks assuming the delay for core network is approximately 100 ms, the tolerable delay for air interface should be strictly lower than 150 ms. Hence, assuming that both users are HSPA users, tolerable delay for buffering, scheduling and detection is below 80 ms. If total delay exceeds 200-250 ms, the two speakers may result in overlapping each other's messages which naturally leads to deteriorated quality of service.

B. HARQ Transmissions

In HSUPA systems synchronous HARQ is assumed which means that retransmissions take place after fixed duration from the previous transmission, commonly referred as *Round Trip Time (RTT)*. For the 10 ms TTI, 4 parallel processes are specified in [15] leading to RTT of 40 ms. Therefore, the maximum allowed transmissions is two when the delay requirements described above are taken into account. For 2 ms TTI, [15] defines 8 parallel processes leading to 16 ms RTT. In this case, up to 4 transmissions could be contemplated without exceeding the delay margin as possible retransmissions can delay the sending of new packets. Maximum transmission numbers with different TTI lengths are analyzed in more detail in [2].

C. Scheduling

Scheduling for uplink is necessary to keep the interference levels reasonable and thus improving the probability to get transmissions through. In HSUPA two different scheduling schemes are defined: scheduled transmissions controlled by Node B and *Non-Scheduled Transmissions (NST)* controlled by the *Radio Network Controller (RNC)*.

Scheduled transmissions are controlled by Node B so that UEs will signal at each time instant of how much resources they would need and then Node B assigns maximum transmit rate for each user so that the interference levels will not be exceeded. However, the downside of scheduled transmissions is that when, for instance, VoIP is considered satisfactory minimum bit rate might not be achieved and in addition each request requires time and resource consuming signaling.

TABLE I. MAIN SIMULATION ASSUMPTIONS

| Feature/Parameter | Value / Description |
|----------------------------------|---|
| Cell layout | Hexagonal grid, 3 sectors / site, 19 sites / 57 sectors, Wrap-around |
| Inter-site distance | 500m with 10 dB penetration loss 1732m with 20 dB penetration loss |
| Channel model | Vehicular A |
| UE velocity | 3 kmph |
| Scheduling algorithm | Non-scheduled |
| Max active set size | 3 |
| Max. HARQ transmissions | 4 // 2 ms TTI 2 // 10 ms TTI |
| Number of HARQ processes | 8 // 2 ms TTI 4 // 10 ms TTI |
| UE max Tx power | 21 dBm |
| Call length | 60 seconds |
| Slot length | 2/3 milliseconds |
| Voice activity | 0.5 |
| Inactivity/activity periods | neg. exp. distribution, mean 3 sec |
| VoIP packet size | 320 bits |
| VoIP packet interarrival time | 20 ms |
| SID packet interarrival time | 160 ms |
| UL DTX | [on, off] |
| Outage observation window length | 10 seconds |
| Frame error criteria | 5 % |
| Consecutive frame error criteria | 0.3 % |
| Noise rise capacity criteria | 6 dB |
| Outage capacity criteria | 5 % |

NSTs are controlled by RNC which defines a minimum data rate at which the UE can transmit without any previous request. This reduces signaling overhead and consequently processing delays. To meet the tight delay requirements set for VoIP application, NST is the most suitable choice as it enables the UE to transmit the VoIP packets as soon as they arrive to the physical layer and free HARQ processes are available.

D. TTI Length Classifier

As mentioned earlier, 3GPP has specified for HSUPA that terminals can be configured with either 10 ms (mandatory support) or 2 ms (optional support) TTI. Configuration between TTI lengths is controlled by the RNC. In general, the RNC will need to be fairly conservative in re-configuring TTIs, since the RLC re-configuration procedure can require several hundreds of ms and the UE must not lose coverage during this time.

In this study, the impact re-configuration is neglected as we are utilizing quasi-static simulator where UEs do not actually move. The classification which UE uses 10 ms and which 2 ms TTI is based on UE reported path loss and it is done always in the beginning of the call.

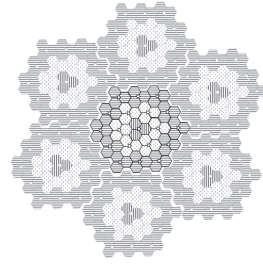


Figure 3. Wrap-around simulation scenario

TABLE II. UL DTX ASSUMPTIONS

| Feature/Parameter | Value / Description |
|-----------------------|---------------------|
| DTX cycle 1 length | 60 slots |
| DTX cycle 2 length | 120 slots |
| Inactivity timer | 36 slots |
| DPCCH burst 1 length | 3 slots |
| DPCCH burst 2 length | 3 slots |
| Short preamble length | 2 slots |
| Long preamble length | 4 slots |
| Postamble length | 1 slot |

In real networks this decision could be made, i.e., based on UE's E_c/N_0 difference between the UE's serving cell and any other cell. If the difference is smaller than a certain predefined range, the terminal would be assigned to use 10 ms TTI. Another option would be to assign TTI groups based on the power headroom reports coming from terminals. As with the E_c/N_0 based solution, if the headroom would be below the predefined range, the user would be assigned to use 10 ms TTI.

V. SIMULATION METHODOLOGY AND ASSUMPTIONS

This VoIP on HSUPA study has been performed using a quasi-static time driven system simulator, also utilized in [2] [4] [6] [7]. All necessary RRM algorithms as well as their interactions are modeled in the simulator and detailed simulation of the users within multiple cells is included. The fast fading channel is explicitly modeled for each UE according to the ITU Vehicular-A profile which is modified for chip interval. A wrap-around multi-cell layout modeling realistic interference conditions is utilized in this study. The principle of wrap-around is roughly that the radio conditions of the actual simulation area are replicated around the area where UEs are located. The wrap-around scenario is illustrated in

Figure 3. Main parameters used in the system simulation are summarized in TABLE I. and UL DTX parameters are listed in TABLE II.

A. VoIP traffic

Each VoIP call consist of activity and silence periods during which either voice or *Silence Indicator (SID)* packets are generated at constant intervals. The duration of these periods is distributed according to parameterized negative exponential distribution.

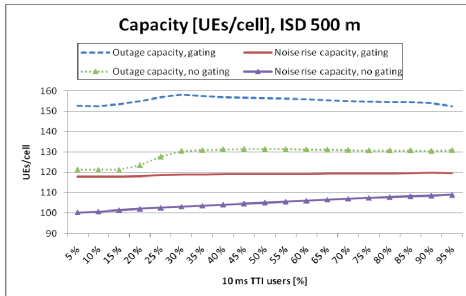


Figure 4. Outage and noise rise capacity in ISD 500 m cell

The size of the VoIP and SID packets are given as parameters as well as the interval between successive packets. In this study VoIP packet is assumed to be 38 bytes and the inter-arrival time between packets is 20 ms. SID packets, used to generate comfort noise in real systems, are assumed to be 14 bytes by their size and they are generated on 160 ms intervals during silence periods. *Robust Header Compression (ROCH)* is not modeled explicitly but ideal ROCH is assumed by taking it into account in packet sizes.

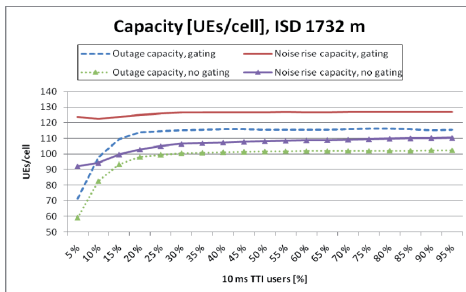


Figure 5. Outage and noise rise capacity in ISD 1732 m cell

B. Quality of service criteria for VoIP

VoIP *Quality of Service (QoS)* is monitored through outage criterion based on packet delay, error rate and *Noise Rise (NR)* criterion based on increased interference level. User is considered to be in outage if at least 5 % of the packets are not received correctly within the delay budget, i.e., 80 ms when

monitored over a 10 seconds on period. Additionally, the user is considered to be in outage if 0.3 % of consecutive frames are not received successfully. Consecutive frame error occurs when the frame is not received within delay budget and the previous frame was also incorrectly received. Further, the capacity is defined as the maximum number of VoIP users per cell, which can be supported without exceeding a 5 % cell wide outage level. Whereas, a noise rise criterion is defined so that mean level should not exceed 6.0 dB. When overall capacity is discussed in this paper it means the minimum of the two: outage and noise rise.

VI. SIMULATION RESULTS

As Figure 4. shows, noise rise acts as a limiting factor in 500 m ISD cell as UEs are not power limited in such a small cell. Different splits, in regard of users assigned to 2 ms or 10 ms TTIs, have only a minor effect on noise rise capacity while gating is used. However, when gating is not used, the higher the number of 10 ms TTI users, the higher the noise rise capacity is. This is caused by the fact that without UL DTX the transmissions are continuous, i.e., DPCCCH is transmitted all the time and thus 2 ms TTI cannot utilize the gaps between the data transmissions to reduce the interference. Whereas, 10 ms TTI has lower power offset between control and data so the interference levels are lower.

In contrast to noise rise capacity, different splits have a more noticeable effect on outage capacity in 500 m cell, as shown in Figure 4. With gating the highest capacity is reached when roughly 30 % of users are assigned to use 10 ms TTI. Similar effect can be seen when gating is not used, with the exception that the capacity does not suffer from higher amount of 10 ms TTI users. The improvement in outage is caused by the fact that good users can utilize shorter TTI length and higher number of HARQ transmissions efficiently.

The VoIP capacity in larger 1732 m cell is illustrated in Figure 5. Unlike in the smaller cell, outage acts as the limiting factor in regard of capacity in larger cell. This happens due to the fact that UEs are more likely to be power limited than interference limited in larger cells. Both noise rise and outage capacity reach their peak performance when at least 30 % of users are assigned to use 10 ms TTI. With lower splits, the noise rise capacity does not suffer as much as outage capacity. However if the RoT alone were to be used to define capacity, then there could be many UEs with poor *Block Error Rate (BLER)*, whereas if outage alone were used, the RoT could rise to a level that would cause coverage issues for other services and system instability.

The overall capacity is presented in Figure 6. As it can be seen from the figure, in smaller cell when gating is used, all TTI splits provide quite similar capacity. On the other hand, without gating the 10 ms TTI provides slightly higher capacity. In larger cell, with and without gating, the performance can be improved very significantly by introducing mixture of 2 and 10 ms TTI users. In larger cells with only or very high number of 2 ms UEs the capacity can be severely compromised.

Transmit antenna activity with different TTI splits can be seen in Figure 7. The figure shows that antenna activity increases steadily from roughly 48% to 60% when the amount

of users assigned to use 10 ms TTI is increased. Thus, the opportunities for power savings and achievable talk-times reduce quite rapidly.

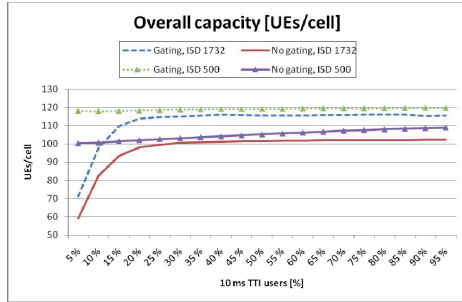


Figure 6. Overall capacity with different TTI splits

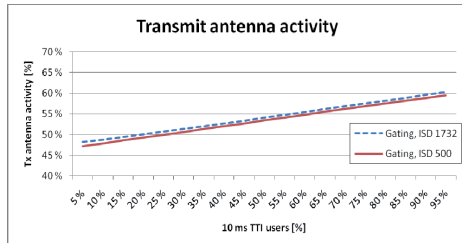


Figure 7. Transmit antenna activity based on different TTI splits

When considering the performance from capacity and Tx activity perspectives, the peak capacity can be attained with 30-35% of users assigned with 10 ms TTI, which translates into roughly 50% antenna activity. Thus, the improvement in battery saving opportunities when compared to the situation where all UEs would be configured to 10 ms TTI is noticeable.

VII. CONCLUSION

The purpose of this paper was to evaluate the benefit of exploiting a mixture of both of the specified transmissions time intervals instead of only one. The performance was investigated with the help of system level simulations and evaluated with different inter-site distances, with and without discontinuous DPCC transmissions.

The results show that with mixed TTIs and large cells the coverage can be extended significantly compared to case where all users use 2 ms TTI. Additionally it is shown, that mixed TTI configuration with roughly 1/3 of the users configured to 10 ms TTI and the rest for 2 ms TTI, provides comparable capacity level with the pure 10 ms TTI setup. However, at the same time battery saving opportunities with mixed TTI configuration are enhanced.

It has also been proposed in 3GPP to merge the best parts of the 2 ms and 10 ms TTI cases by enabling TTI repetition for the 2 ms TTI case when user is close to the cell edge, and thus avoiding the TTI switching procedure. So far the solution has not been approved for inclusion in the specifications.

ACKNOWLEDGMENT

This study is a collaborative work with Nokia and Nokia Siemens Networks. The authors would like to thank all of their co-workers and colleagues for their comments and support.

REFERENCES

- [1] H. Holma, A. Toskala: "HSDPA/HSUPA for UMTS: High Speed Radio Access for Mobile Communications", John Wiley & Sons Ltd, 2006.
- [2] O. Fresan, Tao Chen, E. Malkamaki, T. Ristaniemi: "DPCC Gating Gain for Voice Over IP on HSUPA", IEEE Wireless Communications and Networking Conference, WCNC 2007, 2007.
- [3] M. Bertinelli, J. Jaatinen: "VoIP over HSUPA: link level performance study", 3rd International Symposium on Wireless Communication Systems, ISWCS '06, 2006.
- [4] O. Fresan, Tao Chen, K. Ranta-aho, T. Ristaniemi: "Dynamic Packet Bundling for VoIP Transmission Over Rel7 HSUPA with 10ms TTI Length", 4th International Symposium on Wireless Communication Systems, ISWCS 2007, 2007.
- [5] H. Holma, M. Kuusela, E. Malkamaki, K. Ranta-aho, Tao Chen: "VoIP over HSPA with 3GPP release 7", IEEE 17th International Symposium on Personal, Indoor and Mobile Radio Communications, PIMRC'06, 2006.
- [6] Tao Chen, G. Charbit, K. Ranta-aho, O. Fresan, T. Ristaniemi: "VoIP end-to-end performance in HSPA with packet age aided HSDPA scheduling", IEEE 19th International Symposium on Personal, Indoor and Mobile Radio Communications, PIMRC 2008, 2008.
- [7] Tao Chen, M. Kuusela, E. Malkamaki: "Uplink Capacity of VoIP on HSUPA", IEEE 63rd Vehicular Technology Conference, VTC 2006-Spring, 2006.
- [8] You Jin Kang, Junsu Kim, Dan Keun Sung, Seunghyun Lee: "Hybrid Scheduling Algorithm for Guaranteeing QoS of Real-Time Traffic in High Speed Uplink Packet Access (HSUPA)", IEEE 18th International Symposium on Personal, Indoor and Mobile Radio Communications, PIMRC 2007, 2007.
- [9] K. Aho, J. Aijanen, T. Ristaniemi: "Impact of Mobility to the VoIP over HSUPA System Level Performance", IEEE Vehicular Technology Conference, VTC Spring 2008, 2008.
- [10] A. Arjona, C. Westphal, A. Yla-Jaaski, M. Kristensson: "Towards High Quality VoIP in 3G Networks - An Empirical Study", Fourth Advanced International Conference on Telecommunications, AICT '08, 2008.
- [11] J. Prokkola, P.H.J. Perala, M. Hanski, E. Piri: "3G/HSPA Performance in Live Networks from the End User Perspective", IEEE International Conference on Communications, ICC '09, 2009.
- [12] 3GPP Technical Specification Group Radio Access Network: "Physical layer procedures (FDD)", 3GPP TS 25.214, v9.0.0 (2009-09).
- [13] 3GPP Technical Specification Group Radio Access Network: "Continuous connectivity for packet data users", 3GPP TR 25.903, v8.0.0 (2008-12).
- [14] ITU-T: "General Recommendations on the transmission quality for an entire international telephone connection", Recommendation G.114, May 2003.
- [15] 3GPP Technical Specification Group Radio Access Network: "FDD Enhanced Uplink; Overall description", 3GPP TR 25.309, V6.6.0 (2006-03).

PIV

**STREAMLINING HSUPA TTI LENGTHS WITHOUT
COMPROMISING HSUPA CAPACITY**

by

Frans Laakso, Kari Aho, Ilmari Repo, Thomas Chapman 2011

IEEE 73rd Vehicular Technology Conference: VTC2011-Spring

Reproduced with kind permission of IEEE.

Streamlining HSUPA TTI Lengths without Compromising HSUPA Capacity

Frans Laakso
Magister Solutions Ltd.
Hannikaisenkatu 41
FIN-40100 Jyväskylä, Finland
firstname.lastname@magister.fi

Ilmari Repo
Magister Solutions Ltd.
Hannikaisenkatu 41
FIN-40100 Jyväskylä, Finland
firstname.lastname@magister.fi

Kari Aho
Magister Solutions Ltd.
Hannikaisenkatu 41
FIN-40100 Jyväskylä, Finland
firstname.lastname@magister.fi

Thomas Chapman
Roke Manor Research Ltd.
S051 0ZN
Hampshire, United Kingdom
firstname.lastname@roke.co.uk

Abstract— This paper proposes a s.c. 2 ms range extension scheme for High Speed Uplink Packet Access (HSUPA) networks to avoid potential coverage problems and usage of multiple TTI lengths. With range extension UEs in poor radio conditions are configured to send bundles of 2 ms TTI transmissions without HARQ feedback to improve their coverage. This paper analyzes the performance of range extension in comparison with normal 2 ms TTI performance with multiple inter-site distances. The analysis is conducted considering VoIP performance due to its high sensitivity to additional delays and packet loss. The results acquired by using system level simulation tool indicate that using 2 ms range extension can improve system capacity in larger cells where normal 2 ms TTI can result into coverage problems. Moreover, utilizing repeated 2 ms TTIs instead 10 ms TTIs enables increased battery saving opportunities when UL DTX is applied.

Keywords: VoIP, scheduling, range extension, TTI repetition

I. INTRODUCTION

Traditionally voice has been transferred via circuit switched networks, but recently IP-based applications have started to gain more and more popularity. The *Third Generation Partnership Project's (3GPP's)* Releases 5 and 6 took a major step toward enhanced IP support by introducing *High Speed Downlink Packet Access (HSDPA)* and *High Speed Uplink Packet Access (HSUPA)* evolutions [1]. Due to these enhancements for the first time also voice could be transmitted over a packet switched network with higher spectral efficiency than a traditional circuit switched network. Following from the HSDPA and HSUPA evolutions, 3GPP has introduced a number of enhancements that further improve and make IP based voice services feasible. These include, for instance, an architectural framework and IP multimedia subsystem to provide a secure and reliable means for wireless and wired communication, and *Continuous Packet Connectivity (CPC)* features to provide, e.g., battery saving opportunities and reducing the interference levels.

II. MOTIVATION AND RELATED STUDIES

Previous studies regarding HSUPA (VoIP) performance have focused on various performance enhancing techniques, such as *Discontinuous DPCCCH transmissions (UL DTX)*, i.e., *Dedicated Physical Control Channel (DPCCCH)* gating, see, e.g., [2] [3] [4] [5] and [6]. These extensive studies for VoIP have shown noticeable gains in terms of capacity, battery savings and meeting the delay requirements.

In [2] coverage when both 10 ms and 2 ms TTIs are present in the system and can be configured to be used depending on the UEs path loss are investigated. The results indicate that a “mixed” TTI approach offers extended coverage with good battery saving opportunities when compared to normal 2 ms TTI performance. The purpose of this paper is to extend the “mixed” TTI and other previous studies by proposing a 2 ms *Range Extension (RE)* -scheme. With Range extension 2 ms TTI transmissions are repeated if the UE is found to be coverage limited, thus eliminating the need to configure for two different TTIs. This makes possible for the scheduler to manage only one *Transmission Time Interval (TTI)* instead of two, and as such reduce the number of required radio link reconfiguration procedures. Additionally, various services have tight delay requirements and as such the shorter 2 ms TTI in conjunction with range extension enables the coverage limited UEs to meet the requirements better. Furthermore, Release 7 enhancements such as UL DTX are of less benefit in conjunction with the 10 ms TTI, as presented in Figure 1. and thus UEs can benefit from a range extension technique that avoids the necessity to utilize the 10ms TTI in large cells.

The proposed scheme is evaluated with a time driven quasi-static system simulator from two-fold perspective: maximum achievable capacity per cell and battery saving opportunities. The used simulator represents a HSUPA network in detail including commonly accepted models for, e.g., channel profiles, fading and propagation.

III. DISCONTINUOUS DPCCH TRANSMISSIONS

Before 3GPP Release 7, *Dedicated Physical Control Channel (DPCCH)* was defined to be transmitted continuously regardless whether there is actual user data to be transmitted or not, thus highly loading the cell and draining the UE battery with continuous transmissions. An ideal solution for mitigating the impact of continuous DPCCH would be to keep the UE silent during the periods when it is not transmitting any data and activate the control channels just for the transmission periods. However, that could compromise the fast power control.

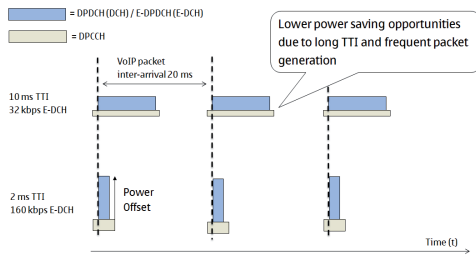


Figure 1. Example of VoIP traffic with different TTIs

Release 7 addresses this problem with discontinuous DPCCH transmissions [7] [8]. With UL DTX the transmission of DPCCH is controlled by data transmissions and various different timers which are introduced in more detail in [2] [7] and [8]. This approach provides increased battery saving opportunities during the times when turning off the transmit circuitry is possible, i.e., no data or mandatory control transmissions are present.

IV. VOIP OVER HSUPA

In this section, key HSUPA and VoIP features and assumptions in terms of this study are depicted. These include delay requirements, *Hybrid Automatic Repeat Request (HARQ)* transmissions and scheduling.

A. Delay Requirements

One of the most critical factors affecting VoIP quality of service is delay. Total transmission delay is the sum of the compression, decompression, processing, buffering/queuing, transmission and the network delays. According to the ITU e-model [9], the maximum acceptable mouth-to-ear delay for voice is in the order of 250 ms. In the respect of HSPA networks assuming the delay for core network is approximately 100 ms, the tolerable delay for air interface should be strictly lower than 150 ms. Hence, assuming that both users are HSPA users, tolerable delay for buffering, scheduling and detection is below 80 ms.

B. HARQ Transmissions

In HSUPA systems synchronous HARQ is used which means that retransmissions take place after fixed duration from the previous transmission, commonly referred as *Round Trip Time (RTT)*. For 2 ms TTI, [10] defines 8 parallel processes,

leading to a 16 ms RTT. In this case, up to 4 transmissions could be tolerated without exceeding the delay margin as possible retransmissions can delay the sending of new packets. Maximum transmission numbers with different TTI lengths are analyzed in more detail in [3].

C. Scheduling

Scheduling for uplink is necessary in order to keep the interference levels reasonable and thus improving the probability to get transmissions through. In this paper *Non Scheduled Transmissions (NST)* are assumed. NSTs are controlled by *Radio Network Controller (RNC)* which defines a minimum data rate at which the UE can transmit without any previous request. This reduces signaling overhead and consequently processing delays. NSTs are the most suitable choice for delay sensitive VoIP application as those enable the UE to transmit the VoIP packets as soon as they arrive to the physical layer and free HARQ processes are available.

V. RANGE EXTENSION MODELING

In this section, the selected range extension scheme is presented in detail. The following sections cover actual RE scheme, the switching criteria between normal 2 ms TTI and 2 ms TTI RE modes, and finally HARQ operation with 2 ms TTI RE.

A. Range Extension Scheme and Requirements

As mentioned before, with RE UE is configured to send a bundle of 2 ms TTI transmissions without HARQ feedback. Regarding RE, a scheme with three s.c. *super-HARQ (S-HARQ)* processes, i.e., bundles of consecutive 2 ms TTI transmissions of same packet is presented in this paper. The selection is done due to similarity to TTI bundling in *Long Term Evolution (LTE)*, which is presented in [11] [12].

In the selected scheme each RE bundle consists of 4 consecutive 2 ms transmissions and there are 3 S-HARQ processes as Figure 2. illustrates. In other words, the RTT for super-HARQ processes is 12 TTIs and three packets can be accommodated at the time. Each S-HARQ is assumed to have maximum of three transmissions per S-HARQ.

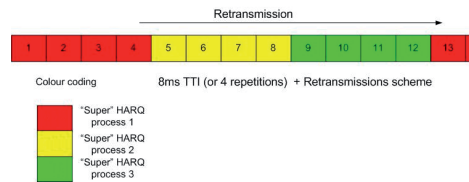


Figure 2. Illustration of the selected range extension scheme

When moving to RE mode, the outer loop power control switches from targeting 1% residual BLER following the 4th transmission of the 2 ms TTI to targeting 10% residual BLER following the 2nd range extension bundle. As the number of repeated TTIs is higher than the number of non repeated TTIs, the E-DPDCH power offset for repeated TTIs is lower than non repeated TTIs in order to keep power control stable.

Additionally, E-DPCCH is multiplexed with E-DPDCH and both are transmitted with each repetition within the RE bundle. In addition CPC cannot be applied during RE mode but only during normal 2 ms mode. Finally, for the purposes of these simulations it is assumed that the Node Bs have perfect knowledge of when RE has been applied.

B. Switching criteria for 2 ms TTI Range Extension

A decision to use either normal 2 ms TTI transmissions or RE mode is made in the beginning of HARQ cycle; every 8 TTIs when in 2 ms mode and every 12 TTIs when in range extension mode. From now on, this is referred as the switch point, see Figure 3. If the UE is not at the switch point, it will continue its transmissions in the current mode even if the criteria for switching would indicate otherwise.

To make the switch from normal to RE mode there must be data to be transmitted either in HARQ channel or in buffer. Additionally, the *Uplink Power Headroom (UPH)*, i.e., the available UE transmit power after DPCCH, must be below the threshold value. The threshold value for switching is optimized based on the targeted *Quality of Service (QoS)* criteria and defines the ratio between normal 2 ms TTI users and range extension users.

- If the UPH is higher than the set threshold value, the UE should make a regular 2 ms TTI (re-)transmission, as it is expected to have sufficient power to meet the required *Signal to Interference Ratio (SIR)* level
- If the UPH is less than the set threshold value, the UE should switch to RE mode.

The UE is forced to make the switch from RE mode to normal mode if there is no data to be transmitted. Otherwise, the switch can be made if the UPH is above the threshold value.

C. HARQ operation with 2 ms TTI Range Extension

Round Trip Time defines in principle which HARQ channel can be mapped to which super-HARQ. Illustration in Figure 3. shows how HARQ channels are mapped when moving from normal to RE mode. In this study it is assumed that HARQ channels 1 and 2 can be mapped to super-HARQ process 1 even though full 16 ms RTT has not passed. Similarly, channels 1 through 6 can be mapped to super-HARQ process 2 and finally all normal HARQ channels can be mapped to super-HARQ process 3.

If there are more than 3 HARQ processes in use when the UE moves to RE mode, the prioritization of HARQ channels according to delay. Excess packets / pending HARQ will have to wait until one or more super processes are available.

Regarding retransmission, unlike with normal 2 ms transmission, where the HARQ feedback (ACK/NACK) is sent after every individual transmission, in RE mode the feedback is sent at the end of the RE bundle. The Node B combines all of the received transmissions in the bundle before decoding in order to accumulate higher SINR at its receiver.

When moving from RE mode to normal 2 ms TTI mode due to RTT requirements, super-HARQ processes 1 and 2 can

be mapped to HARQ channel 1 and onwards. All super-HARQ processes can be mapped to HARQ channel 5 and onwards, as shown in Figure 4.

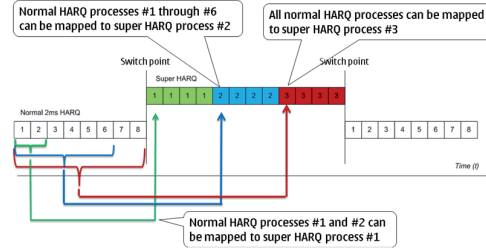


Figure 3. HARQ mapping when switching from normal 2 ms TTI to 2 ms TTI RE

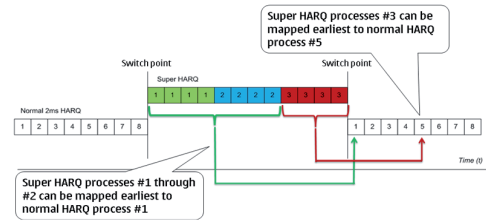


Figure 4. HARQ mapping when switching from 2 ms TTI RE to normal 2 ms TTI operation

VI. SIMULATION METHODOLOGY AND ASSUMPTIONS

The proposed range extension scheme is benchmarked by using a quasi-static time driven system simulator, also utilized in, e.g., [2] [3] [4] [6]. All necessary RRM algorithms as well as their interactions are modeled in the simulator and detailed simulation of the users within multiple cells is included. The fast fading channel is explicitly modeled for each UE according to the ITU Vehicular-A profile which is modified for chip interval. A wrap-around multi-cell layout modeling realistic interference conditions is utilized in this study. The principle of wrap-around is roughly that the radio conditions of the actual simulation area are replicated around the area where UEs are located. The wrap-around scenario is illustrated in Figure 5. The main parameters used in the system simulation are summarized in TABLE I. and UL DTX parameters are listed in TABLE II. In the following subsections the most essential parts of the modeling are elaborated.

A. VoIP traffic

Each VoIP call consist of activity and silence periods during which either voice or *Silence Indicator (SID)* packets are generated at constant intervals. The duration of these periods is distributed according to parameterized negative exponential distribution.

The size of the VoIP and SID packets are given as parameters as well as the interval between successive packets. In this study a VoIP packet is assumed to be 38 bytes and the inter-arrival time between packets is 20 ms. SID packets, used to generate comfort noise in real systems, are assumed to be 14 bytes by their size and they are generated on 160 ms intervals during silence periods. *Robust Header Compression (ROCH)* is not modeled explicitly but ideal ROCH is assumed by taking it into account in packet sizes.

TABLE I. MAIN SIMULATION ASSUMPTIONS

| Feature/Parameter | Value / Description |
|----------------------------------|---|
| Cell layout | Hexagonal grid, 3 sectors / site, 19 sites / 57 sectors, Wrap-around |
| Inter-site distance | 500m with 10 dB penetration loss 1732m with 20 dB penetration loss |
| Channel model | Vehicular A |
| UE velocity | 3 kmph |
| Scheduling algorithm | Non-scheduled |
| Max active set size | 3 |
| Max. HARQ transmissions | 4 // 2 ms TTI 3 // 2 ms TTI RE |
| Number of HARQ processes | 8 // 2 ms TTI 3 // 2 ms TTI RE |
| Transmissions in RE-bundle | 4 |
| Power control target | 1% after 4 th Tx // 2 ms TTI 10% after 2 nd bundle // RE |
| UE max Tx power | 21 dBm |
| Call length | 60 seconds |
| Slot length | 2/3 milliseconds |
| Voice activity | 0.5 |
| Inactivity/activity periods | neg. exp. distribution, mean 3 sec |
| VoIP packet size | 320 bits |
| VoIP packet interarrival time | 20 ms |
| SID packet interarrival time | 160 ms |
| UL DTX | [on, off] |
| Outage observation window length | 10 seconds |
| Frame error criteria | 5 % |
| Consecutive frame error criteria | 0.3 % |
| Noise rise capacity criteria | 6 dB |
| Outage capacity criteria | 5 % |

B. Quality of service criteria for VoIP

VoIP *Quality of Service (QoS)* is monitored through outage criterion based on packet delay, error rate and *Noise Rise (NR)* criterion based on interference level. User is considered to be in outage if at least 5 % of the packets are not received correctly

within the delay budget, i.e., 80 ms when monitored over a 10 seconds on period. Additionally, the user is considered to be in outage if 0.3 % of consecutive frames are not received successfully. Consecutive frame error occurs when the frame is not received within delay budget and the previous frame was also incorrectly received. Further, the capacity is defined as the maximum number of VoIP users per cell, which can be supported without exceeding a 5 % cell wide outage level. In addition, a noise rise criterion is defined so that mean level should not exceed 6.0 dB. When the overall capacity is discussed in this paper it refers the minimum of the two: outage and noise rise.

TABLE II. UL DTX ASSUMPTIONS

| Feature/Parameter | Value / Description |
|-----------------------|---------------------|
| DTX cycle 1 length | 60 slots |
| DTX cycle 2 length | 120 slots |
| Inactivity timer | 36 slots |
| DPCCCH burst 1 length | 3 slots |
| DPCCCH burst 2 length | 3 slots |
| Short preamble length | 2 slots |
| Long preamble length | 4 slots |
| Postamble length | 1 slot |

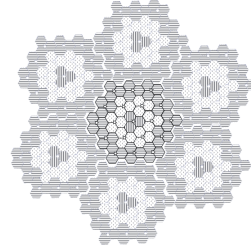


Figure 5. Wrap-around simulation scenario

VII. SIMULATION RESULTS

In the small cell (ISD 500 m) RE mode slightly outperforms normal 2 ms TTI without gating as Figure 6. shows. With gating the performance numbers are almost identical. As the smaller cell scenario is interference limited, rather than the users being power limited, only a very limited number of UEs will be configured to use RE mode. Range extension improves the probability to get transmissions through in power outage situation but as such does not reduce the interference. As practically no users are configured to use RE mode in the smaller cell, the differences also in possible battery saving opportunities are minimal, as seen in Figure 7.

In large cell range extension clearly outperforms normal 2 ms TTI, both with and without gating, by showing over 200 % increase in capacity, as can be seen in Figure 8. . Gating offers

slightly improved capacity for normal 2 ms TTI users in large cell, but RE mode users benefit from gating noticeably more.

Additionally, the cost of RE mode in terms of possible battery saving opportunities is very minimal, as illustrated in Figure 9. Moreover, as [2] indicates with 2 ms TTI and thus with RE the power saving opportunities are much higher than with 10 ms TTI. Taking both the improvement in capacity and the minor increase in transmit antenna activity into account, the benefits offered by RE mode clearly outweigh the negative effects.

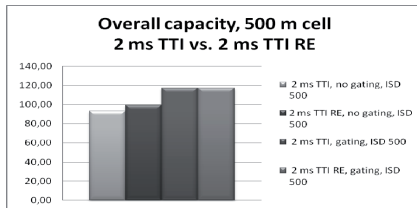


Figure 6. Overall capacity in ISD 500 m cell

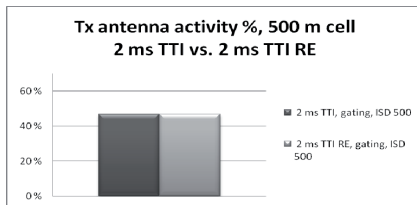


Figure 7. Transmit antenna activity in ISD 500 m cell

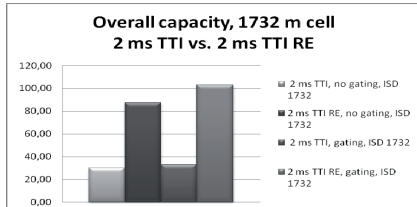


Figure 8. Overall capacity in ISD 1732 m cell

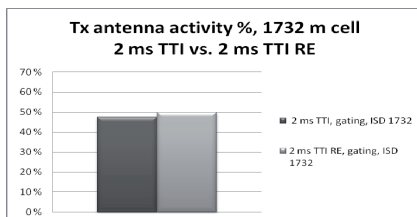


Figure 9. Transmit antenna activity in ISD 1732 m cell

VIII. CONCLUSION

The purpose of this paper was to propose and evaluate the performance of s.c. 2 ms range extension scheme to avoid potential coverage problems and usage of multiple TTI lengths. The performance was investigated with the help of system level simulations with different inter-site distances and with and without discontinuous DPCC transmissions.

The results indicate that coverage problems in large cell can be mitigated very efficiently with range extension when compared to normal 2 ms TTI mode. The results show over 200 % performance enhancement in terms of capacity. In the smaller cell, RE mode shows no adverse effects and offers similar performance with normal 2ms TTI mode. Additionally, the trade-off in battery saving opportunities between normal 2 ms TTI and RE mode is minimal.

ACKNOWLEDGMENT

This study is a collaborative work with Nokia and Nokia Siemens Networks. The authors would like to thank all of their co-workers and colleagues for their comments and support.

REFERENCES

- [1] H. Holma, A. Toskala: "HSDPA/HSUPA for UMTS: High Speed Radio Access for Mobile Communications", John Wiley & Sons Ltd, 2006.
- [2] F. Laakso, K. Aho, I. Repo, T. Chapman: "Extended HSUPA Coverage and Enhanced Battery Saving Opportunities with Multiple TTI Lengths", IEEE 21st International Symposium on Personal, Indoor and Mobile Radio Communications, PIMRC'10, 2010.
- [3] O. Fresan, Tao Chen, E. Malkamaki, T. Ristaniemi: "DPCC Gating Gain for Voice Over IP on HSUPA", IEEE Wireless Communications and Networking Conference, WCNC 2007, 2007.
- [4] O. Fresan, Tao Chen, K. Ranta-aho, T. Ristaniemi: "Dynamic Packet Bundling for VoIP Transmission Over Rel'7 HSUPA with 10ms TTI Length", 4th International Symposium on Wireless Communication Systems, ISWCS 2007, 2007.
- [5] H. Holma, M. Kuusela, E. Malkamaki, K. Ranta-aho, Tao Chen: "VoIP over HSPA with 3GPP release 7", IEEE 17th International Symposium on Personal, Indoor and Mobile Radio Communications, PIMRC'06, 2006.
- [6] Tao Chen, M. Kuusela, E. Malkamaki: "Uplink Capacity of VoIP on HSUPA", IEEE 63rd Vehicular Technology Conference, VTC 2006-Spring, 2006.
- [7] 3GPP Technical Specification Group Radio Access Network: "Physical layer procedures (FDD)", 3GPP TS 25.214, v9.0.0 (2009-09).
- [8] 3GPP Technical Specification Group Radio Access Network: "Continuous connectivity for packet data users", 3GPP TR 25.903, v8.0.0 (2008-12).
- [9] ITU-T: "General Recommendations on the transmission quality for an entire international telephone connection", Recommendation G.114, May 2003.
- [10] 3GPP Technical Specification Group Radio Access Network: "FDD Enhanced Uplink; Overall description", 3GPP TR 25.309, V6.6.0 (2006-03).
- [11] R. Susitaival, M. Meyer: "LTE Coverage Improvement by TTI Bundling", IEEE 69th Vehicular Technology Conference, VTC 2009-Spring, April 2009.
- [12] Jing Han, Haiming Wang: "Principle and Performance of TTI Bundling For VoIP in LTE FDD Mode", IEEE Wireless Communications and Networking Conference, WCNC 2009, April 2009.

PV

**INTRODUCING SWITCHED ANTENNA TRANSMIT
DIVERSITY FOR HIGH SPEED UPLINK PACKET ACCESS**

by

Kari Aho, Ilmari Repo, Petri Eskelinen, Frans Laakso 2011

18th International Conference on Telecommunications

Reproduced with kind permission of IEEE.

Introducing Switched Antenna Transmit Diversity for High Speed Uplink Packet Access

Kari Aho
Magister Solutions
Hannikaisenkatu 41
FIN-40100 Jyväskylä, Finland
kari.aho@magister.fi

Petri Eskelinen
Magister Solutions
Hannikaisenkatu 41
FIN-40100 Jyväskylä, Finland
petri.eskelinen@magister.fi

Ilmari Repo
Magister Solutions
Hannikaisenkatu 41
FIN-40100 Jyväskylä, Finland
ilmari.repo@magister.fi

Frans Laakso
Magister Solutions
Hannikaisenkatu 41
FIN-40100 Jyväskylä, Finland
frans.laakso@magister.fi

Abstract—3GPP is investigating uplink transmit diversity alternatives for HSUPA. This paper addresses uplink transmit diversity from the perspective of open loop where additional feedback information is not available. Furthermore, the focus will be on switched antenna transmit diversity where only one antenna is active at the time even though UE is equipped with multiple transmit antennas. Five different algorithms are presented and benchmarked in system level in various conditions against baseline performance without Tx diversity. The studies show achievable gains when the UE velocity is low but practical algorithms get only fraction of the possible gain and improper algorithms can lead to even performance loss.

Keywords: SATD, HSUPA, Open Loop Transmit Diversity

I. INTRODUCTION

The *Third Generation Partnership Project's (3GPP's)* Releases 5 and 6 took major steps toward enhancing packet data capabilities of cellular networks by standardizing *High Speed Downlink Packet Access (HSDPA)* and *High Speed Uplink Packet Access (HSUPA)* evolutions [1]. Following Release 6, various performance enhancements, such as dual cell HSDPA and HSUPA, higher order modulation, discontinuous reception and transmission were introduced to further enhance performance. In October 2009 a study item was opened in 3GPP to cover open loop transmit diversity options for uplink. Previously transmit diversity has been considered only for downlink (see, e.g., [2], [3]), for instance due to cost and size requirements of the small hand-held terminals. However, due to increasing demand of higher performance also in the uplink, diversity techniques were considered as potential performance enhancement for HSUPA as well. During various *Radio Access Network Radio Layer 1 (RAN1)* work group [4] meetings possible schemes, assumptions and performance of open loop beamforming and *Switched Antenna Transmit Diversity (SATD)* were evaluated

and discussed. The findings are summarized in the 3GPP Technical Report 25.863 [5].

The purpose of this paper is to introduce and benchmark five different open loop switched antenna transmit diversity algorithms under the 3GPP simulation assumptions. Analysis will be conducted with the help of a quasi-static time driven system level simulator used previously, e.g., to support findings for [5]. Theoretically, SATD can offer 3 dB gain over non-diversity performance [5] and in this paper the gain is evaluated on system level with the respect of different channels, UE velocities and load conditions.

II. SWITCHED ANTENNA TRANSMIT DIVERSITY

Regardless of SATD the UE transmits the *Dedicated Physical Control Channel (DPCCH)*, *Enhanced-DPCCH (E-DPCCH)*, *Enhanced Dedicated Data Channel (E-DPDCH)* and *High Speed-DPCCH (HS-DPCCH)* as in the current specifications. The difference with SATD being that UE possesses two transmit antennas and is able to switch its transmit chain between the antennas as Figure 1. illustrates.

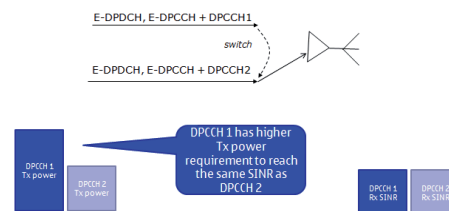


Figure 1. Principle of SATD

The UE autonomously decides at each evaluation interval which transmit antenna is better and thus which to use. In soft handover, it may be the case that the best UE antenna may

differ for different cells. In this paper it is assumed that the UE bases its antenna selection on the serving NodeB. Moreover, since the network is not aware of the UEs transmit diversity scheme, any filtering of channel estimations between slots at the Node B will smear the channel impulse responses from the two antennas after switching as the switch is invisible to the network.

In the following subsections five different SATD algorithms for deciding the best antenna are presented. First the so called Genie (TX1) algorithm is presented. Genie is not realistic but represents an upper performance bound for UE TX diversity algorithms. After TX1 algorithm four "practical algorithms" which use existing performance indicators to decide the used antenna are introduced.

A. TX1: Genie Aided Switching

With Genie aided switching UE makes switching decisions every evaluation period, e.g. radio frame (10 ms), based on ideal knowledge of the channel impulse responses from the two antennas. The selected transmit antenna ($j=1,2$) is the one that maximizes:

$$\frac{1}{15} \sum_{k=1}^{15} \sum_{l=1}^L \left(|h_{1,j}(l,k)|^2 + |h_{2,j}(l,k)|^2 \right). \quad (1)$$

In (1) k is a slot index, l is a multipath index and $h_{i,j}(l,k)$ represents the channel impulse response from between transmit antenna j and receive antenna i . In the simulation environment this algorithm can be implemented simply by selecting the antenna with best fading conditions as that will result into same outcome as the equation above. See Figure 2. for reference of the Genie algorithm.

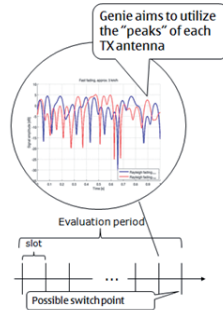


Figure 2. TX1, Genie aided switching

B. TX2: TPC Aided Switching 1

With *Transmit Power Control (TPC)* command aided switching the UE will every time interval, e.g., radio frame (10 ms), check the sum of TPC commands where power UP command represents $+1$ and power DOWN -1 . If the sum of the commands is higher than 0 then the switch is made as that

would indicate that the current antenna needs on average more power than in previous evaluation period and other antenna could potentially be in better situation. In addition, a forced switch is made every forced switch time interval, e.g., 4 frames, if the sum of TPC commands does not trigger the switch earlier. Figure 3. illustrates TX2 algorithm.

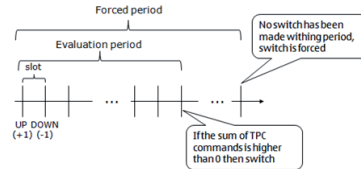


Figure 3. TX2, TPC aided switching 1

C. TX3: TPC Aided Switching 2

Another practical algorithm presented in this paper is also based on TPC commands. As Figure 4. shows, here the UE switches Tx antennas periodically every time interval, e.g., radio frame (10 ms), and then monitors the following PC command for the new antenna. If the command after the switch is DOWN switched antenna is kept in use, otherwise the previous antenna is switched back into use

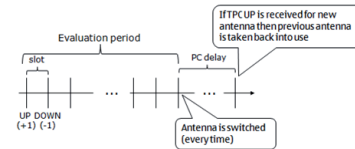


Figure 4. TX3, TPC aided switching 2

D. TX4: DPCCH Aided Switching

Practical algorithm TX4 is based on UE checking periodically every time interval the last known DPCCH level of each antenna and switches to the antenna indicating the best antenna, see Figure 5. for reference. A forced switch is made every forced switch time interval, e.g., 4 frames if performance indicator level does not trigger the switch.

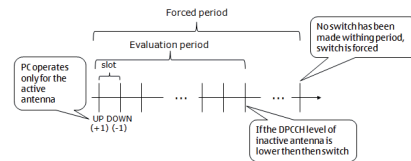


Figure 5. TX4, DPCCH aided switching

E. TX5: Periodical Switch

Finally, the simplest switching algorithm, is based on periodical switch between antennas. This means that antennas are changed every time interval, e.g., radio frame (10 ms), regardless of the channel conditions of different antennas.

F. Power Selection Algorithms

In addition to switching algorithms the DPCCH transmit power level for the new antenna needs also to be decided after each switch. In this paper two different power algorithms are modeled and studied. These algorithms are shown in Figure 6. and described shortly in the following:

- *Pwr keep* which results into using the power level of the antenna that was switched away.
- *Pwr old* which indicates the use of the last known power level of the new antenna.

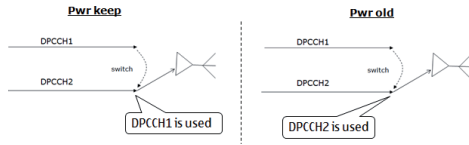


Figure 6. Transmit Power Selection Algorithms

G. Antenna Imbalance

When deploying multiple antennas to a user device it is likely that antennas are not exactly alike. Antenna imbalance is a term representing the difference in efficiency between Tx antennas. There exists two main types of imbalances:

- Short term antenna imbalance which models the spatial difference between antennas, i.e., different slow fading conditions between the antennas.
- Long term antenna imbalance which models the difference caused by, e.g., manufacturing reasons.

For the sake of modeling purposes both long and short term imbalances are fixed for the duration of the call. Short term imbalance is randomized according to Gaussian distribution with standard deviation of 2.25 dB. Long term imbalance is fixed to 0 dB.

III. SIMULATION METHODOLOGY AND ASSUMPTIONS

This study has been performed by using a comprehensive quasi-static time driven system simulator. The simulator has been utilized in the past in various international publications as well as supporting 3GPP standardization work, see, e.g., [6]. The simulation tool enables detailed simulation of users in multiple cells with realistic call generation, propagation and fading which are adopted from [7] and updated according to 3GPP requirements.

A. Quasi-static Simulation Approach

The term “Quasi-static” approach means that UEs are stationary but both slow (log normal) and fast fading are explicitly modeled. Fast fading is modeled for each UE according to the ITU channel profiles [8] which are modified for chip interval. Statistical confidence is reached through running multiple drops, i.e., independent simulation iterations. In each step terminal locations, fading, etc. are randomized but the statistics are gathered and averaged over all drops.

TABLE I. MAIN SIMULATION ASSUMPTIONS

| Feature/Parameter | Value / Description |
|------------------------------|---|
| Cell Layout | Hexagonal grid, 19 NodeBs, 3 sectors per Node B with wrap-around |
| Inter-site Distance | 1000 m with 10 dB penetration loss |
| Channel Model | Pedestrian A, Vehicular A |
| UE Velocity | [3, 30] kmph |
| Log Normal Fading | Standard Deviation : 8dB Inter-NodeB Correlation: 0.5 Intra-NodeB Correlation: 1.0 Correlation Distance: 50m |
| NodeB Receiver | Rake (2 antennas per cell) |
| UE Max. Tx Power | 23 dBm |
| TTI Length | 2 ms |
| Max. HARQ Transmissions | 4 |
| Number of HARQ Processes | 8 |
| Short Term Antenna Imbalance | Gaussian distribution, STD 2.25 dB |
| Long term Antenna Imbalance | 0 dB |
| Tx Antenna Correlation | uncorrelated |
| SATD Switching Periods | Evaluation period: 10 ms Forced switch: 140 ms |
| Number of UEs per Sector | [1, 2, 4, 10] |
| UE Distribution | Uniform over the whole area |
| Traffic Type | Full Buffer |
| Scheduling algorithm | Proportional Fair, Forgetting factor: 0.01 |
| Uplink power headroom | Averaged over 100 ms (not antenna specific) |

B. Simulation Assumptions

Main parameters used in the system simulation are summarized in TABLE I. For simulation scenario a wrap-around multi-cell layout illustrated in Figure 7. is utilized.

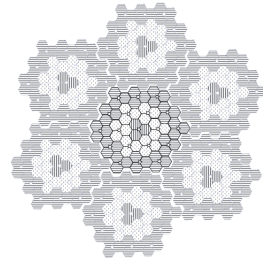


Figure 7. Wrap-around simulation scenario

The purpose of the wrap-around is to model the interference correctly also for outer cells. This is achieved by limiting the UE placement around the actual simulation area but replicating the cell transmissions around the whole simulation area to offer more realistic interference situation

throughout the scenario. In Figure 7. the actual simulation area is highlighted in the center. UEs are created to the scenario according to uniform distribution which results into some cells being more heavily loaded while others can be even empty.

IV. SIMULATION RESULTS

Figure 8. and Figure 9. illustrate the performance of different SATD algorithms in terms of cell throughput in a Pedestrian A 3 kmph channel. As those figures show, in general, SATD is able to increase the system level performance by 10-20 % depending on the algorithm and load conditions.

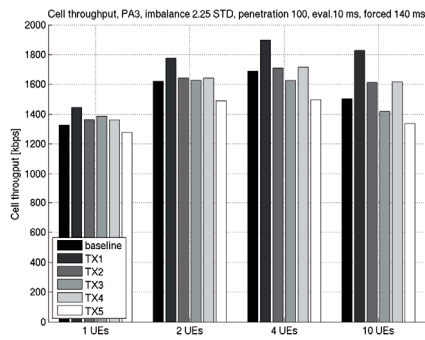


Figure 8. Algorithm Comparison, Pwr keep, Cell throughput, PedA 3 kmph

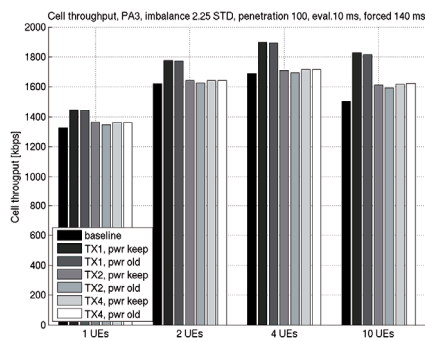


Figure 9. Power and SATD algorithms, Cell throughput, PedA 3 kmph

The gain from SATD is caused mainly by additional diversity and due to UEs being able to utilize the antenna which is in better channel situation. Utilizing the better antenna reduces the average required DPCCH (and total) Tx power as Figure 10. shows. Due to reduced Tx power also the interference levels are reduced, especially at cell edge where the interference levels are generally the highest. On the one hand this benefits the poorer (cell edge) UEs which are often

power (or interference) limited. On another hand UEs in better channel conditions are able to benefit from the reduced interference as well. Due to the reduced DPCCH Tx powers and interference levels the NodeB is able to schedule higher allocations to UEs in good channel conditions. Higher allocations will increase the cell throughput but also the interference within the system. Still, cell edge UEs experience reduced interference of the neighboring cells caused by other cell edge UEs. Naturally, NodeB scheduling decisions control the interference levels as well and thus benefit also the cell edge UEs which need less power for DPCCH with SATD.

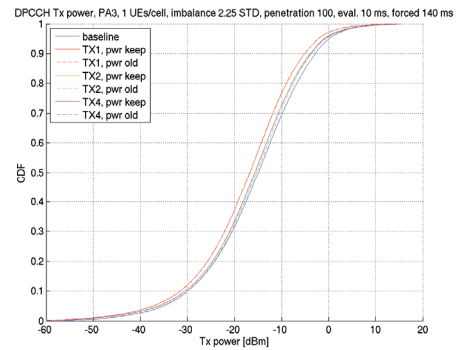


Figure 10. DPCCH Tx Power Distribution, PedA 3 kmph

In terms of algorithm performance, as expected, TX5, based only on periodic changing of TX antennas, results in poorest performance and in fact does not provide gain over the baseline but even losses. This is due to power control being affected by the switching and the fact that UE can potentially switch to a much poorer antenna resulting into system loss. With algorithms TX1, TX2 and TX4 the performance can be enhanced with all load conditions as Figure 8. and Figure 9. illustrate. TX1 represents an upper limit of the performance as the switches are based on accurate channel information. However, TX1 would not be possible to implement without actual feedback channel, hence the name Genie algorithm. Practical algorithms TX2 and TX4 utilizing available averaged channel information (TPC or DPCCH level) are able to provide gain but do not meet the upper limit. TX3 indicates gain with low load but once the load increases the performance gain turns into loss. This is due to the fact that with higher load the (varying) interference conditions become more dominant, and a decision to keep the newly switched antenna is based on solely one transmit power command is bound to be inaccurate.

In addition, the power selection algorithms shown in Figure 9. do not show very significant difference in these studies. Apart from, in general, pwr keep, i.e. keeping same DPCCH power in use for both antennas regardless of the switch, is showing slightly higher performance. The reason for that is that the antennas in this study are considered rather similar to each other with the exception of channel conditions and short term antenna imbalance which is assumed to be rather small

(standard deviation 2.25 dB). Thus, it is better to keep the power level in use that is power controlled continuously.

As it was stated above SATD is able to provide benefit over the baseline when the UE velocity is low, namely 3 kmph. However, in faster changing channel selecting and utilizing the best antenna continuously becomes much more challenging. This is demonstrated in Figure 11, where the performance in terms of cell throughput in Vehicular A 30 kmph channel is depicted. As that figure shows the potential gains even with TX1 are more limited and with practical algorithms SATD can lead to 'no gain' situations in some cases. The difficulty to select the best antenna is illustrated in Figure 12, which shows the number of antenna switches per second in both channels. As can be seen from that the amount of switches increases significantly with TX1 when comparing PedA 3 kmph and VehA 30 kmph channels. The increased amount is caused by the UE trying to follow the faster changing channel. With TX2 and TX4 the amount of switches does not increase as those algorithms are based on averaged key performance indicators and thus the impact of channel is more filtered.

V. CONCLUSION

The purpose of this paper was to evaluate transmit diversity for HSUPA from the perspective of open loop where no additional feedback information is available. The performance was addressed through switched antenna transmit diversity where only one antenna is active at the time even though UE would be equipped with multiple transmit antennas.

This paper presents and benchmarks five different algorithms for SATD in various conditions against baseline performance without Tx diversity. The studies show that the Genie (TX1) algorithm can provide gains with all cell loading points and channels. The gains in VehA are, however, significantly lower. For practical algorithms, improper switching decisions can bring some loss of performance even in PedA channel but a properly selected algorithm can provide gain. VehA channel is more difficult environment for the practical algorithms and closer fine-tuning would be in order to avoid possible losses.

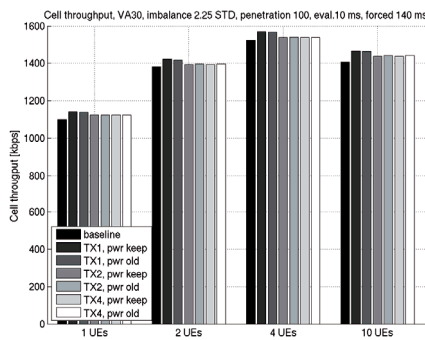


Figure 11. Power and SATD algorithms, Cell throughput, VehA 30 kmph

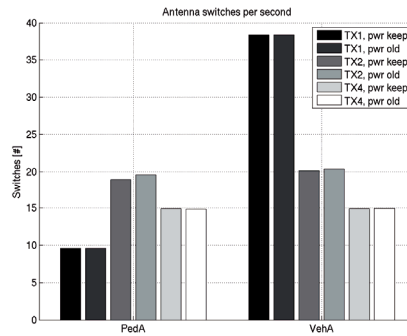


Figure 12. Amount of Antenna Switches per Second

ACKNOWLEDGMENTS

This study is a collaborative work with Nokia and Nokia Siemens Networks. The authors would like to thank all of their co-workers and colleagues for their comments and support. In addition authors would like to express their gratitude to Thomas Chapman from Roke Manor for his valuable comments and contributions on the work.

REFERENCES

- [1] H. Holma, and A. Toskala: "HSDPA/HSUPA for UMTS: High Speed Radio Access for Mobile Communications", John Wiley & Sons Ltd, 2006.
- [2] R.T Derryberry, S.D. Gray, D.M. Ionescu, G. Mandyam, and B. Raghathan, "Transmit diversity in 3G CDMA systems", *Communications Magazine, IEEE*, vol.40, no.4, pp.68-75, Apr 2002.
- [3] A. Hottinen, R. Wichman, "Transmit diversity by antenna selection in CDMA downlink," *Spread Spectrum Techniques and Applications, 1998. Proceedings., 1998 IEEE 5th International Symposium on*, vol.3, no., pp.767-770 vol.3, 2-4 Sep 1998
- [4] Third Generation Partnership Project (3GPP), Radio Access Network Radio Layer 1 Work Group, <http://3gpp.org/RAN1-Radio-layer-1>, cited September 2010.
- [5] Third Generation Partnership Project (3GPP), "Universal Terrestrial Radio Access (UTRA); Uplink transmit diversity for High Speed Packet Access (HSPA)", *Technical Report, TR 25.863*, May 2010.
- [6] I. Repo, K. Aho, S. Hakola, T. Chapman, and F. Laakso, "Enhancing HSUPA system level performance with dual carrier capability", In *Proceedings of 5th IEEE International Symposium on Wireless Pervasive Computing (ISWPC)*, Modena, Italy, May 2010.
- [7] Third Generation Partnership Project (3GPP), "Selection Procedures for the Choice of Radio Transmission Technologies of the UMTS", *Technical Requirement, TR 101 112 (UMTS 30.03)*, 1998.
- [8] ITU-R, "Guidelines for Evaluation of Radio Transmission Technologies for IMT-2000", *Recommendation, ITU-R M.1225*, 1997.

PVI

**ON HSUPA OPEN LOOP SWITCHED ANTENNA TRANSMIT
DIVERSITY PERFORMANCE IN VARYING LOAD
CONDITIONS**

by

Petri Eskelinen, Ilmari Repo, Kari Aho, Frans Laakso 2011

IEEE 73rd Vehicular Technology Conference: VTC2011-Spring

Reproduced with kind permission of IEEE.

On HSUPA Open Loop Switched Antenna Transmit Diversity Performance in Varying Load Conditions

Petri Eskelinen
Magister Solutions
Hannikaisenkatu 41
FIN-40100 Jyväskylä, Finland
firstname.lastname@magister.fi

Kari Aho
Magister Solutions
Hannikaisenkatu 41
FIN-40100 Jyväskylä, Finland
firstname.lastname@magister.fi

Ilmari Repo
Magister Solutions
Hannikaisenkatu 41
FIN-40100 Jyväskylä, Finland
firstname.lastname@magister.fi

Frans Laakso
Magister Solutions
Hannikaisenkatu 41
FIN-40100 Jyväskylä, Finland
firstname.lastname@magister.fi

Abstract—The Switched Antenna Transmit Diversity (SATD) scheme is a promising transmit diversity technique to improve the performance in High Speed Uplink Packet Access (HSUPA) systems. Antenna switching rests on a technique where only one antenna is active at a time even if the UE is equipped with multiple transmit antennas. Switching and antenna selection can be based on different methods and criteria and this paper provides simulative analysis of three different open loop antenna switching algorithms for the HSUPA systems. Furthermore, the focus will be on evaluating corresponding system level performance compared to the single Tx antenna performance when bursty traffic is assumed. The studies show that there are achievable gains and thus system performance may be enhanced by applying the antenna switching scheme, especially when the mobile velocity is low.

Keywords: SATD, HSUPA, Open Loop Transmit Diversity

I. INTRODUCTION

The *Third Generation Partnership Project's (3GPP)* Releases 5 and 6 took major steps toward enhancing packet data capabilities of cellular networks by standardizing *High Speed Downlink Packet Access (HSDPA)* and *High Speed Uplink Packet Access (HSUPA)* evolutions [1]. After that several additional performance enhancements have been introduced e.g. *Multiple-Input and Multiple-Output (MIMO)* technologies, higher order modulation, discontinuous reception and transmission as a few examples. 3GPP started a study item to find out potential options for *open loop transmit diversity (OLT)* in October 2009. The transmit diversity has already been studied for downlink direction and due to that the study item covers only uplink performance evaluation. Transmit diversity techniques have been considered as potential performance enhancement for HSUPA. During various *Radio Access Network Radio Layer 1 (RAN1)* work group [2] meetings possible schemes, assumptions and performance of open loop beamforming and *Switched Antenna Transmit Diversity (SATD)* were evaluated and discussed. The findings are gathered to Technical Requirement 25.863 [3].

II. MOTIVATION AND RELATED STUDIES

The open loop transmit diversity schemes for HSUPA have been recently investigated by 3GPP. Contributions [4], [5], [6] and [7] provide SATD results for 1 km and 2.8 km Inter Site Distance (ISD) with simulation assumptions aligned to 3GPP assumptions. All contributions above assume static number of users with full buffer traffic.

This paper extends previous studies of SATD performance with a scenario where users arrive dynamically to the system according to Poisson process. Once users arrive to the system they upload a file and leave the system when the upload is completed thus creating a network environment where data transmissions are bursty. Bursty traffic is more representative of the real world conditions where users do not send data all the time.

III. SWITCHED ANTENNA TRANSMIT DIVERSITY

With SATD the User Equipment (UE) possesses two transmit antennas and is able to switch its radio frequency (RF) chain between the antennas as shown in Figure 1. Regardless, the UE transmits *Dedicated Physical Control Channel (DPCCCH)*, *Enhanced-DPCCH (E-DPCCH)*, *Enhanced Dedicated Data Channel (E-DPDCH)* and *High Speed-DPCCH (HS-DPCCH)* as in the current specifications.

The UE autonomously decides which transmit antenna should be used due to the requirement by the 3GPP that the network is not aware of the UEs transmit diversity scheme and thus any feedback from NodeB for antenna selection is not available. According to the 3GPP Technical Specification TR 25.863 [3] the theoretic maximum gain from SATD can be calculated by assuming ideal channel state information at the UE and the perfect inner loop power control (to achieve combined receive power target P). Then the transmit antenna which has the larger channel gain will be chosen every time switch is made. With the assumptions above, the instantaneous transmit power is:

$$\frac{P}{\max_{j=1,2} \left\{ |h_{1,j}|^2 + |h_{2,j}|^2 \right\}}. \quad (1)$$

The average transmit power needed for switched antenna scheme is:

$$E \left[\frac{P}{\max_{j=1,2} \left\{ |h_{1,j}|^2 + |h_{2,j}|^2 \right\}} \right] = \int_0^{\infty} \frac{P}{x} f(x) dx = P/2. \quad (2)$$

The probability distribution of the denominator in Eq. (2) within the expectation can be derived as following:

Define two random variables: $X_j = |h_{1,j}|^2 + |h_{2,j}|^2, j=1,2$

They are independent and identically distributed with probability distribution function xe^{-x} . The probability distribution function of the random variable $\max(X_1, X_2)$ can be further derived based on the formula for maximum of two independent random variables:

$$f(x) = 2xe^{-x} [1 - (1+x)e^{-x}]. \quad (3)$$

Finally, the expectation is evaluated as follows:

$$E \left[\frac{P}{\max_{j=1,2} \left\{ |h_{1,j}|^2 + |h_{2,j}|^2 \right\}} \right] = \int_0^{\infty} \frac{P}{x} 2xe^{-x} [1 - (1+x)e^{-x}] dx = P/2 \quad (4)$$

Thus relative to the baseline, there is ideally a 3 dB gain by using switched antenna transmit diversity.

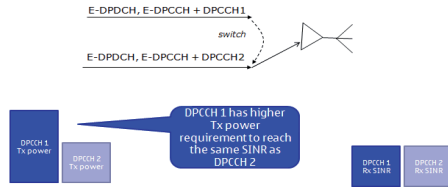


Figure 1. Principle of SATD

IV. ANTENNA SWITCHING ALGORITHMS

In this study three different Uplink Tx diversity antenna switching algorithms are simulated against single Tx antenna performance. First algorithm (TX1) is not realistic because of the algorithm's knowledge of the channel impulse responses and it represents the upper performance bound for a UE TX diversity algorithm. In addition, TX2 and TX4 implement "a practical algorithm" possible for real open loop implementations. The studied algorithms are described shortly below:

A. TX1: Genie Aided Switching

With Genie aided switching UE makes a switching decision every evaluation period, e.g. radio frame (10 ms), based on ideal knowledge of the channel impulse responses from the two antennas. The selected antenna is the one that maximizes:

$$\frac{1}{15} \sum_{k=1}^{15} \sum_{l=1}^L \left(|h_{1,j}(l,k)|^2 + |h_{2,j}(l,k)|^2 \right). \quad (5)$$

In Eq. (5) k is a slot index, l is a multipath index and $h_{i,j}(l,k)$ represents the channel impulse response from between transmit antenna j and receive antenna i . In the simulation environment this algorithm can be implemented simply by selecting the antenna with best fading conditions.

B. TX2: TPC Aided Switching 1

With *Transmit Power Control (TPC)* command aided switching, the UE will every time interval check the sum of TPC commands. Power UP command represents $+I$ and power DOWN $-I$. If the sum of the commands is higher than 0 then the switch is made. A forced switch is made every forced switch time interval if performance indicator levels do not trigger the switch.

C. TX4: DPCCH Aided Switching

The UE checks periodically every time interval the last known DPCCH level of each antenna and switches to the antenna indicating the best antenna. A forced switch is made every forced switch time interval if performance indicator levels do not trigger the switch.

V. TRAFFIC MODEL

In this study bursty traffic model is used to evaluate switched antenna performance for HSUPA. Used traffic model is based on *Next Generation Mobile Networks (NGMN) File Transfer (FTP)* traffic model [8] in which traffic is generated using fixed number of users, with a statistical distribution. Model defines the size of the file to be transferred and the reading time required before the next transfer. However, this way simulation will be burdened by the high number of inactive users that do not transfer any data actively and are only waiting their reading time to be expired.

Method used in this study is a simplification of NGMN model by utilizing dynamic arrival of users instead of reading times. Users arrive to the system according to Poisson process and uniform distribution. Once user arrives it uploads a file and leaves the system when the file data is transferred. For the period of the file transfer the data is assumed to upload as quickly as the network allows (i.e. similar to full buffer user). Dynamic arrival of users generates load to the system that is dependent on two variables: the file size S and the Poisson distributed arrival rate λ . Thus, the offered load (Mbps) is defined as:

$$\text{Offered load traffic} = \lambda * S \quad (6)$$

TABLE I. MAIN SIMULATION ASSUMPTIONS

| Feature/Parameter | Value / Description |
|---------------------------------|--|
| Cell Layout | Hexagonal grid, 19 NodeBs, 3 sectors per NodeB with wrap-around |
| Inter-site Distance | [1000, 2800] m with 10 dB penetration loss |
| Channel Model | Pedestrian A, Vehicular A |
| UE Velocity | [3, 30] kmph |
| Log Normal Fading | Standard Deviation: 8dB Inter-NodeB Correlation: 0.5 Intra-NodeB Correlation: 1.0 Correlation Distance: 50m |
| NodeB Receiver | Rake (2 antennas per cell) |
| UE Max. Tx Power | 23 dBm |
| TTI Length | 2 ms |
| Max. HARQ Transmissions | 4 |
| Number of HARQ Processes | 8 |
| Short Term Antenna Imbalance | Gaussian distribution, STD 2.25 dB |
| Long term Antenna Imbalance | 0 dB |
| Switched Antenna Switch Periods | Evaluation period: 10 ms Forced switch: 140 ms |
| Tx Antenna Correlation | uncorrelated |
| Offered load traffic | [0.25; 0.50; 0.75; 1.00; 1.25; 1.50; 1.75] Mbps |
| UE Distribution | Uniform over the whole area |
| Traffic Type | File Transfer with variable load (fixed file size 2 Mbits) |
| Scheduling algorithm | Proportional Fair, Forgetting factor: 0.01 |
| Uplink power headroom | Averaged over 100 ms (not antenna specific) |

VI. SIMULATION METHODOLOGY AND ASSUMPTIONS

This study has been performed by using a comprehensive quasi-static time driven system simulator. The simulator has been utilized in the past in various international publications as well as supporting 3GPP standardization work, see, e.g., [9]. Simulation tool enables detailed simulation of users in multiple cells with realistic call generation, propagation and fading (adopted from [10]).

A. Quasi-static Simulation Approach

Quasi-static approach means that UEs are stationary but both slow (log normal) and fast fading are explicitly modeled. Fast fading is modeled for each UE according to the ITU channel profiles which are modified for chip interval [11]. Statistical confidence is reached through running multiple drops, i.e., independent simulation iterations. In each step terminal locations, fading, etc. are randomized but the statistics are gathered and averaged over all drops.

B. Simulation Assumptions

Main parameters used in the system simulation are summarized in TABLE I. As a simulation scenario wrap-around multi-cell layout is utilized in this study. The purpose of

the wrap-around is to model the interference correctly also for outer cells. This is achieved by limiting the UE placement around the actual simulation area but replicating the cell transmissions around the whole simulation area to offer more realistic interference situation throughout the scenario. A UE is able to connect to the outer cells. The wrap-around scenario is illustrated in Figure 2. with actual simulation area highlighted in the center. UEs are created to the scenario according to uniform distribution. This result in some cells being more heavily loaded while others can be even empty, resulting in more accurate imitation of real network behavior.

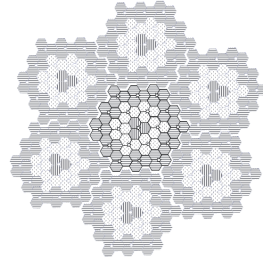


Figure 2. Wrap-around simulation scenario

VII. SIMULATION RESULTS

With used simulation assumptions cell can fully serve offered traffic loads up to 1.00 Mbps, after which served and offered load start to differ, as shown in Figure 3. This is the point after which SATD starts to show noticeable performance enhancement over the baseline in terms of cell throughput. SATD is providing notable gain over the baseline with higher loads especially in PedA 3 kmph channel. This is due to a lower pilot powers and/or decreased interference levels, which are the result of better utilization of changing channel conditions. In general, SATD improves the system ability to serve higher offered loads.

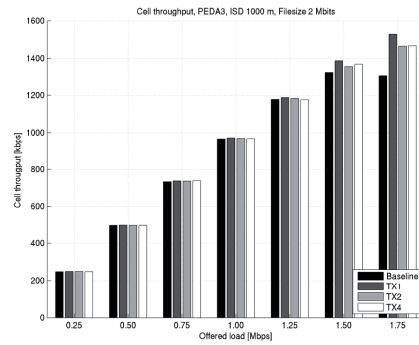


Figure 3. Cell throughput, ISD 1000 m, PedA 3 kmph

The average user throughput results in Figure 4. and Figure 5. confirm clearly that there are noticeable gains from SATD and the user throughput, as well as the cell throughput gains, can be seen especially in the PedA 3 kmph channel conditions. As expected, the best performance is achieved by using genie aided TX1 algorithm which has the perfect knowledge of the channel situation, as described earlier in this paper. The differences between the performance of TX2 and TX4 practical algorithms are minor, but in general TX4 performs slightly better. With both ISDs the antenna switching can bring approximately 10 - 20 % of performance increase to the user throughput.

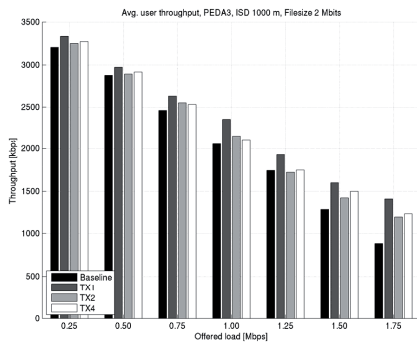


Figure 4. Average user throughput, ISD 1000, PedA 3 kmph

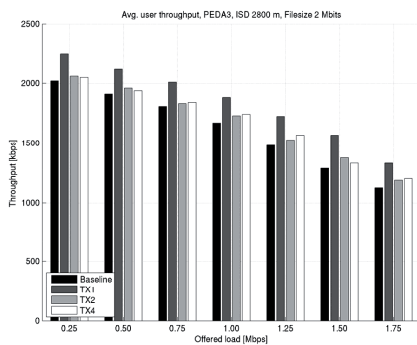


Figure 5. Average user throughput, ISD 2800, PedA 3 kmph

By increasing the offered load, interference becomes more and more dominant, causing DPCCH power to be increased accordingly, as seen in Figure 6. . Due to being able to utilize the antenna which has the higher channel gain, SATD uses less DPCCH and total power. Thus, SATD causes less interference which in turn enables NodeB to schedule higher allocations. The result of higher allocations is again increased interference within the system, but with greater traffic-to-pilot ratio.

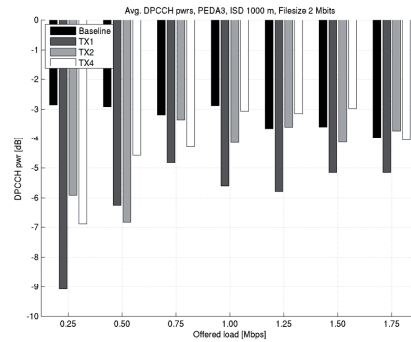


Figure 6. DPCCH Avg. Tx power, ISD 1000 m, PedA 3 kmph

With lower loads in small cells, the transmit power is not generally an issue and power savings when SATD is assumed do not increase throughput, but when offered load increases gain from antenna switching can clearly be seen. Because of this, one of the main advantages of SATD is the improved performance provided for cell edge users, which are most often limited by their power headroom. Cell edge UEs can utilize the decreased DPCCH power by increasing the transmit power of the data channel, thus having higher probability for a successful transmission. This is why gains can be seen in larger cell also with lower loads, as seen in Figure 5.

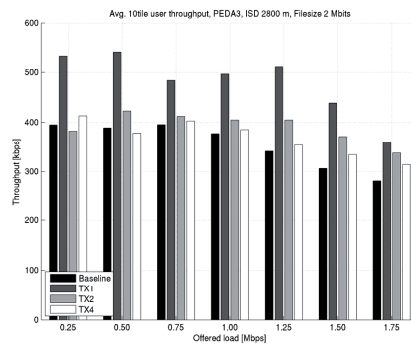


Figure 7. User Throughput, 10%-ile, ISD 2800 m, PedA 3 kmph

Moreover, the 10th percentile average user throughput, illustrated in Figure 7. represent the poorer, cell edge UEs. With ISD of 2800 m and all offered loads, substantial gains can be observed with PedA 3 kmph and it can be concluded that the higher transmit power utilization and lower interference increases especially the performance of UEs in worst channel conditions. However, this effect improves also the performance of users closer to cell centre, as the UEs in question can be allocated with even higher data rates.

In most cases there are achievable throughput and transmit power gains from utilizing SATD, but like seen in Figure 8, and Figure 9, some configurations may also lead to losses. In general, achieved gain of using antenna switching results from a higher tolerance to the continuously changing channel conditions and interference, but with highest loads, system gets too congested and unstable for practical algorithms, especially in VehA 30 kmph channel. Moreover, when the channel changes too rapidly, utilizing SATD can also result in some losses. Thus, this aspect is very important to take into account when applying and selecting the antenna switching algorithms and configurations.

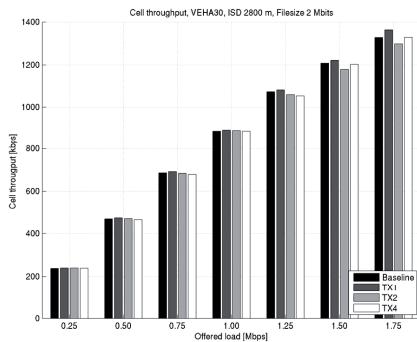


Figure 8. Cell throughput, ISD 2800 m, VehA 30 kmph

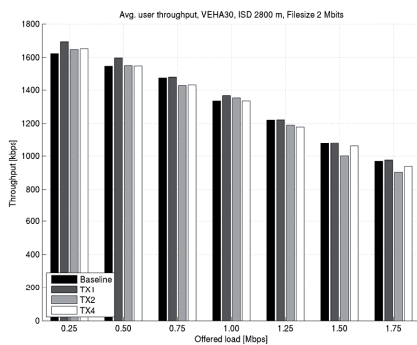


Figure 9. Average user throughput, ISD 2800, VehA 30 kmph

VIII. CONCLUSION

The purpose of this paper was to evaluate performance of open loop switched antenna transmit diversity using bursty traffic with different offered load levels. The paper indicates that SATD can be used to enhance the performance of HSUPA systems with realistic traffic conditions and not only with full buffer traffic.

In general, the results show that SATD can bring substantial gain over the baseline performance. The gain is higher either with higher loads or in larger cell where terminals are more likely to be power limited. This due to the fact that the performance enhancements from SATD are mainly due to lowered interference conditions and transmit power requirements. Moreover, the reduction in DPCCH transmit power helps especially the performance of power limited cell edge users.

ACKNOWLEDGMENT

This study is a collaborative work with Nokia and Nokia Siemens Networks. The authors would like to thank all of their co-workers and colleagues for their comments and support. In addition the authors would like to express their gratitude to Thomas Chapman from Roke Manor Research for his valuable comments and contributions on the work.

REFERENCES

- [1] H. Holma, A. Toskala: "HSDPA/HSUPA for UMTS: High Speed Radio Access for Mobile Communications", John Wiley & Sons Ltd, 2006.
- [2] Third Generation Partnership Project (3GPP), Radio Access Network Radio Layer 1 Work Group, <http://3gpp.org/RAN1-Radio-layer-1>, cited September 2010.
- [3] Third Generation Partnership Project (3GPP), "Universal Terrestrial Radio Access (UTRA): Uplink transmit diversity for High Speed Packet Access (HSPA)", Technical Requirement, TR 25.863, May 2010.
- [4] R1-102074, "Revised system level results on switched antenna Tx diversity in a 1km cell", NSN, Nokia, RAN1#60bis
- [5] R1-102077, "Text proposal on revised system level results on SATD in a 1km cell", NSN, Nokia, RAN1#60bis
- [6] R1-102075, "System level results on switched antenna Tx diversity in a 2.8km cell", NSN, Nokia, RAN1#60bis
- [7] R1-102078, "Text proposal on system level results for a 2.8km cell", NSN, Nokia, RAN1#60bis
- [8] Next Generation mobile Networks (NGMN), "NGMN Radio Access Performance Evaluation Methodology", A White Paper by NGMN Alliance, January 2008
- [9] I. Repo, K. Aho, S. Hakola, T. Chapman, and F. Laakso, "Enhancing HSUPA system level performance with dual carrier capability", In Proceedings of 5th IEEE International Symposium on Wireless Pervasive Computing (ISWPC), Modena, Italy, May 2010.
- [10] Third Generation Partnership Project (3GPP), "Selection Procedures for the Choice of Radio Transmission Technologies of the UMTS", Technical Requirement, TR 101 112 (UMTS 30.03), 1998.
- [11] ITU-R, "Guidelines for Evaluation of Radio Transmission Technologies for IMT-2000", Recommendation, ITU-R M.1225, 1997.

PVII

**SWITCHED ANTENNA TRANSMIT DIVERSITY
IMPERFECTIONS AND THEIR IMPLICATIONS TO HSUPA
PERFORMANCE**

by

Ilmari Repo, Kari Aho, Petri Eskelinen, Frans Laakso 2011

18th International Conference on Telecommunications

Reproduced with kind permission of IEEE.

Switched Antenna Transmit Diversity Imperfections and Their Implications to HSUPA Performance

Ilmari Repo
Magister Solutions
Hannikaisenkatu 41
FIN-40100 Jyväskylä, Finland
ilmari.repo@magister.fi

Petri Eskelinen
Magister Solutions
Hannikaisenkatu 41
FIN-40100 Jyväskylä, Finland
petri.eskelinen@magister.fi

Kari Aho
Magister Solutions
Hannikaisenkatu 41
FIN-40100 Jyväskylä, Finland
kari.aho@magister.fi

Frans Laakso
Magister Solutions
Hannikaisenkatu 41
FIN-40100 Jyväskylä, Finland
frans.laakso@magister.fi

Abstract—3GPP is investigating uplink transmit diversity alternatives for HSUPA. This paper focuses on a transmit diversity scheme using switching between two transmit antennas without additional feedback information. The special focus of this paper is on various non-ideal conditions that occur in real implementations, such as antenna imbalance, correlation and the existence of multiple different SATD algorithms in the network simultaneously. The studies show that transmit antenna correlation somewhat decreases performance but still keeps gains over the baseline, antenna imbalance reduces situations where the switching is feasible and that using a mixture of algorithms can bring down the gains.

Keywords: SATD, HSUPA, Open Loop Transmit Diversity

I. INTRODUCTION

The Third Generation Partnership Project (3GPP) has studied and specified multiple improvements since the original Release '99 WCDMA was specified. In Releases 5 and 6 data transfer took a major step as *High Speed Downlink Packet Access (HSDPA)* and *High Speed Uplink Packet Access (HSUPA)* evolutions were introduced. After that, higher order modulation and multicarrier HSDPA and HSUPA have been adopted in the specifications. In the downlink, multiple antenna techniques are already in specifications, see e.g. [1].

The development of 3/3.5G technology is still ongoing and currently one topic under investigation is open loop uplink transmit diversity. The proposed schemes do not require additional signaling or knowledge from the network, therefore it should be made sure that the algorithms work in all conditions and with users a mixture of users using different transmit diversity algorithms. Both antenna switching and beamforming are being discussed in 3GPP and this paper will focus on the former, referred later in this paper as *Switched Antenna Transmit Diversity (SATD)*. The theoretical gain from switching between transmit antennas arises from the difference in fading due to rapidly changing channel conditions. If the

978-1-4577-0024-8/11/\$26.00 ©2011 IEEE

User Equipment (UE) i.e. the mobile terminal is able to sense which antenna is better, it can switch to that antenna and ideally be able to transmit with less transmit power than when being limited to having only one possible transmit antenna.

Baseline SATD performance has been analyzed in [2]. This paper aims to extend the analysis by considering non-idealities that are present in actual networks. These non-idealities include transmit antenna correlation caused by the transmitters being physically close to each other and experiencing similar fading, antenna imbalance caused by either slow fading or device physical capabilities and the situation where there is not only one but multiple open-loop SATD algorithms in use in the network at the same time.

II. SWITCHED ANTENNA TRANSMIT DIVERSITY

In Switched Antenna Transmit Diversity UE transmits the data and control channels, i.e., *Dedicated Physical Control Channel (DPCCH)*, *Enhanced DPCCH (E-DPCCH)*, *Enhanced Dedicated Physical Data Channel (E-DPDCH)* and *High Speed DPCCH (HS-DPCCH)* in the same way than in the case of normal HSUPA operation. The UE however has 2 transmit antennas and it is able to switch its *Radio Frequency (RF)* chain between the antennas.

The investigated scheme with SATD is open loop, which means that there is no additional feedback information from the Node B that tells the UE which transmit antenna it should use. The UE can control the selection of transmit antenna autonomously and in this study it is assumed that the decision on antenna is made once per 10 milliseconds. Since the network is not aware of the UEs transmit diversity scheme, any filtering of channel estimations between slots at the Node B will be degraded due to change in the channel impulse responses from the two antennas after switching.

The principle of SATD is presented in Figure 1. In practice, there are two options for deciding transmit power after antenna

switch. Either use the previous active DPCCCH power or previous DPCCCH power from the new antenna that is being switched to. In this study the first option is used.

In case of *Soft Handover (SHO)*, it may be the case that the best UE antenna may differ for different cells. In these simulations the UE antenna selection is based on the Node B with the lowest instantaneous path loss, which includes the fast fading component, and considers the best antenna to each Node B.

In the following subsections the simulated SATD algorithms are presented. The first one is so called ideal algorithm which requires more information than is available in real networks. It is used as the theoretical upper limit for the practical approaches.

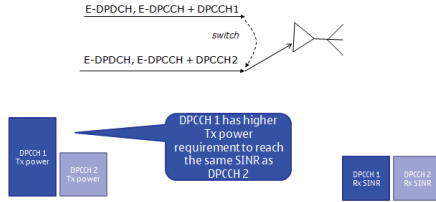


Figure 1. Principle of SATD

A. TX1: Genie Aided Switching

With Genie aided switching the UE makes a switching decision every *evaluation period*, radio frame (10 ms), based on ideal knowledge of the channel impulse responses from the two transmit antennas. The selected transmit antenna j is the one that maximizes:

$$\frac{1}{15} \sum_{k=1}^{15} \sum_{l=1}^L \left(|h_{1,j}(l,k)|^2 + |h_{2,j}(l,k)|^2 \right) \quad (1)$$

In (1) k is a slot index, l is a multipath index and $h_{i,j}(l,k)$ represents the channel impulse response from between transmit antenna j and receive antenna i . In the simulation environment this algorithm can be implemented simply by selecting the antenna with best fading conditions as that will result into same outcome as the equation above.

As the Node B receiver should be unaware of the antenna switch. The Genie is not realistic, but represents the upper performance bound for a UE TX diversity algorithm in a network that is not aware of the existence of antenna switching UEs.

B. TX2: TPC Aided Switching 1

As mentioned previously, with open loop the UE does not have knowledge of the channel impulse responses, etc. and thus must implement an algorithm that can be used in real network

for deciding which antenna to use. In HSUPA *Transmit Power Control (TPC)* commands are sent from the Node B to UE every slot. With TPC aided switching the UE will count the sum of TPC commands. Power UP command represents $+1$ and power DOWN -1 . If the sum of the commands gathered for the length of the evaluation period (10 ms) is higher than 0 then the switch is made. In addition, a forced switch is made every 14 frames, if the sum of TPC commands does not trigger the switch earlier.

C. TX3: TPC Aided Switching 2

Another practical algorithm presented in this paper is also based on TPC commands. In this algorithm UE switches transmit antennas periodically every 10 ms, and then monitors the next TPC command for the new antenna. If the command after the switch is DOWN switched antenna is kept in use, otherwise previous antenna is switched back into use. A forced switch is made every 14 frames, if the switch is not triggered earlier.

D. TX4: DPCCCH Aided Switching

With practical algorithm TX4 the UE checks periodically every 10 ms the last known DPCCCH level of each antenna and switches to the antenna indicating the best antenna. A forced switch is made every 14 frames, if the switch is not triggered earlier.

E. TX5: Periodical Switch

Finally, the simplest switching algorithm is based on periodical switch between antennas. This means that antennas are changed every time interval, regardless of the channel conditions of different antennas.

III. TRANSMIT ANTENNA CORRELATION

The transmit antennas of user devices are relatively close to each other and could experience some degree of correlation. For Switched Antenna Transmit Diversity a high level of correlation between antennas is not desired because it will reduce the probability of the other antenna having better channel conditions when one antenna is experiencing a fade. Transmit antenna correlation can be represented using the Kronecker model [3],

$$R_{TX} = \begin{bmatrix} 1 & r_{tx} \\ r_{tx} & 1 \end{bmatrix}, R_{RX} = \begin{bmatrix} 1 & 0 \\ 0 & 1 \end{bmatrix}, \quad (2)$$

$$H_{kron} = R_{RX}^{1/2} G (R_{TX}^{1/2})^T, \quad (3)$$

where R_{TX} and R_{RX} are transmit and receive correlation matrices and G contains independent channel impulse responses. The amount of transmit correlation is represented by r_{tx} and should be between 0 and 1. The resulting Kronecker matrix H_{kron} should then be normalized to obtain correlating channel impulse responses.

$$H = \frac{1}{E\{tr\{H_{kron} H_{kron}^H\}\}} H_{kron} \approx \frac{1}{tr\{H_{kron} H_{kron}^H\}} H_{kron} \quad (4)$$

In the simulator pre-calculated correlating fading files for each antenna are used in order to reduce computational complexity. The fading data is read from the correlating files synchronously for each antenna and for each multipath component.

IV. ANTENNA IMBALANCE

When deploying multiple antennas to a user device it is probable that the antennas are not exactly alike regarding their transmit capabilities. Antenna imbalance is used to represent the TX power (EIRP) difference between transmit antennas with different efficiencies. The two main causes of power imbalance are short and long term imbalance. Short term antenna imbalance models the spatial difference between antennas i.e. different slow fading conditions between the antennas. Causes for short term imbalance can include for example an object in the path of one of the antennas. Long term antenna imbalance models the difference caused by e.g. manufacturing reasons.

In terms of this study both the long and short term imbalance are fixed for the duration of the call. Short term imbalance is randomized according to Gaussian distribution with 0 dB mean and standard deviation of 2.25 dB. Long term imbalance is fixed to -4 dB when it is on. Antenna imbalance is modeled in the simulator by modifying the pre-calculated fading values for each multipath of the secondary antenna during runtime. The imbalance is then also taken into account when calculating the interference caused by other UEs.

V. SIMULATION METHODOLOGY AND ASSUMPTIONS

This study has been performed by using a comprehensive quasi-static system simulator that has been used in the past in various international publications as well as supporting 3GPP standardization work, see e.g. [4]. The simulation tool enables detailed simulation of users in multiple cells with realistic call generation, propagation and fading (adopted from [5]).

A. Quasi-static Simulation Approach

The term “Quasi-static” approach means that UEs are stationary but both slow and fast fading are explicitly modeled. Fast fading is modeled as a function of time for each UE according to the ITU channel profiles which are modified every chip interval [6]. Statistical confidence is obtained through running multiple drops, i.e., independent simulation iterations. In each iteration mobile terminal locations, fading, imbalance and other random variables are varied. The statistics are gathered and averaged over all drops. *Actual Value Interface (AVI)* mapping is used for mapping link level E_b/N_0 values to frame error rates [7].

B. Traffic and Channel Models

A full buffer traffic generation model is assumed, which means that the UEs constantly have data in their transmit

buffers and the data is transmitted as fast as allowed by the Node B scheduling grants allocated to users according to *Proportional Fair (PF)* metric. Both Pedestrian A channel with 3 km/h and a Vehicular A channel at 30 km/h are simulated in order to observe the impact of increased velocity to antenna switching algorithms.

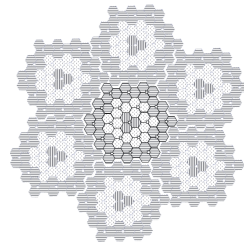


Figure 2. Wrap-around simulation scenario.

TABLE I. MAIN SIMULATION ASSUMPTIONS

| Feature/Parameter | Value / Description |
|------------------------------|---|
| Cell Layout | Hexagonal grid, 19 Node Bs, 3 sectors per Node B with wrap-around |
| Inter-site Distance | 1000 m with 10 dB penetration loss |
| Channel Model | Pedestrian A, Vehicular A |
| UE Velocity | [3, 30] kmph |
| Log Normal Fading | Standard Deviation : 8dB Inter-NodeB Correlation: 0.5 Intra-NodeB Correlation: 1.0 Correlation Distance: 50m |
| NodeB Receiver | RAKE (2 antennas per cell) |
| UE Max. Tx Power | 23 dBm |
| TTI Length | 2 ms |
| Max. HARQ Transmissions | 4 |
| Number of HARQ Processes | 8 |
| Short Term Antenna Imbalance | {Zero-mean Gaussian (STD 2.25 dB), off} |
| Long term Antenna Imbalance | {0, -4} dB |
| Tx Antenna Correlation | {Uncorrelated, 0.3, 0.7} |
| Number of UEs per Sector | [1, 2, 4, 10] |
| UE Distribution | Uniform over the whole area |
| Traffic Type | Full Buffer |
| Scheduling algorithm | Proportional Fair, Forgetting factor: 0.01 |
| Uplink power headroom | Averaged over 100 ms (not antenna specific) |
| Power algorithm | Keep Transmit Power after antenna switch |

C. Simulation scenario and parameters

The main parameters used in the system simulation are summarized in TABLE I. A hexagonal wrap-around multi-cell

layout is utilized. Wrap-around is used to model the interference correctly also for outer cells. This is achieved by limiting the UE placement inside the actual simulation area but replicating the cell transmissions around the whole simulation area to offer more realistic interference situation throughout the scenario. A UE is also able to connect to the replicated cells for example, as part of SHO active set. The wrap-around scenario is illustrated in Figure 2. with actual simulation area in the center and the replicas surrounding it. UEs are created according to a uniform spatial distribution over the whole area. This will result into some cells being more heavily loaded while others can be even empty.

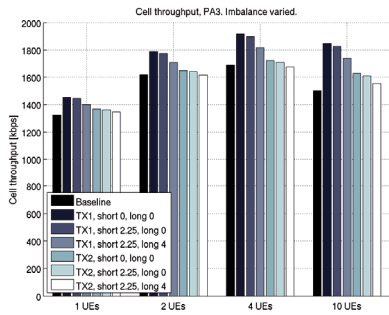


Figure 3. Cell throughput, Antenna imbalance, PedA 3 km/h.

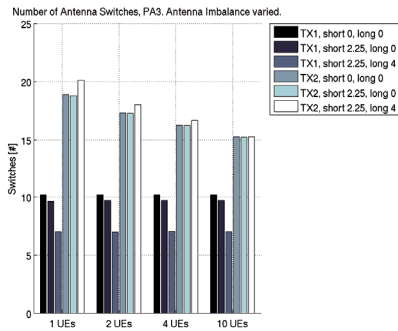


Figure 4. Antenna Switches per second, Antenna Imbalance, PedA 3 km/h.

VI. SIMULATION RESULTS

In this section the simulation results are depicted as bar plots that are grouped by the avg. number of UEs per sector. The most important performance indicators are cell throughput and the Tx power levels regarding both control and data channel power. The average number of antenna switches per second is also used to show how the change in antenna

imbalance affects antenna selection. Cell throughput is defined as the mean throughput of all 57 sectors in the scenario.

Figure 3. shows the performance of SATD with different antenna imbalance values in terms of cell throughput in Pedestrian A channel using the ideal TX1 (Genie) algorithm and a practical algorithm TX2. The results indicate that assuming -4 dB long term imbalance decreases cell throughput when compared to ideal case without imbalance with both the ideal TX1 and the practical TX2 algorithms. When only short term imbalance is assumed, the performance is closer to the ideal situation, but a small consistent drop in throughput is observed in spite of the fact that the short term imbalance is modeled zero-mean and has 50% probability to be positive.

Figure 4. shows the number of antenna switches per second with the same antenna imbalance combinations. The number of antenna switches decreases with the TX1 algorithm when the imbalance increases, because the antenna that has better fading conditions is better than the other antenna more of the time. However, TX2 as a practical algorithm does not have accurate information about quality of antennas and the channel. Therefore antenna is switched more often than would be optimal.

In Figure 5. Figure 6. the cell throughput is shown using both ideal and practical open loop algorithms, namely TX1, TX2 and TX4, using transmit antenna correlations 0, 0.3 and 0.7 along with baseline. In Pedestrian A channel all SATD algorithms have gain over baseline with 0 and 0.3 correlation and the cell throughput with practical algorithms can go slightly below baseline when the amount of correlation goes up to 0.7. The practical algorithms do not suffer from increased correlation as much as the ideal TX1. In Vehicular A channel with velocity of 30 km/h fast power control and switches are not able to keep up with the rapid changes in channel conditions. The gains over baseline are smaller even with zero correlation. However, increasing correlation does not cause the throughput to go lower and in the cases where there is gain with uncorrelating channel, there still is gain with highly correlating antennas.

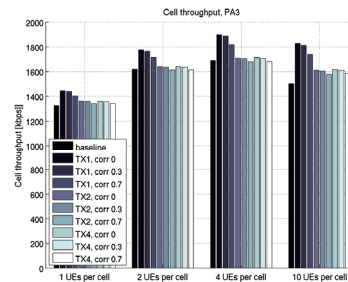


Figure 5. Cell Throughput, Antenna Correlation, PedA 3 km/h.

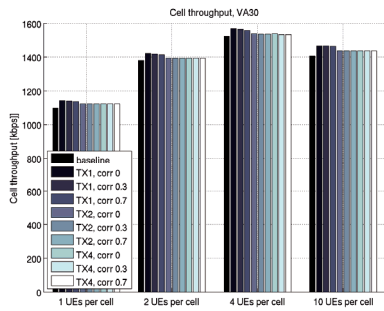


Figure 6. Cell Throughput, Antenna Correlation, VehA 30 km/h.

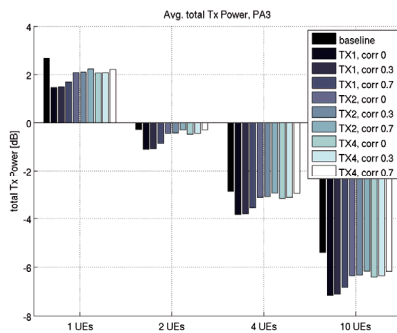


Figure 7. Total Tx Power, Antenna Correlation, PedA 3 km/h.

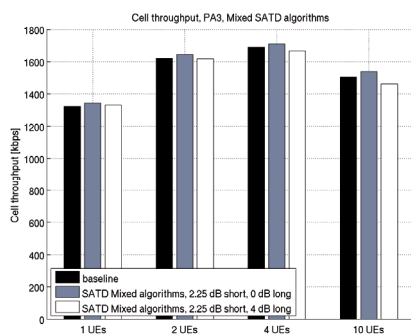


Figure 8. Cell Throughput, Mixed SATD Algorithm, PedA 3 km/h.

Figure 7. shows how correlation impacts the mean total transmit powers in terms of PA3 where SATD is able to provide most of the gain. SATD in general should decrease the required transmit powers due to usage of antenna with better fading conditions. In PA3 channel both of the practical algorithms TX2 and TX4 show minor increase over the uncorrelated case when correlation increases.

In a real network, it is possible that UEs will have different antenna selection schemes that may affect to system level performance. Figure 8. shows the cell throughput in PA3 channel in the case where the UEs have random distribution of SATD algorithms TX2, TX3, TX4 and TX5. Thus, network contains algorithms, like TX5, that might cause even losses for single UEs. The results show that without long term imbalance there is still system level gain over baseline, but with 4dB long term imbalance the throughput is not improved over baseline.

VII. CONCLUSION

The purpose of this paper was to evaluate Switched Antenna Transmit Diversity performance regarding correlation of the transmit antennas and antenna imbalance and with a population of mixed algorithms. It was shown that especially long term antenna imbalance can reduce the achievable gain by SATD since it reduces the time when second antenna is better. It was also shown that antenna correlation, which is inherently present in real implementations, has an impact on SATD performance especially in PA3 channel. It was also shown that using mixture of different SATD open-loop algorithms simultaneously might lead to system performance being lowered close to, or below baseline level.

ACKNOWLEDGMENTS

This study is a collaborative work with Nokia and Nokia Siemens Networks. The authors would like to thank all of their co-workers and colleagues, especially Thomas Chapman, for their comments and support on the work.

REFERENCES

- [1] Holma, H.; Toskala, A.; Ranta-aho, K.; Pirsankari, J.; "High-Speed Packet Access Evolution in 3GPP Release 7, *Communications Magazine, IEEE*, vol.45, no.12, pp.29-35, December 2007
- [2] 3GPP TSG-RAN WG1 Meeting #60bis R1-102074, "Revised system level results on switched antenna Tx diversity in a 1km cell", NSN, Nokia, RAN1#60bis
- [3] Kai Yu; Bengtsson, M.; Ottersten, B.; McNamara, D.; Karlsson, P.; Beach, M.; "Modeling of wide-band MIMO radio channels based on NLoS indoor measurements," *Vehicular Technology, IEEE Transactions on*, vol.53, no.3, pp. 655-665, May 2004.
- [4] I. Repo, K. Aho, S. Hakola, T. Chapman, and F. Laakso, "Enhancing HSUPA system level performance with dual carrier capability", In Proc. of 5th IEEE ISWPC, Modena, Italy, May 2010.
- [5] Third Generation Partnership Project (3GPP), "Selection Procedures for the Choice of Radio Transmission Technologies of the UMTS", Technical Requirement, TR 101 112 (UMTS 30.03), 1998.
- [6] ITU-R, "Guidelines for Evaluation of Radio Transmission Technologies for IMT-2000", Recommendation, ITU-R M.1225, 1997.
- [7] S. Hämmäläinen, P. Slanina, M. Hartman, A. Lappeteläinen, H. Holma, Salonaho O., "A Novel Interface Between Link and System Level Simulations", in Proc. of ACTS97, Aalborg, Denmark, October, 1997.

PVIII

**BEAMFORMING TRANSMIT DIVERSITY USING POWER
CONTROL COMMANDS FOR HIGH SPEED UPLINK PACKET
ACCESS**

by

Frans Laakso, Kari Aho, Ilmari Repo, Petri Eskelinen, Marko Lampinen 2011

IEEE 74th Vehicular Technology Conference: VTC2011-Fall

Reproduced with kind permission of IEEE.

Beamforming Transmit Diversity Using Power Control Commands for High Speed Uplink Packet Access

Frans Laakso, Kari Aho, Ilmari Repo, Petri Eskelinen
Magister Solutions, Ltd.
Hannikaisenkatu 41
FIN-40100 Jyväskylä, Finland
firstname.lastname@magister.fi

Marko Lampinen
Renesas Mobile Corporation
Elektroniikkatie 10
FIN-90590 Oulu, Finland
firstname.lastname@renesasmobile.com

Abstract—3GPP is investigating uplink transmit diversity alternatives for High Speed Uplink Packet Access (HSUPA). This paper studies beamforming transmit diversity where the UE transmitter applies a weight vector to the transmit antennas. In contrast to the traditional beamforming where transmitter is aware of the channel state through channel state feedback, a practical scheme which relies on existing power control commands to calculate the weight vector is investigated. This approach allows autonomous determination of the weight vector by the UE. Additionally, an ideal algorithm which always selects the optimal weight vectors is presented in order to obtain upper boundary for the performance. Both algorithms are benchmarked in various conditions on system level against baseline performance without transmit diversity. The studies show that ideally open loop beamforming is capable of providing gain in simulated conditions. However, the power control command dependent realistic algorithm is able to provide gain only when the low velocity Pedestrian A 3 kmph channel is used. With more complex and higher velocity Vehicular A 30 kmph channel the realistic algorithm is not able to provide gain and reaches only baseline level performance.

Keywords: *Beamforming, HSUPA, transmit diversity*

I. INTRODUCTION

The *Third Generation Partnership Project's (3GPP's)* Releases 5 and 6 took major steps toward enhancing packet data capabilities of cellular networks by standardizing *High Speed Downlink Packet Access (HSDPA)* and *High Speed Uplink Packet Access (HSUPA)* evolutions [1]. Following Release 6, various performance enhancements, such as dual cell HSDPA and HSUPA, higher order modulation, discontinuous reception and transmission were introduced to further enhance performance. In October 2009 a study item was opened in 3GPP to cover open loop transmit diversity options for uplink. This study item covers the study of beamforming transmit diversity schemes without channel state feedback. Hence the studied schemes are called open loop transmit diversity schemes and they should not be mixed with the space-time block codes. Previously transmit diversity has been considered only for downlink, e.g., due to cost and size requirements of the small hand-held terminals. Both open loop space-time block codes and closed loop beamforming based on channel state feedback have been specified for the downlink.

However, due to increasing demand of higher performance also in the uplink, diversity techniques were considered as potential performance enhancement for HSUPA. During various *Radio Access Network Radio Layer 1 (RAN1)* work group [2] meetings possible schemes, assumptions and performance of open loop *Beamforming Transmit Diversity (BFTD)* and *Switched Antenna Transmit Diversity (SATD)* were evaluated and discussed. The findings are summarized in the 3GPP Technical Report 25.863 [3].

Different open loop beamforming transmit diversity concepts are presented in [4] [5] [6]. As explained in [4], the diversity transmitter which employs beamforming can provide two types of gain; coherent gain from beamforming and incoherent gain from mitigation of channel fades, i.e., the classical diversity gain. If the radio channels of different transmit antennas are highly correlated, which typically is the case in small hand-held devices, they can be used to form a beam and the coherent gain becomes dominant.

The purpose of this paper is to introduce and benchmark two different single stream open loop beamforming transmit diversity algorithms under the 3GPP simulation assumptions. Analysis will be conducted with the help of a quasi-static time driven system level simulator used previously, e.g., to support findings for [3]. Theoretically, beamforming can offer 3 dB gain over non-diversity performance [3] and in this paper the gain is evaluated on system level with Rake and *Linear Minimum Mean Square Error (LMMSE)* receivers. Moreover, two cell sizes, 1000 m and 2800 m, and two radio channels, Pedestrian A 3 kmph and Vehicular A 30 kmph, are simulated in respect of different UE velocities and load conditions.

II. OPEN LOOP BEAMFORMING TRANSMIT DIVERSITY

The open loop beamforming scheme illustrated in Figure 1. contains a single power control loop based on the post receiver combined *Signal to Interference-Noise Ratio (SINR)* across all transmit and receive antennas at the NodeB and each antenna branch is transmitted with 50% of the total transmit power. Only one *Dedicated Physical Control Channel (DPCCH)* is sent and the coded, modulated, spread and filtered signal transmitted from each antenna is the same; however a phase offset, determined by weight vectors, is applied between the

antennas. As such the phase adjustments are applied also for the *High Speed Dedicated Physical Control Channel (HS-DPCCH)*, *E-DCH Dedicated Physical Control Channel (E-DPCCH)* and *E-DCH Dedicated Physical Data Channel (E-DPDCH)*. Regarding the soft handover, the selected weights are applied to all of the links in UEs active set.

The phase offset is set autonomously by the UE and should maximize the SINR at the receiver. The network is not aware of the phase offset applied by the UE, but will receive a pilot signal based on a combination of the two transmitter antenna signals and base its channel estimation on this. Changing of the phase offset by the UE will result in a change in the channel estimate; however filtering of the channel estimates will smear these changes. The phase offset may be changed by the UE every slot.

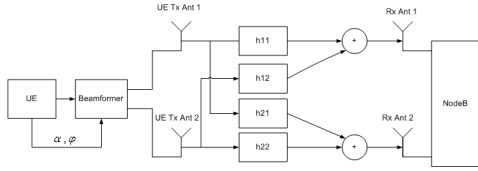


Figure 1. Principle of Open Loop BFTD

The SINR calculation for downlink Rx diversity system presented in [7] has been modified for uplink with a 2x2 antenna configuration that incorporates both beamforming transmit diversity and diversity reception. The formula of E-DPDCH SINR with LMMSE receiver is shown in (1). The channel coefficient matrix of the numerator has been replaced with a new combined channel coefficient matrix. The denominator (2), i.e., the interference part of the SINR equation consists of the self-interference from *Enhanced Dedicated Channel (E-DCH)* and the pilot, and also of the noise and other UE interference. The assumption is made that the other UE interference is white.

$$SINR = S_f \frac{P_{EDCH}}{N_c P} \frac{P |\mathbf{w}^T \mathbf{H}_C^T \hat{\boldsymbol{\delta}}|^2}{I} \quad (1)$$

where

$$I = P_{tot} \mathbf{w}^T \mathbf{H}_C^T \hat{\boldsymbol{\delta}} \hat{\boldsymbol{\delta}}^T \mathbf{H}_C \mathbf{w}^* + \mathbf{w}^T \mathbf{C}_w \mathbf{w}^* \quad (2)$$

In the formula above, P_{EDCH}/P is the fraction of the total transmit power used by all E-DPDCHs and N_c is the number of *spreading factor = 4 (SF4)* equivalent codes used for E-DPDCH. The *effective processing gain* S_f is equal to 4, as the SF2 codes are transmitted with twice the power of the SF4 codes. P_{tot} is the total UE transmit power used by E-DPDCH, E-DPCCH and the DPCCCH.

\mathbf{H}_c is a $(F+L) \times (F \times N_{Rx})$ combined channel coefficient matrix which represents the effective channels from the beamforming transmitter to the receive antennas 1 and 2. Multiplication by the channel coefficient matrix models the

convolution between the transmitted signal and the channel. The channel coefficient matrix is defined as

$$\mathbf{H}_C = \begin{bmatrix} \mathbf{h}_c & 0 & 0 & \dots & 0 \\ 0 & \mathbf{h}_c & 0 & \dots & 0 \\ \vdots & 0 & \mathbf{h}_c & \ddots & \vdots \\ 0 & \vdots & 0 & \ddots & 0 \\ 0 & 0 & \dots & 0 & \mathbf{h}_c \end{bmatrix}^T \quad (3)$$

wherein matrix \mathbf{h}_c includes the path loss, shadowing, antenna gain and fast fading components and is formed by weighting the impulse responses between the transmit and receive antennas (\mathbf{h}_{11} , \mathbf{h}_{12} , \mathbf{h}_{21} , \mathbf{h}_{22}) with the transmit antenna weights (\mathbf{w}_1 , \mathbf{w}_2):

$$\mathbf{h}_c = \begin{bmatrix} w_1 \mathbf{h}_{11}[0] + w_2 \mathbf{h}_{21}[0] & \dots & w_1 \mathbf{h}_{11}[L] + w_2 \mathbf{h}_{21}[L] \\ w_1 \mathbf{h}_{12}[0] + w_2 \mathbf{h}_{22}[0] & \dots & w_1 \mathbf{h}_{12}[L] + w_2 \mathbf{h}_{22}[L] \end{bmatrix} \quad (4)$$

The delay of equalizer is presented in (5) by $\boldsymbol{\delta}$ and is defined with $\hat{\boldsymbol{\delta}}$ as follows:

$$\boldsymbol{\delta} = \begin{bmatrix} 0 & \dots & 0 & 1 & 0 & \dots & 0 \end{bmatrix}^T \quad (5)$$

$$\hat{\boldsymbol{\delta}} = \text{diag} \left(\begin{bmatrix} 1 & \dots & 1 & 0 & 1 & \dots & 1 \end{bmatrix} \right) \quad (6)$$

\mathbf{C}_w is the combined covariance matrix for the noise and other UE interference. The calculation of the receiver filter \mathbf{w} is presented in (7) for Rake and in (8) for LMMSE.

$$\mathbf{w} = \mathbf{H}_C^H \quad (7)$$

$$\mathbf{w} = \sqrt{P_{tot}} \mathbf{H}_C (P_{tot} \mathbf{H}_C \mathbf{H}_C^T + \mathbf{C}_w)^{-1} \boldsymbol{\delta} \quad (8)$$

In the following subsections two different BFTD algorithms for deciding the used beamforming weight vectors are presented. First the so called Genie algorithm is presented. Genie is not a realistic option for real networks but represents an upper performance boundary for UE Tx diversity algorithms. A realistic "practical algorithm", which uses existing performance indicators to formulate the used weights, and as such is applicable to real networks, is introduced after the Genie algorithm.

A. Genie Aided Beamforming

In the Genie scenario [3], the UE has perfect knowledge of the channel impulse responses from the two antennas. The phase offset between antennas is implemented by applying a beamforming weight to each antenna. The beamforming weights $\underline{\mathbf{w}} = [w_1 \ w_2]^H$ are adjusted every slot (0.67msec); in each slot, they are calculated to maximize:

$$\sum_{l=1}^L \mathbf{w}^H H_l(k)^H H_l(k) \mathbf{w} \quad (9)$$

where $H_l(k)$ is a 2x2 matrix of channels between transmit and receive antennas for the l^{th} multipath in the k^{th} slot. The calculation is done to all of the links in UEs active set and the weight resulting in the highest power is selected. To simplify evaluation of the above formulation, a limited set of 8 weight vectors is defined. Each weight vector is defined as

$$[\mathbf{w}_1 \quad \mathbf{w}_2] = [1 \quad e^{-j\theta}]$$

where $\theta = \{0, 0.25\pi, 0.5\pi, 0.75\pi, \pi, 1.25\pi, 1.5\pi, 1.75\pi\}$

For the Genie the weight selection is calculated and applied on a slot by slot basis and no delays are assumed with the application of weights.

B. Terminal Power Control Aided Practical Algorithm

In the practical beamforming scenario [3], the UE does not have access to channel impulse response vectors and must estimate every slot the weight vector to apply based on the *Terminal Power Control (TPC)* commands and the following algorithm:

Let TPC command DOWN be represented by -1 and TPC command UP by +1.

1. Initial relative phase between two transmitters is $\Delta\phi = -\delta/2$ for the first slot (#1 slot). ϵ is kept zero until two TPC commands become available to the UE.
2. Apply relative phase for the next slot $\Delta\phi = \Delta\phi + \delta$
3. Determine new relative phase: (TPC1 and TPC2 correspond to slot (1,2),(3,4), ..., (i*2-1, i*2), where $i = 1$ to n)
 - a. if $TPC1 > TPC2$, $\Delta\phi = \Delta\phi + \epsilon$
 - b. if $TPC2 > TPC1$, $\Delta\phi = \Delta\phi - \epsilon$
 - c. otherwise, no change
4. Apply relative phase for the next slot $\Delta\phi = \Delta\phi - \delta$ and go to step 2.

For the algorithm above, $\Delta\phi$ represents the weight phase offset which is defined by applying relative phase shifts with parameter defined values δ and ϵ . As such the total available amount of different weights depends on the relative shift values. Smaller relative shift values result in larger amount of possible weight phase offsets and vice versa. For purposes of these simulations the relative shift values δ and ϵ were defined by 3GPP simulation assumptions.

As is the case with the Genie, for the practical algorithm the weight selection is also updated on a slot by slot basis and no additional delays are assumed with the actual application of weights. However, as power control commands are used to formulate the weights, the parameter defined delay with TPC commands affects the practical algorithm performance.

III. SIMULATION METHODOLOGY AND ASSUMPTIONS

This study has been performed by using a comprehensive quasi-static time driven system simulator. The simulator has been utilized in the past in various international publications as well as supporting 3GPP standardization work, see, e.g., [3] [5] [8]. This simulation tool enables detailed simulation of users in multiple cells with realistic call generation, propagation and fading which are adopted from [6] and updated according to 3GPP requirements.

TABLE I. MAIN SIMULATION ASSUMPTIONS

| Feature/Parameter | Value / Description |
|--------------------------------------|---|
| Cell Layout | Hexagonal grid, 19 NodeBs, 3 sectors per Node B with wrap-around |
| Inter-site Distance | [1000, 2800] m with 10 dB penetration loss |
| Channel Model | Pedestrian A, Vehicular A |
| UE Velocity | PedA: 3 kmph VehA: 30 kmph |
| Log Normal Fading | Standard Deviation : 8dB Inter-NodeB Correlation: 0.5 Intra-NodeB Correlation: 1.0 Correlation Distance: 50m |
| NodeB Receiver | [Rake, LMMSE] (2 antennas per cell) |
| UE Max. Tx Power | 23 dBm |
| TTI Length | 2 ms |
| Max. HARQ Transmissions | 4 |
| Number of HARQ Processes | 8 |
| Short Term Antenna Imbalance | 2.25 dB |
| Long term Antenna Imbalance | 0 dB |
| Tx Antenna Correlation | Uncorrelated |
| Number of UEs per Sector | [0.25, 0.5, 1, 2, 4, 10] |
| UE Distribution | Uniform over the whole area |
| Traffic Type | Full Buffer |
| Scheduling algorithm | Proportional Fair, Forgetting factor: 0.01 |
| Uplink power headroom | Averaged over 100 ms |
| Shift values for practical algorithm | $\delta = 48$ degrees $\epsilon = 12$ degrees |

A. Quasi-static Simulation Approach

The term ‘‘Quasi-static’’ approach means that UEs are stationary but both slow (log normal) and fast fading are explicitly modeled. Fast fading is modeled for each UE according to the *International Telecommunication Union (ITU)* channel profiles [9] and with a jakes model modified for chip interval. Statistical confidence is reached through running multiple drops, i.e., independent simulation iterations. In each step UE locations, fading, etc. are randomized but the statistics are gathered and averaged over all drops.

B. Simulation Assumptions

Main parameters used in the system simulation are summarized in TABLE I. For the simulation scenario a wrap-around multi-cell layout, illustrated in Figure 2, is utilized.

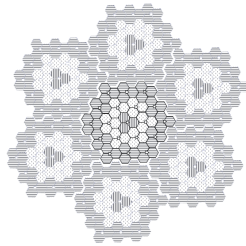


Figure 2. Wrap-around simulation scenario

The purpose of the wrap-around is to model the interference correctly also for outer cells. This is achieved by limiting the UE placement around the actual simulation area, but replicating the cell transmissions around the whole simulation area to offer more realistic interference situation throughout the scenario. In Figure 2, the actual simulation area is highlighted in the center. UEs are created to the scenario according to uniform distribution which results into some cells being more heavily loaded while others can be even empty.

IV. SIMULATION RESULTS

Average user throughputs for ISD 1000m with different cell loads and channels are shown in Figure 3. through Figure 4. The figures show that the Genie can provide up to 12% and the realistic practical algorithm up to a 6% performance enhancement over baseline case with PedA. With LMMSE the absolute throughput is higher, but the relative gains remain similar regardless of the receiver.

With the richer multipath profile and faster changing VehA channel the Genie still shows noticeable performance gains over the baseline case; however, the practical algorithm is not able to bring performance gain over the baseline. Additionally, LMMSE brings clear gain over the Rake receiver.

Average user throughputs for ISD 2800m with different cell loads and channels are shown in Figure 5. and Figure 6. Based on the results for the larger cell, the Genie can provide up to 15% and the practical algorithm up to a 10% performance enhancement over baseline case with PedA. As was the case with the smaller cell size, different receivers have no noticeable effect on the relative throughput gains. Additionally, the trends with different channels are similar to the smaller cell size results; the Genie manages to retain its performance gain for the most part, but the practical algorithm is not able to offer gain over the baseline case and can even result in losses.

The throughput gains are fundamentally due to the signal energy being received more efficiently and, on the other hand, the power of the interfering signals being lower due to the spatial filtering. These two facts affect the transmit power of UEs as seen in the *Cumulative Distribution Function (CDF)* of

DPCCH Tx power in Figure 7. As the UEs are required to use less power than in the baseline case and the power control is able to reduce the transmit powers, less power is needed to get the transmissions through and higher bitrates can be scheduled without generating more interference to the cell or exceeding the maximum UE transmit power.

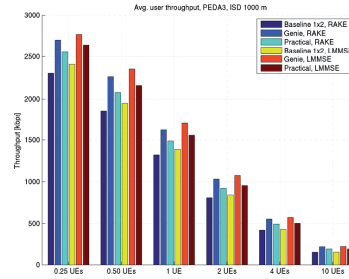


Figure 3. Average user throughput, PedA 3 kmph, ISD 1000m

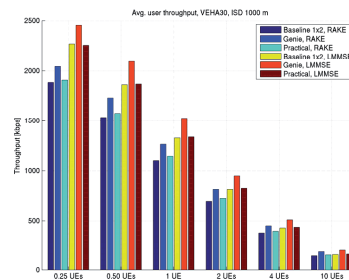


Figure 4. Average user throughput, VehA 30 kmph, ISD 1000m

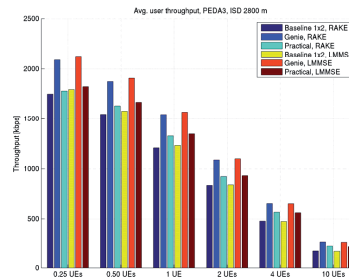


Figure 5. Average user throughput, PedA 3 kmph, ISD 2800m

As a trend the Genie algorithm demonstrates the lowest DPCCH power, resulting in higher throughput gains as more Tx power is available for data transmission. For the VehA 30 kmph, the DPCCH Tx power in Figure 8. illustrates noticeably

smaller Tx power gains for the practical algorithm, which explains the lack of performance improvement over the baseline case due to the algorithm not being able to follow up on the channel properly.

V. CONCLUSION

This paper presents and benchmarks two different algorithms for open loop beamforming transmit diversity in various conditions against baseline performance without transmit diversity. The studies show that the user throughput gains of up to 6 % are possible in a PedA 3 kmph channel with the realistic practical algorithm. However, with more complex and faster changing VehA 30 kmph channel the power control command dependent practical algorithm is not able to provide gains over baseline.

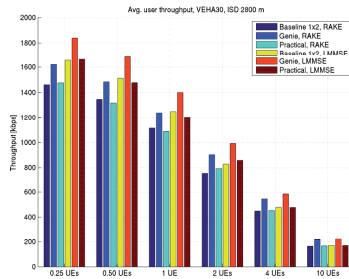


Figure 6. Average user throughput, VehA 30 kmph, ISD 2800m

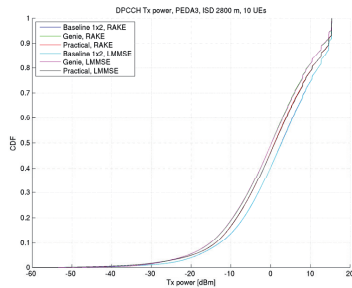


Figure 7. DPCCH Tx power, PedA 3 kmph, ISD 2800m, 10 UEs/cell

The system behavior with transmit diversity is complex and in these simulations all transmit diversity UEs exhibit the same behavior because they use the same algorithm. If a variety of different types of beamforming algorithms were to be present in a system, it is possible that the gain in throughput experienced by different types of users would be complex to predict and dependent on UE mix, load level and channel type.

Thus, although it can be demonstrated that open loop beamforming can show gains in a homogenous system for some load levels and channel types, it cannot be concluded as

easily that the gain is universally applicable in a real deployment, nor that the introduction of open loop beamforming would not harm legacy user performance due to the interaction between interference and power control in the uplink.

ACKNOWLEDGMENTS

This study is a collaborative work between Magister Solutions Ltd. and Renesas Mobile Corporation. The authors would like to thank all of their co-workers and colleagues for their comments and support.

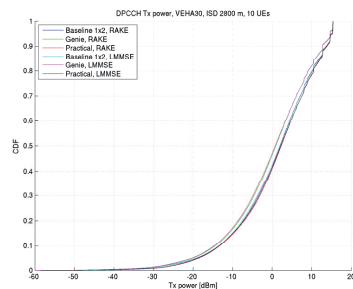


Figure 8. DPCCH Tx power, VehA 30 kmph, ISD 2800m, 10 UEs/cell

REFERENCES

- [1] H. Holma, A. Toskala: "HSDPA/HSUPA for UMTS: High Speed Radio Access for Mobile Communications", John Wiley & Sons Ltd, 2006.
- [2] Third Generation Partnership Project (3GPP), Radio Access Network Radio Layer 1 Work Group, <http://3gpp.org/RAN1-Radio-layer-1>, cited September 2010.
- [3] Third Generation Partnership Project (3GPP), "Universal Terrestrial Radio Access (UTRA); Uplink transmit diversity for High Speed Packet Access (HSPA)", Technical Report, TR 25.863, May 2010.
- [4] S. Wang, E. Abreu, H. Harel, K. Kludt, P. Chen, "Mobile transmit beamforming diversity on UMTS/HSUPA networks." In Proceedings of Sarnoff Symposium, 2010 IEEE , vol., no., pp.1-6, 12-14 April 2010.
- [5] P. Eskelinen, K. Aho, I. Repo and F. Laakso, "On HSUPA open loop switched antenna transmit diversity performance in varying load conditions", In Proceedings of IEEE Vehicular Technology Conference (VTC), Budapest, Hungary, May 2011.
- [6] Third Generation Partnership Project (3GPP), "Uplink transmit diversity for High Speed Packet Access", Technical specification, TR 25.863 V10.0.0, 2010-07.
- [7] T. Nihtilä, "Performance of Advanced Transmission and Reception for High Speed Downlink Packet Access," Ph.D. dissertation, pp. 49-51, University of Jyväskylä, 2008.
- [8] F. Laakso, K. Aho, I. Repo and T. Chapman, "Extended HSUPA coverage and enhanced battery saving opportunities with multiple TTI lengths", In Proceedings of 21th IEEE International Symposium on Personal, Indoor and Mobile Radio Communications (PIMRC), Istanbul, Turkey, September 2010.
- [9] ITU-R, "Guidelines for Evaluation of Radio Transmission Technologies for IMT-2000", Recommendation, ITU-R M.1225, 1997.

PIX

**INTRODUCING DUAL PILOT CLOSED LOOP TRANSMIT
DIVERSITY FOR HIGH SPEED UPLINK PACKET ACCESS**

by

Tuomas Hiltunen, Frans Laakso, Petri Eskelinen, Kari Aho, Ilmari Repo, Arto
Lehti 2011

IEEE 74th Vehicular Technology Conference: VTC2011-Fall

Reproduced with kind permission of IEEE.

Introducing Dual Pilot Closed Loop Transmit Diversity for High Speed Uplink Packet Access

Tuomas Hiltunen,
Frans Laakso, Petri Eskelinen, Kari Aho, Ilmari Repo
Magister Solutions Ltd.
Tampere, Finland
firstname.lastname@magister.fi

Arto Lehti
Renasas Mobile Corporation
Oulu, Finland
firstname.lastname@renasasmobile.com

Abstract—The alternatives for HSUPA uplink transmit diversity are being currently investigated in 3GPP. This paper addresses the uplink transmit diversity from the perspective of closed loop beamforming where NodeB determines transmit antenna weights, and additional feedback is used for signaling the optimal weights to the user equipment. More precisely, this paper introduces a novel transmit diversity technique which involves transmitting two non-beamformed DPCCH (pilot) signals from two antennas whereas the actual data part of the signal is beamformed. Additionally, the dual pilot transmit diversity technique is benchmarked on system level in various conditions against the baseline system performance without transmit diversity. The studies show cell level throughput gains up to 53 % in Pedestrian A channel and up to 26 % in Vehicular A channel comparing to the baseline system. The highest relative gains are achieved in highly loaded cells with long inter-site distances.

Keywords: HSUPA, beamforming, system simulations

I. INTRODUCTION

High Speed Packet Access (HSPA) is the evolution of Wideband Code Division Multiple Access (WCDMA) technology and the standardization of these technologies is run by Third Generation Partnership Project (3GPP). HSPA uplink (HSUPA) was introduced in 3GPP Release 6. The purpose of HSUPA is to improve the performance of uplink dedicated transport channels, that is, increase the data rate and reduce the packet delay [1]. In Releases 7 and 8 a set of new techniques has been added into HSPA standard, such as downlink MIMO (multiple input, multiple output) and higher order modulation, which enables operators to increase the lifespan of their third generation (3G) networks.

A work item for HSUPA closed loop transmit diversity (CLTD) [2] was opened in 3GPP in 2010 and a study on uplink spatial multiplexing is expected to be started in the near future as well. Inspired by this, a set of system level studies has been carried out to investigate the possibilities of the closed loop transmit diversity. Earlier the concept of transmit diversity has been mostly studied in the context of downlink, see, e.g., [3], due to the restrictions in mobile terminal design (antenna placement) and production costs. The uplink transmit diversity has become more feasible due to the improved production techniques and the fact that some HSPA terminals already have two antennas fitted as they can employ more than one antenna in the reception of downlink signal.

Different HSUPA open loop transmit diversity concepts are presented in [4]-[6]. As explained in [4], the diversity transmitter which employs beamforming can provide two types of gain, coherent gain from beamforming and incoherent gain from mitigation of channel fades, i.e., the classical diversity gain. If the radio channels of different transmit antennas are highly correlated, which typically is the case in small handheld devices, they can be used for forming a beam and the coherent gain becomes dominant [4]. Beamforming can be seen as a form of spatial filtering which separates the signals of different user equipments (UE) that are spatially separated. Due to this spatial filtering the interference seen by the NodeB is lower than without beamforming especially in heavily loaded cells. Theoretically the reduced interference level should also improve the performance of legacy terminals in the network. However, active beams of CLTD UEs may cause rapid interference variations in the cell (flashlight effect) which makes the estimation of channel quality more challenging also for the legacy UEs.

This paper contains the description of a single stream dual pilot closed loop beamforming transmit diversity concept and a set simulation results from various simulation scenarios with different system parameters. The study has been carried out using a quasi-static time driven system simulator which simulates the HSUPA network with a resolution of a slot (0.667 ms). The simulation approach is used, for trials in real networks are laborious and analytical models are not able to fully capture the dynamics of the radio network. This paper evaluates the performance of CLTD with Rake and Linear Minimum Mean Square Error (LMMSE) receivers. Moreover, two cell sizes, 1000 m and 2800 m, and two radio channel models, Pedestrian A (PA3) and Vehicular A (VA30), are simulated.

The concept of transmit diversity is presented in Section 2 and system parameters are presented in Section 3. The simulation results can be found in Section 4. Section 5 concludes the paper.

II. DUAL PILOT TRANSMIT DIVERSITY

A. Dual Pilot Closed Loop Transmit Diversity Concept

The transmit diversity scheme introduced in this paper is illustrated in Fig. 1.

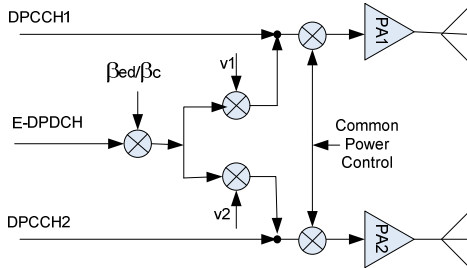


Figure 1. Dual pilot closed loop diversity transmitter

In the presented transmission scheme, two *Dedicated Physical Control Channels* (DPCCH) are transmitted independently from different antennas. DPCCH is the channel that carries the pilot symbols and therefore two DPCCHs are needed in order to obtain knowledge of the whole channel matrix. Beamforming is carried out by precoding the signal with a weight vector $[v_1, v_2]$. The DPCCHs are transmitted without weighting, whereas beamforming is applied to the *High Speed Dedicated Physical Control Channel* (HS-DPCCH), *E-DCH Dedicated Physical Control Channel* (E-DPCCH) and *E-DCH Dedicated Physical Data Channel* (E-DPDCH). For simplicity, HS-DPCCH and E-DPCCH are left out from Fig. 1. There is a single power control loop based on the post receiver combined SINR at the NodeB (across all Tx and Rx antennas) and each antenna branch is transmitted with 50 % of the total power. The DPCCH pilots are transmitted on different OVSF codes. However, since the branches combine over the air, the traffic to pilot ratio $\beta\delta/\beta c$ is set as E-DPDCH power over the total power on DPCCH1 and DPCCH2. That is, the two pilots are transmitted with half of the power allocated to a single DPCCH in non-Tx diversity uplink transmission.

B. Antenna Weight Selection

The key difference to open loop transmit diversity is that the NodeB sets the user equipment antenna weights. It should also be noted that unlike in open loop, the NodeB is aware of when the phase has been changed and can thus maintain optimal channel estimation. If the UE is in soft handover, the weights selected by the *-serving NodeB* are used in the transmitter and the selected weights are signaled in the uplink to inform non-serving basestations about the used Tx weights. The antenna weights are selected from a set of four possibilities which are shown in (1). It is shown in [7] that most of the beamforming gain can be captured by using a codebook of four weights. The codebook is designed so that it is enough to change only v_2 , while v_1 remains constant.

$$v_1 = \frac{1}{\sqrt{2}} \quad (1)$$

$$v_2 \in \left\{ \frac{1+j}{2}, \frac{1-j}{2}, \frac{-1+j}{2}, \frac{-1-j}{2} \right\}$$

The weight selection is updated on a slot by slot basis. To select the correct weights, the NodeB should evaluate the SINR with each of the weight possibilities based on the received pilots. The transmit antenna weight vector that would have maximized the SINR in the current slot is selected for the next slot. However, an additional two slot delay is assumed in applying the weights in the transmitter to model the delay of feedback signaling. Thus, the total transmit antenna weight delay is three slots. Note that no feedback signaling errors are considered, which yields slightly optimistic results.

C. SINR Model

The SINR calculation for downlink Rx diversity system presented in [8] has been modified for uplink with a 2x2 antenna configuration that incorporates both beamforming transmit diversity and diversity reception. The formula of E-DPDCH SINR is shown in (2). The channel coefficient matrix of the numerator has been replaced with a new *combined channel coefficient matrix* \mathbf{H}_C . P_{EDCH}/P is the fraction of the total transmit power used by all E-DPDCHs and N_c is the number of *spreading factor* = 4 (SF4) equivalent codes used for E-DPDCH. The *effective processing gain* S_f is equal to 4, as the SF2 codes are transmitted with twice the power of the SF4 codes.

$$SINR = S_f \frac{P_{EDCH}}{N_c P} \frac{P |\mathbf{w}^T \mathbf{H}_C^T \delta|^2}{I}, \quad (2)$$

where

$$I = P_{tot} \mathbf{w}^T \mathbf{H}_C^T \hat{\delta} \hat{\delta}^T \mathbf{H}_C \mathbf{w}^* + P_{DPCCH1} \mathbf{w}^T \mathbf{H}_1^T \delta \mathbf{H}_1 \mathbf{w}^* + P_{DPCCH2} \mathbf{w}^T \mathbf{H}_2^T \delta \mathbf{H}_2 \mathbf{w}^* + \mathbf{w}^T \mathbf{C}_w \mathbf{w}^*. \quad (3)$$

The denominator (3), i.e., the interference part of the SINR equation consists of the self-interference from *Enhanced Dedicated Channel* (E-DCH), self-interference from the two pilots and the last term which represents noise and other UE interference. P_{DPCCH1} and P_{DPCCH2} are the transmit powers of DPCCH1 and DPCCH2 respectively, and P_{tot} is the total UE Tx power used by all E-DPDCHs and the E-DPCCH. The assumption is made that the other UE interference is white. \mathbf{H}_1 and \mathbf{H}_2 are $(F+L) \times (F \times N_{Rx})$ channel coefficient matrices representing the channels from transmit antennas 1 and 2 to the receive antennas. Here F is the length of the receive filter \mathbf{w} , L equals the length of the channel normalized to chip interval and N_{Rx} is the number of receive antennas. \mathbf{H}_C is the combined channel coefficient matrix that represents the effective channels from the beamforming transmitter to the receive antennas 1 and 2. Multiplications by the channel coefficient matrices in (2) and (3) model the convolution between the transmitted signal and the channel. The channel coefficient matrices are defined as

$$\mathbf{H}_i = \begin{bmatrix} \mathbf{h}_i & \mathbf{0}_{(N_{Rx} \times 1)} & \cdots & \mathbf{0}_{(N_{Rx} \times 1)} \\ \mathbf{0}_{(N_{Rx} \times 1)} & \mathbf{h}_i & \cdots & \vdots \\ \vdots & \vdots & \ddots & \mathbf{0}_{(N_{Rx} \times 1)} \\ \mathbf{0}_{(N_{Rx} \times 1)} & \mathbf{0}_{(N_{Rx} \times 1)} & \cdots & \mathbf{h}_i \end{bmatrix}^T, (i=1,2)$$

$$\mathbf{H}_C = \begin{bmatrix} \mathbf{h}_C & \mathbf{0}_{(N_{Rx} \times 1)} & \cdots & \mathbf{0}_{(N_{Rx} \times 1)} \\ \mathbf{0}_{(N_{Rx} \times 1)} & \mathbf{h}_C & \cdots & \vdots \\ \vdots & \vdots & \ddots & \mathbf{0}_{(N_{Rx} \times 1)} \\ \mathbf{0}_{(N_{Rx} \times 1)} & \mathbf{0}_{(N_{Rx} \times 1)} & \cdots & \mathbf{h}_C \end{bmatrix}^T$$

wherein \mathbf{h}_i is a $N_{Rx} \times (L+1)$ impulse response matrix of the channels between transmit antenna i and receive antennas 1 and 2, including the pathloss, shadowing, antenna gain and fast fading components

$$\mathbf{h}_i = \begin{bmatrix} \mathbf{h}_{i1}[0] & \mathbf{h}_{i1}[1] & \cdots & \mathbf{h}_{i1}[L] \\ \mathbf{h}_{i2}[0] & \mathbf{h}_{i2}[1] & \cdots & \mathbf{h}_{i2}[L] \end{bmatrix}, (i=1,2). \quad (5)$$

Matrix \mathbf{h}_C is formed from \mathbf{h}_1 and \mathbf{h}_2 by weighting the impulse responses with the transmit antenna weights:

$$\mathbf{h}_C = \begin{bmatrix} v_1 \mathbf{h}_{11}[0] + v_2 \mathbf{h}_{21}[0] & \cdots & v_1 \mathbf{h}_{11}[L] + v_2 \mathbf{h}_{21}[L] \\ v_1 \mathbf{h}_{12}[0] + v_2 \mathbf{h}_{22}[0] & \cdots & v_1 \mathbf{h}_{12}[L] + v_2 \mathbf{h}_{22}[L] \end{bmatrix}. \quad (6)$$

The delay of equalizer is modeled by means of δ . δ and $\hat{\delta}$ are defined as follows

$$\delta = \begin{bmatrix} \underbrace{0 \cdots 0}_L & 1 & 0 & \cdots & 0 \end{bmatrix}^T$$

$$\hat{\delta} = \text{diag} \left(\begin{bmatrix} \underbrace{1 \cdots 1}_L & 0 & 1 & \cdots & 1 \end{bmatrix} \right). \quad (7)$$

\mathbf{C}_w is the combined covariance matrix for the noise and other UE interference. The calculation of the receiver filter \mathbf{w} is presented in (8) for Rake and in (9) for LMMSE.

$$\mathbf{w} = \mathbf{h}_C^H \quad (8)$$

$$\mathbf{w} = \sqrt{P_{tot}} \mathbf{H}_C (P_{tot} \mathbf{H}_C \mathbf{H}_C^T + P_{DPCCH1} \mathbf{H}_1 \mathbf{H}_1^T + P_{DPCCH2} \mathbf{H}_2 \mathbf{H}_2^T + \mathbf{C}_w)^{-1} \delta. \quad (9)$$

III. SIMULATION METHODOLOGY AND SYSTEM PARAMETERS

The results presented in Section 4 are obtained using a *quasi-static* simulation tool which enables multi-cell and multi-user simulations with realistic call generation, radio propagation and fading models that are based on [9] and that have been updated according to 3GPP requirements. The same simulation framework has been used in several publications presented in international conferences as well as in supporting 3GPP standardization work, see, e.g., [10].

A. Quasi-static Simulation Approach

In a quasi-static simulator, mobiles remain stationary but both slow and fast fading are modeled thereby providing an accurate simulation model. The fast fading modeling is based on ITU-T channel models [11] which are modified for chip interval. SINR calculation is the core of the simulator and the user throughput is evaluated based on the SINR. Also the channel estimation error is taken into account in the SINR to throughput mapping. To compensate for the fact that the mobiles are not moving, several simulation drops are run to achieve a statistical confidence over the results. The duration of a drop is 10 s. The number of drops is set as a function of the number of UEs in the simulation so that more drops are run for low numbers of UEs / cell.

B. Simulation Scenario

The simulated network presented in Fig. 2 consists of a center cell site and two bands of surrounding cells. Each cell site accommodates three sectors. The layout is replicated around the 19 centermost cells. This is called a *wrap-around* scenario. UEs are distributed over the 19 centermost cells and the statistics are collected from that area only. However, the transmissions of the UEs are replicated in the surrounding cells to create a realistic interference environment for the outermost cells. Moreover, the UE locations are following uniform distribution, thus the actual number of UEs per cell may vary.

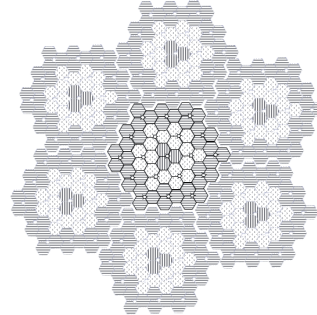


Figure 2. Simulation scenario

C. System Parameters

The most important simulation parameters are presented in Table 1.

TABLE I. SYSTEM PARAMETERS

| Feature/Parameter | Value / Description |
|---------------------------------------|---|
| Cell Layout | Hexagonal, 19 NodeBs, 3 sectors/NodeB, wrap-around |
| Inter-site Distance | 1000 m (penetration loss 10 dB), 2800 m (PL 20 dB) |
| Channel Model | Pedestrian A, Vehicular A |
| UE Velocity | PA: 3 kmph; VA: 30 kmph |
| Log Normal Fading | Standard Deviation : 8 dB Inter-NodeB Correlation: 0.5 Intra-NodeB Correlation: 1.0 Correlation Distance: 50 m |
| NodeB Receiver | Rake, LMMSE (2 Rx ant.) |
| Rise over Thermal (RoT) target | 6dB |
| UE Max. Tx Power | 23 dBm |
| Max. HARQ Transmissions | 4 |
| Number of HARQ Processes | 8 |
| TTI Length | 2 ms |
| Beamforming Tx weight signaling delay | 2 slots |
| Tx Antenna Correlation | Uncorrelated |
| Number of UEs per Sector | [1, 2, 4, 10] |
| Traffic Type | Full Buffer |
| Scheduling algorithm | Proportional Fair, Forgetting factor: 0.01 |

IV. SIMULATION RESULTS

Fig. 3–6 present the cell level throughputs of CLTD and baseline 1x2 system. Simulations show that in the 1000 m cell (Fig. 3 and 4) there is little difference between the performance of Rake and LMMSE receivers when the PA3 channel model is considered. Only in the VA30 channel, which has a richer multipath profile, LMMSE brings clear gain over the Rake receiver. However the relative performance improvement related to the CLTD is almost equal for both receivers.

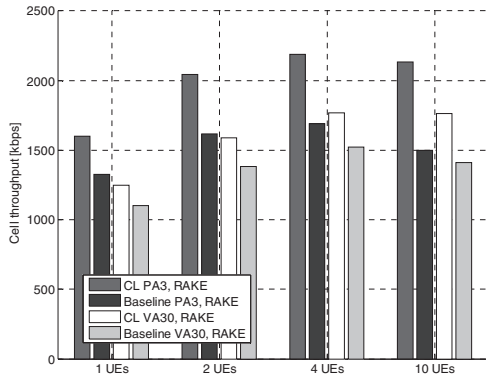


Figure 3. Cell throughput, ISD 1000 m, Rake

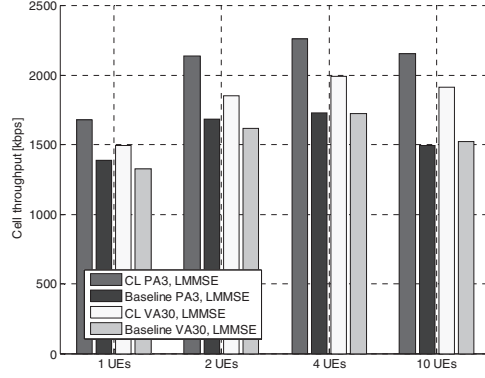


Figure 4. Cell throughput, ISD 1000 m, LMMSE

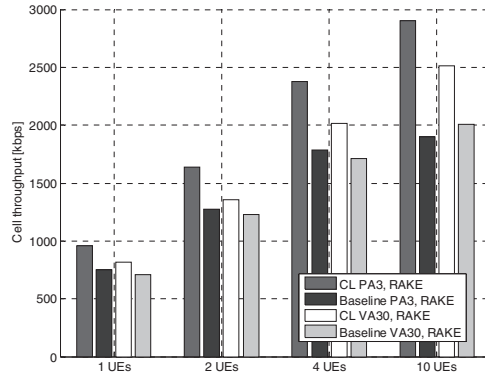


Figure 5. Cell throughput, ISD 2800 m, RAKE

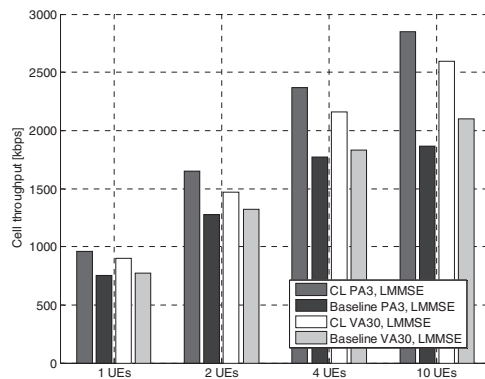


Figure 6. Cell throughput, ISD 2800 m, LMMSE

In the PA3 channel, the relative gains from CLTD are in the range of 21–44 %, varying heavily as a function of cell load. In VA30 the gain is varying between 13–26 %.

Similarly, the cell level throughput statistics are presented for the 2800 m cell in Fig. 5 and 6. In the large cell the CLTD gains are ranging between 28–53 % in PA3 and between 10–25 % in VA30. In the PA3 channel the throughput gains are higher in the 2800 m cell. This is due to the fact that in the large cell UEs are more likely to be power limited yet the power limitation can be eased by Tx diversity. In VA30, the relative throughput improvement is roughly equal with both ISDs, which results from more rapidly changing radio channel. The beamformer is not able to follow the changes in the channel state well enough to exploit the gain potential originating from the relaxed power constraints. In all of the studied cases, the more UEs in the cell, the higher the gains from dual pilot transmit diversity compared to the baseline HSUPA.

The throughput gains are fundamentally due to the signal energy being received more efficiently and, on the other hand, the power of the interfering signals being lower due to the spatial filtering. These two facts affect the transmit power of UEs as seen in the cumulative distribution function (CDF) of DPCCH Tx power in Fig. 7. It shows clearly that when closed loop transmit diversity is used, UEs can get along with less power than in the baseline case and the power control is able to reduce the transmit powers. The dashed and the dotted lines represent the CDFs of individual DPCCH powers. The lines are overlapping for there is only one common power control loop. When less power is needed to get the transmissions through, higher bitrates can be scheduled without generating more interference to the cell or exceeding the maximum UE power.

V. CONCLUSIONS

According to the simulation results presented in this paper it can be stated that dual pilot transmit diversity is beneficial in all of the studied cases, although the gains are higher in the PA3 channel than in VA30, which is due to a more frequency selective channel and higher UE velocity of VA30. The gain mechanism of dual pilot closed loop transmit diversity is similar to other transmit diversity algorithms; by using two transmit antennas a better receiver SIR can be achieved without increasing the total transmission power, which enables scheduling of the UEs with higher bitrates.

In the 1000 m cell and in the PA3 channel the relative gains from CLTD comparing to the 1x2 baseline system are in the range of 21–44 %. In VA30, the gain is varying between 13–26 %. The results in the 2800 m cell are following the same trend so that CLTD gains are ranging between 28–53 % in the PA3 and between 10–25 % in the VA30 channel. The gain is varying heavily as a function of cell load. The highest gains are achieved with high network load levels such as 10 UE/s cell. Simulations show that in the VA30 channel, which has a richer multipath profile, LMMSE brings a clear gain over Rake receiver. However, the relative performance improvement related to the CLTD is almost equal for both receivers.

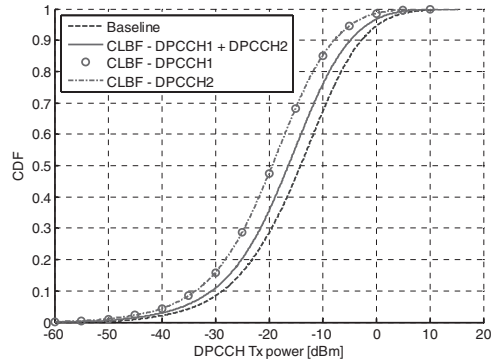


Figure 7. DPCCH Tx power, PA3, 10 UEs/cell, ISD 1000 m

ACKNOWLEDGMENT

This study is done in collaboration between Magister Solutions and Renesas Mobile Corporation. The authors would like to thank all of their co-workers and colleagues for their comments and support.

REFERENCES

- [1] E. Dahlman, S. Parkvall, J. Sköld, P. Beming, 3G evolution – HSPA and LTE for mobile broadband, 1st ed., Academic Press, 2007.
- [2] Third Generation Partnership Project (3GPP), Work Item Description, Uplink Transmit Diversity for HSPA, RP-101438, RAN #50.
- [3] J. Hamalainen, R. Wichman, "Closed-loop transmit diversity for FDD WCDMA systems," In Proc. of the 34th Asilomar Conference on Signals, Systems and Computers, Pacific Grove, CA, October 2000.
- [4] S. Wang, E. Abreu, H. Harel, K. Kludt, P. Chen, "Mobile transmit beamforming diversity on UMTS/HSUPA networks," In Proc. of Samoff Symposium, Princeton, New Jersey, April 2010.
- [5] P. Eskelinen, K. Aho, I. Repo and F. Laakso, "On HSUPA open loop switched antenna transmit diversity performance in varying load conditions", In Proc. of IEEE Vehicular Technology Conference (VTC), Budapest, Hungary, May 2011, in press.
- [6] Third Generation Partnership Project (3GPP), "Uplink transmit diversity for High Speed Packet Access", Technical specification, TR 25.863 V10.0.0, 2010-07.
- [7] P. Eskelinen, F. Laakso, K. Aho, T. Hiltunen, I. Repo, "Impact of practical codebook limitations on HSUPA closed loop transmit diversity", In Proc. of IEEE Vehicular Technology Conference (VTC), San Francisco, CA, September 2011, in press.
- [8] T. Nihtila, "Performance of Advanced Transmission and Reception for High Speed Downlink Packet Access," Ph.D. dissertation, pp. 49-51, University of Jyväskylä, 2008.
- [9] Third Generation Partnership Project (3GPP), "Selection procedures for the choice of radio transmission technologies of the UMTS", Technical requirement, TR 101 112 (UMTS 30.03), 1998.
- [10] F. Laakso, K. Aho, I. Repo and T. Chapman, "Extended HSUPA coverage and enhanced battery saving opportunities with multiple TTI lengths", In Proc. of 21th IEEE International Symposium on Personal, Indoor and Mobile Radio Communications (PIMRC), Istanbul, Turkey, September 2010.
- [11] ITU-R, "Guidelines for evaluation of radio transmission technologies for IMT-2000", Recommendation, ITU-R M.1225, 1997.

PX

**IMPACT OF PRACTICAL CODEBOOK LIMITATIONS ON
HSUPA CLOSED LOOP TRANSMIT DIVERSITY**

by

Petri Eskelinen, Frans Laakso, Kari Aho, Tuomas Hiltunen, Ilmari Repo, Arto
Lehti 2011

IEEE 74th Vehicular Technology Conference: VTC2011-Fall

Reproduced with kind permission of IEEE.

Impact of Practical Codebook Limitations on HSUPA Closed Loop Transmit Diversity

Petri Eskelinen, Frans Laakso, Kari Aho,
 Tuomas Hiltunen, Ilmari Repo
 Magister Solutions Ltd.
 Hannikaisenkatu 41
 FIN-40100 Jyväskylä, Finland
 firstname.lastname@magister.fi

Arto Lehti
 Renesas Mobile Europe
 Elektroniikkatie 10
 FIN-90590 Oulu, Finland
 arto.lehti@renesasmobile.com

Abstract— Different alternatives for uplink transmit diversity for HSUPA are being investigated in 3GPP. This paper compares the performance of two-antenna beamforming using closed loop feedback information against the baseline single antenna transmission. With beamforming, multiple transmit antennas are utilized and the UE transmitter applies a weight vector to the transmit antennas in order to amplify the received signal. In this paper, the impact of different codebook sizes, delays and update intervals related to antenna weights are studied utilizing a comprehensive system level simulator. The studies show that increasing codebook size provides relatively higher performance gain over the baseline. However, increasing the number of available beamforming antenna weights will also increase signaling overhead. In terms of weight update interval the best performance is achieved with one slot interval and if the interval is prolonged to the length of *Transmission Time Interval (TTI)*, namely 3 slots, then the performance with higher mobile velocity can be compromised. Similarly, the results with different feedback delays show that additional delays in fast fading channel should be avoided.

Keywords: Beamforming, HSPA, Codebook design, weight signaling delay, weight update interval

I. INTRODUCTION

The *Third Generation Partnership Project's (3GPP's)* Releases 5 and 6 took major steps toward enhancing packet data capabilities of cellular networks by standardizing *High Speed Downlink Packet Access (HSDPA)* and *High Speed Uplink Packet Access (HSUPA)* evolutions [1]. Following Release 6, various performance enhancements were introduced to further enhance performance which enables operators to increase the lifespan of their *third generation (3G)* networks. Previously transmit diversity was considered only for downlink direction, but due to increasing demand of higher performance on the uplink, diversity techniques were considered as potential performance enhancement also for HSUPA. In October 2009 a study item was opened in 3GPP to cover *Open Loop Transmit Diversity (OLTD)* options for uplink, followed by a study item for *Closed Loop Transmit Diversity (CLTD)* [2] in 2010. Inspired by this, a set of system level studies has been carried out to investigate the possibilities of the closed loop transmit diversity. During various *Radio Access Network Radio Layer 1 (RANI)* work group [3] meetings possible schemes, assumptions and performance of open loop *Beamforming Transmit Diversity (BFTD)* and *Switched Antenna Transmit Diversity (SATD)* were evaluated and discussed. The findings are summarized in the 3GPP Technical Report 25.863 [4].

The purpose of this paper is to introduce and benchmark *Closed Loop Beamforming (CLBF)* transmit diversity under practical codebook limitations and deepen the earlier OLTD studies [5][6][7]. The simulations presented consider various important configuration aspects and requirements of CLBF, such as codebook size, weight update interval and weight feedback delay. Simulations assume RAKE receiver and *Inter-Site Distance (ISD)* of 2800 m where UEs are likely to get power limited. Analysis will be conducted with the help of a quasi-static time driven system level simulator used previously, e.g., to support findings for [4]. Theoretically, BFTD can offer 3 dB gain over non-diversity performance and in this paper the gain is evaluated on system level with the respect of different channels, UE velocities and load conditions using the 3GPP simulation assumptions and schemes.

II. CLOSED LOOP BEAMFORMING TRANSMIT DIVERSITY

In this paper pre-coded dual pilot beamforming scheme illustrated in Figure 1, is assumed. In the scheme, phase adjustments are applied for the pilot as well as to the data channels and sent using both antennas. Moreover, the TX power on the two antenna branches is exactly the same and there is a single power control loop based on the post receiver combined (across all TX and RX antennas) SINR at the NodeB.

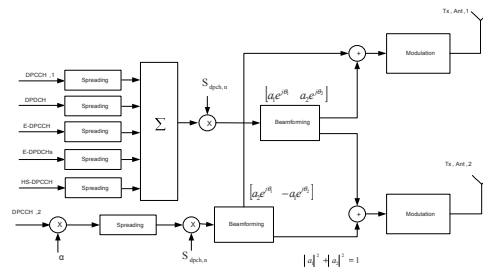


Figure 1. Dual pilot closed loop diversity transmitter [8]

A. Antenna Weight Selection

Pre-coding (beamforming) weight vector is determined by the serving NodeB and fed back to the UE that applies the phase shift between antennas. To select the correct weights, the NodeB should evaluate the received power with each of the

weight possibilities based on the received pilots. In the NodeB receiver the beamforming weight vector

$$\mathbf{w} = [w_1 \quad w_2]^H \quad (1)$$

is calculated to maximize the received power for the previous slot:

$$\sum_{l=1}^L \mathbf{w}^H H_l(k)^H H_l(k) \mathbf{w} \quad (2)$$

where $H_l(k)$ is a 2x2 matrix of channels between transmit and receive antennas for the l^{th} multipath in the k^{th} slot. The channel matrix is constructed based on realistic channel estimates of the true channels. The calculation in (2) is done only for the link between UE and serving NodeB and the weight resulting in the highest power is selected and applied for all links. To simplify evaluation of the above formulation, a limited set of weights is defined and used as a codebook.

B. Codebook Design

The codebook is designed so that from (1) it is enough to change only w_2 while w_1 remains constant. The size of the codebook determines how many weights can be used for w_2 from the set of weights presented in Figure 2. and it affects on the resolution of beamforming method: the more weights in codebook the more optimal weight can be calculated.

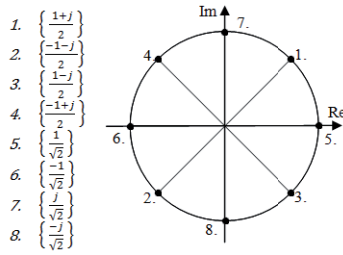


Figure 2. Beamforming codebook weights for w_2

Weights are selected in numerical order, e.g. if codebook size four is assumed, first four weights are used for w_2 like presented in (3).

$$w_1 = \frac{1}{\sqrt{2}} \quad (3)$$

$$w_2 \in \left\{ \frac{1+j}{2}, \frac{1-j}{2}, \frac{-1+j}{2}, \frac{-1-j}{2} \right\}$$

C. Beamforming

As presented in Figure 1. the primary pilot, DPCC with E-DPCC, E-DPDC and HS-DPCC channels are pre-coded with the primary beamforming weight vector

$$[w_1 \quad w_2] = [a_1 e^{j\theta_1} \quad a_2 e^{j\theta_2}] \quad (4)$$

where $a_1^2 + a_2^2 = 1$ and $\theta_i \in \{0, \frac{\pi}{4}, \frac{\pi}{2}, \frac{3\pi}{4}, \pi, \frac{5\pi}{4}, \frac{3\pi}{2}, \frac{7\pi}{4}\}$. The beamforming phase is then denoted by $\theta_2 - \theta_1$.

The scaled *Secondary Pilot Channel (S-DPCCH)* is pre-coded with the orthogonal secondary beamforming weight vector

$$[w_3 \quad w_4] = [a_2 e^{j\theta_1} \quad -a_1 e^{j\theta_2}] \quad (5)$$

In this paper it is assumed that

$$a_1 = \frac{1}{\sqrt{2}} = a_2. \quad (6)$$

For the UE the beamforming weights are adjusted at every slot (0.67msec), but the weight selection in NodeB can be updated more sparsely e.g. on TTI basis. The combinations of update rate, delay in pre-coding vector application and the codebook size used in this study are detailed in simulation assumptions.

III. SIMULATION METHODOLOGY AND ASSUMPTIONS

This study has been performed by using a comprehensive quasi-static time driven system simulator. The simulator has been utilized in the past in various international publications as well as supporting 3GPP standardization work, see, e.g., [9]. The simulation tool enables detailed simulation of users in multiple cells with realistic call generation, propagation and fading which are adopted from [10] and updated according to 3GPP requirements.

TABLE I. MAIN SIMULATION ASSUMPTIONS

| Feature/Parameter | Value / Description |
|------------------------------|---|
| Cell Layout | Hexagonal, 19 NodeBs, 3 sectors/NodeB, wrap-around |
| Inter-site Distance | 2800 m with 10 dB penetration loss |
| Channel Model | Pedestrian A, Vehicular A |
| UE Velocity | [3, 30] kmph |
| Log Normal Fading | Standard Deviation : 8dB Inter-NodeB Correlation: 0.5 Intra-NodeB Correlation: 1.0 Correlation Distance: 50m |
| NodeB Receiver | RAKE (2 antennas per cell) |
| UE Max. Tx Power | 23 dBm |
| TTI Length | 2 ms |
| Uplink HARQ | 8 HARQ Processes Max. 4 HARQ Transmissions |
| Short Term Antenna Imbalance | Gaussian distribution: $\mu = 0, \sigma = 2.25$ dB |
| Long term Antenna Imbalance | 0 dB |
| Tx Antenna Correlation | uncorrelated |
| Codebook Size | [2, 4, 8] weights |
| Weight Feedback Delay | [2, 5, 11, 23, 47, 95] slots |
| Weight Update Interval | [1, 3, 6, 9] slots |
| Number of UEs per Sector | [0.25, 0.5, 1, 2, 4, 10] |
| UE Distribution | Uniform over the whole area |
| Traffic Type | Full Buffer |
| Scheduling algorithm | Proportional Fair, Forgetting factor: 0.01 |
| Uplink power headroom | Averaged over 100 ms (not antenna specific) |

A. Simulation Assumptions

Main parameters used in the system simulation are summarized in TABLE I. For simulation scenario a wrap-around multi-cell layout, illustrated in Figure 3, is utilized. The purpose of the wrap-around is to model the interference correctly also for outer cells. This is achieved by limiting the UE placement around the actual simulation area but replicating the cell transmissions around the whole simulation area to offer more realistic interference situation throughout the scenario. In Figure 3, the actual simulation area is highlighted in the center.

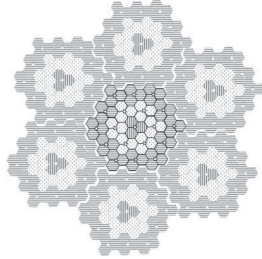


Figure 3. Wrap-around simulation scenario

B. Quasi-static Simulation Approach

The term ‘‘Quasi-static’’ approach means that UEs are stationary but both slow (log normal) and fast fading are explicitly modeled. Statistical confidence is reached through running multiple drops, i.e., independent simulation iterations. In each step terminal locations, fading, etc. are randomized but the statistics are gathered and averaged over all drops.

C. Channel models

The fast fading model used in these simulations is based on tapped-delay line model according to the ITU recommendations of channel models [11] that are characterized by the number of taps, the time delay relative to the first tap, the average power relative to the strongest tap and the Doppler spectrum of each tap. ITU-models are modified so that the delay and powers between paths are normalized to at least one chip-time. TABLE II. shows the tap delays and powers for Vehicular A (VA) and Pedestrian A (PA) channels in accordance of normalized ITU recommendations.

TABLE II. PATH DELAYS AND POWERS FOR PEDESTRIAN A AND VEHICULAR A ENVIRONMENTS

| Tap | Vehicular A | | Pedestrian A | |
|-----|------------------------|--------------------|------------------------|--------------------|
| | Relative delay (chips) | Average power (dB) | Relative delay (chips) | Average power (dB) |
| 1 | 0 | -3.14256 | 0 | -0.24 |
| 2 | 1 | -4.14256 | 1 | -13.01 |
| 3 | 3 | -12.1426 | 2 | -25.72 |
| 4 | 4 | -13.1426 | - | - |
| 5 | 7 | -18.1426 | - | - |
| 6 | 10 | -23.1426 | - | - |

Because the UE mobility is modeled through channel model, the channel characteristics change in time domain. The

time for which the channel characteristics can be assumed to be constant is called coherence time. This is a simplistic definition in the sense that exact measurement of coherence time requires using the autocorrelation function.

Coherence time can be calculated through Doppler power spectrum that gives the statistical power distribution of the channel for a signal transmitted at just one frequency f . While the power delay profile is caused by multipath, the Doppler spectrum is caused by motion of the objects in the channel. As a UE moves relative to NodeB, it causes a Doppler shift which is produced by a vehicular antenna traveling among the stationary scatterers. Knowing [12] that the largest magnitude of Doppler power spectral density occurs when the scatterer is directly ahead of the moving antenna platform or directly behind it, the magnitude of the frequency shift is

$$f_{Dmax} = \frac{v}{c} f_c \quad (7)$$

where f_{Dmax} is the maximum Doppler frequency, v is UE velocity, f_c the carrier frequency and c speed of light. In equation (7) f_{Dmax} is positive when the transmitter and receiver move toward each other, and negative when moving away from each other. The Doppler shifts between different signal components forms the Doppler power spectrum in the range $\pm f_{Dmax}$ around the carrier frequency, f_c .

The width of the Doppler power spectrum is called as the Doppler spread, denoted by f_d . In a typical Rayleigh fading multipath environment, the Doppler shift of each arriving multipath is generally different and the effect on the received signal is seen as a Doppler spreading of the transmitted signal frequency, rather than a shift.

The Doppler spread, f_d , and the coherence time, T_c , are inversely related. Therefore, the approximate relationship between the two can be defined as

$$T_c \approx \frac{1}{f_d} \quad (8)$$

When T_c is defined more precisely as the time duration over which the channel's response to a sinusoid has a correlation greater than 0.5, the relationship between T_c and f_d is approximately

$$T_c \approx \frac{9}{16\pi f_d} \quad (9)$$

A popular method to use (8) and (9) is to define T_c as the geometric mean [12]. This will result in equation

$$T_c = \sqrt{\frac{9}{16\pi f_d^2}} \approx \frac{0.423}{f_d} \quad (10)$$

Thus, if the UE moves fast, the Doppler spread is large and the coherence time will be small, i.e., the channel is fast fading channel. Coherence time, calculated by using the equation (10), gives 114.17 slots for PA3 channel. When VA30 is assumed the channel coherence time is ten times smaller, namely 11.42 slots, due to the higher velocity of UEs. Accordingly the Doppler spread of 55.59 Hz in VA30 channel is ten times higher than Doppler spread in PA3 channel.

IV. SIMULATION RESULTS

In figure legends and tables the “Baseline” represents simulation results carrying only the basic HSUPA capable UEs (i.e. no Tx diversity) utilized with one transmit antenna. All other legends in the figures equal to pre-coded Dual Pilot Closed Loop Beamforming cases. This paper shows the impact of different codebook sizes, weight update intervals and weight feedback delays. The performance is evaluated through cell throughputs in addition to DPCCH transmit power. All throughput values presented in tables are shown in kbps.

A. Codebook Size

TABLE III. show the cell throughput in terms of different codebook sizes. The results indicate that increased codebook size provides relatively higher performance gain. However, beamforming can provide significant gain over the baseline even with the smallest codebook size.

TABLE III. IMPACT OF CB SIZE ON CELL THROUGHPUT

| Codebook size | Average number of users per cell | | | | | | |
|---------------|----------------------------------|-------|-------|--------|--------|--------|--------|
| | 0.25 | 0.50 | 1 | 2 | 4 | 10 | |
| PA3 | Baseline | 429.2 | 758.7 | 1206.7 | 1656.0 | 1912.2 | 1683.6 |
| | CB size 2 | 486.5 | 858.1 | 1420.9 | 2021.1 | 2376.5 | 2305.2 |
| | CB size 4 | 508.3 | 894.8 | 1490.9 | 2132.8 | 2531.8 | 2507.5 |
| | CB size 8 | 511.6 | 906.4 | 1510.3 | 2159.7 | 2573.0 | 2556.4 |
| VA30 | Baseline | 358.8 | 661.3 | 1116.5 | 1509.4 | 1795.8 | 1642.0 |
| | CB size 2 | 378.9 | 687.0 | 1164.1 | 1718.9 | 2012.3 | 1941.9 |
| | CB size 4 | 385.4 | 699.8 | 1191.4 | 1769.4 | 2089.7 | 2047.2 |
| | CB size 8 | 386.7 | 705.5 | 1199.7 | 1781.9 | 2108.4 | 2069.7 |

Higher amount of weights in codebook means also higher signalling overhead and thus selection of codebook size is not only matter of the highest achievable gain in the uplink. Increasing number of codes from two to four has much more significant impact on the throughput levels than increasing codebook size from four to eight.

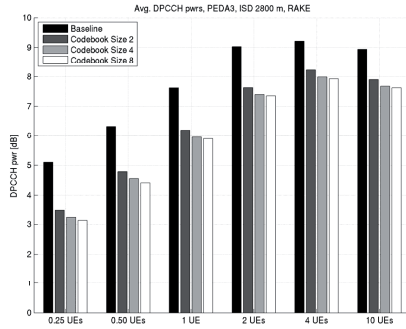


Figure 4. Impact of CB size on average DPCCH Tx powers

One of the main characteristics of beamforming is that it eases the power limitation experienced by UEs in worst channel conditions. Like illustrated in Figure 4, beamforming

decreases the DPCCH Tx power providing a possibility to use higher amount of power allocation for data transmission. Thus, UEs can have significant performance gain due to a higher transmit power utilization.

As shown in results above, the codebook size affects directly on beamforming functionality: the more weights in codebook the more optimal phase can be used to maximize the received power, and thus providing higher gain over baseline.

B. Weight Update Interval

TABLE IV. illustrates the cell throughput for both PA3 and VA30 channels in terms of different weight update intervals. Expectedly, slow fading PA3 is more robust against longer update intervals because the channel coherence time is long enough for calculated weight to be optimal enough in 3 slot periods. However, the transmit diversity gain starts to degrade notably when the update interval is longer than 1 TTI, but regardless the studied update interval, the cell throughput performance stays clearly above the baseline level.

TABLE IV. IMPACT OF WEIGHT UPDATE INTERVAL ON CELL THROUGHPUT

| Update Interval | Average number of users per cell | | | | | | |
|-----------------|----------------------------------|-------|-------|--------|--------|--------|--------|
| | 0.25 | 0.50 | 1 | 2 | 4 | 10 | |
| PA3 | Baseline | 429.2 | 758.7 | 1206.7 | 1656.0 | 1912.2 | 1683.6 |
| | 1 slot | 508.3 | 894.8 | 1490.9 | 2132.8 | 2531.8 | 2507.5 |
| | 3 slots | 504.6 | 899.0 | 1514.7 | 2092.1 | 2550.3 | 2475.7 |
| | 6 slots | 499.6 | 871.0 | 1469.4 | 2092.7 | 2487.5 | 2367.0 |
| | 9 slots | 480.0 | 892.8 | 1436.3 | 2000.8 | 2329.4 | 2238.4 |
| VA30 | Baseline | 358.8 | 661.3 | 1116.5 | 1509.4 | 1795.8 | 1642.0 |
| | 1 slot | 385.4 | 699.8 | 1191.4 | 1769.4 | 2089.7 | 2047.2 |
| | 3 slots | 361.6 | 654.2 | 1106.9 | 1532.0 | 1846.2 | 1637.8 |
| | 6 slots | 363.7 | 667.5 | 1081.2 | 1559.0 | 1800.4 | 1647.7 |
| | 9 slots | 363.5 | 644.7 | 1091.8 | 1547.2 | 1767.9 | 1661.1 |

The results shows that in PA3 channel beamforming weights could be updated per TTI basis without compromising cell throughput, but in fast fading VA30 the beamforming weights must be updated every slot to prevent performance degradation. As it can be seen, the VA30 channel is very sensitive to the update interval. When applying 1 TTI update interval instead of 1 slot the performance drops noticeably. VA30 is more rapidly changing radio channel with short coherence time, which results the optimal weight to change rapidly between consecutive slots. If weight update interval is 3 slots or more, the beamformer is not able to follow the changes in the channel state well enough and also losses against the baseline cell throughput can be observed.

C. Weight Feedback Delay

The cell throughput with different weight feedback delays for PA3 and VA30 channels are shown in TABLE V. Here the weights are updated every slot but an additional delay from signalling them to the UE is introduced. It should be noted that because the signalled weights are calculated according to the information of previous slot, weight will be effective in UE one additional slot later that feedback delay itself. In this way the total delays would be 1, 2, 4, 8, 16 and 32 TTIs in addition to the ideal case with only 1 slot delay.

Increasing feedback delay decreases the performance gain against the baseline in terms of cell throughput and the channel model has a strong effect on result due to a different coherence time between channels. The results indicate similar behaviour as update interval results did, i.e., in VA30 additional delays can cause problems in terms of achievable gains, especially if the delays are quite long.

A UE in PA3 channel can tolerate feedback delay almost 20 slots until cell throughput start to decrease notably. However, feedback delay can cause only minor loss when compared to the baseline even if delay would be near 100 slots. Cell throughput in VA30 channel decreases already with 2 slot feedback delay and it can be seen that if delay is 11 slots or longer, the cell throughput drops in baseline level and after that the increasing the delay further does not affect on performance.

TABLE V. IMPACT OF WEIGHT FEEDBACK DELAY ON CELL THROUGHPUT

| Feedback delay | Average number of users per cell | | | | | | |
|----------------|----------------------------------|-------|-------|--------|--------|--------|--------|
| | 0.25 | 0.50 | 1 | 2 | 4 | 10 | |
| PA3 | Baseline | 429.2 | 758.7 | 1206.7 | 1656.0 | 1912.2 | 1683.6 |
| | 0 slots | 508.4 | 898.0 | 1489.8 | 2131.4 | 2536.2 | 2506.8 |
| | 2 slots | 508.3 | 894.8 | 1490.9 | 2132.8 | 2531.8 | 2507.5 |
| | 5 slots | 506.8 | 894.3 | 1485.0 | 2124.6 | 2533.7 | 2496.6 |
| | 11 slots | 505.2 | 890.9 | 1481.2 | 2110.8 | 2517.9 | 2468.5 |
| | 23 slots | 497.7 | 876.7 | 1450.9 | 2066.6 | 2435.7 | 2366.1 |
| | 47 slots | 472.2 | 825.4 | 1353.3 | 1900.5 | 2192.4 | 2035.6 |
| | 95 slots | 427.7 | 739.6 | 1195.0 | 1646.8 | 1844.1 | 1592.5 |
| | Baseline | 358.8 | 661.3 | 1116.5 | 1509.4 | 1795.8 | 1642.0 |
| | 0 slots | 390.4 | 712.3 | 1213.7 | 1812.2 | 2161.1 | 2144.5 |
| VA30 | 2 slots | 385.4 | 699.8 | 1191.4 | 1769.4 | 2089.7 | 2047.2 |
| | 5 slots | 370.9 | 672.6 | 1135.0 | 1663.7 | 1918.5 | 1807.8 |
| | 11 slots | 357.5 | 645.7 | 1086.4 | 1571.1 | 1786.2 | 1628.6 |
| | 23 slots | 357.6 | 645.7 | 1085.8 | 1569.3 | 1787.0 | 1624.9 |
| | 47 slots | 359.1 | 647.0 | 1086.8 | 1574.1 | 1789.7 | 1636.0 |
| | 95 slots | 357.0 | 643.8 | 1084.6 | 1569.9 | 1782.4 | 1623.4 |

V. CONCLUSION

The purpose of this paper was to evaluate transmit diversity for HSUPA from the perspective of closed loop feedback information with several limitations. This paper showed system level performance of closed loop beamforming with different alternatives for codebook sizes, weight update intervals and feedback delays.

We presented simulation results with three different codebooks sizes and according to the results the highest number of codes provided best performance, as could be expected. Disadvantage of this method is large downlink signaling overhead, which is due to the large size of the beamforming codebook. However, in these studies the size of the codebook can be reduced from eight to four with only a 2% penalty in performance. Reducing the size of the codebook to two weights decreases cell throughput approximately 10% that is much more significant difference.

Studies provided limits for feasible weight update interval and weight feedback delay, which preserve the cell throughput performance. The update interval and delay are critical

especially for channels with high vehicular speeds, in which the coherence time of channel is very low. In terms of weight update interval the best performance is achieved with 1 slot interval and if the interval is prolonged to 1 TTI then the performance in faster fading VA30 channel can be compromised. Finally, the signaling feedback delays show the similar effects as update intervals and thus additional delays should be avoided.

ACKNOWLEDGMENTS

This study is done in collaboration between Magister Solutions and Renesas Mobile Corporation. The authors would like to thank all of their co-workers and colleagues for their comments and support.

REFERENCES

- [1] H. Holma, A. Toskala: "HSDPA/HSUPA for UMTS: High Speed Radio Access for Mobile Communications", John Wiley & Sons Ltd, 2006.
- [2] Third Generation Partnership Project (3GPP), "Uplink Transmit Diversity for HSPA", Work Item Description, RP-101438, RAN #50.
- [3] Third Generation Partnership Project (3GPP), Radio Access Network Radio Layer 1 Work Group, <http://3gpp.org/RAN1-Radio-layer-1>, cited September 2010.
- [4] Third Generation Partnership Project (3GPP), "Universal Terrestrial Radio Access (UTRA); Uplink transmit diversity for High Speed Packet Access (HSPA)", Technical Report, TR 25.863, May 2010.
- [5] K. Aho, I. Repo, P. Eskelinen and F. Laakso, "Introducing Switched Antenna Transmit Diversity for High Speed Uplink Packet Access", In Proceedings of 18th IEEE International Conference on Telecommunications (ICT), Ayia Napa, Cyprus, May 2011.
- [6] I. Repo, K. Aho, P. Eskelinen and F. Laakso, "Switched Antenna Transmit Diversity Imperfections and Their Implications to HSUPA Performance", In Proceedings of 18th IEEE International Conference on Telecommunications (ICT), Ayia Napa, Cyprus, May 2011.
- [7] P. Eskelinen, I. Repo, K. Aho and F. Laakso, "On HSUPA Open Loop Switched Antenna Transmit Diversity Performance in Varying Load Conditions", In Proceedings of 73rd IEEE Vehicular Technology Conference (VTC), Budapest, Hungary, May 2011.
- [8] Yibo Jiang, Haitong Sun, Sharad Sambhwani, Jilei Hou, "Uplink Closed Loop Transmit Diversity for HSPA", Qualcomm Incorporated, May 19, 2010.
- [9] I. Repo, K. Aho, S. Hakola, T. Chapman, and F. Laakso, "Enhancing HSUPA system level performance with dual carrier capability", In Proceedings of 5th IEEE International Symposium on Wireless Pervasive Computing (ISWPC), Modena, Italy, May 2010.
- [10] Third Generation Partnership Project (3GPP), "Selection Procedures for the Choice of Radio Transmission Technologies of the UMTS", Technical Requirement, TR 101 112 (UMTS 30.03), 1998.
- [11] ITU-R, "Guidelines for Evaluation of Radio Transmission Technologies for IMT-2000", Recommendation, ITU-R M.1225, 1997.
- [12] Bernard Sklar, "Rayleigh Fading Channels in Mobile Digital Communication Systems Part I: Characterization", IEEE Communications Magazine 35 (7): 90 – 100, July 1997.

PXI

**IMPACT OF AMPLITUDE COMPONENT ON HSUPA CLOSED
LOOP TRANSMIT DIVERSITY PERFORMANCE**

by

Petri Eskelinen, Frans Laakso, Marko Lampinen 2012

IEEE 75th Vehicular Technology Conference: VTC2012-Spring

Reproduced with kind permission of IEEE.

Impact of Amplitude Component on HSUPA Closed Loop Transmit Diversity Performance

Petri Eskelinen, Frans Laakso
Magister Solutions Ltd.
Hannikaisenkatu 41
FIN-40100 Jyväskylä, Finland
firstname.lastname@magister.fi

Marko Lampinen
Renesas Mobile Corporation
Elektroniikkatie 10
FIN-90590 Oulu, Finland
marko.lampinen@renesasmobile.com

Abstract— 3GPP is investigating uplink transmit diversity alternatives for High Speed Uplink Packet Access (HSUPA). This paper addresses uplink transmit diversity from the perspective of Closed Loop Beamforming (CLBF) when amplitude component is included in the beamforming codebook. This allows transmitter to divide the total transmit power unequally to transmit antennas based on the feedback from the NodeB. This study includes the investigation of the potential benefits of antenna selection and amplitude adaptation as part of the feedback. Furthermore, the focus will be on evaluating corresponding system level performance when long term antenna imbalance is assumed. The studies show that there are achievable gains and thus system performance may be enhanced by applying the amplitude component, especially when the antenna imbalance is high. However, the trends indicate that gains are mainly seen by the cell edge users, thus introducing amplitude component in the codebook increases coverage and fairness.

Keywords: Beamforming, HSUPA, Codebook design

I. INTRODUCTION

The Third Generation Partnership Project's (3GPP's) Releases 5 and 6 took major steps toward enhancing packet data capabilities of cellular networks by standardizing High Speed Downlink Packet Access (HSDPA) and High Speed Uplink Packet Access (HSUPA) [1]. Following Release 6, various performance enhancements were introduced to further enhance performance which enables operators to increase the lifespan of their third generation (3G) networks. In 2010 a study item was opened in 3GPP to cover Closed Loop Transmit Diversity (CLTD) [2]. Inspired by this, a set of system level studies has been carried out to investigate the possibilities and potential performance enhancements for HSUPA using the closed loop transmit diversity.

The purpose of this paper is to introduce and benchmark the beamforming when amplitude information is included in the codebook. For that, this study will examine the performance of CLBF with three different types of amplitude schemes listed below:

1. no additional amplitude component, meaning equally divided power between the transmit antennas
2. an additional amplitude component deploying the unequal power split between the transmit antennas
3. an amplitude that allows transmitter to use only one antenna at the time, i.e. antenna switching

In addition to listed schemes, mixed scenarios are also studied. This means that the amplitude components are utilized in the way that allows beamforming with both equal and unequal power distributions between the two transmit antennas. With these assumptions, this study will deepen the earlier CLTD studies, e.g. [3], that assumes equal transmit power for each antenna branch. Moreover, the antenna switching, i.e. Switched Antenna Transmit Diversity (SATD), has been studied more extensively in open loop perspective, see, e.g. [4].

Simulations in this paper assume RAKE receiver and Inter-Site Distance (ISD) of 2800 m where User Equipment (UE) are more likely to get power limited. Analysis will be conducted with the help of a quasi-static time driven system level simulator using the 3GPP simulation assumptions and schemes. The rest of this document is organized as follows: in section II, the system model is presented and the basic Closed Loop Beamforming Transmit Diversity method is introduced briefly. Section III describes the simulation methods and assumptions adopted in this study and section IV summarizes the simulation results. Finally, section V concludes the paper.

II. CLOSED LOOP BEAMFORMING TRANSMIT DIVERSITY

In this paper pre-coded dual pilot beamforming scheme illustrated in Figure 1. is assumed. In the scheme, phase and amplitude adjustments are applied for the pilot as well as to the data channels. Moreover, there is a single power control loop based on the post receiver combined (across all TX and RX antennas) Signal to Interference-plus-Noise Ratio (SINR) at the NodeB, but the total TX power for the two antenna branches is divided in respect of the signaled amplitudes that defines the offset, e.g., 80/20 power split between antennas. Either of the antennas can have the larger portion of the power.

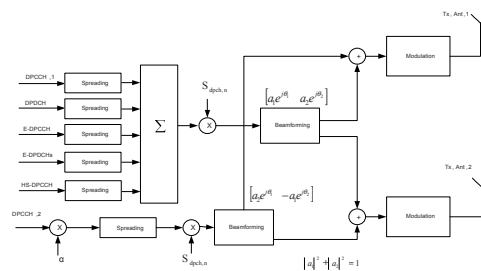


Figure 1. Dual pilot closed loop diversity transmitter [5]

Pre-coding weight vector, a.k.a. codeword, is determined by the serving NodeB and fed back to the UE that applies the phase and amplitude shifts between antennas. To select the correct weights, the NodeB evaluates the received power with each of the weight possibilities based on the received pilots. In the NodeB receiver the beamforming weight vector (1)

$$\underline{w} = [w_1 \quad w_2]^H \quad (1)$$

is calculated to maximize the received power for the previous slot:

$$\sum_{l=1}^L \underline{w}^H H_l(k)^H H_l(k) \underline{w} \quad (2)$$

where $H_l(k)$ is a 2x2 matrix of channels between transmit and receive antennas for the l^{th} multipath in the k^{th} slot. The calculation in (2) is done only for the link between UE and serving NodeB and the weight resulting in the highest power is selected and applied for all links.

As presented in Figure 1. the primary pilot, DPCCCH with E-DPCCCH, E-DPDCH and HS-DPCCCH channels are pre-coded with the primary beamforming weight vector

$$[w_1 \quad w_2] = [a_1 e^{j\theta_1} \quad a_2 e^{j\theta_2}] \quad (3)$$

where the phase $\theta_i \in \{0, \frac{\pi}{4}, \frac{3\pi}{4}, \frac{5\pi}{4}, \frac{7\pi}{4}\}$ and amplitude a_i belong to a finite set depending on the case. The beamforming phase offset is then denoted by $\theta_2 - \theta_1$ and the relation of a_1 to a_2 reflects the selected codebook power offset.

The scaled *Secondary Pilot Channel (S-DPCCCH)* is pre-coded with the orthogonal secondary beamforming weight vector (4)

$$[w_3 \quad w_4] = [a_2 e^{j\theta_1} \quad -a_1 e^{j\theta_2}]. \quad (4)$$

A. Codebook Design

Codebook (CB) defines a limited set of codewords to simplify equation (2). To study the potential benefits of having amplitude in addition to phase in the codebook, this paper will introduce various codebook combinations: codebook with only *antenna switching (AS)* codewords, codebook with phase only and codebook with phase and amplitude components. Relation between required signaling bits and codebook sizes for each scheme are shown in TABLE I.

TABLE I. CODEBOOK DESIGN

| Signaling | 1 bit | 2 bits | 3 bits | | 4 bits |
|-----------|-------|---------------|---------------|-----------------|-----------------|
| CB size | 2 | 4 | 6 | 8 | 12 |
| Scheme | AS | 4 Phases only | 4 Phases + AS | 4 Phases, 2 Amp | 4 Phases, 3 Amp |

In the phase only scheme most of the beamforming gain can be captured using a codebook size four [3], thus in this study one out of 4 possible phases presented in (5) is selected for pre-coding. The codebook is designed so that it is enough to change only the phase θ_2 while the phase θ_1 remains constant. Moreover, the signal inputs to the two antennas have equal amplitude ($a_1 = 1/\sqrt{2} = a_2$) making it unnecessary to signal amplitude feedback in downlink direction.

$$w_1 = 1/\sqrt{2} \\ w_2 \in \left\{ \frac{1+j}{2}, \frac{1-j}{2}, \frac{-1+j}{2}, \frac{-1-j}{2} \right\} \quad (5)$$

The antenna switching codeword is special kind of amplitude component, because the phase selection becomes unnecessary. This corresponds to antenna selection where the data and control channels are transmitted on the selected antenna along with the primary pilot. However, the secondary pilot is still transmitted on the other antenna. For (3) this means that when AS is applied at the UE and primary antenna is selected for the transmission $a_1 = 1, a_2 = 0$ and both $\theta_1, \theta_2 = 0$, i.e., the included weight vectors in the codebook are [1,0] and [0,1]. These codewords can also be included in the 4 phase codebook and this case refers to a 6 entry codebook that contains 4 equal power precoding vectors with 4 different phases, as shown in (5), and 2 additional AS codewords: [1,0] and [0,1].

When amplitude component, other than AS, is included in the codebook, it will replace the equal transmit power between antenna branches. For example, if amplitude component for the 80/20 power split is used, weight selection out of 4 phases uses 2 bits and amplitude information is conveyed by an additional bit, thus 3 bits are transmitted to the UE. However, in mixed scenarios the additional amplitudes are included in the codebook in the way that reserves the equal power split, i.e., "mixed" in this case refers to scenario where UE is able to divide the total transmit power between the antennas either evenly or unevenly. For that, the equal power will need its own, explicit, amplitude. For example, if codebook contains four phases and two amplitudes (e.g. 80/20 and 20/80), the size of the codebook is 8. Now, including the 50/50 amplitude for the equal power split increases the number of amplitudes to 3 and thus codebook size to 12 that will need in total 4 bits for mapping the codewords as shown in last column of TABLE I.

III. SIMULATION METHODOLOGY AND ASSUMPTIONS

This study has been performed by using a comprehensive quasi-static time driven system simulator which simulates HSUPA with a slot resolution. The term "Quasi-static" approach means that UEs are stationary but both slow (log normal) and fast fading are explicitly modeled. Statistical confidence is reached through running multiple drops, i.e., independent simulation iterations. In each step terminal locations, fading, etc. are randomized but the statistics are gathered and averaged over all drops. The simulator has been utilized previously in various international publications, see, e.g. [3] and [4], as well as supporting 3GPP standardization work. The simulation tool enables detailed simulation of users in multiple cells with realistic call generation, propagation and fading which are adopted from [6] and updated according to 3GPP requirements.

A. Simulation Assumptions

The beamforming weights are adjusted at every slot (0.67msec) and absolute feedback from NodeB to UE is used meaning that the exact codeword is signaled to the UE. Because signaling delay is two slots and the signaled weight is

calculated with the information of previous slot, total delay is three slots. The combinations of phases and amplitudes used in this study with all the main parameters used in the system simulation are summarized in TABLE II.

TABLE II. MAIN SIMULATION ASSUMPTIONS

| Feature/Parameter | Value / Description |
|------------------------------|---|
| Cell Layout | Hexagonal, 19 NodeBs, 3 sectors/NodeB, wrap-around |
| Inter-site Distance | 2800 m with 10 dB penetration loss |
| Channel Model | Pedestrian A 3 kmph |
| Log Normal Fading | Standard Deviation : 8dB Inter-NodeB Correlation: 0.5 Intra-NodeB Correlation: 1.0 Correlation Distance: 50m |
| NodeB Receiver | RAKE (2 antennas per cell) |
| UE Max. Tx Power | 23 dBm |
| TTI Length | 2 ms |
| Uplink HARQ | 8 HARQ Processes Max. 4 HARQ Transmissions |
| Short Term Antenna Imbalance | Gaussian distribution: $\mu = 0, \sigma = 2.25$ dB |
| Long term Antenna Imbalance | [0, 4, 10] dB |
| Tx Antenna Correlation | Uncorrelated |
| Codebook | AS only (100/0, 0/100) 4 Ph only (50/50) 4 Ph + 2 Amp (80/20, 20/80) 4 Ph + 3 Amp (50/50, 80/20, 20/80) 4 Ph + AS (50/50, 100/0, 0/100) |
| Weight Feedback | Delay: 2 slots Update Interval: 1 slot Bit Error Rate: 2 % |
| Number of UEs per Sector | [0.25, 0.5, 1, 2, 4, 10] |
| UE Distribution | Uniform over the whole area |
| Traffic Type | Full Buffer |
| Scheduling algorithm | Proportional Fair, Forgetting factor: 0.01 |
| Uplink power headroom | Averaged over 100 ms (not antenna specific) |

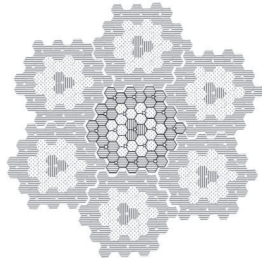


Figure 2. Wrap-around simulation scenario

For simulation scenario a wrap-around multi-cell layout, illustrated in Figure 2, is utilized. The purpose of the wrap-around is to model the interference correctly also for outer cells. This is achieved by limiting the UE placement around the

actual simulation area but replicating the cell transmissions around the whole simulation area to offer more realistic interference situation throughout the scenario. In Figure 2, the actual simulation area is highlighted in the center. Statistics are collected from all cells. UEs are distributed uniformly around the simulation area which can result into some cells being more loaded than others.

B. Channel models

The fast fading model used in these simulations is based on tapped-delay line model according to the *International Telecommunication Union (ITU)* recommendations of channel models [7] that are characterized by the number of taps, the time delay relative to the first tap, the average power relative to the strongest tap and the Doppler spectrum of each tap. ITU-models are modified so that the delay and powers between paths are normalized to at least one chip-time. See [3] for more detailed information of the tap delays and powers for *Pedestrian A (PedA)* and *Vehicular A (VehA)* channels in accordance of normalized ITU recommendations.

C. Antenna Imbalance

When deploying multiple antennas to a user device it is likely that the antennas are not exactly alike. Naturally, the environment or user may cause different fading loss to other transmit antenna, but in addition to that, also the physical transmit capabilities between the antennas may differ and antenna imbalance is used to represent these transmit power differences. In this study antenna imbalance is implemented in the same fashion with [4], i.e., short and long term imbalance are used. Short term antenna imbalance models difference in slow fading conditions between the antennas caused by an object in the path of the antenna for example. Long term antenna imbalance models the difference caused by, e.g., manufacturing reasons. In terms of this study both the long and short term imbalance are fixed for the duration of the call but short term imbalance is randomized according to Gaussian distribution with 0 dB mean and standard deviation of 2.25 dB. In this study the power degradation caused by antenna imbalance is always applied on second transmit antenna called as diversity antenna.

IV. SIMULATION RESULTS

In the presented figures and tables the “Baseline” represents simulation results carrying only the basic HSUPA capable UEs utilizing one transmit antenna and all other results equal to CLBF cases. Moreover, different schemes of amplitude components are presented in tables as relative powers between antenna branches. Either of the antennas can have the larger portion of the power, e.g., 80/20 specifies general power split in which either antenna 1 or antenna 2 can have 80% of the power while the other antenna has 20% of the power. The performance is evaluated through cell and user throughputs in addition to total transmit power. All throughput values presented in tables are shown in kbps.

The amplitude component usages in respect of antenna imbalances are shown in TABLE III. Naturally, the phase only 50/50 power split is not included in the table because it does not have additional amplitude component. In general, when there is no long term imbalance between the transmit antennas,

all amplitude components, other than 50/50, are equally probable and the more antenna imbalance is assumed the more UE will use the amplitude component that favors its stronger primary antenna. According to the amplitude component usages in mixed scheme including 80/20 power split, equal transmit power between the antennas is not seen as good option when compared to the unequal power split, because in this case amplitude components are used most of the time regardless of the antenna imbalance.

The mixed scenario results with AS (50/50, 100/0) shows that even if 4 dB of the transmit power send through the diversity antenna would fade away due to the antenna imbalance, the 50/50 power split is still used over 50 % of time and thus can be seen as better option than AS. However, assuming 10 dB antenna imbalance chances the situation to favor AS codewords because in this situation transmission through both antennas would lose too much transmit power.

TABLE III. AMPLITUDE COMPONENT USAGE IN RESPECT OF ANTENNA IMBALANCE

| Scheme | | Amplitude component usage | | | | |
|--------|--------------|---------------------------|-------|-------|-------|-------|
| | | 50/50 | 80/20 | 20/80 | 100/0 | 0/100 |
| 0 dB | 100/0 | - | - | - | 50 % | 50 % |
| | 80/20 | - | 50 % | 50 % | - | - |
| | 50/50, 80/20 | 26 % | 37 % | 37 % | - | - |
| | 50/50, 100/0 | 64 % | - | - | 18 % | 18 % |
| 4 dB | 100/0 | - | - | - | 79 % | 21 % |
| | 80/20 | - | 78 % | 22 % | - | - |
| | 50/50, 80/20 | 20 % | 66 % | 14 % | - | - |
| | 50/50, 100/0 | 51 % | - | - | 43 % | 6 % |
| 10 dB | 100/0 | - | - | - | 96 % | 4 % |
| | 80/20 | - | 95 % | 5 % | - | - |
| | 50/50, 80/20 | 6 % | 91 % | 3 % | - | - |
| | 50/50, 100/0 | 17 % | - | - | 82 % | 1 % |

TABLE IV. IMPACT OF AMPLITUDE COMPONENT ON CELL THROUGHPUT

| Scheme | | Average number of users per cell | | | | | |
|----------|--------------|----------------------------------|--------------|---------------|---------------|---------------|---------------|
| | | 0.25 | 0.50 | 1 | 2 | 4 | 10 |
| Baseline | | 429.2 | 758.7 | 1206.7 | 1656.0 | 1912.2 | 1683.6 |
| 0 dB | 100/0 | 464.5 | 812.3 | 1330.6 | 1859.1 | 2116.2 | 1961.1 |
| | 50/50 | 505.6 | 891.4 | 1477.7 | 2116.1 | 2508.1 | 2479.2 |
| | 80/20 | 505.1 | 886.7 | 1470.8 | 2081.9 | 2440.7 | 2379.7 |
| | 50/50, 80/20 | 506.3 | 890.0 | 1472.9 | 2093.0 | 2458.5 | 2399.9 |
| | 50/50, 100/0 | 505.0 | 887.6 | 1467.8 | 2078.8 | 2435.7 | 2356.7 |
| 4 dB | 100/0 | 436.9 | 762.4 | 1252.4 | 1769.4 | 2029.7 | 1868.2 |
| | 50/50 | 466.6 | 826.3 | 1402.2 | 2052.6 | 2493.0 | 2476.9 |
| | 80/20 | 469.4 | 824.3 | 1372.8 | 1990.2 | 2356.7 | 2284.6 |
| | 50/50, 80/20 | 469.8 | 826.2 | 1383.3 | 2001.1 | 2377.3 | 2304.7 |
| | 50/50, 100/0 | 465.3 | 817.7 | 1361.0 | 1960.4 | 2305.5 | 2215.1 |
| 10 dB | 100/0 | 428.0 | 736.4 | 1196.9 | 1668.0 | 1879.4 | 1666.7 |
| | 50/50 | 422.0 | 745.4 | 1272.5 | 1897.7 | 2314.1 | 2280.2 |
| | 80/20 | 436.7 | 762.8 | 1263.6 | 1813.5 | 2120.4 | 1987.6 |
| | 50/50, 80/20 | 436.0 | 762.3 | 1266.3 | 1815.6 | 2124.8 | 1988.3 |
| | 50/50, 100/0 | 431.6 | 747.0 | 1223.2 | 1719.0 | 1961.2 | 1776.8 |

Cell throughputs in respect of different schemes and cell loads are show in TABLE IV. When comparing the phase only

beamforming (50/50) with all other transmit power distributions, the phase only scheme outperforms other clearly and applying an amplitude component seems mainly to decrease the beamforming gain. In terms of cell throughput, the diversity gain is in the lowest level when the AS is used. Moreover, if antenna imbalance is raised up to 10 dB the performance with AS component drops quite close to the baseline level. This is due to the weight selection percentages shown in TABLE III. in which it could be seen that mainly the primary antenna is used for transmission and that effectively degrades UE to basic HSUPA device with no transmit diversity.

The main observation from the cell throughput results is that the overall system performance will decrease if any of the studied amplitude component is included in the CLBF codebook. However, as shown in TABLE V. applying an amplitude component can provide notable gain in terms of the 10th percentile user throughput (cell edge UEs) where the results show increased performance, with and without antenna imbalance, when compared to the phase only scheme (50/50). In general, the amplitude component for 80/20 power split seems to work better than adding antenna switching codewords. Only in the case of the highest studied imbalance AS codewords can result into higher performance than other power distributions, but still mostly at lower level than the baseline.

TABLE V. IMPACT OF AMPLITUDE COMPONENT ON 10TH PERCENTILE USER THROUGHPUT

| Scheme | | Average number of users per cell | | | | | |
|----------|--------------|----------------------------------|---------------|---------------|--------------|--------------|--------------|
| | | 0.25 | 0.50 | 1 | 2 | 4 | 10 |
| Baseline | | 262.8 | 184.8 | 126.3 | 73.0 | 51.8 | 45.6 |
| 0 dB | 100/0 | 364.2 | 301.2 | 198.8 | 95.7 | 78.1 | 72.8 |
| | 50/50 | 386.6 | 319.2 | 216.8 | 98.5 | 82.9 | 81.0 |
| | 80/20 | 420.8 | 338.8 | 241.2 | 111.4 | 91.8 | 83.7 |
| | 50/50, 80/20 | 415.2 | 338.4 | 220.8 | 115.4 | 88.4 | 84.0 |
| | 50/50, 100/0 | 402.4 | 324.8 | 228.8 | 113.0 | 88.8 | 82.8 |
| 4 dB | 100/0 | 269.2 | 220.4 | 135.4 | 65.5 | 50.1 | 46.4 |
| | 50/50 | 264.8 | 232.2 | 143.7 | 68.2 | 52.2 | 46.0 |
| | 80/20 | 300.2 | 245.2 | 160.9 | 75.9 | 57.6 | 53.3 |
| | 50/50, 80/20 | 300.2 | 244.3 | 160.4 | 74.6 | 56.5 | 52.8 |
| | 50/50, 100/0 | 280.4 | 242.1 | 167.4 | 71.4 | 55.7 | 51.9 |
| 10 dB | 100/0 | 242.80 | 192.60 | 124.27 | 59.60 | 45.60 | 36.57 |
| | 50/50 | 194.93 | 152.20 | 100.70 | 48.16 | 32.35 | 25.69 |
| | 80/20 | 234.00 | 202.07 | 128.27 | 60.97 | 42.60 | 33.82 |
| | 50/50, 80/20 | 236.20 | 190.27 | 122.88 | 57.70 | 43.26 | 34.29 |
| | 50/50, 100/0 | 241.20 | 201.20 | 118.52 | 60.60 | 44.40 | 35.56 |

In general, the antenna imbalance causes significant decrease on the performance of already power limited CLBF UEs. Especially with the highest loads it can cause the performance to drop below the baseline. In terms of 10th percentile user throughput results, the most notable losses against baseline can be seen with phase only CLBF affected by 10 dB antenna imbalance. Some losses can also be seen with amplitude components but this is the case where the gain from including amplitude components in the codebook is most visible. In other words, this means that amplitude components can benefit the UEs in worst channel conditions regardless the

antenna imbalance but it will also help UE to tolerate against it by directing more transmit power through the better antenna.

TABLE VI. summarizes the user performance in good channel conditions and shows that phase only beamforming overcomes amplitude components even with the 10 dB antenna imbalance. This is possible because even if the phase only UEs are not capable to adjust to the antenna imbalance by weighting the better antenna, they can compensate the power limitation by increasing the transmit power as shown in Figure 3. This only applies for the UEs in good channel conditions because UEs in worst channel conditions are more likely to be power limited and already transmitting with the full power.

TABLE VI. IMPACT OF AMPLITUDE COMPONENT ON 90TH PERCENTILE USER THROUGHPUT

| Scheme | Average number of users per cell | | | | | | |
|-----------------|----------------------------------|---------------|---------------|---------------|---------------|---------------|--------------|
| | 0.25 | 0.50 | 1 | 2 | 4 | 10 | |
| Baseline | 2946.5 | 2829.9 | 2541.2 | 1871.2 | 922.4 | 278.0 | |
| 0 dB | 100/0 | 2943.2 | 2839.6 | 2611.6 | 2043.2 | 1060.0 | 335.3 |
| | 50/50 | 3291.3 | 3175.2 | 2915.2 | 2297.6 | 1231.6 | 416.0 |
| | 80/20 | 3202.3 | 3091.9 | 2841.2 | 2267.2 | 1203.2 | 400.6 |
| | 50/50, 80/20 | 3222.5 | 3122.2 | 2855.2 | 2250.4 | 1217.6 | 404.6 |
| | 50/50, 100/0 | 3203.8 | 3106.7 | 2845.2 | 2245.2 | 1206.8 | 395.5 |
| 4 dB | 100/0 | 2917.2 | 2836.5 | 2579.2 | 2017.2 | 1051.6 | 330.8 |
| | 50/50 | 3261.4 | 3166.6 | 2904.6 | 2352.0 | 1305.4 | 439.0 |
| | 80/20 | 3165.8 | 3065.2 | 2802.6 | 2239.2 | 1201.6 | 400.6 |
| | 50/50, 80/20 | 3173.1 | 3079.7 | 2809.2 | 2252.0 | 1218.4 | 404.5 |
| | 50/50, 100/0 | 3134.9 | 3046.5 | 2773.6 | 2215.2 | 1177.2 | 388.4 |
| 10 dB | 100/0 | 2911.9 | 2810.8 | 2525.2 | 1914.6 | 977.6 | 297.0 |
| | 50/50 | 3167.1 | 3076.7 | 2809.6 | 2284.4 | 1291.2 | 422.0 |
| | 80/20 | 3057.8 | 2953.6 | 2691.2 | 2088.4 | 1120.3 | 356.3 |
| | 50/50, 80/20 | 3059.9 | 2951.9 | 2684.4 | 2103.2 | 1126.4 | 354.0 |
| | 50/50, 100/0 | 2947.4 | 2856.4 | 2578.7 | 1998.4 | 1020.6 | 313.0 |

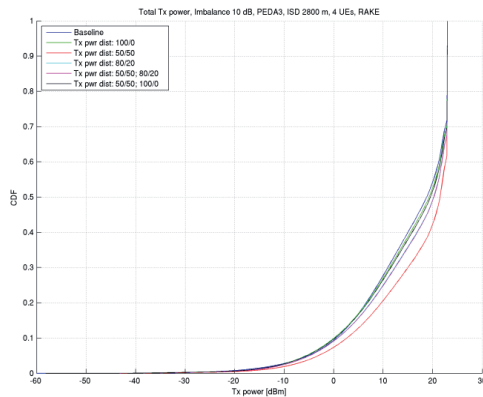


Figure 3. Total Transmit Power, 10 dB antenna imbalance, 4 UEs/cell

Moreover, if amplitude components are compared to the default 50/50 power distribution the results of 90th percentile user throughput indicate that the more antenna imbalance is

assumed the lower gains can be achieved with the amplitudes. However, it was shown in TABLE V. that in the same scenarios amplitude components shows notable gains to UEs in the worst channel conditions. In other words, these cell edge UEs are able to use higher data rates TABLE V. thus consuming the higher share of the *Rise Over Thermal (RoT)* target. The outcome can be seen as an increased fairness in the user perspective but on the contrary this will decrease the system performance in terms of cell throughput as it was seen in TABLE IV.

V. CONCLUSION

When compared to the baseline performance CLBF with an amplitude component show gain in overall system in terms of cell throughput but when comparing CLBF performance with and without amplitude component, the system performance will decrease in all situations if any of the studied amplitude components are included in the CLBF codebook.

On the other hand, the benefits of transmitting amplitude information can clearly be seen in 10th percentile user throughput results which mean that the amplitude component can provide increased coverage and fairness in the system and as such can be seen useful. However, applying the amplitude component will increase the number of available beamforming weights and thus also the feedback requirements generating more signaling overhead in downlink direction.

For the cell edge UEs, it is shown that the higher the imbalance the higher is the benefit from amplitude component. With amplitude components CLBF can adapt to the power limitation caused by the long distance to the serving NodeB and also mitigate the impact of power loss caused by antenna imbalance.

ACKNOWLEDGMENTS

This study is done in collaboration between Magister Solutions and Renesas Mobile Corporation. The authors would like to thank all of their co-workers and colleagues for their comments and support.

REFERENCES

- [1] H. Holma, A. Toskala: "HSDPA/HSUPA for UMTS: High Speed Radio Access for Mobile Communications", John Wiley & Sons Ltd, 2006.
- [2] Third Generation Partnership Project (3GPP), "Uplink Transmit Diversity for HSPA", Work Item Description, RP-101438, RAN #50.
- [3] P. Eskelinen, F. Laakso, K. Aho, T. Hiltunen, I. Repo and A. Lehti, "Impact of Practical Codebook Limitations on HSUPA Closed Loop Transmit Diversity", In Proceedings of 74th IEEE Vehicular Technology Conference (VTC), San Francisco, United States, September 2011.
- [4] I. Repo, K. Aho, P. Eskelinen and F. Laakso, "Switched Antenna Transmit Diversity Imperfections and Their Implications to HSUPA Performance", In Proceedings of 18th IEEE International Conference on Telecommunications (ICT), Ayia Napa, Cyprus, May 2011.
- [5] Yibo Jiang, Haitong Sun, Sharad Sambhwani, Jilei Hou, "Uplink Closed Loop Transmit Diversity for HSPA", Qualcomm Incorporated, May 19, 2010.
- [6] Third Generation Partnership Project (3GPP), "Selection Procedures for the Choice of Radio Transmission Technologies of the UMTS", Technical Requirement, TR 101 112 (UMTS 30.03), 1998.
- [7] ITU-R, "Guidelines for Evaluation of Radio Transmission Technologies for IMT-2000", Recommendation, ITU-R M.1225, 1997.

PXII

**PERFORMANCE OF ABSOLUTE AND RECURSIVE FEEDBACK
METHODS WITH HSUPA CLOSED LOOP TRANSMIT
DIVERSITY**

by

Frans Laakso, Petri Eskelinen, Marko Lampinen 2012

23rd IEEE International Symposium on Personal, Indoor and Mobile Radio
Communications (PIMRC 2012)

Reproduced with kind permission of IEEE.

Performance of Absolute and Recursive Feedback Methods with HSUPA Closed Loop Transmit Diversity

Frans Laakso, Petri Eskelinen
Magister Solutions, Ltd.
Hannikaisenkatu 41
FIN-40100 Jyväskylä, Finland
firstname.lastname@magister.fi

Marko Lampinen
Renesas Mobile Corporation
Elektronikkatie 10
FIN-90590 Oulu, Finland
firstname.lastname@renesasmobile.com

Abstract—3GPP is investigating uplink transmit diversity alternatives for High Speed Uplink Packet Access. This paper presents a closed loop beamforming transmit diversity scheme where NodeB determines the transmit antenna weight vectors and feedback is used for signaling the optimal weights to the user equipment. Two promising feedback method candidates are presented and benchmarked in various conditions on system level against the baseline performance without transmit diversity. In each time slot the absolute feedback method signals the whole weight vector information, while the recursive feedback method signals only a single bit and the weight vector is recursively calculated from multiple bits sent over consecutive time slots. The results show that both feedback methods are capable of providing gain over the baseline in simulated conditions. However, while the recursive feedback method requires less signaling bits per slot, it is more vulnerable to the effects of weight signaling errors due to the signaling error propagation.

Keywords: Beamforming, HSUPA, transmit diversity, closed loop

I. INTRODUCTION

The *Third Generation Partnership Project's (3GPP's)* Releases 5 and 6 took major steps toward enhancing packet data capabilities of cellular networks by standardizing *High Speed Downlink Packet Access (HSDPA)* and *High Speed Uplink Packet Access (HSUPA)* evolutions [1]. In Releases 7, 8 and 9 a set of new techniques has been added into HSPA standard, such as dual cell HSDPA and HSUPA, downlink MIMO (*Multiple Input, Multiple Output*) and discontinuous reception and transmission.

In October 2009 a study item was opened in 3GPP to cover open loop transmit diversity options for uplink. This study item covers the study of beamforming transmit diversity schemes without channel state feedback. Hence the studied schemes are called open loop transmit diversity schemes and they should not be mixed with the space-time block codes. Followed by it, a study item for HSUPA *Closed Loop Transmit Diversity (CLTD)* [2] was opened in 3GPP in 2010. Note that both open loop space-time block codes and closed loop beamforming based on channel state feedback have been specified for the downlink. However, due to increasing demand of higher performance also in the uplink, diversity techniques were

considered as potential performance enhancement for HSUPA. Inspired by this, a set of system level studies has been carried out to investigate the possibilities of the closed loop transmit diversity.

As explained in [3], the diversity transmitter which employs beamforming can provide two types of gain; coherent gain from beamforming and incoherent gain from mitigation of channel fades, i.e., the classical diversity gain. If the radio channels of different transmit antennas are highly correlated, which typically is the case in small hand-held devices, they can be used to form a beam and the coherent gain becomes dominant [3]. Beamforming can be seen as a form of spatial filtering which separates the signals of different *User Equipment (UE)* that are spatially separated. Due to this spatial filtering the interference seen by the NodeB is lower than without beamforming especially in heavily loaded cells. Theoretically the reduced interference level should also improve the performance of legacy terminals in the network. However, active beams of CLTD UEs may cause rapid interference variations in the cell which makes the estimation of channel quality more challenging also for the legacy UEs.

The purpose of this paper is to introduce and benchmark a single stream dual pilot closed loop beamforming transmit diversity concept with pilot channel pre-coding under the 3GPP simulation assumptions. Analysis will be conducted with the help of a quasi-static time driven system level simulator. The remainder of this document is organized as follows: In Section II, the system model is presented and the basic transmit diversity method is introduced briefly. Section III describes the feedback schemes in detail. Section IV presents the simulator and simulation assumptions adopted in this study and section V presents the simulation results. Finally, section VI concludes the paper.

II. CLOSED LOOP BEAMFORMING TRANSMIT DIVERSITY WITH PRE-CODED PILOT

In the presented transmission scheme, illustrated in Figure 1, two *Dedicated Physical Control Channels (DPCCH)* are transmitted independently from different antennas. DPCCH is the channel that carries the pilot symbols and therefore two DPCCHs are needed in order to obtain knowledge of the whole

channel matrix. Beamforming is carried out by pre-coding the signal with a weight vector $[w_1, w_2]$. In addition to the DPCCHs, beamforming is also applied to the *High Speed Dedicated Physical Control Channel (HS-DPCCH)*, *E-DCH Dedicated Physical Control Channel (E-DPCCH)* and *E-DCH Dedicated Physical Data Channel (E-DPDCH)*. For simplicity, HS-DPCCH and E-DPCCH are left out from Fig. 1. The scheme includes a single power control loop based on the post receiver combined *Signal to Interference-Noise Ratio (SINR)* across all transmit and receive antennas at the NodeB and each antenna branch is transmitted with 50% of the total transmit power. The DPCCH pilots are transmitted on different *Orthogonal Variable Spreading Factor (OVSF)* codes. However, since the branches combine over the air, the traffic to pilot ratio β_d/β_c is set as E-DPDCH power over the total power on DPCCH1 and DPCCH2. That is, the two pilots are transmitted with half of the power allocated to a single DPCCH in non-Tx diversity uplink transmission.

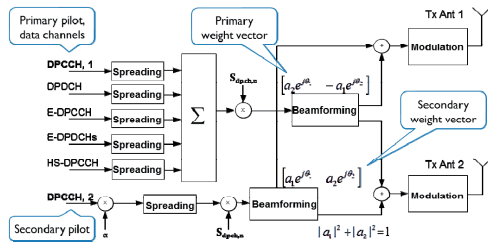


Figure 1. Principle of Closed Loop BFTD with pre-coded pilot

The SINR calculation for downlink Rx diversity system presented in [4] has been modified for uplink with a 2x2 antenna configuration that incorporates both beamforming transmit diversity and diversity reception. The formula of E-DPDCH SINR with Rake receiver is shown in (1). The channel coefficient matrix of the numerator has been replaced with a new combined channel coefficient matrix \mathbf{H}_c . The denominator (2), i.e., the interference part of the SINR equation consists of the self-interference from *Enhanced Dedicated Channel (E-DCH)* and the pilots, and also of the noise and other UE interference. The assumption is made that the other UE interference is white.

$$SINR = S_f \frac{P_{EDCH}}{N_c P} \frac{P |w^T \mathbf{H}_c^T \delta|^2}{I} \quad (1)$$

where

$$I = P_{tot} w^T \mathbf{H}_c^T \hat{\delta} \hat{\delta}^T \mathbf{H}_c w^* + P_{DPCCH2} w^T \mathbf{H}_2^T \hat{\delta} \hat{\delta}^T \mathbf{H}_2 w^* + w^T \mathbf{C}_w w^* \quad (2)$$

In the formula above, P_{EDCH}/P is the fraction of the total transmit power used by all E-DPDCHs and N_c is the number of *spreading factor* = 4 (SF4) equivalent codes used for E-DPDCH. The *effective processing gain* S_f is equal to 4, as the

SF2 codes are transmitted with twice the power of the SF4 codes. P_{tot} is the total UE transmit power used by E-DPDCH, E-DPCCH and the DPCCH1. Respectively, DPCCH2 is the transmit power of scaled *secondary pilot channel (S-DPCCH)*.

\mathbf{H}_c is a $(F+L) \times (F \times N_{Rx})$ combined channel coefficient matrix which represents the effective channels from the beamforming transmitter to the receive antennas 1 and 2. Here F is the length of the receive filter w , L equals the length of the channel normalized to chip interval and N_{Rx} is the number of receive antennas. Multiplication by the channel coefficient matrix models the convolution between the transmitted signal and the channel. The channel coefficient matrix is defined as

$$\mathbf{H}_c = \begin{bmatrix} \mathbf{h}_c & 0 & 0 & \dots & 0 \\ 0 & \mathbf{h}_c & 0 & \dots & 0 \\ \vdots & 0 & \mathbf{h}_c & \ddots & \vdots \\ 0 & \vdots & 0 & \ddots & 0 \\ 0 & 0 & \dots & 0 & \mathbf{h}_c \end{bmatrix}^T \quad (3)$$

wherein matrix \mathbf{h}_c includes the path loss, shadowing, antenna gain and fast fading components and is formed by weighting the impulse responses between the transmit and receive antennas ($\mathbf{h}_{11}, \mathbf{h}_{12}, \mathbf{h}_{21}, \mathbf{h}_{22}$) with the transmit antenna weights (w_1, w_2):

$$\mathbf{h}_c = \begin{bmatrix} w_1 \mathbf{h}_{11}[0] + w_2 \mathbf{h}_{21}[0] & \dots & w_1 \mathbf{h}_{11}[L] + w_2 \mathbf{h}_{21}[L] \\ w_1 \mathbf{h}_{12}[0] + w_2 \mathbf{h}_{22}[0] & \dots & w_1 \mathbf{h}_{12}[L] + w_2 \mathbf{h}_{22}[L] \end{bmatrix} \quad (4)$$

The delay of equalizer is presented in (5) by δ and is defined with $\hat{\delta}$ as follows:

$$\delta = \begin{bmatrix} 0 & \dots & 0 & 1 & 0 & \dots & 0 \end{bmatrix}^T \quad (5)$$

$$\hat{\delta} = \text{diag} \left(\begin{bmatrix} 1 & \dots & 1 & 0 & 1 & \dots & 1 \end{bmatrix} \right) \quad (6)$$

\mathbf{C}_w is the combined covariance matrix for the noise and other UE interference. The calculation of the receiver filter w is presented in (7) for Rake.

$$w = \mathbf{H}_c^H \quad (7)$$

The algorithm used for selecting the weight vectors is described in the following subsection.

A. Weight Vector Selection Algorithm

The phase offset between antennas is implemented by applying a beamforming weight to each antenna. The beamforming weights $w = [w_1 \ w_2]^H$ are adjusted every slot (0.67msec); in each slot, they are calculated to maximize:

$$\sum_{k=1}^L w^H H_i(k) H_i(k) w \quad (8)$$

where $H_i(k)$ is a 2x2 matrix of channels between transmit and receive antennas for the i^{th} multipath in the k^{th} slot. The calculation is done to all of the links in UEs active set and the weight resulting in the highest power is selected. The antenna weights are selected from a set of four vectors. The possible weight vectors are defined as

$$[w_1 \ w_2] = [a_1 e^{j\theta_1} \ a_2 e^{j\theta_2}] \quad (9)$$

where $a_1^2 + a_2^2 = 1$ and $\theta = \{0.25\pi, 0.75\pi, 1.25\pi, 1.75\pi\}$.

The scaled S-DPCCH is pre-coded with the orthogonal secondary beamforming weight vector

$$[w_3 \ w_4] = [a_2 e^{j\theta_1} \ -a_1 e^{j\theta_2}] \quad (10)$$

where in this scheme it is assumed that

$$a_1 = \frac{1}{\sqrt{2}} = a_2 \quad (11)$$

The weight selection is calculated and applied on a slot by slot basis and a 2 slot signaling delay is assumed with the application of weights. To select the correct weights, the NodeB should evaluate the SINR with each of the weight possibilities based on the received pilots. The transmit antenna weight vector that would have maximized the SINR in the current slot is selected for the next slot. However, an additional two slot delay is assumed in applying the weights in the transmitter to model the delay of feedback signaling. Thus, the total transmit antenna weight delay is three slots.

It should be noted that unlike in open loop beamforming, the NodeB is aware of when the phase has been changed and can thus maintain optimal channel estimation. If the UE is in soft handover, the weights selected by the serving NodeB are used in the transmitter and the selected weights are signaled in the uplink to inform non-serving NodeBs about the used Tx weights. It is shown in [5] that most of the beamforming gain can be captured by using a codebook of four weights.

III. FEEDBACK METHODS

Two distinctive feedback methods are investigated in this paper; the absolute and the recursive feedback method. In the absolute feedback method, the information for the whole beamforming vector, i.e. 2 bits, is transmitted in every feedback period whereas in the recursive feedback method, one bit per feedback update period is transmitted. For the recursive feedback method, the feedback bits of the current and previous time slots are combined to form the pre-coding vector. This approach has potential to offer increased tolerance against individual signaling errors as only part of the weight vector would have incorrect information in the case of an error. In addition the scheme requires less signaling bits per time slot, which would offer increased motivation to use such a scheme. However, compared to the absolute scheme, a single signaling error affects the weight selection for a longer time period as the full weight vector is constructed from the information over multiple time slots.

The use of pre-coded pilot means that channel estimate for the demodulation is directly available from the channel

estimate. However, the non-beamformed channel needs to be calculated in order to derive the channel for feedback calculation. The receiver uses the already signaled beamforming weight to solve the non-beamformed channel. The applied beamforming weight in the transmitter is not necessarily the same as the assumed one in the receiver if feedback error occurs and the receiver is not aware of the feedback error. This causes error propagation for the recursive feedback method. The absolute feedback method suffers also from the error propagation but the memory effect is shorter.

A. Recursive feedback algorithm

The recursive feedback method for this study was adapted from downlink Closed loop mode 1 -transmit diversity [6] and is defined as follows:

In each slot, UE calculates the optimum phase adjustment, ϕ , for antenna 2, which is then quantized into ϕ_Q having two possible values as follows:

$$\phi_Q = \begin{cases} \pi, & \text{if } \pi/2 < \phi - \phi_r(i) \leq 3\pi/2 \\ 0, & \text{otherwise} \end{cases} \quad (12)$$

where:

$$\phi_r(i) = \begin{cases} 0, & i = 2k, \forall k \in \mathbb{Z} \\ \pi/2, & i = 2k+1, \forall k \in \mathbb{Z} \end{cases} \quad (13)$$

If $\phi_Q = 0$, a command '0' is send to the UE.

Correspondingly, if $\phi_Q = \pi$, command '1' is send to the UE. Due to rotation of the constellation the received commands are interpreted according to TABLE I. which shows the mapping between phase adjustment, ϕ_i , and received feedback command for each uplink slot.

TABLE I. PHASE ADJUSTMENTS, ϕ , CORRESPONDING TO FEEDBACK COMMANDS FOR THE SLOTS

| Slot | Even slot | Uneven slot |
|-------|-----------|-------------|
| Bit 0 | 0 | $\pi/2$ |
| Bit 1 | π | $-\pi/2$ |

The weight w_2 is then calculated by averaging the received phases over 2 consecutive slots. Algorithmically, w_2 is calculated as follows:

$$w_2 = \frac{\sum_{i=n-1}^n \cos(\phi_i)}{2} + j \frac{\sum_{i=n-1}^n \sin(\phi_i)}{2} \quad (14)$$

$$\text{where: } \phi_i \in \{0, \pi, \pi/2, -\pi/2\} \quad (15)$$

For antenna 1, w_1 is constant:

$$w_1 = 1/\sqrt{2} \quad (16)$$

IV. SIMULATION METHODOLOGY AND ASSUMPTIONS

This study has been performed by using a comprehensive quasi-static time driven system simulator. The simulator has been utilized in the past in various international publications as well as supporting 3GPP standardization work, see, e.g., [5]. This simulation tool enables detailed simulation of users in multiple cells with realistic call generation, propagation and fading which are adopted from [7] and updated according to 3GPP requirements.

A. Quasi-static Simulation Approach

The term “Quasi-static” approach means that UEs are stationary but both slow (log normal) and fast fading are explicitly modeled. Fast fading is modeled for each UE according to the *International Telecommunication Union (ITU)* channel profiles [8] and with a jakes model modified for chip interval. Statistical confidence is reached through running multiple drops, i.e., independent simulation iterations. In each step UE locations, fading, etc. are randomized but the statistics are gathered and averaged over all drops.

B. Simulation Assumptions

Main parameters used in the system simulation are summarized in TABLE II. For the simulation scenario a wrap-around multi-cell layout, illustrated in Figure 2, is utilized.

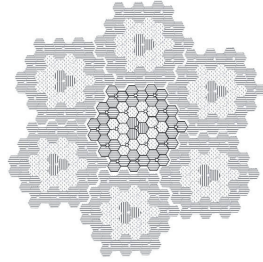


Figure 2. Wrap-around simulation scenario

The purpose of the wrap-around is to model the interference correctly also for outer cells. This is achieved by limiting the UE placement around the actual simulation area, but replicating the cell transmissions around the whole simulation area to offer more realistic interference situation throughout the scenario. In Figure 2 the actual simulation area is highlighted in the center. UEs are created to the scenario according to uniform distribution which results into some cells being more heavily loaded while others can be even empty.

V. SIMULATION RESULTS

Average user throughputs for ISD 2800m with different cell loads and channels are shown in Figure 3 and Figure 4. The figures show that both CLBF feedback methods indicate gain over the baseline without transmit diversity in both channels, but the gains in PedA channel are higher. When 0% feedback BER is assumed, the performance with both the absolute and recursive feedback methods match closely. However, when

BER value is increased, the absolute feedback method performs better and the performance gain over recursive feedback increases as BER increases. The difference in performance can be seen already with the error rates below 10%, which are likely within the expected relevant error rate limits.

TABLE II. MAIN SIMULATION ASSUMPTIONS

| Feature/Parameter | Value / Description |
|-------------------------------|--|
| Cell Layout | Hexagonal grid, 19 NodeBs, 3 sectors per Node B with wrap-around |
| Inter-site Distance | 2800 m with 10 dB penetration loss |
| Channel Model and UE Velocity | PedA: 3 kmph VehA: 30 kmph |
| Log Normal Fading | Standard Deviation : 8dB Inter-NodeB Correlation: 0.5 Intra-NodeB Correlation: 1.0 Correlation Distance: 50m |
| NodeB Receiver | Rake (2 antennas per cell) |
| UE Max. Tx Power | 23 dBm |
| TTI Length | 2 ms |
| Max. HARQ Transmissions | 4 |
| Number of HARQ Processes | 8 |
| Short Term Antenna Imbalance | 2.25 dB |
| Long term Antenna Imbalance | 0 dB |
| Tx Antenna Correlation | Uncorrelated |
| Number of UEs per Sector | [0.25, 0.5, 1, 2, 4, 10] |
| UE Distribution | Uniform over the whole area |
| Traffic Type | Full Buffer |
| Scheduling algorithm | Proportional Fair, Forgetting factor: 0.01 |
| Uplink power headroom | Averaged over 100 ms |
| Channel Estimation | 3 slot filtering, utilized through Actual Value Interface (AVI) tables, estimator is ideally aware on applied antenna weight |
| Pre-coding Codebook Size | 4 phases |
| Amplitude Component Offsets | 0.5 / 0.5 |
| Weight Signalling Feedback | [Absolute, Recursive] |
| Number of Feedback Bits | 1 bit for recursive feedback method 2 bits for absolute feedback method |
| Weight Signaling BER | [0, 5, 10, 20]% |

Figure 5 and Figure 6 illustrate the 50th percentile throughput. With 50th percentile throughputs the performance gain of absolute feedback method over recursive feedback method is noticeable as BER increases, especially with PedA3 channel. The performance of recursive feedback at 5 % feedback error rate is almost the same as absolute feedback at 10 % error rate. Or alternatively at 5 % feedback error level the absolute feedback method achieves 5% higher throughput.

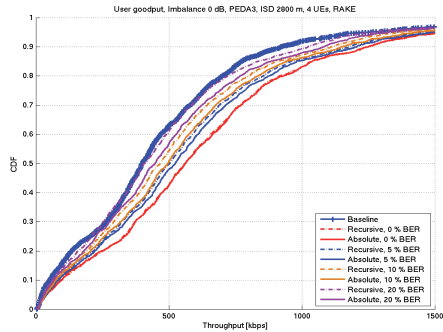


Figure 3. Average user throughput, PedA 3 kmph, ISD 2800m

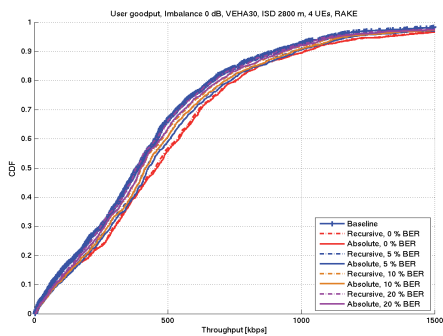


Figure 4. Average user throughput, VehA 30 kmph, ISD 2800m

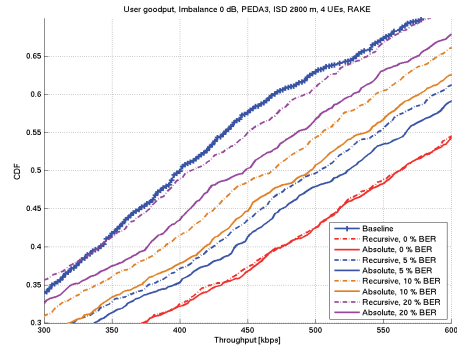


Figure 5. 50th percentile throughput, PedA 3 kmph, ISD 2800m

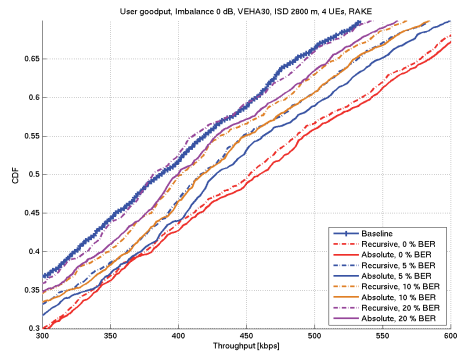


Figure 6. 50th percentile throughput, VehA 30 kmph, ISD 2800m

VI. CONCLUSION

This paper presents and benchmarks two different weight vector feedback methods for closed loop beamforming transmit diversity in various conditions against the baseline performance. The studies show that when comparing performance between the recursive and the absolute feedback the benefit of having absolute feedback comes in increased tolerance for weight signaling bit errors which translates into higher achievable throughput rates. Moreover, it is shown that the higher the BER the higher is the benefit from absolute feedback over recursive. Hence, even with the more relevant 5-10% error rates, the longer memory effect with the recursive feedback signaling error propagation results in large enough impact to overcome the increased individual signaling error tolerance from distributing the weight signaling bits over multiple time slots.

ACKNOWLEDGMENTS

This study is a collaborative work between Magister Solutions Ltd. and Renesas Mobile Corporation. The authors would like to thank all of their co-workers and colleagues for their comments and support.

REFERENCES

- [1] H. Holma, A. Toskala: "HSDPA/HSUPA for UMTS: High Speed Radio Access for Mobile Communications", John Wiley & Sons Ltd, 2006.
- [2] Third Generation Partnership Project (3GPP), Radio Access Network Radio Layer 1 Work Group, <http://3gpp.org/RAN1-Radio-layer-1>, cited September 2010.
- [3] S. Wang, E. Abreu, H. Harel, K. Kludt, P. Chen, "Mobile transmit beamforming diversity on UMTS/HSUPA networks." In Proceedings of Sarnoff Symposium, 2010 IEEE, vol., no., pp.1-6, 12-14 April 2010.
- [4] T. Nihtila, "Performance of Advanced Transmission and Reception for High Speed Downlink Packet Access," Ph.D. dissertation, pp. 49-51, University of Jyväskylä, 2008.
- [5] P. Eskelinen, F. Laakso, K. Aho, T. Hiltunen, I. Repo, "Impact of practical codebook limitations on HSUPA closed loop transmit diversity", In Proc. of IEEE Vehicular Technology Conference (VTC), San Francisco, CA, September 2011.
- [6] Third Generation Partnership Project (3GPP), "Technical Specification Group Radio Access Network; Physical layer procedures (FDD)", Technical Specification, TS 25.214, V10.3.0, 2011-06
- [7] Third Generation Partnership Project (3GPP), "Selection Procedures for the Choice of Radio Transmission Technologies of the UMTS", Technical Requirement, TR 101 112 (UMTS 30.03), 1998.
- [8] ITU-R, "Guidelines for Evaluation of Radio Transmission Technologies for IMT-2000", Recommendation, ITU-R M.1225, 1997.

PXIII

**UPLINK WEIGHT SIGNALING FOR HSUPA CLOSED LOOP
TRANSMIT DIVERSITY**

by

Frans Laakso, Petri Eskelinen, Marko Lampinen 2012

23rd IEEE International Symposium on Personal, Indoor and Mobile Radio
Communications (PIMRC 2012)

Reproduced with kind permission of IEEE.

Uplink Weight Signaling for HSUPA Closed Loop Transmit Diversity

Frans Laakso, Petri Eskelinen
Magister Solutions, Ltd.
Hannikaisenkatu 41
FIN-40100 Jyväskylä, Finland
firstname.lastname@magister.fi

Marko Lampinen
Renesas Mobile Corporation
Elektroniikkatie 10
FIN-90590 Oulu, Finland
firstname.lastname@renesasmobile.com

Abstract—3GPP is investigating uplink transmit diversity alternatives for High Speed Uplink Packet Access. This paper studies closed loop beamforming transmit diversity where NodeB determines transmit antenna weight vectors and additional feedback is used for signaling the optimal weights to the user equipment. The used transmit antenna weights are signaled back to the NodeB in order to ensure correct decoding. This approach is benchmarked against the results where the used weights are not signaled back to the NodeB. Performance is analyzed in various conditions on system level against the performance without uplink weight signaling. The results show that signaling the used weights increases the performance over the case without uplink signaling especially with higher bit error rates. However, uplink weight signaling requires additional signaling bits which may not be justified if weight feedback bit error rates are expected to be low. Additionally when uplink weight signaling is used, even if the weight signaled in downlink were correctly received, signaling errors can happen in uplink which also will result in incorrect decoding at the NodeB.

Keywords: *Beamforming, HSUPA, transmit diversity, closed loop, uplink weight signaling*

I. INTRODUCTION

The *Third Generation Partnership Project's (3GPP's)* Releases 5 and 6 took major steps toward enhancing packet data capabilities of cellular networks by standardizing *High Speed Downlink Packet Access (HSDPA)* and *High Speed Uplink Packet Access (HSUPA)* evolutions [1]. In Releases 7, 8 and 9 a set of new techniques has been added into HSPA standard, such as dual cell HSDPA and HSUPA, downlink MIMO (*Multiple Input, Multiple Output*) and discontinuous reception and transmission.

A study item for HSUPA *Closed Loop Transmit Diversity (CLTD)* [2] was opened in 3GPP in 2010. This study item covers the study of *uplink (UL)* beamforming transmit diversity schemes with channel state feedback, hence the studied schemes are called closed loop transmit diversity schemes. Note that closed loop beamforming based on channel state feedback have been specified for the *downlink (DL)*. Due to increasing demand of higher performance also in the uplink, diversity techniques were considered as potential performance enhancement for HSUPA.

In our previous study on performance of absolute and recursive feedback methods with CLTD we concluded that

both 2x2 beamforming feedback methods are capable of providing gain over the 1x2 baseline in simulated conditions [3]. However, the recursive feedback method was shown to suffer from larger performance reduction with signaling errors. In this paper we summarize and benchmark a single stream dual pilot closed loop beamforming transmit diversity uplink weight signaling concept with pilot channel pre-coding where the used weights are signaled back to the NodeB in an effort to reduce the effects of downlink signaling errors.

The study is conducted with the help of a quasi-static time driven system level simulator and the simulations are done under the 3GPP assumptions. The remainder of this document is organized as follows: In Section II, the system model is presented and the basic transmit diversity method is introduced briefly. Section III describes the feedback schemes in detail. Section IV summarizes the simulation assumptions adopted in this study and section V presents the simulation results. Finally, section VI concludes the paper.

II. CLOSED LOOP BEAMFORMING TRANSMIT DIVERSITY WITH PRE-CODED PILOT

As explained in [4], the diversity transmitter which employs beamforming can provide two types of gain; coherent gain from beamforming and incoherent gain from mitigation of channel fades, i.e., the classical diversity gain. If the radio channels of different transmit antennas are highly correlated, which typically is the case in small hand-held devices, they can be used to form a beam and the coherent gain becomes dominant [4]. Beamforming can be seen as a form of spatial filtering which separates the signals of different *User Equipment (UE)* that are spatially separated. Due to this spatial filtering the interference seen by the NodeB is lower than without beamforming, especially in heavily loaded cells.

In the presented transmission scheme, illustrated in Figure 1, two *Dedicated Physical Control Channels (DPCCH)* are transmitted independently from different antennas. DPCCH is the channel that carries the pilot symbols and therefore two DPCCHs are needed in order to obtain knowledge of the whole channel matrix. Beamforming is carried out by pre-coding the signal with a weight vector $[w_1, w_2]$. In addition to the DPCCHs, beamforming is also applied to the *High Speed Dedicated Physical Control Channel (HS-DPCCH)*, *E-DCH Dedicated Physical Control Channel (E-DPCCH)* and *E-DCH Dedicated Physical Data Channel (E-DPDCH)*. For simplicity,

HS-DPCCH and E-DPCCH are left out from Fig. 1. The scheme includes a single power control loop based on the post receiver combined *Signal to Interference-Noise Ratio (SINR)* across all transmit and receive antennas at the NodeB and each antenna branch is transmitted with 50% of the total transmit power. The DPCCH pilots are transmitted on different *Orthogonal Variable Spreading Factor (OVSF)* codes. However, since the branches combine over the air, the traffic to pilot ratio β_d/β_c is set as E-DPCCH power over the total power on DPCCH1 and DPCCH2. That is, the two pilots are transmitted with half of the power allocated to a single DPCCH in non-Tx diversity uplink transmission.

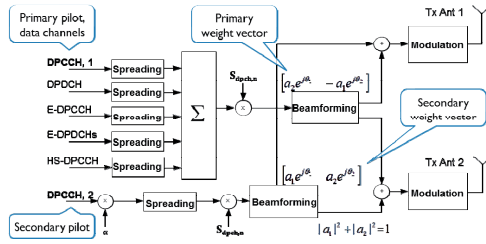


Figure 1. Principle of Closed Loop BFTD with pre-coded pilot

The SINR calculation for the studied closed loop beamforming scheme with pre-coded pilots is presented in [3]. The algorithm used for selecting the weight vectors is described in the following subsection.

A. Weight Vector Selection Algorithm

The phase offset between antennas is implemented by applying a beamforming weight to each antenna. The beamforming weights $\underline{w} = [w_1 \ w_2]^H$ are adjusted every slot (0.67msec); in each slot, they are calculated to maximize:

$$\sum_{l=1}^L \underline{w}^H H_l(k)^H H_l(k) \underline{w} \quad (1)$$

where $H_l(k)$ is a 2x2 matrix of channels between transmit and receive antennas for the l^{th} multipath in the k^{th} slot. The calculation is done to all of the links in UEs active set and the weight resulting in the highest power is selected. The antenna weights are selected from a set of four vectors. Each weight vector is defined as

$$[w_1 \ w_2] = [a_1 e^{j\theta_1} \ a_2 e^{j\theta_2}] \quad (2)$$

where $a_1^2 + a_2^2 = 1$ and $\theta = \{0.25\pi, 0.75\pi, 1.25\pi, 1.75\pi\}$.

The scaled S-DPCCH is pre-coded with the orthogonal secondary beamforming weight vector

$$[w_3 \ w_4] = [a_2 e^{j\theta_1} \ -a_1 e^{j\theta_2}] \quad (3)$$

where it is assumed that

$$a_1 = 1/\sqrt{2} = a_2 \quad (4)$$

The weight selection is calculated and applied on a slot by slot basis. To select the correct weights, the NodeB evaluates the SINR with each of the weight possibilities based on the received pilots. The transmit antenna weight vector that would have maximized the SINR in the current slot is selected for the next slot. However, an additional two slot delay is assumed in applying the weights in the transmitter to model the delay of feedback signaling. Thus, the total transmit antenna weight delay is three slots.

It should be noted that the NodeB is aware of when the phase has been changed and can thus maintain optimal channel estimation. If the UE is in soft handover, the weights selected by the serving NodeB are used in the transmitter and the selected weights are signaled in the uplink to inform non-serving NodeBs about the used Tx weights. It is shown in [5] that most of the beamforming gain can be captured by using a codebook of four weights.

III. FEEDBACK METHODS

Two distinctive feedback methods are investigated in this paper; the absolute and the recursive feedback method. In the absolute feedback method, the information for the whole beamforming vector, i.e. 2 bits, is transmitted in every feedback period whereas in the recursive feedback method, one bit per feedback update period is transmitted. For the recursive feedback method, the feedback bits of the current and previous periods are combined to form the pre-coding vector. This approach has potential to offer increased tolerance against individual signaling errors and, in addition to requiring less signaling bits per time slot, would be the motivation for using such a scheme.

The use of pre-coded pilot means that channel estimate for the demodulation is directly available from the channel estimate. However, the non-beamformed channel needs to be calculated in order to derive the channel for feedback calculation. The receiver uses the already signaled beamforming weight to solve the non-beamformed channel. The applied beamforming weight in the transmitter is not necessarily the same as the assumed one in the receiver if feedback error occurs and the receiver is not aware on the feedback error. This results in error propagation for both of the feedback methods, but the memory effect is shorter with the absolute feedback method.

A. Recursive feedback algorithm

The recursive feedback method was adapted from downlink Closed loop mode 1 -transmit diversity [6] and is defined as follows:

In each slot, UE calculates the optimum phase adjustment, ϕ , for antenna 2, which is then quantized into ϕ_Q having two possible values as follows:

$$\phi_Q = \begin{cases} \pi, & \text{if } \pi/2 < \phi - \phi_r(t) \leq 3\pi/2 \\ 0, & \text{otherwise} \end{cases} \quad (5)$$

where:

$$\phi_r(i) = \begin{cases} 0, & i = 2k, \forall k \in \mathbb{Z} \\ \pi/2, & i = 2k+1, \forall k \in \mathbb{Z} \end{cases} \quad (6)$$

If $\phi_Q = 0$, a command '0' is send to the UE. Correspondingly, if $\phi_Q = \pi$, command '1' is send to the UE. Due to rotation of the constellation the received commands are interpreted according to TABLE I. which shows the mapping between phase adjustment, ϕ_i , and received feedback command for each uplink slot.

TABLE I. PHASE ADJUSTMENTS, ϕ_i , CORRESPONDING TO FEEDBACK COMMANDS FOR THE SLOTS

| Slot | Even slot | Uneven slot |
|------|-----------|-------------|
| Bit | 0 | $\pi/2$ |
| | 1 | $-\pi/2$ |

The weight w_2 is then calculated by averaging the received phases over 2 consecutive slots. Algorithmically, w_2 is calculated as follows:

$$w_2 = \frac{\sum_{i=n-1}^n \cos(\phi_i)}{2} + j \frac{\sum_{i=n-1}^n \sin(\phi_i)}{2} \quad (7)$$

where:

$$\phi_i \in \{0, \pi, \pi/2, -\pi/2\} \quad (8)$$

For antenna 1, w_1 is constant:

$$w_1 = 1/\sqrt{2} \quad (9)$$

B. Error propagation with the investigated feedback methods

The following section provides a simplified description on how a single weight signalling error propagates with the absolute signalling method:

1. NodeB signals the weight vector which should be used to the UE.
2. A signalling error occurs and the UE uses the sub-optimal weight vector for transmission.
3. NodeB receives the transmission and bases its next weight vector on the channel estimate from the transmission with sub-optimal weights.
4. The UE receives the weight vector correctly, but the weights are based on the sub-optimal transmission and as such the following transmission to NodeB is also sub-optimal.
5. NodeB receives the transmission and bases its feedback on the channel with correct weights. The error is corrected.

With recursive feedback method, a single weight signalling error propagates as follows:

1. NodeB signals the bit which is used to refine the weight vector to the UE.
2. A signalling error occurs and as the most current weight vector bit is erroneous, the UE uses the sub-optimal weight vector for transmission.
3. NodeB receives the transmission and bases its next weight vector bit on the sub-optimal channel estimate.
4. The UE receives the latest bit correctly, but as the bit is based on the sub-optimal transmission and also the erroneous bit the NodeB previously signalled is still used, the following transmission to NodeB is also sub-optimal.
5. NodeB receives the transmission and bases its feedback bit on the channel with sub-optimal channel estimate.
6. The UE receives the bit correctly and both bits used by the algorithm are now correctly received, but the bits are still based on the previous sub-optimal transmissions. As such the following transmission to NodeB is also possibly sub-optimal.
7. NodeB receives the transmission and bases its feedback bit on the channel with sub-optimal weights.
8. NodeB receives the transmission and bases its feedback on the channel with correct weights. The error is corrected.

C. Uplink weight signalling

The investigated approach aims to eliminate the use of sub-optimal channel estimates in the weight selection by adjusting the currently used estimates based on the difference between the original calculated signalling bit and the bit signalled back from the UE. This approach reduces the signalling error memory effect, but does not improve the already sent data transmissions, thus completely removing the error effects. As such the expected performance is not on par with the completely error free results, but the investigated approach should still offer visibly improved performance. The investigated approach is relatively straightforward and requires few additional NodeB resources compared to the feedback methods, namely the mechanics for comparing the signalling bits and channel estimates for recalculating the new weights are needed. However, the bi-directional weight signalling introduces new challenges in terms of additional signalling resources and possible uplink signalling errors. For the purposes of this study the uplink signalling errors and signalling overhead are not considered as the focus is on investigating the upper bound of achievable performance.

IV. SIMULATION METHODOLOGY AND ASSUMPTIONS

This study has been performed by using a comprehensive quasi-static time driven system simulator. The simulator has been utilized in the past in various international publications as well as supporting 3GPP standardization work, see, e.g., [5] [7]. This simulation tool enables detailed simulation of users in multiple cells with realistic call generation, propagation and

fading which are adopted from [8] and updated according to 3GPP requirements.

A. Quasi-static Simulation Approach

The term “Quasi-static” approach means that UEs are stationary but both slow (log normal) and fast fading are explicitly modeled. Fast fading is modeled for each UE according to the *International Telecommunication Union (ITU)* channel profiles [9] and with a jakes model modified for chip interval. Statistical confidence is reached through running multiple drops, i.e., independent simulation iterations. In each step UE locations, fading, etc. are randomized but the statistics are gathered and averaged over all drops.

B. Simulation Assumptions

Main parameters used in the system simulation are summarized in TABLE II. For the simulation scenario a wrap-around multi-cell layout, illustrated in Figure 2, is utilized.

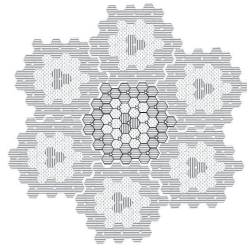


Figure 2. Wrap-around simulation scenario

The purpose of the wrap-around is to model the interference correctly also for outer cells. This is achieved by limiting the UE placement around the actual simulation area, but replicating the cell transmissions around the whole simulation area to offer more realistic interference situation throughout the scenario. In Figure 2 the actual simulation area is highlighted in the center. UEs are created to the scenario according to uniform distribution which results into some cells being more heavily loaded while others can be even empty.

V. SIMULATION RESULTS

Average user throughputs for ISD 2800m with different cell loads and feedback methods are shown in Figure 3 and Figure 4. The figures show that the investigated uplink weight signaling approach can offer improved performance with both of the benchmarked feedback methods. When 0% downlink feedback BER is assumed, the uplink signaling approach provides identical results, which is to be expected. However, when BER value is increased, the uplink signaling performs increasingly better. The difference in performance can be seen already with the error rates below 10%, which are likely within the expected relevant error rate limits. It can be also seen that the improvement is more noticeable with the recursive feedback method, which corroborates with the more drastic error specific propagation with the said method.

Figure 5 illustrates the 10th percentile user throughput with recursive feedback. It can be seen that for users in poor channel conditions the benefits from improved error correction are most tangible, in numerous cases improving performance compared to the case without uplink signaling by up to 10-15%. However, these results are obtained without any uplink signaling errors and as such present the upper bound on achievable performance.

As previously investigated in [3], both beamforming feedback methods provide gain over the 1x2 baseline results.

TABLE II. MAIN SIMULATION ASSUMPTIONS

| Feature/Parameter | Value / Description |
|-------------------------------|--|
| Cell Layout | Hexagonal grid, 19 NodeBs, 3 sectors per Node B with wrap-around |
| Inter-site Distance | 2800 m with 10 dB penetration loss |
| Channel Model and UE Velocity | PedA: 3 kmph |
| Log Normal Fading | Standard Deviation : 8dB Inter-NodeB Correlation: 0.5 Intra-NodeB Correlation: 1.0 Correlation Distance: 50m |
| NodeB Receiver | Rake (2 antennas per cell) |
| UE Max. Tx Power | 23 dBm |
| TTI Length | 2 ms |
| Max. HARQ Transmissions | 4 |
| Number of HARQ Processes | 8 |
| Short Term Antenna Imbalance | 2.25 dB |
| Long term Antenna Imbalance | 0 dB |
| Tx Antenna Correlation | Uncorrelated |
| Number of UEs per Sector | [0.25, 0.5, 1, 2, 4, 10] |
| UE Distribution | Uniform over the whole area |
| Traffic Type | Full Buffer |
| Scheduling algorithm | Proportional Fair, Forgetting factor: 0.01 |
| Uplink power headroom | Averaged over 100 ms |
| Channel Estimation | 3 slot filtering, utilized through Actual Value Interface (AVI) tables, estimator is ideally aware on applied antenna weight |
| Pre-coding Codebook Size | 4 phases |
| Amplitude Component Offsets | 0.5 / 0.5 |
| Weight Signalling Feedback | [Absolute, Recursive] |
| Number of Feedback Bits | 1 bit for recursive feedback 2 bits for absolute feedback |
| Downlink Weight Signaling BER | [0, 5, 10, 20]% |
| Uplink Weight Signaling BER | 0% |

VI. CONCLUSION

This paper presents and benchmarks an uplink weight signaling approach for two different feedback methods for closed loop beamforming transmit diversity in various conditions against the performance without uplink signaling. The results show that the benefits from improved error correction can lead to noticeable gains, in numerous cases improving performance compared to the case without uplink signaling by up to 10-15%. The difference in performance can be seen already with the error rates below 10%, which are likely within the expected relevant error rate limits. It can be also seen that the improvement is more noticeable with the recursive feedback method, which corroborates with the more drastic error specific propagation with the said method.

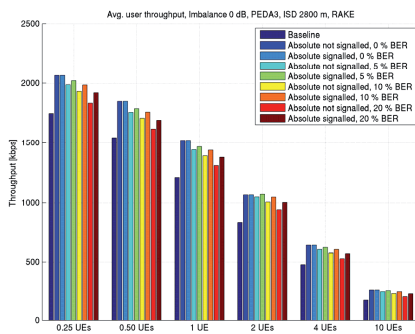


Figure 3. Average user throughput, absolute feedback, PedA 3 kmph, ISD 2800m

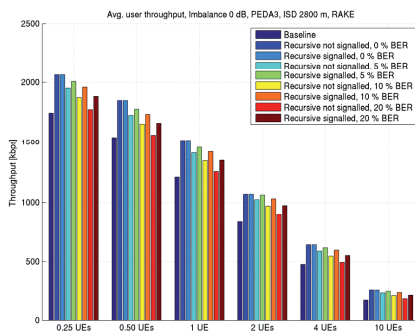


Figure 4. Average user throughput, recursive feedback, PedA 3 kmph, ISD 2800m

However, these results are obtained without uplink signaling errors and as such present the upper bound on achievable performance. Additionally, even though the investigated uplink signaling method is relatively

straightforward, a new bi-directional weight signalling is needed and as such introduces new challenges.

ACKNOWLEDGMENTS

This study is a collaborative work between Magister Solutions Ltd. and Renesas Mobile Corporation. The authors would like to thank all of their co-workers and colleagues for their comments and support.

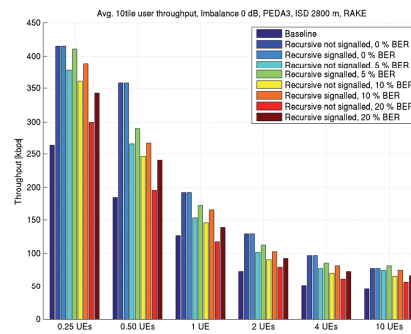


Figure 5. 10th percentile user throughput, recursive feedback, PedA 3 kmph, ISD 2800m

REFERENCES

- [1] H. Holma, A. Toskala: "HSDPA/HSUPA for UMTS: High Speed Radio Access for Mobile Communications", John Wiley & Sons Ltd, 2006.
- [2] Third Generation Partnership Project (3GPP), Radio Access Network Radio Layer 1 Work Group, <http://3gpp.org/RAN1-Radio-layer-1>, cited September 2010.
- [3] F. Laakso, P. Eskelinen, M. Lampinen, "Performance of Absolute and Recursive Feedback Methods with HSUPA Closed Loop Transmit Diversity", In Proc. of 23rd IEEE International Symposium on Personal, Indoor and Mobile Radio Communications (PIMRC), Sydney, Australia, September 2012.
- [4] S. Wang, E. Abreu, H. Harel, K. Kludt, P. Chen, "Mobile transmit beamforming diversity on UMTS/HSUPA networks," In Proceedings of Sarnoff Symposium, 2010 IEEE, vol., no., pp.1-6, 12-14 April 2010.
- [5] P. Eskelinen, F. Laakso, K. Aho, T. Hiltunen, I. Repo, "Impact of practical codebook limitations on HSUPA closed loop transmit diversity", In Proc. of IEEE Vehicular Technology Conference (VTC), San Francisco, CA, September 2011.
- [6] Third Generation Partnership Project (3GPP), "Technical Specification Group Radio Access Network; Physical layer procedures (FDD)", Technical Specification, TS 25.214, V10.3.0, 2011-06
- [7] Third Generation Partnership Project (3GPP), "Universal Terrestrial Radio Access (UTRA); Uplink transmit diversity for High Speed Packet Access (HSPA)", Technical Report, TR 25.863, V10.0.0, 2010-07.
- [8] Third Generation Partnership Project (3GPP), "Selection Procedures for the Choice of Radio Transmission Technologies of the UMTS", Technical Requirement, TR 101 112 (UMTS 30.03), 1998.
- [9] ITU-R, "Guidelines for Evaluation of Radio Transmission Technologies for IMT-2000", Recommendation, ITU-R M.1225, 1997.